Bioresponsive Polymer-Protein Conjugates as a Unimolecular Drug Delivery System

Helena Rosalind Petra Gilbert
MRPharmS

A thesis submitted to Cardiff University in partial fulfilment of the requirements for the degree of Doctor of Philosophy

Centre for Polymer Therapeutics
Welsh School of Pharmacy
Cardiff University
United Kingdom

ProQuest LLC
789 East Eisenhower Parkway
P.O. Box 1346
Ann Arbor, MI 48106-1346

For my mother, father and brother

Acknowledgements

I would first and foremost like to acknowledge the insight of Prof. Ruth Duncan, in generating the concept of masked and reinstated protein activity; central to this thesis. I am greatly appreciative of the opportunity given to me to contribute to this exciting area of research and also wish to acknowledge BBSRC for funding my PhD studentship. I would furthermore like to thank Prof. Duncan for her support and guidance, without which this research would not have been possible.

I would like to thank both my parents and brother for their support and encouragement, which has enabled me to persist in completing this work. Furthermore, I wish to thank my father for inspiring me to explore the idea of research and my mother for her faith in my ability to do anything I set my mind to. Julian, your endless love, support, tolerance and selflessness is amazing and only a small part of the reason I love you so much. Thank you.

Finally, I wish to acknowledge all of my friends and colleagues, past and present, in the Centre for Polymer Therapeutics. Thank you for your friendship, support, assistance and intellectual help! I wish to thank all of you for being a part of my journey. Sarah and Cat; I'm so glad I met you two. Your friendship and parallel PhD experience in a different subject has kept PhDs in perspective for me. Thank you all!

Abstract

PEGylation has become very popular for the generation of nanomedicines with improved protein delivery properties, despite its lack of biodegradability. Researchers usually try to maximise retained protein activity during PEGylation. However, this proof of principle study aimed to create an inactive peptide or enzyme product, using a biodegradable polymer, that would elicit minimal activity/non-specific toxicity on administration. Following triggered site-specific degradation of the polymer, the hypothesis was that protein activity could be slowly regenerated in the general circulation or localised to a specific target site.

Model conjugates were synthesised by coupling dextrin (degraded by amylase) to trypsin and melanocyte stimulating hormone (MSH), to test this concept and targeted delivery for both an enzyme and a receptor-binding ligand. Hyaluronic acid (HA; degraded by hyaluronidase) conjugates of trypsin and ribonuclease A were also synthesised. The latter was intended to develop the possibility of designing novel anti-cancer conjugates.

A higher molecular weight dextrin (47,200 g/mol, 26 mol % succinoylation) was shown to best mask (34 %) trypsin activity and reinstate 58 % of the activity by addition of amylase. When a HA fraction (molecular weight ~130,000 g/mol) was prepared by acid hydrolysis and conjugated to trypsin (4 % w/w), trypsin activity was masked to 6 % and immediately re-instated to 24 % on addition of hyaluronidase. Similarly, the dextrin-MSH conjugate reduced melanin production to 11 % of the control and only restored to 33 % on addition of amylase. RNase A alone was not cytotoxic (up to 1 mg/mL), whereas, the HA-RNase A conjugate (0.1 mg/mL RNase A equivalent) was cytotoxic in B16F10 and CV-1 cells (72 h).

This work provides proof of principle for the concept of using biodegradable polymers to mask and reinstate conjugated protein activity in the presence of the appropriate enzyme 'unmasking' trigger.

Contents

List of Figures

List of Tables

Abbreviations

ALL	Acute lymphoblastic leukaemia
ANOVA	Analysis of variance
AP	Ammonium persulfate
ARG	Arginine
ASP	Aspartic acid
ATCC	American type culture collection
B16F10	Murine melanoma cell line
BAEE	Na-benzoyl-arginine-ethyl-ester
BAPNA	$_{N}$-Benzoyl-$_{L}$-arginine-$_{p}$-Nitroanilide
BCA	Bicinchoninic acid
BSA	Bovine serum albumin
BS-RNase	Bovine seminal ribonuclease
^{13}C	Carbon-13
CB	Coomassie blue
Contd	Continued
CR	Controlled release
CT	Clinical trials
Cu	Copper sulfate
CV-1	African green monkey fibroblasts
CYS	Cysteine
D_2O	Deuterated water
ddH_2O	double distilled water
DMAP	4-dimethylaminopyridine
DMEM	Dulbecco's minimal essential media
DMF	N,N-dimethylformamide
DMSO	Dimethyl sulphoxide
EC_{50}	Effective concentration to achieve 50 % maximal response
ECACC	European collection of cell cultures
ECM	Extracellular matrix
EDC	1-ethyl-3(3-dimethylaminopropyl)carbodiimide
EDTA	Trypsin-ethylenediaminetetraaceticacid
EGF	Epidermal growth factor
EPR	Enhanced permeability and retention effect
Equiv.	Equivalent
ER	Endoplasmic reticulum
ERT	Enzyme replacement therapy
FACS	Flow angle cytometry
FBS	Foetal bovine serum
FDA	Food and drug administration
FPLC	Fast protein liquid chromatography
FT-IR	Fourier transform infrared spectroscopy
FU	Fluorouracil
GCSF	Granulocyte colony stimulating factor
GLU	Glutamic acid
GLY	Glycine
GPC	Gel permeation chromatography
GRAS	Generally approved substances
^{1}H	Hydrogen-1

HA	Hyaluronic acid
HAase	Hyaluronidase
HCl	Hydrochloric acid
HGH	Human growth hormone
HIS	Histidine
HMW	High molecular weight
HPMA	N-'(2-hydroxypropyl)methacrylamide
IA	Intra-articular
IC_{50}	Concentration which inhibits cell growth by 50 %
IHABP	Intracellular HA binding proteins
IP	Inter-peritoneal
IR	Infra-red
IT	Intra-tumoral
IV	Intra-venous
Kcat	Turnover rate
Km	Affinity constant
LMW	Low molecular weight
lq	Liquid
LEU	Leucine
LYS	Lysine
mAb	Monoclonal antibodies
MC-Rs	Melanocortin receptors
MET	Methionine
ML2	Human myeloid leukaemia cell line
MLC	Mixed lymphocyte culture
Mn	Number average molecular weight
mPEG	Monomethoxy-PEG
MSH	Melanocyte stimulating hormone
MTT	3-(4,5-dimethylthiazol-2-yl)-2,5-diphenyl-2H-terazoliumbromide
Mw	Weight average molecular weight
MWCO	Molecular weight cut-off
N_2	Nitrogen
NA	Not applicable
NAD	Not adjusted
NaOH	Sodium hydroxide
NAp	p-Nitroanilide
NC	Not characterised
ND	Not determined
NF	Not fractionated
NMR	Nuclear magnetic resonance
NS	Not stated
OG	Oregon green
OG-CAD	Oregon green cadaverine
$p \leq$	Probability less than or equal to
PBS	Phosphate buffered saline
PD10	Prepacked sephadex G25 column
PDI	Polydispersity index
PEG	Polyethylene glycol
PEI	Polyethylenimine

PELT	Polymer enzyme liposome therapy
PHE	Phenylalanine
pKa	Acid dissociation constant
PLGA	Poly(DL-lactide-co-glycolide)
ppm	parts per million
PR	Phenol red
R	Receptor
r^2	Correlation coefficients
RA	Rheumatoid arthritis
RES	Reticulo-endothelial system
Rc HA	Rooster comb hyaluronic acid
RI	Refractive index
RIs	Ribonuclease inhibitors
RNase A	Ribonuclease A
RPMI	Rose park memorial institute
RT	Room temperature
Russ.	Russian translation
S	Substrate concentration
SC	Sub-cutaneous
SCID	Severe combined immunodeficiency disease
SD	Standard deviation
SDS	Sodium dodecyl sulphate
SDS-PAGE	Sodium dodecyl sulphate polyacrylamide gel electrophoresis
SEC	Size exclusion chromatography
SEM	Standard error of the mean
SER	Serine
SFR	Synthesised using a fixed ratio of dextrin to trypsin
SMA	Styrene maleic anhydride
SMANCS	Styrene-co-maleic anhydride-neocarzinostatin
STE	Synthesised using an excess of trypsin
Sulfo-NHS	N-hydroxysulfosuccinimide
TEMED	N,N,N,N'-tetra-methyl-ethylenediamine
TLC	Thin layer chromatography
TNBS	2,4,6-trinitrobenzenesulfonate
TNF	Tumour necrosis factor
TRIZMA HCl	Tris[hydroxymethyl]aminomethane hydrochloride
tRNA	transfer RNA
TYR	Tyrosine
UV	Ultraviolet
UV-vis	Ultraviolet-visible
V	Velocity
Vb	Bed volume
Vmax	Maximum velocity
Vo	Void volume

Chapter 1

General Introduction

1.0 INTRODUCTION

Polymer-protein conjugation was first applied to pharmaceuticals in 1982, when Vladimir Torchilin conjugated the polysaccharide dextran to the enzyme streptokinase (Torchilin et al., 1982 *Russ.*). 'Streptodekase' was the first polymer-protein conjugate to be used clinically (Figure 1.1). The conjugate showed significant benefits over the free streptokinase, enabling both a reduction in the frequency of administration and a significant reduction in adverse drug reaction (reviewed by Torchilin, 2000). In parallel to the development of Streptodekase, in the late 1970s, Davis and Abuchowski were also working on polymer-protein conjugation for drug development (reviewed by Davis, 2002). Their research demonstrated that when the polymer, polyethylene glycol (PEG) was covalently bound to proteins, termed PEGylation, the protein became non-immunogenic whilst experiencing little loss of activity (Abuchowski et al., 1977). In addition, PEGylation was also able to alter the pharmacokinetic and pharmacodynamic properties of the protein (Abuchowski and Davis, 1979). The pioneering work of Torchilin and the partnership of Davis and Abuchowski paved the way for the development of the field of polymer-protein conjugation.

In 1990 PEG-adenosine deaminase (Adagen™) was the first polymer-protein conjugate to be approved by the Food and Drug Administration (FDA). This was shortly followed in 1994 by the approval of PEG-L-asparaginase (Oncaspar®). With the exception of styrene-co-maleic anhydride-neocarzinostatin (SMANCS) marketed in Japan in 1993 (Maeda et al., 1985; reviewed by Maeda and Konno, 1997) and the aforementioned Streptodekase, which contain the polymer dextran, PEG is the most widely used polymer for protein conjugation (Table 1.1 and 1.2).

Despite the success and growing popularity of PEGylation, it suffers from several significant limitations. In particular, PEG is not a biodegradable polymer. This presents issues of renal elimination and its potential accumulation following chronic administration. In addition, continuous expression of protein activity and reductions in conjugated protein activity are also limitations of PEG conjugation.

The aim of the present study was to develop a novel approach for polymer-protein conjugation avoiding the pitfalls of PEGylation. It was hypothesised that a biodegradable polymer could be used to create polymer-protein conjugates that would be inactive whilst in transit, eliciting minimal activity and minimal non-specific

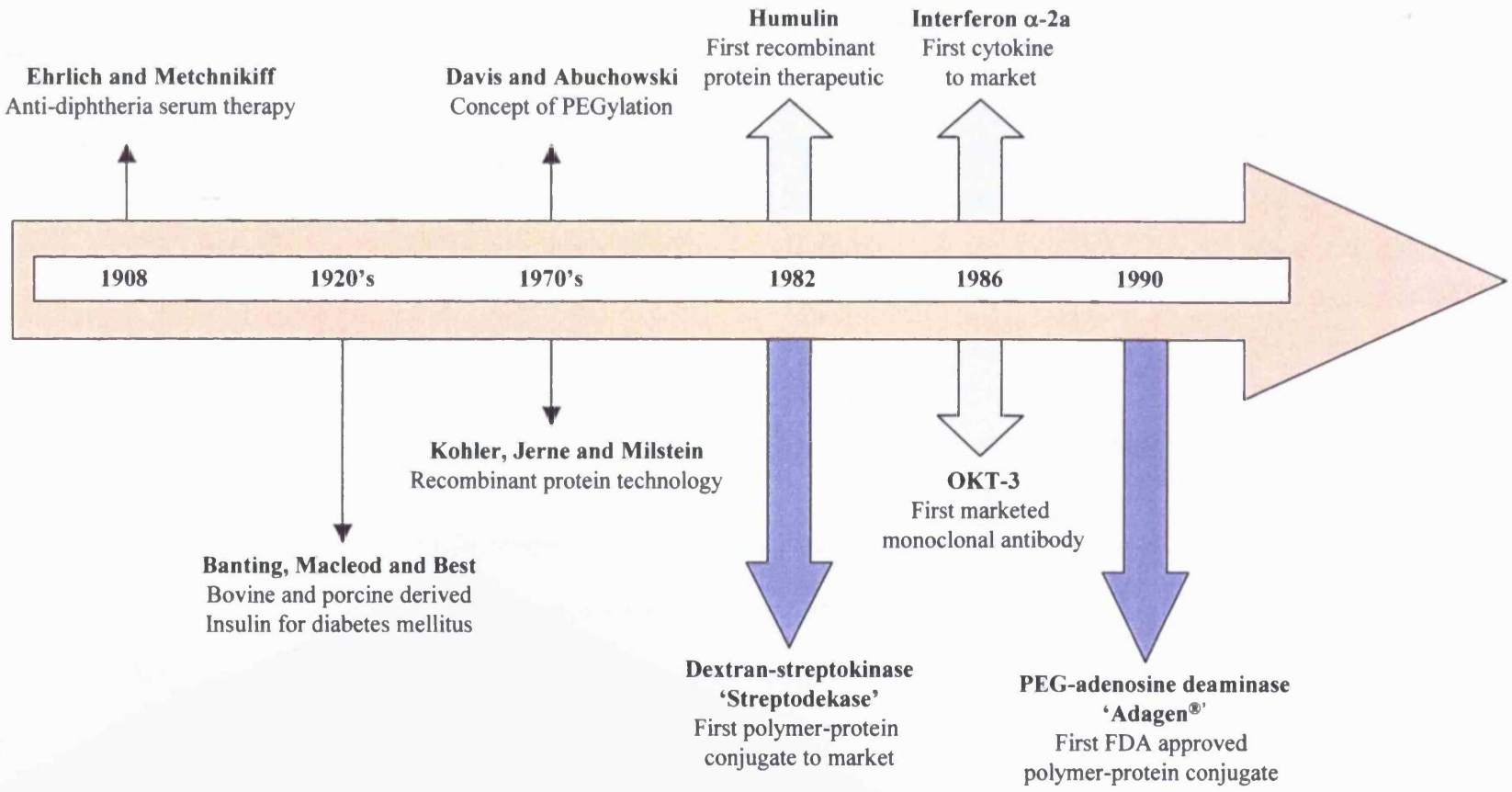

Figure 1.1 Timeline of key events in the development of protein therapeutics, adapted from Nagle et al., (2003).

Table 1.1 Polymer-protein conjugates currently on the market and in clinical trials

Year / status	Drug name	Polymer-protein combination	Indication	Reference
1982	Streptodekase	Dextran-streptokinase	Cardiovascular and ophthalmologic	Torchilin et al., 1982
1990	Adagen™	PEG-adenosine deaminase	SCID syndrome	Levy et al., 1988
1993	SMANCS	Zinostatin-Stimalmer	Hepatocellular carcinoma	Maeda and Konno, 1997
1994	Oncaspar®	PEG-L-asparaginase	Acute lymphoblastic leukaemia	Graham, 2003
2000	PEG Intron®	PEG-interferon alpha-2b	Hepatitis C	Wang et al., 2002
CT (P III)†	PEG Intron®	PEG-interferon alpha-2b	Renal cell carcinoma	Odaimi et al., 2004
			Advanced melanoma (stage IV)	Krown et al., 2004
CT (P II)†	PEG Intron®	PEG-interferon alpha-2b	Chronic myeloid leukaemia	NIH, 2006a
			Gastrointestinal carcinoid tumour	NIH, 2003a
			Brain and CNS tumours	NIH, 2007a
2002	Pegasys®	PEG-interferon alpha-2a	Hepatitis C	Reviewed by Reddy et al., 2002
CT (P III)†	NS‡	PEG-interferon alpha-2a	Chronic hepatitis B and C	NIH, 2005a
CT (P I)†	NS‡	PEG-interferon alpha-2a	Non-melanomatous skin cancer	NIH, 2007b
2002	Neulasta®	PEG-G-CSF††	Chemotherapy induced neutropenia	Reviewed by Kinstler et al., 2002
	PEG-filgrastim			

Contd.

Table 1.1 Polymer-protein conjugates currently on the market and in clinical trials (Contd.)

Year / status	Drug name	Polymer-protein combination	Indication	Reference
2002	Pegvisomant	PEG-HGH[‡‡]	Acromegaly	Reviewed by Parkinson et al., 2003
CT (P III)[†]	CDP870	PEG-Anti TNF FAB	Rheumatoid arthritis	Chapman et al., 1999
	(certolizumab pegol)			NIH, 2003b
CT (P II)[†]	CDP870	PEG-Anti TNF FAB	Crohn's disease	NIH, 2006b
	(certolizumab pegol)		Chronic plaque psoriasis	NIH, 2005b
CT (P II)[†]	PEG-haemoglobin	PEG-haemoglobin	Melanoma	PhRMA, 2004
	(Ro 50-3821)		Anaemia	NIH, 2003c
CT (P I)[†]	LYSODASE	PEG-Glucocerebrosidase	Gaucher disease	Enzon, 2004
				NIH, 1993
CT (P II)[†]	pegsunercept	PEG-sTNF-a-R1	Rheumatoid Arthritis	PhRMA, 2004
CT (P I)[†]	ADI-PEG	PEG-Arginine deiminase	Metastatic Melanoma	NIH, 2003d
CT (P II)[†]	ADI-PEG	PEG-Arginine deiminase	Hepatocellular carcinoma	NIH, 2003e

[†]CT is an abbreviation for clinical trials; PI, PII or PIII represents phase one, two or three

[‡]NS indicates not stated

[††]G-CSF is an abbreviation for Granulocyte colony stimulating factor

[‡‡]HGH defines Human growth hormone

[†††] TNF and R stand for tumour necrosis factor and receptor respectively

Table 1.2 Experimental PEG-protein conjugates

Protein classification	Protein	Experimental model	Reference
Enzyme	Adenosine phosphorylase	Adenosine deaminase deficiency	Brewerton et al., 2003
	Catalase	Pharmacokinetic studies	Gordon et al., 1990
	Chymotrypsin	Characterisation of binding sites	Schering et al., 2004
	Galactosidase (α and β)	Assessment of activity and properties	Beecher et al., 1990 ; Matsuo et al., 1997
	Glutaminase	Anticancer agent	Harzmann et al., 2004
	Lysozyme	Identification of PEGylation site	Veronese et al., 2001a
	Trypsin	Activity studies	Abuchowski and Davis, 1979 ; Zhang et al., 2001
	Urokinase	Activity studies	Garman and Kalindjian, 1987 ; Sakuragawa et al., 1986
Hormone	Glucagon	Efficacy and pharmacokinetics	Lee et al., 2004
	Insulin	Microencapsulation, administration route	Reviewed by Hinds and Wan Kim, 2002
	Melanin	Biotechnological application	Ishii et al., 1995
Cytokine	Erythropoietin	Animal studies into therapeutic effect	Malik et al., 2000
	Granulocyte-macrophage colony stimulating factor	*In vivo* studies on efficacy and immunogenicity	Malik et al., 1992
	Interleukin (-6, –2 and -15)	Imunogenicity	Gonzalez-Garcia et al., 1996

Contd.

Table 1.2 Experimental PEG-protein conjugates (Contd.)

Protein classification	Protein	Experimental model	Reference
Other	Avidin	Structure activity relationship study	Caliceti et al., 2002
	Biphalin	Animal studies; analgesia	Huber et al., 2003
	Desmopressin	Animal studies, efficacy	Veronese, 2004
	FAB	Half-life and retention of activity	Chapman et al., 1999
	Haemoglobin	Effect of PEG size on properties	Manjula et al., 2003
	Ovalbumin	Melanoma	Jackson et al., 1987

†TNF stands for tumour necrosis factor

toxicity. By triggered degradation of the bound polymer, it was hoped to slowly regenerate protein activity, and / or localise it to a particular target site.

This introduction reviews the challenges of protein delivery and in particular the development of the field of polymer-protein conjugation. The specific areas of biodegradable polymers, and bioresponsive or triggered degradation of polymer conjugates, are also discussed. To investigate this concept, the biodegradable polymers dextrin and hyaluronic acid (HA), the enzymes trypsin and ribonuclease A (RNase A), and peptide melanocyte stimulating hormone (MSH) were chosen as the models. These polymers and proteins are described in more detail in subsequent sections (sections 1.7.1 and 1.7.2 respectively), explaining the rationale for their choice.

1.1 Therapeutic proteins in clinical use; their challenges and approaches to overcome them

Between 1996 and 2004 there were over 70 approvals of new indications for protein therapeutics by the FDA (FDA, 2004). They are used in a variety of clinical indications, but despite the increasing use of proteins as parenteral therapeutic agents, there remains a number of physico-chemical and biological challenges to their use (Table 1.3).

Firstly, proteins are renowned for their poor aqueous solubility (reviewed by Ishii et al., 1995 and Matsushima et al., 1996), which may cause them to precipitate and cause processing difficulties. The lack of protein stability further contributes to its vulnerability to chemical degradation and denaturation, when exposed to conditions, such as excessive pH (Glazer et al., 1963; Orlando, 1962) and temperature (Arakawa et al., 1993), that can limit the possible shelf-life of the protein.

Secondly, following the systemic administration of a protein therapeutic, a number of biological issues are encountered. Reticulo-endothelial system (RES) clearance, rapid renal filtration of small proteins and rapid metabolism (reviewed by Roberts et al., 2002) can all cause rapid decreases in blood level leading to poor pharmacokinetic profiles (Inada et al., 1990; Lee et al., 2004). Proteins (particularly humanised proteins) can activate the immune system. They are detected by their antigenic epitopes, leading to the generation of anti-protein antibodies and can also cause complement-activation (Gonzalez-Garcia et al., 1996; Malik et al., 1992). Immune-complex formation can cause rapid clearance of a protein from the systemic

Table 1.3 Challenges for the delivery of therapeutic proteins

(adapted from Pasut et al., 2004)

Type of challenge	Issue
Physicochemical	Poor solubility
	Susceptibility to pH
	Susceptibility to temperature
Biological	Rapid RES[†] clearance
	Rapid renal elimination
	Rapid metabolism
	Immunogenicity
	Sensitivity on repeated administration
	Proteolytic degradation

[†] RES; reticulo-endothelial system

circulation by either RES uptake, or inactivation (reviewed by Roberts et al., 2002). Repeated exposure to foreign proteins may further result in anaphylaxis (reviewed by Nucci et al., 1991).

Thirdly, the inherent susceptibility of proteins to degradation by host proteolytic enzymes further contributes to their short circulating half-life (Chapman et al., 1999; Matsuo et al., 1997). Finally, non-specific accumulation of proteins in organs and tissues, other than the target, can reduce target cell concentration (reviewed by Torchilin and Lukyanov, 2003).

Polymer-protein conjugation is just one of a number of approaches that have been applied to overcome the aforementioned issues surrounding protein delivery. It was chosen for this study because of the substantial background of work previously conducted on PEG-protein conjugation (section 1.1).

1.2 Polymer-protein conjugates

Polymer-protein conjugates are one class of an ever-growing family of water-soluble delivery systems that have been termed 'polymer therapeutics'. This umbrella term also encompasses polymeric micelles, polymer-drug conjugates and polymeric drugs to which the drug is covalently bound, and polyplexes (polymer DNA complexes) (Figure 1.2). The common feature of these systems is that they are nano-sized polymer delivery systems, featuring water-soluble polymers. The nature of covalent components classes them as new chemical entities rather then drug delivery systems (reviewed by Duncan, 2003).

Polymer-protein conjugates represent a tripartite structure composed of a water-soluble polymer (bearing a functional group), a covalent linker and a protein. Conjugation is either at specific site(s) on the protein or it can be random. The polymer used can either contain inherent functionality, or it must first be chemically activated in order to incorporate a suitable functional group for protein conjugation. Methods of polymer activation and linker design are further discussed in section 1.3.

Conjugation of a therapeutic protein to a carrier polymer has many advantages. Polymer-protein conjugates can improve protein chemical stability (reviewed by Pasut et al., 2004), increase resistance to proteolytic degradation (Cunningham-Rundles et al., 1992; Lee et al., 2004; Malik et al., 2000), decreased immunogenicity and

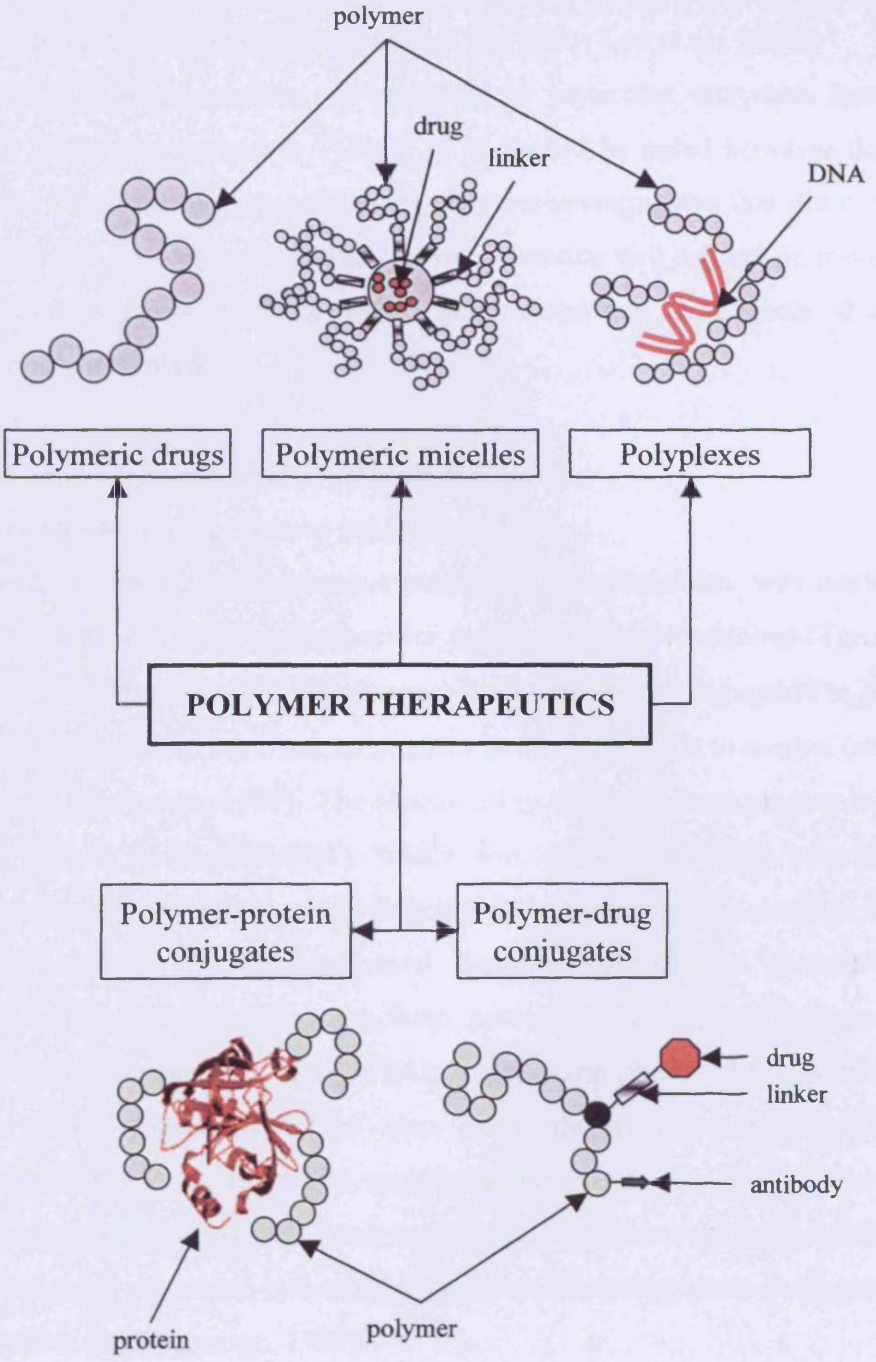

Figure 1.2 Categories of polymer therapeutics including; polymeric drugs, polymeric micelles, polyplexes, polymer-drug conjugates and polymer-protein conjugates (adapted from Duncan, 2003).

displayed recognition by pre-existing antibodies (Gonzalez-Garcia et al., 1996; Savoca et al., 1979). These effects result in longer circulation times, and dramatically altered pharmacokinetic profile of the protein (Harris et al., 2001; Lee et al., 2004).

Since 1982, large numbers of proteins, in particular enzymes, have been conjugated to PEG (summarised in Table 1.2). It should be noted however that there have also been a number of successful polymer-protein conjugates that did not utilise PEG as the polymer for conjugation. The following section will discuss, in more detail, both PEGylated proteins and the other polymer-protein conjugates that have successfully made it to market.

Polymer-protein conjugates currently used as therapeutics

1.2.1 Conjugates that use polymers other than PEG

In 1982, the dextran-streptokinase conjugate 'Streptodekase' was marketed in the USSR for the treatment of cardiovascular and ophthalmic conditions (Torchilin et al., 1982. *Russ.*). Dextrans (α,1-6 polyglucose) have since been conjugated to plasmin, haemoglobin and aprotinin, but these conjugates have not made it to market (reviewed in Veronese and Morpurgo, 1999). The unsuitability of dextran-conjugates is mainly attributed to reports of hepatotoxicity which was detected in trials of a dextran-doxorubicin conjugate, where the poorly degradable conjugate accumulated in the liver (Danauser-Reidl et al., 1993). Decreased degradability of the dextran carrier (compared to unmodified dextran) has been associated with modifications of the polymer backbone (Vercauteren et al., 1990; Vercauteren et al., 1992). Both dextran and dextran-protein conjugates have also been shown to induce anti-dextran antibodies, of which greater than 90 % were IgM (Seppala et al., 1985). Dextran is in addition also a less popular choice of polymeric backbone, since the poly-functionality of the polysaccharide can cause both cross-linking and heterogeneous conjugates to be formed (Veronese and Morpurgo, 1999).

An alternative approach was used when the anti-tumour protein neocarzinostatin was conjugated to the hydrophobic polymer, styrene maleic anhydride (SMA) to form the conjugate SMANCS. The polymer SMA was chosen to ensure that SMANCS would remain solubilised in the contrast agent Lipoidol (poppy seed oil), so that it could be administered locally, by cannula, to patients with liver cancer. SMANCS came to market in 1990 and has only ever been licensed in Japan, for the treatment of hepatocellular carcinoma. Conjugation in this instance not only reduced

the immunogenicity of the neocarzinostatin, and its susceptibility to protease degradation, but also increased the half-life of the protein (Maeda et al., 1985; reviewed by Maeda and Konno, 1997).

Although there have been two successful non-PEGylated polymer-protein conjugates to market, all of the most successful polymer-protein conjugates have used PEG (section 1.2.2).

1.2.2 PEGylated proteins in the market

PEG is currently the polymer most widely used for conjugation to proteins. This is mainly because it is inert, non-toxic and water-soluble. The properties of PEG, and reasons why it is so favoured are detailed in section 1.3. PEG has had great success, dominating nearly all of the marketed conjugates, and all of the polymer-protein conjugates, currently in clinical trials (Table 1.1). In 1990, PEG-adenosine deaminase (Adagen™) was the first FDA approved product being licensed for the treatment of severe combined immunodeficiency disease (SCID). The conjugate replenishes levels of adenosine deaminase associated with this "missing-enzyme" syndrome. Adagen™ has proved more efficacious, and safer (less immunogenic), than previous therapies involving blood transfusion or injection of the missing enzyme (Hershfield et al., 1987; Chaffee et al., 1992). Gene therapy has been used to replace adenosine deaminase in SCID children (reviewed by Aiuti et al., 2003; NIH, 1990), but the side effect (later appearance of vector-related leukaemia) has been well publicised (Kohn et al., 2003).

The second FDA approved conjugate, PEG-L-asparaginase (Oncaspar®), came to market in 1994. It was approved for the treatment of acute lymphoblastic leukaemia (ALL). Asparaginase acts by hydrolysing asparagine present in the blood, inhibiting its availability to leukaemic cells which are unable to synthesise their own asparagine (Boos, 2004). L-asparaginase is derived from *E-coli*, and is known to cause hypersensitivity reactions when administered. On conjugation to PEG, the incidence of hypersensitivity reactions was reduced to less than 8 % and the circulating half-life of the protein was increased. This has allowed the frequency of administration to be reduced from daily doses to a regime of once every 2 weeks (Park et al., 1981; reviewed by Thanou and Duncan, 2003).

PEGylated Interferon-α has been marketed as both PEG-Intron® and Pegasys® in 2000 and 2002 respectively. These two formulations are used to treat hepatitis C.

They differ in both the molecular weight of PEG and type of Interferon-α. PEG-Intron® uses a linear mPEG (12,000 g/mol) conjugated to Interferon α-2b (reviewed by Wang et al., 2002), whereas Pegasys® uses a branched PEG (40,000 g/mol) conjugated to Interferon α-2a (Reddy et al., 2001; reviewed by Reddy et al., 2002). Both preparations impart substantially longer half-lives compared to the free protein, enabling once weekly administration instead of daily (Glue et al., 2000; Zeuzem et al., 2000). A comparison of these two conjugates showed that the higher molecular weight, branched PEG used in Pegasys® demonstrated better pharmacokinetics of the protein (reviewed by Reddy et al., 2002).

All of these conjugates are examples of the benefits of PEG conjugation, which include: improved efficacy and safety (decreased immunogenicity and hypersensitivity), and improved dosing regime. Furthermore, it was shown that a high molecular weight branched PEG was most effective (reviewed by Reddy et al., 2002). PEG conjugates on the market displaying similar benefits and containing other proteins include granulocyte colony stimulating factor (GCSF; Neulasta®) (Johnston et al., 2000; reviewed by Kinstler et al., 2002) and human growth hormone (HGH; pegvisomant) (Thorner, 1999; reviewed by Parkinson et al., 2003).

Over the last two decades, the growing number of PEG conjugates in research and undergoing clinical trials has fuelled the continuous development of PEGylation chemistry. There has been an improvement in the control of conjugation reactions as the field of PEGylation evolved. Specifically, the limitations and development of PEG chemistries are discussed in detail in section 1.3.

1.3 PEG and the evolution of PEGylation chemistry

PEG is an inert, non-toxic polymer composed of repeat units of ethylene oxide forming either linear, or branched chains of varying molecular weight (Harris, 1992). PEG is extremely popular as a polymer for protein conjugation. It is also soluble in water, biocompatible and can be synthesised to have a narrow polydispersity (1.01 to 1.1 for PEGs < 5,000 and > 50,000 g/mol respectively). Due to its high level of hydration (2 - 3 water molecules per monomer) PEG also shows an extended flexible structure when in aqueous solutions, increasing the apparent molecular weight by 5 to 10 times its actual size (Harris, 1992; reviewed by Harris and Chess, 2003).

PEG of a molecular weight < 40,000 g/mol is excreted from the body via the kidney, and PEG > 20,000 g/mol is additionally eliminated in the faeces, but over a

longer period of time (Yamaoka et al., 1994). The non-toxic nature of PEG greater than 1,000 g/mol enabled it to be FDA approved as a polymeric excipient for internal use (Harris, 1992; Kibbe, 2000). Molecular weights less than 400 g/mol have however been found to be degraded to toxic metabolites by alcohol dehydrogenase (Harris, 1992).

PEG chains can be prepared to have only one terminal functional group. This made the polymer a favourite for protein conjugation. Early PEGylation chemistry used linear monomethoxy PEG (mPEG) chains with molecular weights of less than 12,000 g/mol (reviewed by Harris and Chess, 2003), but most commonly molecular weights of 5,000 g/mol were used (Levy et al., 1988; Savoca et al., 1979). Before PEG can be covalently attached to a protein, the terminal hydroxyl group must be activated. The method chosen for activation is important as it determines the type of covalent bond that is formed between the polymer and protein, and has subsequent effects on the properties of the conjugate. There are a number of different amino-acid residues to which PEG may be conjugated. These include: arginine (ARG), aspartic acid (ASP), cysteine (CYS), glutamic acid (GLU), histidine (HIS), lysine (LYS), serine (SER), threonine (THR), and tyrosine (TYR), as well as both the N and C-terminal groups (Roberts et al., 2002). The early PEG conjugation chemistry usually used the amino groups of the proteins as conjugation sites (reviewed by Roberts et al., 2002).

The evolution of PEGylation chemistry is discussed in the following sections to illustrate some of the challenges and limitations of polymer-protein conjugation.

1.3.1 Conjugation of PEG to amines

Typically, PEG was first conjugated to the α- or ε-amino group of lysines or to the N-terminal amino acid (Harris, 1992). Depending on the nature of the reactive PEG terminal group, the conjugation method led to the formation of different linkages:

- Amide — PEG-tresylate (Francis et al., 1998)
  PEG–dichlorotriazine (Zalipsky and Lee, 1992)
- Carbamate — PEG-succinimidyl carbonate (Zalipsky and Lee, 1992)
  PEG-benzotriazole carbonate (Zalipsky and Lee, 1992)
  PEG-p-nitrophenyl carbonate (Zalipsky and Lee, 1992)
  PEG-trichlorophenyl carbonate (Zalipsky and Lee, 1992)
  PEG-carbonylimidazole (Zalipsky and Lee, 1992)
- Ester — PEG-succinimidyl succinate (Carter and Meyerhoff, 1985)

Despite the intention of the aforementioned PEG derivatives to be conjugated to amines such as lysine, some of the derivatives (PEG-tresylate, -dichlorotriazine, -succinimidyl carbonate, and –benzotriazole carbonate) preferentially react not only with lysine, but with the hydroxyl groups of serine and tyrosine, and the imidazole side chain of histidine residues, to form sulfamate and imidazolecarbamate linkages respectively (reviewed by Roberts et al., 2002).

Each of these early methods had a number of disadvantages, presenting themselves as challenges for future development of PEGylation chemistry.

1.3.2 Problems of early PEGylation chemistry

The first generation of PEGylated proteins highlighted a number of key issues (Table 1.4); including

- Heterogeneity
- Diol-contamination
- Unstable linkages
- Low molecular weight (LMW) conjugates
- Reductions in protein activity

The non-specific conjugation of PEG to the ε-amino group of lysine on a protein can lead to the formation of heterogeneous conjugates, i.e. a greater polydispersity (reviewed by Zaplinsky, 1995). PEG-diol contamination of mPEG, up to 15 % w/w, can also lead to increased heterogeneity of the product due to protein cross-linking and can result in protein-inactivation (Dust et al., 1990).

Poor selectivity of the first generation of PEG derivatives, in particular PEG-succinimidyl carbonate, -benzotriazole carbonate, -tresylate, and –dichlorotriazine, enabled side-reactions with serine, tyrosine and histidine residues to occur. This created a heterogeneous mixture of conjugates with either the desired linker (amide or carbamate), or an unstable linker (sulfamate or imidazolecarbamate) prone to degradation (reviewed by Roberts et al., 2002).

Random conjugation, such as in the case of first generation PEGylation chemistry, could potentially occur at or near the active site of the protein. This would result in either direct blocking of the active site or steric hindrance. Protein activity was hence typically reduced from the native protein following PEG conjugation.

Table 1.4 Problems associated with first generation PEGylation chemistry

(reviewed by Veronese and Pasut, 2005; Roberts et al., 2002 and Zalipsky and Lee, 1992)

PEG derivative	Bond formed	Associated problems
PEG-tresylate	Amide	Non-specific conjugation can result in a degradable sulfamate linkage
PEG-dichlorotriazine	Amide	Cross linking due to remaining chloride Toxicity
PEG-succinimidyl carbonate PEG-benzotriazole carbonate	Carbamate	Non-specific conjugation to HIS or TYR rather then LYS, produces a hydrolytically unstable imidazolecarbamate linkage Poor reactivity
PEG-carbonylimidazole	Carbamate	Poor reactivity
PEG-p-nitrophenyl carbonate PEG-trichlorophenyl carbonate	Carbamate	Toxic by-products of 4-nitrophenol or 2,4,5-trichlorophenol respectively
PEG-succinimidyl succinate	Ester	Susceptible to hydrolysis Succinate tag left attached to the protein following degradation

For example, random PEGylation of recombinant human Interleukin-1 receptor antagonist reduced the activity to 9.8 % of control (Yu et al., 2007).

The five key issues, described above, were soon overcome through rapid advancements in PEGylation chemistry (section 1.3.3).

1.3.3 Solutions and further optimisation of PEGylation chemistry

The next generation (termed second generation PEGylation chemistry) provided several key solutions to the problems encountered during early development. These included:

- Site-specific conjugation
- Removal of PEG-diol contamination
- Improved linkage and stability
- Use of high molecular weight (HMW) and branched PEGs

The improvements noted above, and discussed in this section, have led to an increase in the number of PEG-protein conjugates currently undergoing clinical trials.

1.3.3.1 Site-specific conjugation

Site-specific conjugation has been utilised to (i) prevent conjugation of the polymer chains to the active-site of the protein, thus limiting the reduction in protein activity noted with the first generation PEG chemistries, and (ii) improve the homogeneity of the resulting PEGylated protein conjugate (Tsutsumi et al., 2000). Site-specific conjugation has been achieved using three main techniques:

- Thiol-reactive PEGs
- Insertion of cysteines into the protein sequence
- Enzymatic conjugation to the N-terminus of the protein

Thiol-reactive PEGs (PEG-maleimide, PEG-vinyl sulfone, PEG-iodoacetamide and PEG-orthopyridyl disulfide) can selectively conjugate cysteine-thiols present in proteins (Chapman et al., 1999). To further increase the control over the location of the conjugation site, cysteine residues have been selectively inserted into a protein sequence using genetic engineering and mutagenesis (Hershfield et al., 1991; Tsutsumi et al., 2000). A disadvantage of using thiol-reactive PEGs however, is that conjugation

may be reversed in the presence of thiol-reducing agents (reviewed by Pasut et al., 2004).

Another approach has been the use of enzymes, such as transglutaminase (reviewed by Sato, 2002; Sato et al., 2000) and subtiligase (Chang et al., 1994), to control the conjugation of PEG to a small peptidic substrate which has been inserted at the N-terminus of the protein.

1.3.3.2 Reduction of PEG-diol contamination

The problem of PEG-diol contamination was overcome by using the PEG derivative PEG-propionaldehyde, which allows aldol-condensation to occur and prevents the formation of PEG diol. Alternatively, ion-exchange chromatography of PEG-COOH has been successfully applied, removing up to 97 % of the diol impurities (reviewed by Pasut et al., 2004).

1.3.3.3 Improved PEG-protein linkage

Some methods of PEG activation applied in the second generation chemistries revolve around the use of mPEG-propionaldehyde, PEG-carboxylic acids and PEG-NHS esters (e.g. PEG succinimidyl ester) to enable thiol-ether linkage to cysteine residues to occur. Branched, and linear, PEG esters of propionic and butanoic acid have also been used to conjugate to histidine residues present on the protein and form stable amide linkages when reacted under physiological conditions (reviewed by Roberts et al., 2002).

1.3.3.4 Larger molecular weight and branched PEGs

Branched PEGs of higher molecular weights (up to 60,000 g/mol) were used to enable targeting by the enhanced permeability and retention (EPR) effect enhancing pharmacokinetic and pharmacodynamic properties. Heterobifunctional PEGs (branched) have also been used to provide multiple conjugation sites on the polymers and to enable targeting of the conjugate to specific sites through the attachment of antibodies, or peptides, as targeting ligands (reviewed by Pasut et al., 2004).

Despite the progress made in the later PEGylation chemistry, resulting in a number of conjugates which are now marketed and undergoing clinical trials (Table 1.1), there still remain two key limitations affecting the use of PEG as the polymer delivery vehicle.

1.3.4 Limitations of PEG-protein conjugation

PEGylation chemistry continues to evolve as PEG remains very popular and has proven clinical use (section 1.3). No matter how far the chemistry advances however, it will not be possible to overcome the most significant limitation of PEG, its lack of biodegradability. As a result, the molecular weight of PEG must be below 40,000 g/mol in order to ensure renal clearance. This limitation can be partly overcome by the use of branched PEGs (described above), but chronic administration of PEG may still lead to problems of accumulation in the body, particularly in the liver (reviewed by Veronese and Pasut, 2005).

A further limitation of PEG is that on conjugation it can irreversibly decrease protein activity. This has been shown for random first generation PEGylation chemistry (Pegasys® only retains 7 % of Interferon-α activity; reviewed by Veronese and Pasut, 2005), site-specific conjugation using thiol reactive PEGs (40 % Interleukin-1 activity retained; Yu et al., 2007) and conjugation to branched PEGs (~20,000 g/mol; 14 - 16 % recombinant human Interleukin 11 activity retained; Takagi et al., 2007). Despite these examples of reduced protein activity, in some cases there has been only a negligible decrease in activity. Particular examples include PEG conjugation to avidin (Caliceti and Veronese, 2003), insulin (Hinds and Wan Kim, 2002) and adenosine phosphorylase (Brewerton et al., 2003). Here, activity following conjugation of the protein was 93.5 – 99 %, 85 - 112 % and 90 % respectively. Balan et al., (2007) have also developed a protocol for the site-specific conjugation of PEG to protein disulfide bonds through a three carbon bridge. They demonstrated a retained L-asparaginase activity following conjugation of four PEG polymers, but also showed significant reductions in activity of Interferon-α2b when the same technique was applied. Furthermore, PEG-protein conjugates express protein activity continuously and thus are neither selective nor site-specific therapeutics. This imparts a greater potential for them to cause side effects. Only by using biodegradable polymers for conjugation, or biodegradable PEG-protein linkers, is it possible to overcome these limitations.

1.4 Biodegradable polymeric backbones

Biodegradable polymers may be divided into two classes: (i) naturally occurring polymers, such as polysaccharides of mammalian, plant or bacterial origin,

and (ii) semi-synthetic polymers made from natural metabolites (reviewed by Brocchini and Duncan, 1999).

Several studies have been carried out involving the chemical modification of a polysaccharide and subsequent analysis of its degradation. Most definitively, and most relevant to this work, is the degradability of dextrin modified by succinoylation. This was investigated by Hreczuk-Hirst et al., (2001a), when dextrin (molecular weight = ~15,500 and 51,000 g/mol) was modified up to 34 mol %, and its degradation by α-amylase measured over time. The degradation of succinoylated dextrin was well characterised and showed that at 34 mol % succinoylation there was little dextrin degradation over 180 min measured by gel permeation chromatography (GPC). At lower degrees of succinoylation, however, the polymer was readily degraded (Hreczuk-Hirst et al., 2001a). Bruneel and Schacht, (1995) modified pullulan by 2-hydroxypropylamine, succinoylation and partial periodate oxidation. They found that the modified pullulan was degraded by the enzymes α- and β-amylase, but that it was not degraded by lysosomal enzymes. When dextran, a structurally similar linear polysaccharide, was modified by reduction to a dialdehyde and also to a monosuccinate ester, however, it was successfully degraded by rat liver lysosomal enzymes (Vercauteren et al., 1992).

All three of these studies have concluded that the rate of degradation is controlled by the extent of modification of the polymer backbone, where greater modification significantly decreases the degradability. As such, this property presents itself as an opportunity to modulate the rate of degradation of the polymer backbone and imparts a controlled release (CR) effect.

It was previously noted (section 1.3.4) that the non-specific expression of PEG conjugated protein activity was a key limitation of PEGylation. Hence, in addition to utilising a biodegradable polymer in this work, a bioresponsive element used to trigger polymer degradation and expression of protein activity was to be incorporated. As such, advances in the current field of stimuli-responsive polymers will be overviewed in the following section.

1.5 Bioresponsive polymers for triggered release of protein payload

Although most polymer-protein conjugates have been prepared by PEGylation, recently a number of studies have examined stimuli-responsive polymer-protein conjugates. Stimuli responsive polymers undergo a large change in property due to a

small stimulus (chemical or physical) (reviewed by Hoffman and Stayton, 2004). Recent reviews of stimuli responsive polymers have identified many types of stimuli that have been utilised to activate or release the bound protein. These include: pH, temperature, radiation; infrared (IR) and ultraviolet (UV), ions (Ca^{2+} and Mg^{2+}), electrical potential and ultrasound, as well as biochemical stimulus using metabolites and enzymes (reviewed by Roy and Gupta, 2003 and Hoffman and Stayton, 2004).

Stimuli responsive polymer-protein conjugates have been synthesised both using random (Chen and Hoffman, 1993; Lackey et al., 1999) and site-specific conjugation (Ding et al., 1999; Shimoboji et al., 2001; Shimoboji et al., 2002; Shimoboji et al., 2003). Stimuli have been used to either induce a change in polymer conformation or to degrade the polymeric component or peptidyl linker in the delivery system. Physical stimuli, such as temperature (Shimoboji et al., 2001; Shimoboji et al., 2003), UV and visible (UV-vis) radiation (Shimoboji et al., 2002) have been used to control ligand protein receptor recognition. Stimuli responsive polymers have also been conjugated, site-specifically, next to the active site of the protein in order to cause steric hindrance (Shimoboji et al., 2001; Shimoboji et al., 2002). Application of physical stimuli were used to cause a change in polymer conformation, reversing the steric hindrance and revealing the active site (reviewed by Hoffman and Stayton, 2004). Similarly, the thermo-sensitive polymer PNIPAAm-E116C-streptavidin conjugate, synthesised by Ding et al., (1999), was used to release bound biotin by temperature cycling which induced a change in the conformation of the polymer.

Chemical methods of activation, such as pH and enzymatic degradation, have also been applied. Polymers (poly(methacrylate) and poly(butyl acrylate)) displaying glutathione- and pH-sensitive properties have been synthesised and conjugated to oligopeptides and oligonucleotides (Bulmus et al., 2003). Enzymatic degradation of the polymers in order to trigger the release of a drug or protein has however had limited application. One exception is in the mechanism of polymer enzyme liposome therapy (PELT), where polymer-enzyme conjugates are administered to trigger the degradation of previously administered liposomal delivery systems (Duncan et al., 2001). Similarly, enzymatic degradation, exploiting enhanced levels of secretory phospholipase A_2 in cancer tissue, has also been used to specifically trigger the degradation of liposomes loaded with the chemotherapeutic agent methotrexate in cancer tissue (Andresen et al., 2004).

Enzymes present in the lysosomal compartment have also been a target to both (i) cleave the linkers of polymer-drug conjugates, and (ii) degrade synthetic polymers used in polymer-drug conjugates (reviewed by Duncan, 2007; Haag and Kratz, 2006). One such example is the tetrapeptide linker glycine-phenylalanine-leucine-glycine (GLY-PHE-LEU-GLY), which is specifically cleaved in the lysosome by the enzyme cathepsin B (a thiol dependent lysosomal protease). The biodegradable linker 'GLY-PHE-LEU-GLY' was utilised in the polymer-anticancer drug conjugate N-'(2-hydroxypropyl)methacrylamide (HPMA) copolymer-doxorubicin (PK1) (reviewed by Duncan, 2003).

To date there are no examples of stimuli responsive biodegradable polymer-protein conjugates, where enzymatic degradation of the polymer is triggered by a biological target, as such, it was considered interesting to work in this area.

1.6 Novel concept of masked activity and triggered degradation

The aim of this study was to develop a new approach for polymer-protein conjugation, that would allow reversible inactivation of a protein by conjugation to a biodegradable polymer (Figure 1.3). Subsequently, using enzyme-triggered degradation of the polymer, it was hoped to re-express protein activity. Ideally the unmasking of activity would occur at particular disease sites. In theory this would allow site-specific activation.

The use of a degradable polymer for protein conjugation would in addition bring a potential advantage over PEG by achieving eventual complete polymer elimination. This would also permit the use of higher molecular weight polymers to optimise the conjugate weight average molecular weight, and thus improve targeting of the conjugate through the EPR effect.

The model polymer-protein and polymer-peptide conjugates chosen to test this hypothesis are described in the following section.

1.7 Model polymer-protein conjugates chosen to test the hypothesis of this research

For the purpose of this research, two model polymers; dextrin and HA, have been chosen which meet the aforementioned requirement of biodegradability. Both are

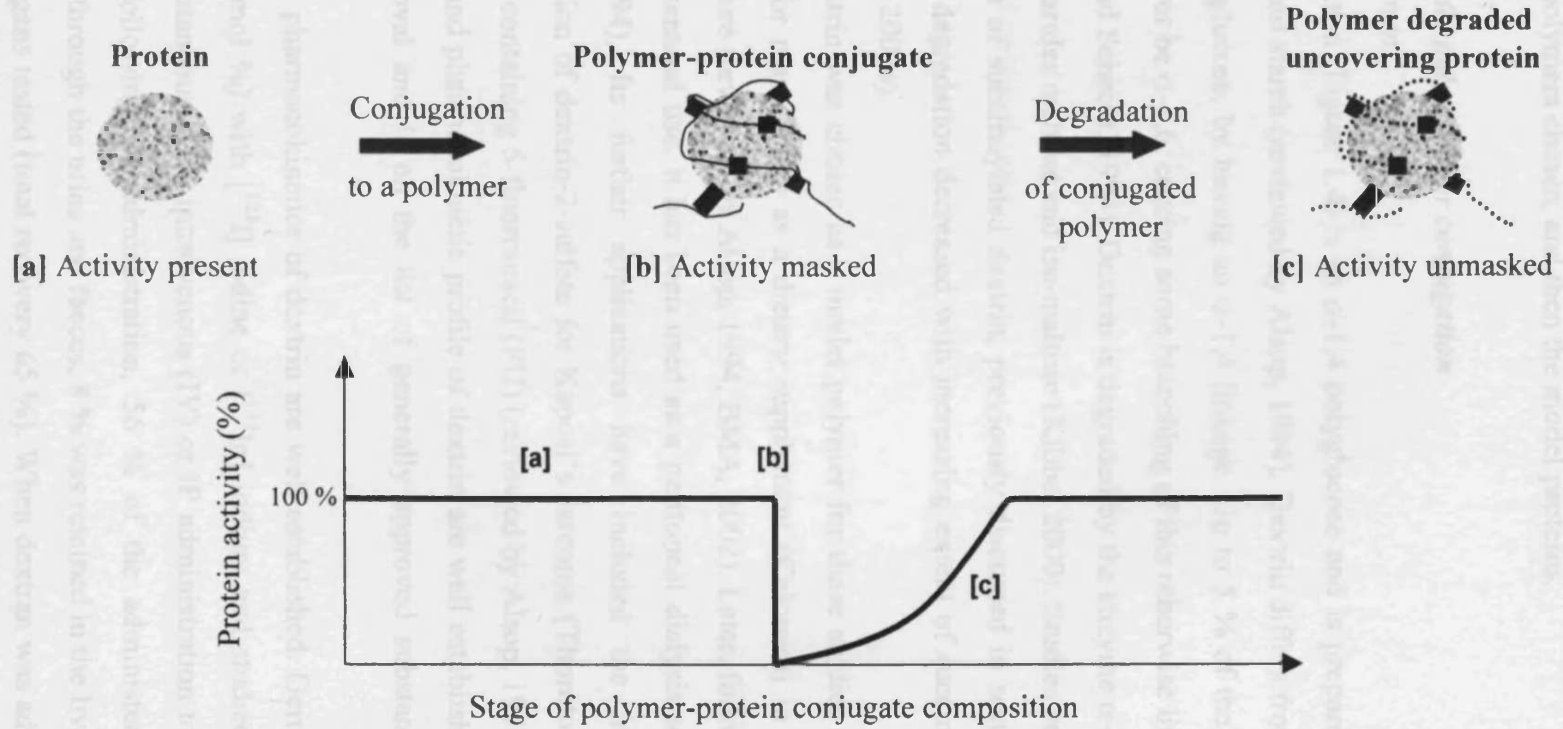

Figure 1.3 Proposed concept of masked and reinstated protein activity. Stage (a) protein retains full activity, (b) conjugation of the protein to a polymer would ideally mask all protein activity, until (c) the polymer is degraded, re-instating the protein activity back to 100 %.

FDA approved and have an established history of clinical use and known pharmacokinetic profiles. For characterisation of protein activity, the enzymes trypsin, RNase A and the peptide MSH were chosen. The following section will discuss firstly, the model polymers chosen, and then the model proteins.

1.7.1 Model polymers for conjugation

1.7.1.1 Dextrin

Dextrin (Figure 1.4) is an α-1,4 polyglucose and is prepared from hydrolysed corn or potato starch (reviewed by Alsop, 1994). Dextrin differs from dextran, which is also a polyglucose, by having an α-1,4 linkage. Up to 5 % of the linkages in dextrin may however be α-1,6, causing some branching of this otherwise linear polysaccharide (Bruneel and Schacht, 1994). Dextrin is degraded by the enzyme α-amylase to produce the disaccharides maltose and iso-maltose (Kibbe, 2000). Studies on amylase-mediated degradation of succinoylated dextrin, previously discussed in section 1.4, found that the rate of degradation decreased with increasing extent of succinoylation (Hreczuk-Hirst et al., 2001a).

Dextrin was chosen as a model polymer for these studies as it has been used clinically for many years as a dietary supplement (Caloreen) in cases of renal and hepatic failure (reviewed by Alsop, 1994; BMA, 2002). Later, following clinical safety data on parenteral use, it has been used as a peritoneal dialysis solution (Mistry and Gokal, 1994). Its further applications have included the inter-peritoneal (IP) administration of dextrin-2-sulfate for Kaposi's sarcoma (Thornton et al., 1999), and IP solution containing 5-fluorouracil (FU) (reviewed by Alsop, 1994) (Table 1.5). Both the safety and pharmacokinetic profile of dextrin are well established and it possesses FDA approval and is on the list of generally approved substances (GRAS) (Day, 2003).

The pharmacokinetics of dextrin are well established. German (2001) labelled dextrin (1 mol %) with [^{125}I] iodine or [^{111}In] indium and studied its biodistribution after sub-cutaneous (SC), intra-venous (IV) or IP administration to rats. It was shown that 1 h following IV administration, 56 % of the administered dose had been eliminated through the urine and faeces, 8 % was retained in the liver and < 1 % was in all other organs tested (total recovery 65 %). When dextran was administered however (reviewed by German, 2001), only 28 % was eliminated, and 50, 13, 3 and 4 % was

(a) Dextrin

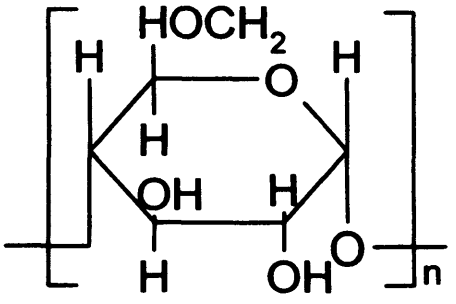

(b) Hyaluronic acid

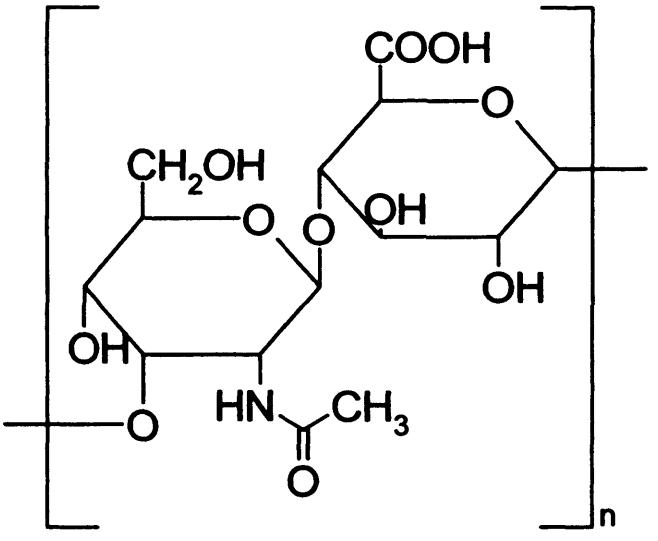

Figure 1.4 Chemical structure of (a) dextrin (α-1,4 polyglucose) and (b) hyaluronic acid (N-acetylglucosamine-1,4-glucuronic acid).

Table 1.5 Application of dextrin in pharmaceutical formulations

Drug name	Formulation / carrier solution	Indication	Reference
Extraneal®	Icodextrin (7.5 % w/v) Peritoneal dialysis solution	Chronic renal failure	Baxter, 2007
Dexemel®	Icodextrin (4 % w/v) Peritoneal dialysis solution	Delivery of cancer chemotherapy	Hosie et al., 2001
Caloreen®	Maltodextrin (source: corn starch)	Malnutrition and malabsorption states	Reviewed by Alsop, 1994 BMA, 2002
Dextrin-2-sulphate (CT phase 1)[†]	Icodextrin (7.5 % w/v) Peritoneal dialysis solution	Antiretroviral for Kaposi's sarcoma	Shaunak et al., 1998 Thornton et al., 1999 NIH, 2005c
5-FU[‡] (CT[†])	Icodextrin (7.5 % w/v)	Abdominal malignancies	Kerr et al., 1996

[†]CT is an abbreviation for clinical trials

[‡]FU stands for fluorouracil

retained in the blood, liver, gastro-intestinal tract and carcass respectively. All other organs tested retained ≤ 1 % of the administered dose. The pharmacokinetics of a dextrin derivative, Icodextrin, used in a peritoneal dialysis solution, has also been studied. Icodextrin absorbed into the systemic circulation and lymphatic system (~20 %) was also shown to produce consistently raised plasma levels of both Icodextrin and its degradation product maltose (Davies, 1994). The raised plasma levels of Icodextrin were found to be stable over the treatment period tested (two years), with no adverse effects detected. Particular concerns had been of changes in subject's osmolality and sodium levels, neither of which occurred (Gokal et al., 1994). Additionally it was found that on the cessation of dialysis, plasma levels of icodextrin and maltose returned to pre-treatment levels within two weeks. Icodextrin metabolites of maltose, maltotriose and maltotetrose were believed to be formed by tissue and plasma α-amylase hydrolysis of the parent dextrin (Davies, 1994). Despite the good profile on both the safety and pharmacokinetics data, there have been isolated case reports of allergic reaction, expressed as exfoliative dermatitis (Fletcher et al., 1998; Goldsmith et al., 2000).

The advantages, and previous use of dextrin, support its suitability as a model polymer in this preliminary system. Dextrin, as well as being biodegradable, is also polyfunctional. Although polyfunctionality was highlighted earlier as a potential disadvantage, causing heterogeneity, this may be used to enable it to surround the protein, and potentially completely mask the proteins activity (Figure 1.3). Cross linking and heterogeneity may however still be a problem. Dextrin was also a good candidate as a model polymer for the reasons later discussed in chapter 3 (section 3.1.4).

1.7.1.2 Hyaluronic acid (HA)

The linear polysaccharide HA (Figure 1.4), composed of N-acetylglucosamine and glucuronic acid units with α-1,4 glycosidic linkage, varies in molecular weight between 2 x 10^6– 10 x 10^6 g/mol, and has an approximate length of 3 - 30 μm. It is a glycosaminoglycan and is found throughout the body, predominantly in connective tissue, cartilage, vitreous humor and synovial fluid (0.5 - 4 mg/mL), where it is essential for normal joint function (Collins, 1987; Ghosh and Guidolin, 2002).

HA was chosen for these studies because it is also a biodegradable linear polysaccharide degraded by the lysosomal enzyme hyaluronidase (HAase). HA acts as one of the key components of the extracellular matrix (ECM) of the joint cavity and is endocytosed *via* the CD44 receptor, and transported to the lysosome (Aguiar et al., 1999) where HAase hydrolyses the 1 - 4 linkage between N-acetyl-beta-D-glucosamine and D-glucuronate (ExPASy, 2004). The CD44 receptor has no hyaluronidase activity itself and there are no enzymes capable of degrading HA outside of the cell (Aguiar et al., 1999). Furthermore, HA is degraded and removed from the body very rapidly. In an arthritic state, such as the arthritic sheep model, the half-life of HA was shown to be even shorter, decreasing from 21 to 11.5 h after induction of arthritis (Ghosh and Guidolin, 2002). Because HA has such a short circulating half-life, it was considered important to modify the degradability of HA to increase its potential circulation time in the body.

HA, used commercially, is either extracted from mammalian sources such as Rooster comb (Rc), bovine vitreous humor, and human umbilical cord, or it is derived by bacterial fermentation. The source of HA affects the salt form, purity and solubility of the polymer. It is FDA approved in several preparations for intra-articular (IA) injection into the osteoarthritic joint (Table 1.6). These formulations are sodium salts of HA derived from bacterial and animal sources, in the molecular weight range of HA found in synovial fluid (4×10^6 - 6×10^6 g/mol). The pharmaceutical application of HA delivery systems and their chemistry of conjugation has been described later in Chapter 5.

1.7.2 Model proteins and peptides for conjugation

Two proteins (trypsin and RNase A) and a peptide (α-MSH) were chosen for conjugation to mimic targeting of the:-

(i) Systemic circulation (trypsin)

(ii) Extracellular receptor binding (MSH)

(iii) Intracellular targeting (RNase A)

The rationale for the choice of proteins is outlined in the following sections.

Table 1.6 Natural synovial hyaluronic acid and preparations of hyaluronic acid used commercially

Hyaluronic acid name	Manufacturer	components	Molecular weight (g/mol)	Source	Reference
Synovial fluid hyaluronate	NA[†]	Glucuronic acid, N-acetylglucosamine	4×10^6 - 6×10^6	Human	Bobic, 2005
Synvisc®	Biomatrix	Hylan G-F 20 (hyaluronan)	$6 \times 10^6 - 23 \times 10^6$	Chicken combs	Ghosh and Guidolin, 2002 Goorman et al., 2000 Clarke et al., 2005
Hyalgan®	Shire	Sodium hyaluronate	$5 \times 10^5 - 7 \times 10^5$	Chicken combs	Kolarz et al., 2003
Fermathron®	Biomet Merck	Sodium hyaluronate	1×10^6	Bacterial fermentation by *Streptococcus equi*	BMA, 2001a
Orthovisc®	Zimmer	Sodium hyaluronate	1×10^6 - 3×10^6	Rooster combs	BMA, 2001a Anika, 2004
Arthrease®	DePuy	Sodium hyaluronate	4×10^6 - 6×10^6	Biosynthetic	Bobic, 2005

[†]NA; not applicable

1.7.2.1 Trypsin; model enzyme for dextrin and HA conjugation

Trypsin (Figure 1.5) is a pancreatic protease (23,400 g/mol) belonging to the subclass of serine proteases (PFAM, 2004). It is expressed in the pancreas and present in the body as an inactive zymogen, particularly located in endothelial and epithelial cells (Hooper, 2002; Mathews and van Holde, 1990). There are three commonly occurring forms of trypsin; α, β and ε-trypsin. Indicating that trypsin purchased commercially and used experimentally may be a combination of active α or β-trypsin and inactive ε-trypsin (ExPASy, 2004).

Trypsin (porcine) is made up of 231 amino acids, ten of which are lysines (Swiss-Prot/TrEMBL, 2003). As previously mentioned (section 1.3), the lysines present in proteins are often used for conjugation to carboxyl functional groups on a polymer. The number of lysines may therefore be viewed as an indicator of the number of potential binding sites. Extensive characterisation information, as well as defined crystal structure and active site information, is available for trypsin. Refinement of the crystal structure of native porcine β-trypsin between 1.5 - 1.8 Å (Huang et al., 1994; Johnson et al., 1999) has revealed a catalytic triad (HIS-57, SER-195 and ASP-102) typical of serine proteases, which also incorporate GLY-93 and SER-219 at the active site (Johnson et al., 1999). Lysines do not make up the composition of the catalytic triad. This reduces the likelihood of direct conjugation to the active site and irreversible reduction in trypsin activity.

The accessibility of lysines present in bovine trypsin was evaluated by Zhang et al., (2001). They studied the conjugation of mPEG (350 g/mol) to bovine trypsin and utilising a 2,4,6-trinitrobenzenesulfonate (TNBS) assay, found that 11 of the 14 lysines available were conjugated to mPEG, (activated by p-nitrophenyl chloroformate). When mPEG was derivatised by acetic acid N-hydroxy-succinimide ester, however, only 8 of the 14 lysines were modified (Murphy and Fagain, 1996). This indicates that not all of the lysines present are necessarily accessible for conjugation, and additionally that different reaction conditions may result in preferential conjugation to particular lysines.

Trypsin catalyses the hydrolysis of peptide bonds, cleaving the carboxyl side of lysine and arginine amino acid residues present in substrates such as $_{N}$-Benzoyl-$_{L}$-arginine-$_{p}$-Nitroanilide (BAPNA) or Na-benzoyl-arginine-ethyl-ester (BAEE) (Hooper, 2002; SIGMA, 1995). The optimum activity of trypsin is between pH 7 - 9 (Hooper, 2002). This pH optimum influenced both the choice of substrate and experimental

(a) Trypsin

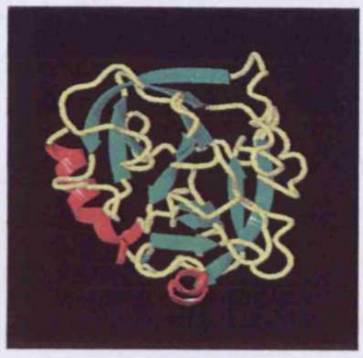

(Expasy, 2004)

(b) α-MSH

N-Acetyl-Ser-Tyr-Ser-Met-Glu-His
NH_2-Val-Pro-Lys-Gly-Trp-Arg-Phe

(Sigma product information, 2005)

(c) RNase A

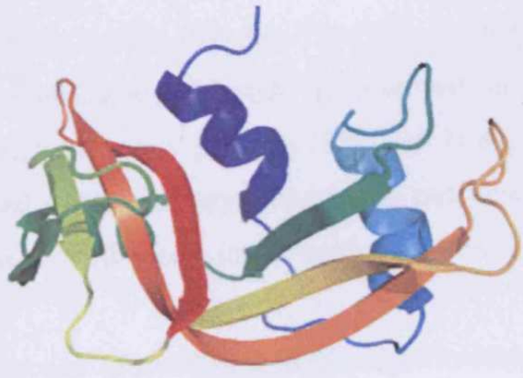

(PDB, 2007)

Figure 1.5 Structure or sequence of the proteins and peptide; (a) trypsin, (b) melanocyte stimulating hormone (MSH) and (c) ribonuclease A (RNase A).

conditions (Fernandez et al., 2003; Johnson et al., 2002) used in enzyme kinetic studies. The catalytic nature of trypsin enables it to increase the rate of hydrolysis without undergoing any change itself (Mathews and van Holde, 1990), thus making it a suitable choice for establishing zero-order kinetics (Cornish-Bowden, 2004). The specifics of trypsin assay conditions will be discussed later in Chapter 3.

Trypsin was chosen as a model protein in the present study as it has been previously conjugated to several polymers (Abuchowski and Davis, 1979; Ding et al., 1998; Murphy and Fagain, 1996; Schering et al., 2004; Zhang et al., 2001) including the biodegradable polymers carboxymethylcellulose (Villalonga et al., 2000) and cyclodextrin (Fernandez et al., 2003). Several preliminary studies in this laboratory have also shown that it is possible to prepare dextrin-trypsin conjugates (Lewis, 2003; Meier, 2002; White, 2002), making it an ideal choice for proof of principle studies for the concept of masked and reinstated protein activity.

1.7.2.2 MSH; model peptide hormone for dextrin conjugation

To further test the hypothesis of this research, at a different level of targeting, the peptide MSH was chosen, for its ability to stimulate a membrane bound receptor in a B16F10 murine melanoma cell line. Mammalian MSH (Figure 1.5) is a tridecapeptide with an amidated serine at its C-terminus. The core sequence of mammalian α-MSH 'Met-Glu-His-Phe-Arg-Trp-Gly' is located at residues 4 to 10 (Eberle, 1988). This melanocortin peptide is involved in the regulation of skin pigmentation *via* the melanogenesis pathway (Tsatmali et al., 2002) (Figure 1.6). It is predominantly produced in the pituitary gland in the pars intermedia, although it may also be found in the skin, particularly in the epidermal keratinocytes and melanocytes (Tsatmali et al., 2002).

The primary function of α-MSH is to stimulate melanin production through the melanogenesis pathway. α-MSH stimulation of the melanocortin receptors (MC-Rs) (7 transmembrane G-protein coupled receptors) initiates conversion of the substrate L-tyrosine to the precursor dopaquinone by the enzyme tyrosinase (Tsatmali et al., 2002), in a concentration-dependent manner (Eberle, 1988). The precursor dopaquinone is subsequently converted in the endoplasmic reticulum (ER) into either eumelanin or phaeomelanin (the two types of melanin), and is released in melanosomes (Tsatmali et al., 2002).

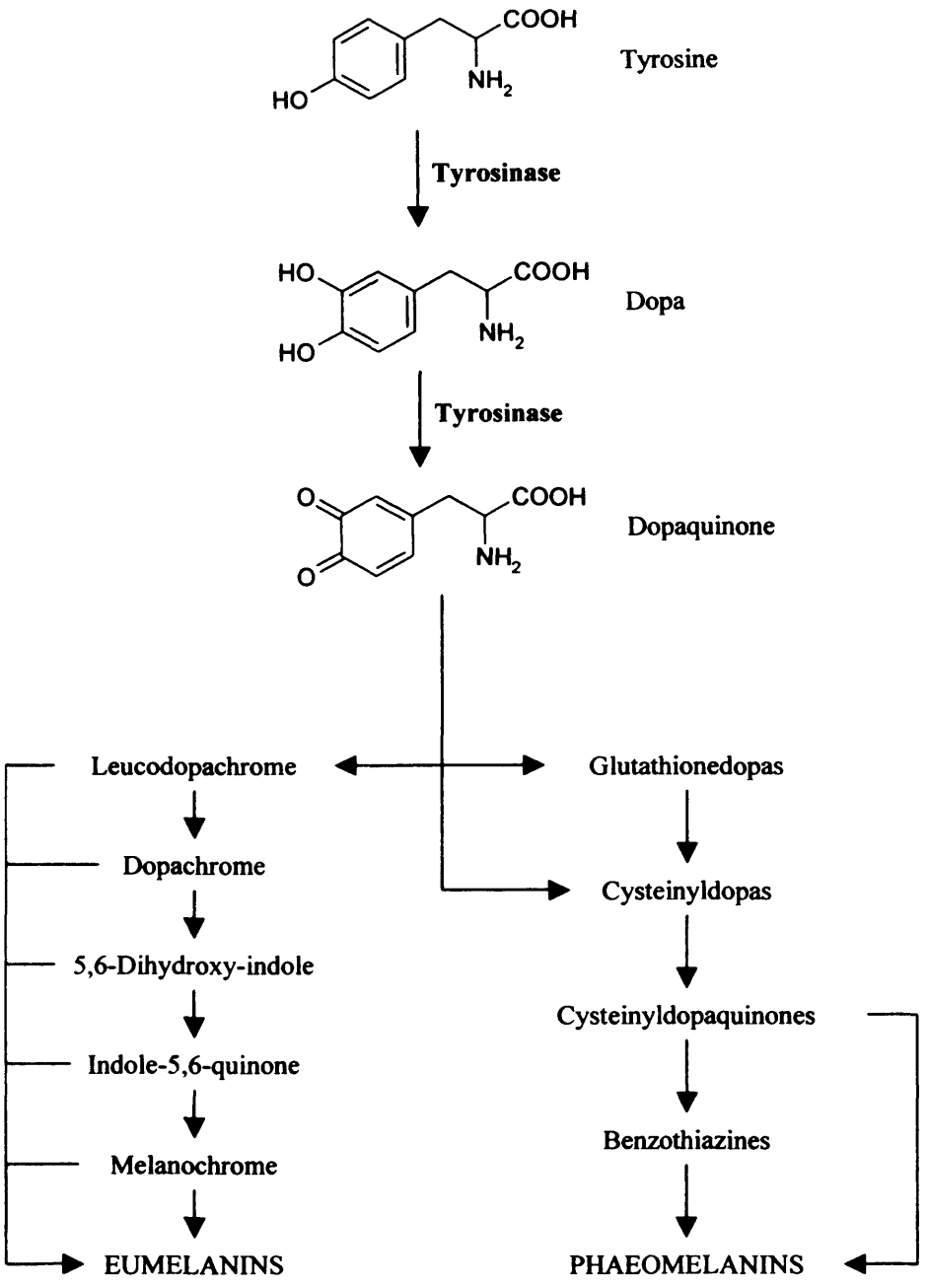

Figure 1.6 Melanogenesis pathway; conversion of tyrosine into eumelanins and phaeomelanins (adapted from Eberle, 1988).

MSH was chosen to establish proof of concept of a peptide / receptor model in B16F10 cells. As MSH (1,640 g/mol) is much smaller than trypsin (23,400 g/mol), the effect of protein molecular weight on the ability to mask protein activity can also be examined. Melanin and tyrosinase assays in B16F10 murine melanoma cells are well established (Eberle, 1988) and have previously been applied to determine the activity of HPMA copolymer conjugated MSH (O'Hare et al., 1993). There are several well established *in vitro* assays (Eberle, 1988; O'Hare et al., 1993) that have been used to quantify MSH activity, either by determining melanin production or tyrosinase activity (Figure 1.7). Within the subgroup of melanoma cell assays, there are two main cell types used; B16F10 and Cloudman S91 cells. B16F10 murine melanoma cells were the cell line of choice by O'Hare et al., (1993), to standardise the melanin assay to enable HPMA copolymer-MSH conjugate activity to be measured. The choice of cell type and melanin assay is discussed in detail in Chapter 4.

Since the 1980's MSH and its synthetic analogues Melanotan I and II have been studied as chemopreventative agents (Bhardwaj and Blanchard, 1998), ligands for melanoma-specific targeting (Ghanem et al., 1991; Rosenkranz et al., 2003), and as potent anti-inflammatory agents (Zhong and Bellamkonda, 2005; Tsatmali et al., 2002). It has also been utilised as a protein in a CR gel formulation of poloxamer 407 (Bhardwaj and Blanchard, 1996). Further details of the delivery systems involving MSH are also discussed in Chapter 4.

1.7.2.3 Ribonuclease A as a potential therapeutic protein

Three commonly used sources of ribonuclease have been used in experimental studies; bovine pancreatic (RNase A), bovine seminal (BS-RNase) and northern leopard frog (Onconase). Human ribonucleases are often found in the extracellular fluid (Erickson et al., 2006), but they can act in the cytosol to degrade transfer ribonucleic acid (tRNA), inhibiting protein synthesis and inducing apoptosis (Ardelt et al., 2003). The mechanism of cellular uptake and intracellular trafficking of ribonuclease is not well known, but it has been suggested that RNase A is internalised using a pathway other than the clathrin- or dynamin-mediated endocytosis (Haigis and Raines, 2002). Although the specific mechanism of action of cytotoxicity of ribonuclease is uncertain, it is thought to be linked to the ability of the ribonuclease to evade ribonuclease inhibitors (RIs) located in the cytosol (0.01 – 0.1 % of the cellular

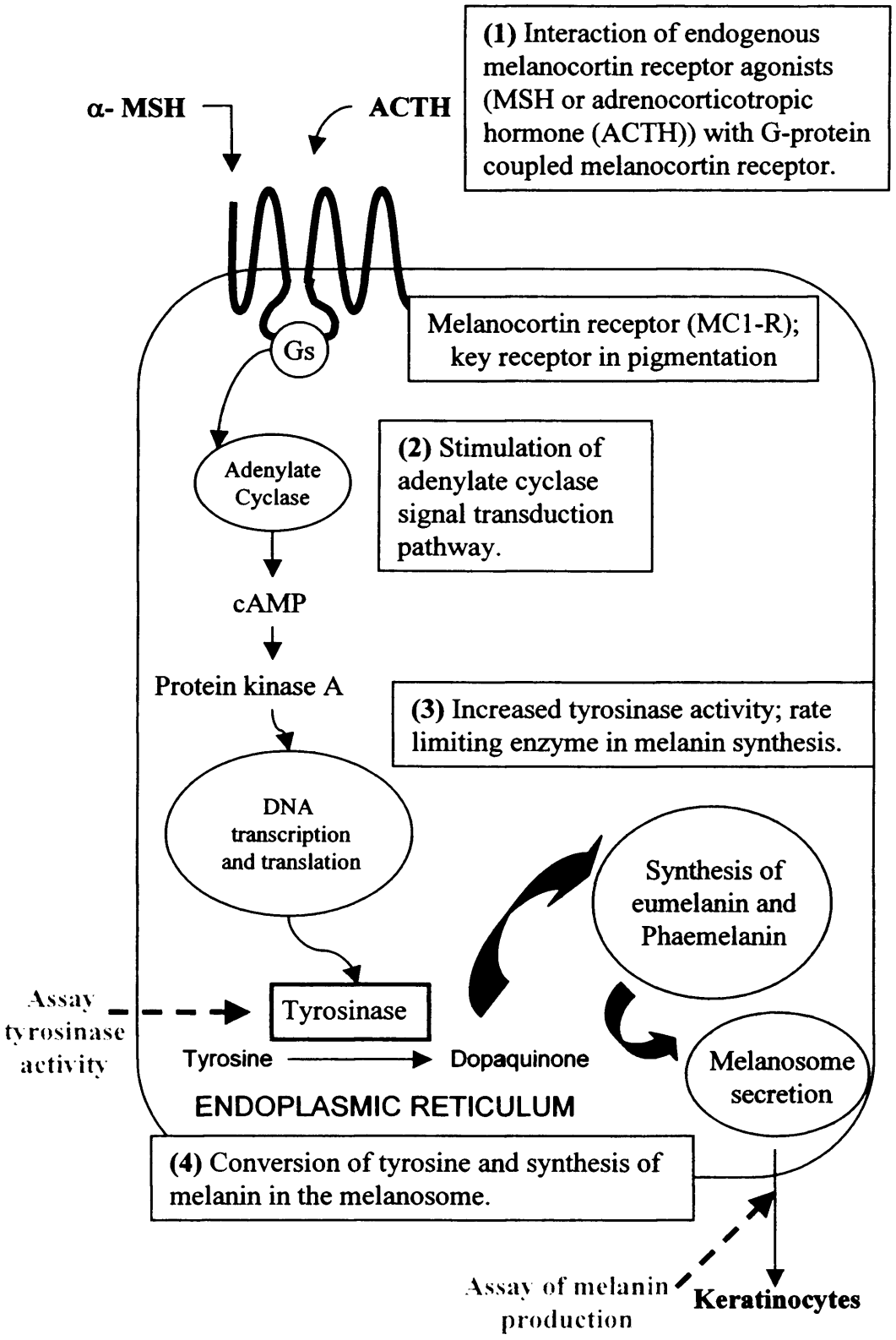

Figure 1.7 Melanocortin receptor activation and subsequent melanogenesis pathway (adapted from Todorovic et al., 2005). The points at which MSH activity may be measured using tyrosinase activity and melanin production assays, are also indicated above.

protein). The normal function of ribonuclease inhibitors is to regulate ribonuclease activity (reviewed in Erickson et al., 2006).

The RNase A family (Figure 1.5) are typically ~ 13,000 g/mol and are used for digestion, angiogensis and host defense (reviewed in Erickson et al., 2006). BS-RNase is a homodimer with two subunits of 124 residues, much larger than Onconase, which is only 104 residues in total. It has been suggested that the greater size of BS-RNase may affect its ability to cross the lipid bilayer and reach the RNA (Matousek et al., 2003).

The activity of ribonucleases as cytotoxic agents is affected by several factors:

- Affinity for the RIs
- Extent of cellular uptake
- Form; unimer, dimer or tetramer
- Route of administration

The affinity of a ribonuclease for the RIs has already been discussed above. Another factor affecting cytotoxicity is the level of cationisation, which can affect the cellular uptake of a ribonuclease. It has been shown that increasing the degree of cationisation increases internalisation *via* binding to glycolipids and glycoproteins on the plasma membrane. This increases the uptake of the ribonuclease and thus increases cytotoxicity (reviewed in Ilinskaya et al., 2004; Eugene Lee et al., 2005).

The affinity of the ribonuclease for the RIs is also affected by the form in which it is present. For example, BS-RNase (dimer) is unstable in mammalian cytosol, reducing the two disulfide bonds to create monomeric subunits. The monomeric subunits are then strongly bound by RIs, blocking ribonuclease activity. Binding to ribonuclease inhibitors has been overcome by conjugation of monomeric subunits to a polymer. Polymer conjugation prevents binding of the monomeric subunit with RIs, yet still enables the subunit to display cytotoxic activity (reviewed in Matousek et al., 2003). Variants of the monomeric BS-RNase have however been created, and are able to evade the RIs and possess greater cytotoxicity than the wild type BS-RNase dimer (Eugene Lee and Raines, 2005).

The mode of administration of the ribonuclease has also been demonstrated to affect cytotoxicity. Studies have shown that free BS-RNase administered by IV, has very poor activity compared to intra-tumoral (IT) administration. When BS-RNase was conjugated to poly(HPMA) however, it was possible to maintain significant

cytotoxicity with IV administration (Ulbrich et al., 2000). This would be expected, as the ribonuclease alone would be susceptible to premature clearance and degradation, negatively affecting its pharmacokinetic profile (discussed in section 1.1). Similarly, RNase A displayed a poor *in vivo* activity profile when administered IV. Cytotoxicity was however found when administered IT (reviewed in Daly et al., 2005). Nonetheless, the typical problems associated with protein delivery highlighted above, make ribonuclease a good candidate for polymer conjugation.

Unfortunately, the choice of model (cell line or animal) to measure ribonuclease induced cytotoxicity is further complicated when the protein is conjugated to a polymer. Michaelis et al., (2002) found that an 3-(4,5-dimethylthiazol-2-yl)-2,5-diphenyl-2H-terazoliumbromide (MTT) assay of BS-RNase-PEG displayed no cytotoxicity in a UKF-NB-3 cell line (evans stage 4 NB) up to a concentration of 100 μg/mL of BS-RNase, whereas unconjugated BS-RNase was cytotoxic in a UKF-NB-3 cell line and had an IC_{50} of 2.18 ± 0.18 μg/mL. Similarly, a poly(HPMA) conjugate of BS-RNase had poor activity when incubated with a human myeloid leukaemia cell line (ML-2) and with stimulated human lymphocytes. This was attributed in part to the huge size of the overall conjugate, which may have prevented penetration into the cell (Ulbrich et al., 2000).

Despite the poor activity of the polymer-ribonuclease conjugates when tested in a cell line, there have been several conjugates which have demonstrated enhanced cytotoxicity when administered into an animal model. Two such examples include BS-RNase-PEG (Michaelis et al., 2002) and poly(HPMA) and PEG (5,000 or 22,000 g/mol) conjugates of RNase A (Pouckova et al., 2004; Soucek et al., 2002; Ulbrich et al., 2000). These polymer-ribonuclease conjugates are discussed further in Chapter 6.

1.8 Aims of this thesis

Feasibility studies for the concept of polymer-protein "activity-masking" and "unmasking" were to be conducted. The enzymes trypsin and RNase A and the receptor-binding ligand MSH were chosen as model proteins. Two polymers were chosen. Dextrin, which can be degraded by amylase, and HA, which is degraded by HAase.

The primary objectives were to optimise the synthesis of dextrin-trypsin conjugates (Chapter 3) in order to define the best molecular weight dextrin (7,700 and

47,200 g/mol) and degree of dextrin succinoylation, for effective masking and reinstatement of trypsin activity. A library of dextrin-trypsin conjugates was to be prepared and the trypsin activity of the conjugates in the presence and absence of amylase determined.

Given success in these primary studies, it was intended to extend this concept to a receptor ligand model. Dextrin-MSH conjugate was considered to be an appropriate choice (Chapter 4). The synthetic, purification and characterisation methods were to be tailored to take account of the smaller size of the peptide MSH than trypsin. Furthermore, MSH activity (free and in conjugate form) was to be tested using methods established to measure melanin release on incubation with MSH, using B16F10 cells.

Having established whether dextrin may mask enzyme and / or peptide activity in a way that allowed triggered activation by amylase, it was considered important to explore the applicability of this concept to other polymers. The second objective of these studies was therefore to explore HA as the masking vehicle. HA, derived from rooster comb, was chosen for these studies. Commercially HA is supplied with a molecular weight of ~900,000 g/mol, so it is first necessary to degrade it to give a lower molecular weight fraction (~100,000 g/mol). The synthesis, purification and characterisation of HA-trypsin conjugates was to be optimised. The activity of the HA-trypsin, in the presence and absence of the polymer degrading enzyme HAase, would then be determined using the method established for dextrin-trypsin conjugates.

The overall objectives of the study were to determine whether this new concept of polymer conjugation could be applied to the development of a potentially therapeutic conjugate, in this instance an anti-cancer conjugate using the enzyme RNase A. An HA-RNase A conjugate was chosen and following synthesis, experiments were to be conducted to test its cytotoxicity in B16F10 and CV-1 cells (high and low CD44 expressing cell lines respectively). In addition, preliminary studies were also to be conducted using HA-oregon green (OG) to follow the cellular uptake of the polymer.

Chapter 2

Materials and General Methods

2.1 Materials

A detailed list of the equipment, compounds, general reagents and their suppliers, for the work described in this thesis is detailed in sections 2.1.1 and 2.1.2.

2.1.1 Equipment

2.1.1.1 Analytical

Size exclusion chromatography (SEC) was carried out using GPC and fast protein liquid chromatography (FPLC). GPC analysis was performed using a JASCO PU-980 high performance liquid chromatography pump (Jasco UK Ltd, UK), with two TSK-gel columns in series (G4000 PW_{XL} followed by G3000 PW_{XL}) and a guard column (Progel PW_{XL}). A Gilson 133 differential refractometer (Gilson Inc, USA) and programmable UV absorbance detector (Severn Analytical, UK) were used as dual channel detectors. PL Caliber Instrument software, version 7.0.4, from Polymer Laboratories (UK) was used for data analysis. FPLC was carried out using an AKTA FPLC system (Amersham Pharmacia Biotech, UK) with a Superdex HR 10/30 SEC column with a UPC-900 detector for UV absorbance (280 nm). Data analysis was conducted using Unicorn 3.20 software (Amersham Pharmacia Biotech, UK). Fourier transform infrared spectroscopy (FT-IR) analysis of the polymers was conducted using an AVATAR OMNI-sampler 360 FT-IR from Nicolet Instrument Corporation (USA) with EZ OMNIC E.S.P. 5.2 software for data analysis. UV-vis absorbance and enzyme activity was measured using a Cary 1G UV-Vis spectrophotometer (Varian, Australia) with Varian 1E software (Varian, Australia). A Sunrise UV-vis absorbance plate reader (Tecan, Austria) was used for analysis of samples in 96 well plates. The fluorescence of OG labelled polymers was read in black flat bottom 96 well plates (Corning Inc, USA), by a Fluorostar Optimar plate reader (BMG labtechnologies, Germany). pH was measured using either a Toledo 320 pH meter (Mettler Toledo, Switzerland) or Hydrion pH indicator paper (Sigma, UK). Thin layer chromatography (TLC) was carried out using TLC plates (0.2 mm, silica 60 with fluorescent indicator UV_{254}) purchased from Macherey-Nagel (Germany).

2.1.1.2 Purification and freeze drying

Purification of samples was carried out using either (i) Spectra/por 7-regenerated cellulose dialysis membrane (Molecular weight cut-off (MWCO) of 2,000, 10,000 or 50,000 g/mol) purchased from Spectrum Laboratories Inc (USA), (ii)

Vivaspin 6 centrifugal filters (Vivascience AG, Sartorius group, Germany) or (iii) prepacked sephadex G25 (PD10) columns (Amersham Biosciences, UK). Samples were freeze dried using a Flexi Dry FD-1.540 freeze dryer (FTS systems, USA) connected to a high vacuum pump (DD75 double stage) from Javac (Australia).

2.1.1.3 Sodium dodecyl sulphate polyacrylamide gel electrophoresis (SDS-PAGE)

SDS-PAGE was used to evaluate the purity of synthesised polymer-protein conjugates. All electrophoresis equipment, including a Power Pac 300 and GelAir Drying Frame were from Bio-Rad (UK). The densiometry of samples loaded on SDS-PAGE gels was measured using an Imaging Densiometer (GS-700, Bio-Rad, USA) with Molecular Analyst software, and subsequently analysed by 1D gel analysis using Image Quant TL v2003.02 software (Amersham Biosciences and Nonlinear Dynamics Ltd. UK).

2.1.1.4 Cell culture and cell assays

A Galaxy S incubator and a Procell incubator (Wolf Laboratories and Jencons-PLS, UK) with Bioair (Bioair, Italy) and Microflow (Servicecare, UK) class II laminar flow hoods were used for all tissue culture. A silver stained Neubauer haemocytometer (Marienfield, Germany) and a bright-field microscope (Inverted DM IL) from Leica (Germany) was used for cell counting. Cells were centrifuged using a Varifuge 3.0 RS, swing out rotor buckets (type 8080, rmax 21.1 cm) made by Heraeus Instruments (Germany). Cell culture consumables (Costar) were purchased from Corning Inc (USA) and pipettes, bijous and universal containers purchased from Elkay (Ireland).

An inverted Leica DM IRB microscope (Germany) with 12-bit cooled monochrome Retiga 1300 camera (Q imaging, Canada) was used to take bright-field images of B16F10 and CV-1 cells. The cell images were then manipulated using Openlab software v 3.0.9 (Improvision, UK). Uptake and binding studies of fluorescently labelled polymers were conducted using a FACS Calibur flow cytometer (Becton Dickinson, UK) with an argon laser (488 nm excitation wavelength) and Cell Quest software (v 3.3). FACS tubes were also purchased from Becton Dickenson (UK).

2.1.2 Compounds and reagents

2.1.2.1 Polymers

Dextrin (~47,200 g/mol) was from ML Laboratories (UK). Dextrin, type 1 from corn (~7,700 g/mol) and HA (~901,400 g/mol) were purchased from Sigma (UK). The characterisation of dextrin and HA, used for the synthesis of polymer-protein conjugates, is shown in Table 2.1. Polyethylenimine (PEI) 50 % w/v in H_2O (750,000 g/mol) and dextran (68,800 g/mol), used as positive and negative controls of cell cytotoxicity, were also purchased from Sigma (UK). Dextrin-OG and HPMA copolymer-OG conjugates used as controls for FACS binding and uptake studies, were donated by Dr. A. Paul and K. Wallom from the Centre for Polymer Therapeutics, Cardiff University.

2.1.2.2 Proteins

The enzymes; salivary α-amylase, porcine pancreatic trypsin (type 1X-S), bovine testes HAase and the peptides; BAPNA and MSH were purchased from Sigma (UK). RNase A was supplied by Applichem (Germany).

2.1.2.3 Molecular weight standards

Gel filtration chromatography molecular weight standards

Pullulan standards of the molecular weights: 5,800, 11,800, 22,800, 47,300, 109,000 and 112,000 g/mol were supplied by Polymer Laboratories Ltd (UK). Dextran blue (2,000,000 g/mol) and glucose (180 g/mol) were purchased from Sigma (UK).

Protein standards of bovine erythrocytes carbonic anhydrase (29,000 g/mol), bovine lung aprotinin (6,500 g/mol), bovine serum albumin (BSA) (66,000 g/mol), horse heart cytochrome c (12,400 g/mol) and alcohol dehydrogenase (150,000 g/mol) were also purchased from Sigma (UK).

SDS-PAGE molecular weight standards

Prestained SDS-PAGE standards; broad range (7,331 - 211,806 g/mol) were purchased from Bio-Rad (USA).

2.1.2.4 Reagents

Acrylamide / bis-acrylamide (40 % solution, mix ratio 37.5 : 1), 1-amino-2-propanol, ammonium persulfate (AP), bicinchoninic acid (BCA) solution, anhydrous

Table 2.1 Characteristics of the polymers used in the synthesis of the polymer-protein conjugates

Polymer	Supplier	Source	Mn[†] (g/mol)	Mw[††] (g/mol)	PDI[‡] (Mw/Mn)
Dextrin	SIGMA	Corn (Type I)	5,200	7,700	1.5
Dextrin	ML LABS	Potato	31,200	47,200	1.5
Rc HA[‡‡]	SIGMA	Rooster comb	774,200	901,400	1.2
HA[‡‡‡]	NA*	Rooster comb	99,600	128,900	1.3

[†] Mn; number average molecular weight

[††] Mw; weight average molecular weight

[‡] PDI indicates the polydispersity

[‡‡] HA; hyaluronic acid. Lower molecular weight fraction derived acid hydrolysis of the rooster comb HA (Rc HA)[‡‡] purchased from SIGMA

* NA; not applicable

calcium chloride, copper (II) sulfate (Cu^{2+}), 1-ethyl-3(3-dimethylaminopropyl)carbodiimide (EDC), hydrochloric acid (HCl), hydrindantin, lithium acetate, ninhydrin, sodium acetate and tris[hydroxymethyl]aminomethane hydrochloride (trizma HCl) were purchased from Sigma (UK).

Bromothymol blue, anhydrous N,N-dimethylformamide (DMF) and anhydrous succinic anhydride were supplied by Aldrich (UK). Bio-Rad (USA) supplied bromophenol blue, coomassie brilliant blue G-250 (CB), 2-mercaptoethanol, sodium dodecyl sulphate (SDS) and N,N,N,N'-tetra-methyl-ethylenediamine (TEMED). Acetic acid, diethyl ether, 4-dimethylaminopyridine (DMAP), paraffin oil, methanol and sodium hydroxide (NaOH) were from Fisher Scientific (UK). Glycine (Electrophoresis Grade) was purchased from ICN Biomedicals (USA) and N-hydroxysulfosuccinimide (Sulfo-NHS) was supplied by Pierce Chemical Company (USA). Oregon green cadaverine ($OG\text{-}_{CAD}$) was purchased from Molecular Probes™ (UK).

FACS Flow and FACS Clean and Rinse formulations were purchased from Becton Dickenson (UK).

2.1.2.5 Cell culture

The B16F10 murine melanoma cell line was purchased from the American type culture collection (ATCC) (USA) and the CV-1 african green monkey kidney fibroblasts were purchased from the European collection of cell cultures (ECACC) (UK). The cell culture media used to maintain these cell lines was Rose Park Memorial Institute (RPMI) 1640 with phenol red (PR) and Glutamax, and Dulbecco's minimal essential media (DMEM) with glucose respectively. In addition, foetal bovine serum (FBS) and trypsin-ethylenediaminetetraaceticacid (EDTA) (0.05 % w/w trypsin, 0.53 mM EDTA) were also purchased from Invitrogen Life Technologies (UK). CO_2 and N_2 (medical grade, 95 % v/v) and liquid N_2 were supplied by BOC (UK). Sigma-aldrich (UK) supplied trypan blue solution (0.4 % w/v), MTT and sterile dimethyl sulphoxide (DMSO).

2.2 Methods

The typical reactions for the synthesis of dextrin-trypsin (Chapter 3), dextrin-MSH (Chapter 4), HA-trypsin (Chapter 5) and HA-RNase A (Chapter 6) conjugates are dealt with in their respective experimental chapters. Both the analytical and

biochemical methods used to characterise these conjugates are however described here (section 2.2.2 and 2.2.3). The steps taken to tailor the characterisation techniques to the analysis of specific polymer-protein conjugates are detailed in the respective experimental chapters. Firstly, the purification techniques used to purify both the functionalised and degraded polymer or the polymer-protein conjugate are described in the following section.

2.2.1 Purification and freeze-drying of the modified polymer and the polymer-protein conjugates

Following the degradation or functionalisation of the parent polymer, or the synthesis of polymer-protein conjugates, the product was purified by one or more of the following methods:

- Dialysis (section 2.2.1.1)
- FPLC fractionation (section 2.2.1.2)
- PD10 desalting columns (section 2.2.1.3)
- Vivaspin 6 centrifugal filters (section 2.2.1.4).

The specific method used has been stated in the appropriate experimental chapter. Following purification, the product was freeze-dried as described in section 2.2.1.5.

2.2.1.1 Dialysis

Solubilised samples were purified by dialysis against double distilled water (ddH_2O) (6 x 5 L) over 48 h. Dialysis membranes (MWCO 2,000, 10,000 or 50,000 g/mol) were chosen according to the size of impurity to be removed.

2.2.1.2 FPLC fractionation

The conjugate reaction mixture (100 μL sample) was first analysed by FPLC (section 2.2.3.4) to identify both the retention time of the conjugate and the presence of impurities. The conjugate reaction mixture was then loaded onto the FPLC column (Superdex 10/30) in 2 mL sample sizes and eluted as described (section 2.2.3.4). The FPLC was however additionally programmed to fractionate the sample into 0.5 mL aliquots. The conjugate fractions were collected, isolating the conjugate fraction from any unconjugated protein and impurities, pooled and then purified using either dialysis

(section 2.2.1.1) or using a PD10 desalting column (section 2.2.1.3). The resulting product was then freeze dried (section 2.2.1.5).

2.2.1.3 Sephadex G25 PD10 desalting column

A prepacked PD10 column was drained and equilibrated with double distilled H_2O (25 mL). Samples (up to 1 mL) were pipetted onto the column and eluted using ddH_2O as a mobile phase. The first 5 mL eluted from the column, containing the conjugate, was collected and freeze dried (section 2.2.1.5). The column was then flushed with 25 mL ddH_2O and stored in ddH_2O.

2.2.1.4 Vivaspin 6 centrifugal filter

The solubilised sample was loaded (6 mL) in the top compartment of a vivaspin centrifugal filtration device and centrifuged at 2000 g for 10 min, causing it to be concentrated. The filtrate was discarded, the retentate topped up to 6 mL with ddH_2O, and the sample re-centrifuged. This was repeated a further two times to remove all phosphate buffered saline (PBS) salts from the dissolved sample. The retentate was then freeze dried (section 2.2.1.5).

2.2.1.5 Freeze drying

Solubilised samples (up to 20 mL) in a plastic tube (50 mL) covered with foil and pierced for ventilation, were snap frozen in liquid N_2 (5 min) and then lyophilised (48 h) to freeze dry the product.

2.2.2 Physicochemical characterisation of parent and functionalised polymers

2.2.2.1 Titration of carboxyl groups incorporated into dextrin by succinoylation

The number of carboxylic acid groups (expressed as mol %) incorporated when dextrin was reacted with succinic anhydride (Chapter 3 and 4) was quantified by titration (Hreczuk-Hirst et al., 2001b). Prior to titration, the pH meter was calibrated using standards of pH 4, 7 and 9.2. Succinoylated dextrin (3 mg) in ddH_2O (2 mL) was titrated against NaOH (5×10^{-4} M), with bromothymol blue indicator (1 % w/v in ethanol, pH range: 6 - 7.6). The end point of the titration was indicated by a change in the solution colour from yellow to blue and a pH of ~7.6. Each sample was titrated three times and the mol % modification, i.e. the number of carboxylic acid groups incorporated, was calculated as below:

Each monomer has one potential site for succinoylation. Therefore, complete succinoylation can be assumed as 100 % site conversion. In this study it was aimed to achieve a range of polymer succinoylation between 2 – 34 % of available sites, by varying the ratio of succinic anhydride and dextrin. If the polymer were to be composed of 100 monomers, and 30 % succinoylation was desired, then 70 % of the dextrin monomers will not be modified and 30 % of the monomers will be succinoylated, giving monomer molecular weights of 180 and 280 g/mol respectively.

Therefore, the theoretical average molecular weight of one monomer in a polymer chain composed of 100 monomers could be calculated using the following equation:

Theoretical monomer molecular weight = (70 % x 180) + (30 % x 280)

Theoretical monomer molecular weight = 210 g/mol

This was then used to calculate the theoretical number of moles COOH in a sample of succinoylated dextrin. The actual number of moles COOH in a sample of succinoylated dextrin was determined by titration, and then the % modification was calculated by the following equation:

% modification = (experimental (mol COOH) / theoretical (mol COOH)) x 100

2.2.2.2 Confirmation of the structure of the parent and modified polymer by FT-IR

Dextrin, succinoylated dextrin, Rc HA and HA fraction were analysed by FT-IR to confirm their structural composition. Samples were analysed, usually using 64 scans, over the mid-infrared (400 - 4000 cm^{-1}) and near-infrared (4000^{+} cm^{-1}) region and the background interference subtracted. Where spectra were not clear, the number of scans was increased from 64 to 300. This improved the signal to noise ratio resulting in a much clearer spectra. Qualitative analysis of FT-IR spectra (% transmittance vs wavenumbers (cm^{-1})) was conducted by interpretation of the peaks in the double-bond region; 2000 - 1500 cm^{-1} (Stuart, 2002).

2.2.2.3 Determination of polymer, protein and polymer-protein conjugate purity, molecular weight and polydispersity using GPC

GPC was used to analyse samples of polymer, modified polymer, protein and polymer-protein conjugate in order to determine their purity and to estimate their molecular weight. Before running the samples, the GPC columns were equilibrated (2 h) with the mobile phase PBS (0.1 M, pH 7.4, filtered (0.2 μm) and sonicated) at a

flow rate of 1 mL/min, and the baseline zeroed against the reference cell every 30 min. The refractive index (RI) detector was set at a sensitivity of 2 and the UV absorbance detector set to 280 nm. Samples (polymer, protein or polymer-protein conjugate) were prepared to a concentration of 3 mg/mL in PBS buffer (pH 7.4) and then filtered (0.2 μm pore size). 60 μL of the solubilised sample was injected onto a G4000PW_{XL} followed by G3000 PW_{XL} column in sequence and analysed over 25 min. Gel filtration standards (pullulan and protein) of known molecular weight and polydispersity were analysed on the columns and the retention times of the standards were used to plot a calibration curve of Log molecular weight against retention time (Figures 2.1 and 2.2). Both the pullulan and protein molecular weight standards used have already been listed in section 2.1.2.3. The retention time of dextran blue (2,000,000 g/mol) and glucose (180 g/mol) were also used to establish the void volume (Vo) and bed volume (Vb) of the column respectively (Meloan, 1999). The molecular weight; number average (Mn) and weight average (Mw), and the polydispersity (PDI) (Mw/Mn) of the analysed samples was then derived from the respective calibration curves using the PL calibre reanalysis software (Figures 2.1 and 2.2). Unless otherwise stated, where molecular weight is stated, this refers to the weight average molecular weight.

2.2.3 Biochemical and analytical characterisation of proteins and polymer-protein conjugates

A combination of methods were used to characterise the free and total protein content of the polymer-protein conjugates. The number of primary amines on trypsin and MSH for polymer conjugation were quantified using a ninhydrin assay (section 2.2.3.1). Whereas, the total protein content of the conjugates were measured using a BCA assay (section 2.2.3.2). In order to identify the presence of free protein in the conjugate, samples were analysed using SDS-PAGE (section 2.2.3.3). Analytical characterisation of the conjugates was carried out using both GPC and FPLC (section 2.2.3.4), to estimate their molecular weight and purity. The method for GPC has already been described in section 2.2.2.3.

2.2.3.1 Ninhydrin assay to quantify the number of primary amines

The number of primary amines of a protein available for polymer conjugation was determined using the ninhydrin assay (Figure 2.3a). Acetate buffer (4 mol/L) was prepared (82 g sodium acetate in 200 mL ddH_2O), adjusted to pH 5.5 and made up to

(a) Chromatogram of pullulan molecular weight standards

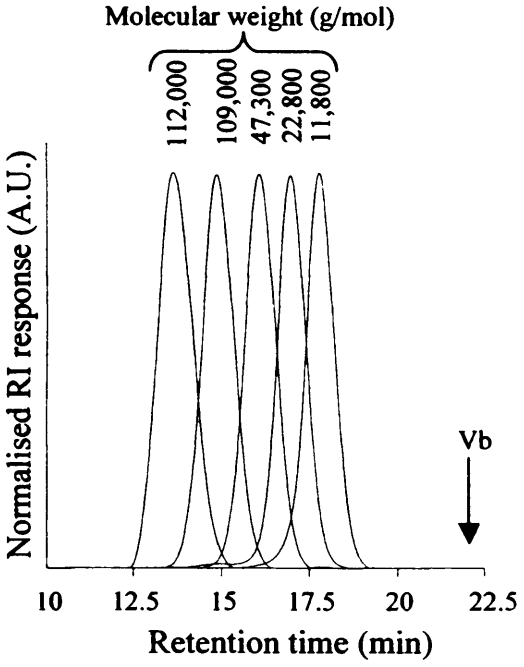

(b) Calibration curve of pullulan molecular weight standards

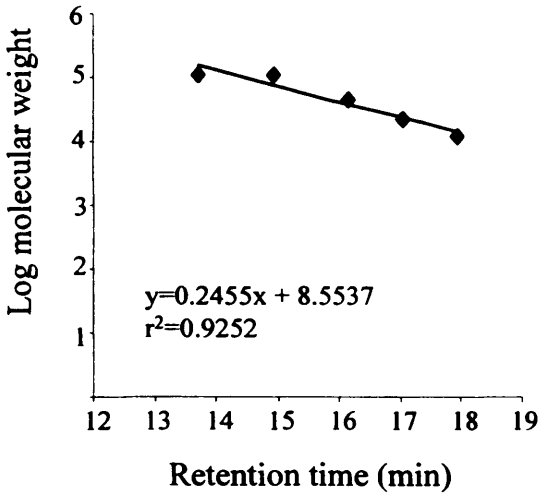

Figure 2.1 GPC analysis of pullulan molecular weight standards using TSK-gel columns G4000PWXL and G3000 PWXL in series. Panel (a) shows the chromatogram of the pullulan standards, where RI represents the refractive index and Vb indicates the bed volume. Panel (b) shows a reconstruction of the calibration curve plotted during GPC analysis using the Polymer Laboratories software, to provide an estimate of sample molecular weight and polydispersity.

(a) Chromatogram of protein molecular weight standards

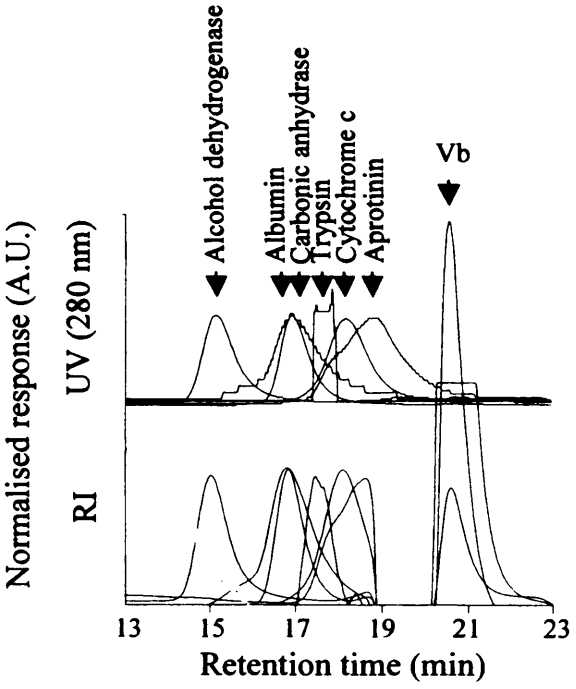

(b) Calibration curve of protein molecular weight standards

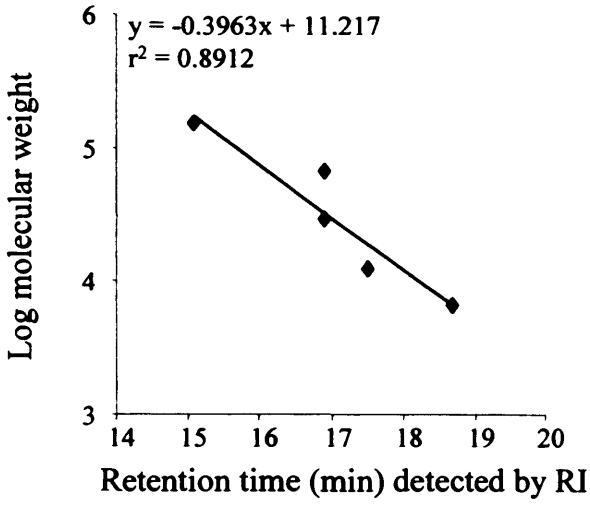

Figure 2.2 GPC analysis of protein molecular weight standards using TSK-gel columns G4000PWXL and G3000 PWXL in series. Panel (a) shows the chromatogram of the protein standards: aprotinin (6,500 g/mol), cytochrome c (12,400 g/mol), carbonic anhydrase (29,000 g/mol), bovine serum albumin (66,000 g/mol) and alcohol dehydrogenase (150,000 g/mol), where Vb represents the bed volume, RI is the refractive index and UV is the ultraviolet absorbance at 280 nm. Panel (b) shows a reconstruction of the calibration curve plotted during GPC analysis using the Polymer Laboratories software, to provide an estimate of sample molecular weight and polydispersity.

(a) Ninhydrin assay mechanism

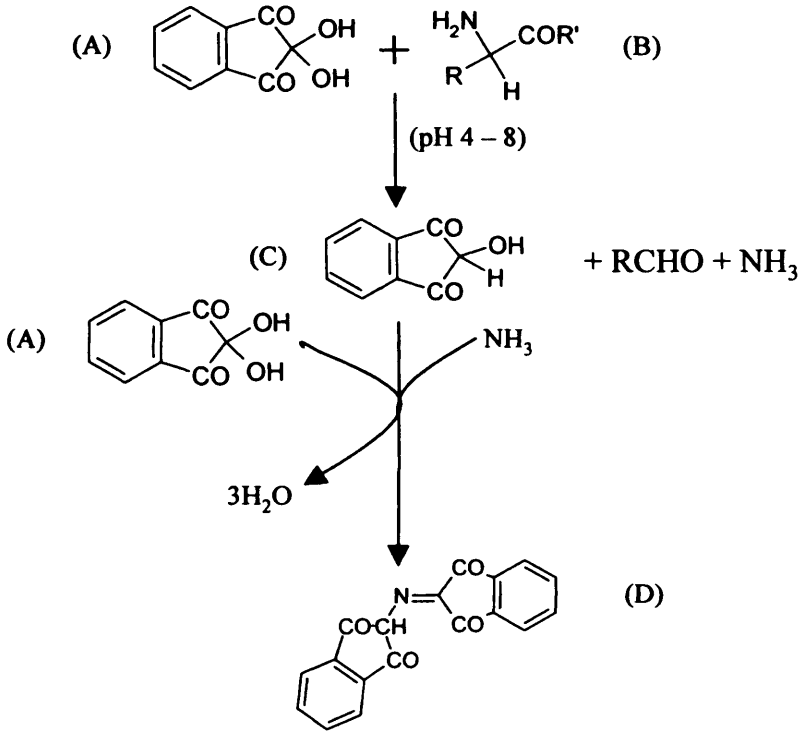

(b) 1-amino-2-propanol calibration curve

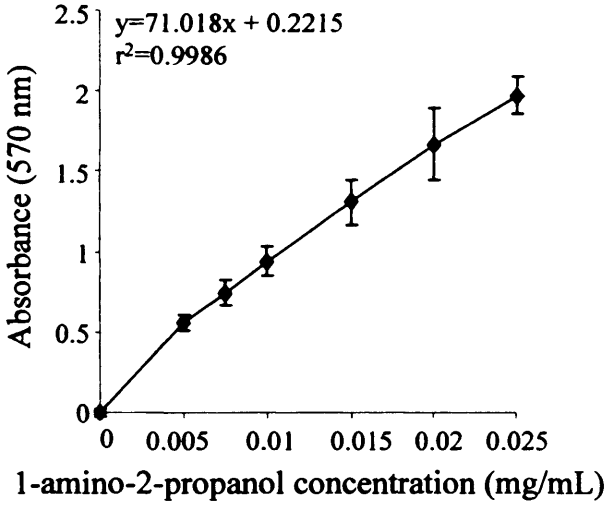

Figure 2.3 Ninhydrin assay to quantify the number of primary amines in a protein for conjugation. Panel (a) Mechanism of the assay; compounds as follows: (A) ninhydrin, (B) primary amine, (C) hydrindantin and (D) diketohydrindylidene-diketohydrindamine. Panel (b) illustrates a typical ninhydrin assay calibration curve using the primary amine standard 1-amino-2-propanol. Data shown represents the mean (n=3) ± SD.

250 mL with ddH_2O. Ninhydrin reagent (ninhydrin 0.8 g and hydrindantin 0.12 g, dissolved in 15 mL DMSO and 5 mL of 4 M lithium acetate) was diluted 1 : 1 (2 mL) with the sample (enzyme, conjugate or 1-amino-2-propanol standard), and transferred to a glass test tube and heated (75 °C for 15 min). The solution was cooled to room temperature (RT) and 3 mL of 50 % v/v ethanol added. 200 μL of sample was pipetted into each sample well in a 96 well plate and the UV-vis absorbance read at 570 nm using a Tecan plate reader. A standard curve was constructed using the reference standard 1-amino-2-propranol (Figure 2.3b).

2.2.3.2 Quantification of the total protein content of the polymer-protein conjugates using a BCA assay

Initially, the BCA assays were conducted using BSA as a protein standard. However, this standard was changed to trypsin, MSH or RNase A to allow direct comparison to the protein content of the corresponding polymer-protein conjugate. The BCA protein assay is based on a colour reaction arising from reduction of Cu^{2+} to Cu^{+} in alkali conditions, enabling complex formation (Stevens, 1998; Figure 2.4a). The purple colour formation increases in intensity with increasing concentration of peptide bonds and the amino acids: tryptophan, cysteine, cystine and tyrosine that are present (Pierce, 2004).

20 μL of sample; conjugate (1 mg/mL in ddH_2O) or protein standard (0.05 – 1 mg/mL in ddH_2O) and 200 μL of BCA reagent (1 mL BCA : 20 μL Cu^{2+}) were added to each sample well, in a 96 well plate, and incubated at 37 °C for 30 min. The UV-vis absorbance was then read at 550 nm, as the complex absorbs strongly at 562 nm (Pierce, 2004). A calibration curve of absorbance against concentration of protein standard was constructed and the absorbance of the conjugate samples related to protein content (Figure 2.4b). This was then expressed as weight percent of protein in the conjugates (% w/w).

2.2.3.3 Characterisation of the purity of the polymer-protein conjugates using SDS-PAGE

SDS-PAGE was used to assess the presence of free protein in the conjugates. The method used was adapted from Kaufman et al., (1995) and the composition of the solutions used appear in Table 2.2.

(a) Mechanism of BCA assay

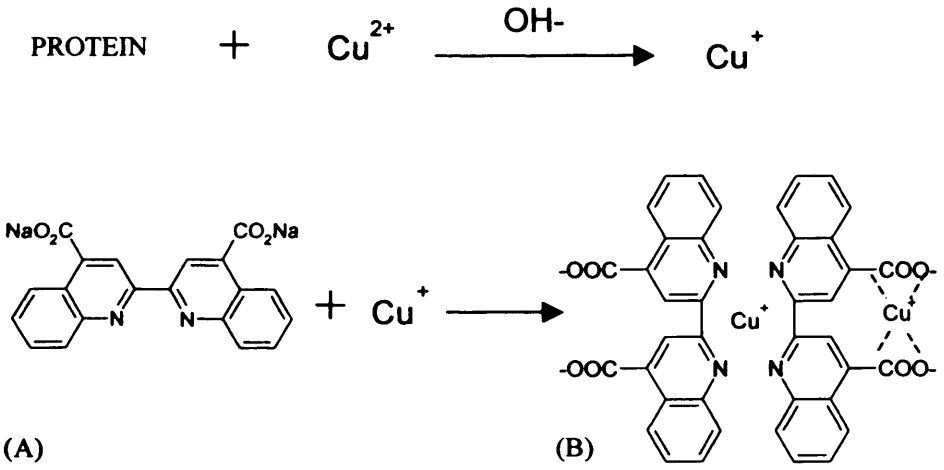

(b) Typical BCA assay calibration curve using BSA as the protein standard

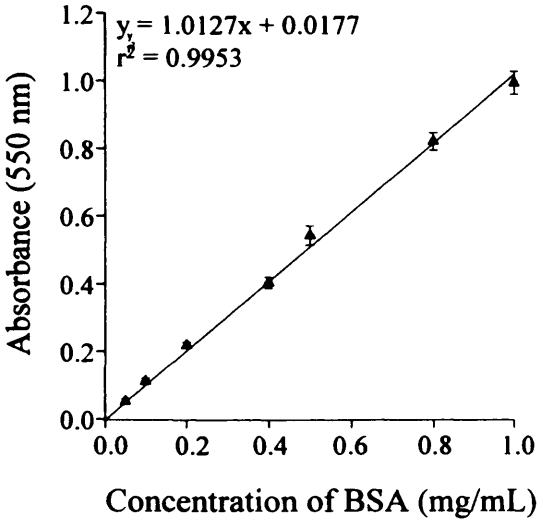

Figure 2.4 BCA assay to determine total protein content of the polymer-protein conjugates. Panel (a) illustrates the mechanism of the BCA assay, where the presence of protein causes the reduction of copper II sulphate (Cu^{2+}) to Cu^{+}, which complexes with BCA (A) to form a purple BCA-Cu complex (B). Panel (b) shows a typical BCA assay calibration curve using bovine serum albumin (BSA) as the protein standard. Data shown represents the mean (n=3) ± SD.

Table 2.2 Composition of separating and stacking gels required to prepare a gel of 12.5 % cross-linkage for SDS-PAGE

Components	Separating gel pH 8.8 (0.375 M tris[††], 20 mL)	Stacking gel pH 6.8 (0.125 M tris[††], 10 mL)
ddH_2O	8.44 mL	5.85 mL
Running buffer pH 8.8 (tris[††] HCl, 1.5 M)	5 mL	0 mL
Stacking buffer pH 6.8 (tris[††] HCl 0.5 M)	0 mL	2.5 mL
10 % w/v SDS[†]	200 µL	100 µL
40 % Acrylamide/Bis-acrylamide	6.25 mL	1 mL
10 % w/v AP[‡]	100 µL	50 µL
TEMED[‡‡]	10 µL	5 µL

[†] SDS; sodium dodecyl sulphate

[‡] AP; ammonium persulphate

[††] Tris is an abbreviation for tris[hydroxymethyl]aminomethane

[‡‡] TEMED is N,N,N,N'-tetra-methyl-ethylenediamine

First, the electrophoresis equipment was assembled (2 glass plates, 0.75 mm spacers, locked into a casting stand) and checked for leakage using ethanol. The separating gel (0.38 M tris, pH 8.8, 12.5 % cross linking, 20 mL) was prepared and pipetted between the glass plates, leaving a 4 cm space at the top. Isopropanol (0.3 mL) was pipetted on top to smooth the gel surface and prevent oxidation, which would impair polymerisation. The gel was then allowed to polymerise at RT for 30 min. The isopropanol was removed and a stacking gel (0.13 M tris, pH 6.8, 10 mL) prepared and pipetted into the remaining space. Sample spacer combs were inserted into the top of the gel, the volume of the stacking gel topped up and the gel left to polymerise at RT for 30 min.

The polymerised gels were removed from the casting stand and assembled in an electrophoresis tank and the tank filled with running buffer (tris HCl buffer, pH 8.3). Conjugate samples (1 mg/mL in ddH_20) and reference samples (trypsin, MSH or RNase A) were prepared by diluting (1 : 1) with denaturing solution (3.8 mL ddH_2O, 5 mL; 0.5 M tris HCl (pH 6.8), 8 mL 10 % w/v SDS, 4 mL glycerol, 2 mL 2-mercaptoethanol, 0.4 mL bromophenol blue 1% w/v) and heated for 5 min at 100 °C. The denatured samples (conjugate or free protein) and the pre-stained protein molecular weight markers were loaded (10 µL) onto the polyacrylamide gels and electrophoresed at 200 V for 50 min. The gel was then rinsed with ddH_2O and stained (1 h) with CB stain (1 % CB 125 mL, methanol 500 mL and acetic acid 100 mL, made up to 1 L with ddH_2O). The gel was cleared of non-specific staining by soaking in a strong destaining buffer (35 % methanol, 5 % acetic acid) for 1 h and then rehydrated using a weak destaining buffer (5 % methanol, 7 % acetic acid) for 30 min. Finally, the gel was rinsed with ddH_2O and dried (2 days) between cellophane sheets, clamped in a Gelair drying frame. The resulting gels were scanned (555 BP, 20 RGG, HEX, AlexaFluor532. Green laser 532) using a densiometer against a background fluorescent plate. The electronic image was then analysed by 1D gel analysis software to determine the intensity of protein bands and molecular weight distribution of the conjugate.

2.2.3.4 Determination of polymer, protein and conjugate purity using FPLC

FPLC was used to determine the purity and to estimate the molecular weight of the polymer-protein conjugates. This technique was primarily used to identify the

presence of free protein in the conjugate (described here) and subsequently to isolate and collect the conjugate fractions, previously described in section 2.2.1.2.

Prior to use, the column (Superdex HR 10/30) was equilibrated with the mobile phase (PBS 0.1 M; pH 7.4, 1 h) at a flow rate of 0.5 mL/min and upper pressure limit of 1.8 mPa. The samples (polymer, protein or polymer-protein conjugate) were prepared to a concentration of 3 mg/mL in PBS buffer (pH 7.4), and then filtered (0.2 μm pore size). 200 μL of the solubilised sample was injected onto the column and analysed over 80 min to ensure complete elution of the sample. Detection was by UV absorbance (280 nm) using a UPC-900 detector to determine the retention time of the sample. Visual analysis of the chromatogram was carried out to determine the presence of free protein in the polymer-protein conjugate or reaction mixture and also to identify the presence of any degradation products. To generate a molecular weight standard calibration curve, proteins of known molecular weight (listed in section 2.1.2.3) were also analysed (Figure 2.5a). A plot of Log molecular weight against retention time was constructed and used to estimate the molecular weight of the polymer-protein conjugates (Figure 2.5b).

2.2.4 Cell culture

2.2.4.1 Defrosting cells

Cryopreserved cells, stored in liquid N_2 were rapidly thawed (37 °C) and re-suspended in cell culture media (10 mL) to dilute the DMSO in the freezing medium. The composition of both the cell culture media and freezing medium for B16F10 and CV-1 cells is described in Table 2.3. The cell suspension was centrifuged (1000 g, 5 min, 20 °C) to remove the cryopreservative, and the supernatant removed. The cells were then re-suspended in 10 mL of fresh media supplemented with 10 % FBS.

2.2.4.2 Maintenance of cell line

Cells were maintained in a 75 cm^3 flask in media supplemented with 10 % FBS and stored at 37 °C in a CO_2 regulated environment. The cells were subcultured twice weekly when > 70 % confluence was achieved. The cells were washed twice with PBS (0.1 M) to remove dead cells and then trypsin-EDTA (4 mL) was added and the cells incubated (37 °C) for 2 min to detach them from the flask. The cell suspension was removed, diluted (up to 10 mL) in complete media (media + 10 % FBS), centrifuged (1000 g, 20 °C, 5 min) and then re-suspended in 10 mL complete media. A split ratio

(a) FPLC chromatogram of protein molecular weight standards

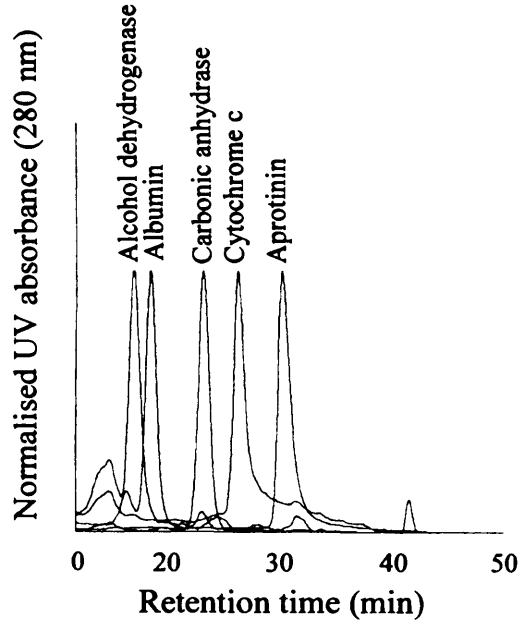

(b) Calibration curve of protein molecular weight standards

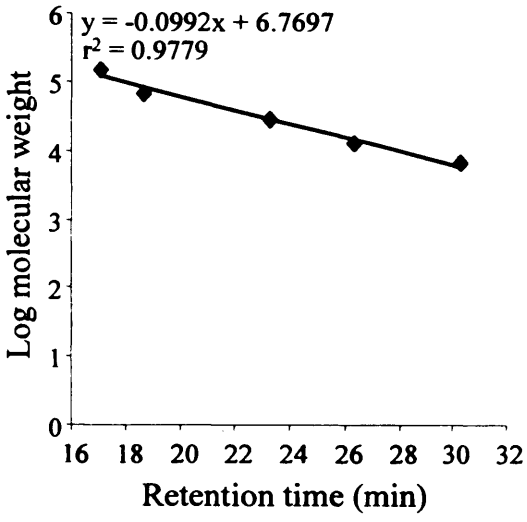

Figure 2.5 FPLC analysis of protein molecular weight standards using a superdex HR 10/30 size exclusion column. Panel (a) shows the chromatogram of the protein standards: aprotinin (6,500 g/mol), cytochrome c (12,400 g/mol), carbonic anhydrase (29,000 g/mol), bovine serum albumin (66,000 g/mol) and alcohol dehydrogenase (150,000 g/mol). UV represents ultraviolet absorbance. Panel (b) represents the calibration curve plotted to provide an estimate of sample molecular weight.

Table 2.3 Cell culture maintenance parameters

Cell line	Origin	Supplier	Passage range	Medium	Freezing medium	Seeding density (cells/mL)	Spilt ratio
B16F10	Murine melanoma	ATCC[†] (USA)	10 - 30	90 % RPMI 1640[‡] + phenol red + Glutamax 10 % FBS[‡‡]	10 % DMSO[‡] 90 % FBS[‡‡]	1 x 10^4 2.5 x 10^4 1 x 10^5	1 : 9
CV-1	African green monkey kidney fibroblasts	EUACC[††] (UK)	19 - 39	90 % DMEM[‡‡] + phenol red + Glucose 10 % FBS[‡‡]	10 % DMSO[‡] 90 % FBS[‡‡]	2.5 x 10^4	2 : 8

[‡] RPMI defines Rose Park Memorial Institute

[‡] DMSO is an abbreviation for dimethyl sulphoxide

[†] ATCC abbreviates the American type culture collection

[‡‡] DMEM defines Dulbecco's minimal essential media

[‡‡] FBS defines foetal bovine serum

[††] ECACC abbreviated the European collection of cell cultures

of 1 : 9 (B16F10) or 2 : 8 (CV-1) was used to subculture the cells and they were maintained and used in experiments for up to 20 passages before defrosting a new aliquot of cells.

2.2.4.3 Counting cells

Cells were prepared for subculture as per section 2.2.4.2, and re-suspended in 10 mL of complete medium. 25 μL of cell suspension was diluted 1 : 1 with trypan blue (0.2 % w/v in PBS), mixed and left to stand (1 min) to stain dead cells blue. 10 μL of this solution was then pipetted under the cover slip on the haemocytometer and viewed using a bright-field microscope. Viable cells located in the two central 0.1 mm^3 squares of the haemocytometer were counted, and the total cell concentration calculated using the following equation:

Viable cells/mL = (Number of cells in both central 0.1 mm^3 squares/2) x 10^4

2.2.4.4 Freezing cells

Aliquots of cells (10^6 cells/mL) were routinely frozen and stored in liquid N_2 to maintain a viable supply of cells of a low passage number. Firstly, cells were counted (section 2.2.4.3), re-centrifuged and re-suspended in freezing medium (10 % DMSO, 90 % FBS; Table 2.3). Aliquots of 1 mL were pipetted into cryogenic vials, wrapped and insulated in polystyrene and kept at –20 °C for 1 h then –80 °C for 24 h, before storing in liquid N_2.

2.2.4.5 Bright-field microscopy and imaging of cell lines

The cells were monitored regularly (~ 4 times/week) using an Inverted DM IL bright-field microscope, to ensure they were growing normally and that there was no signs of infection. The morphology of the cells was observed whilst *in situ* in the cell culturing flasks. Additionally, cells were counted at the point of subculture, using the bright-field microscope as described in section 2.2.4.3. Bright-field images of cell morphology were taken using an inverted Leica DM IRB microscope with 12-bit cooled monochrome Retiga 1300 camera.

2.2.4.6 MTT assay to characterise cell growth and cytotoxicity

The MTT assay was chosen to characterise cell growth so that experiments could be conducted during the exponential growth phase of the cell cycle. The MTT

assay was also used to assess the cytotoxicity of the HA-RNase A conjugate and controls (Chapter 6). This assay measures the formation of formazan crystals (blue) caused by the reduction of MTT by mitochondrial dehydrogenase (Mosmann, 1983) (Figure 2.6a).

Cells were seeded (100 μL) in a 96 well plate to the desired cell density (2.5 x 10^4, 5 x 10^4 and 1 x 10^5 cells/mL) and incubated (37 °C) for 24 h to enable cell adhesion. The outer wells of the 96 well plate were filled with PBS to prevent evaporation of the media and subsequent variations in growth rate. Cell growth was then assessed at 24, 48, 72, 96 and 120 h by adding 20 μL of MTT (5 mg/mL in PBS, sterile filtered) to a single row of the 96 well plate each day. The cells were incubated with MTT for 5 h and then the media / MTT was withdrawn and 100 μL of DMSO added to each well to dissolve the formazan crystals formed. The cells were incubated for a further 30 min to completely dissolve the formazan crystals and then the UV-vis absorbance was measured at 550 nm. A typical growth curve (change in absorbance) over time is shown (Figure 2.6b).

The cytotoxicity of samples (parent polymer or polymer-protein conjugates) and controls (PEI; positive control, dextran; negative control) on both B16F10 and CV-1 cells, seeded at a density of 2.5 x 10^4 cells/mL was measured using the MTT assay. The samples (100 μL of 0.001 – 1 mg/mL in media) were added to the cells, 24 h after subculture and incubated for a further 72 h (37 °C). MTT (20 μL) was added to each of the sample wells 5 h before the end of the 72 h incubation period. The remainder of the assay was carried out as described above.

2.2.5 Statistical Analysis

Samples were analysed in a minimum of three replicates and the error calculated as either standard deviation (SD) or standard error of the mean (SEM) where appropriate. Typically, one-way analysis of variance (ANOVA) followed by a Bonferroni *post hoc* test was used to analyse the results. Unless otherwise stated, probability (p) < 0.05 was deemed to indicate significance.

(a) Reduction of MTT (A) to formazan crystals (B)

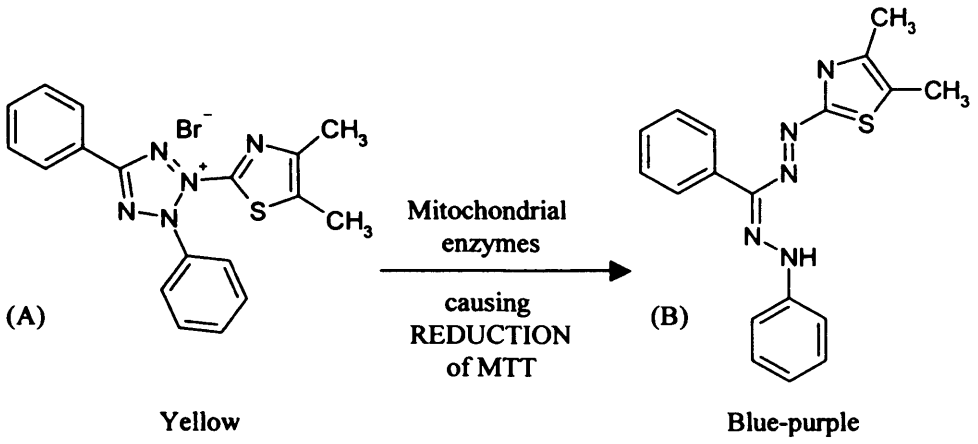

(b) A typical growth curve for B16F10 murine melanoma cells

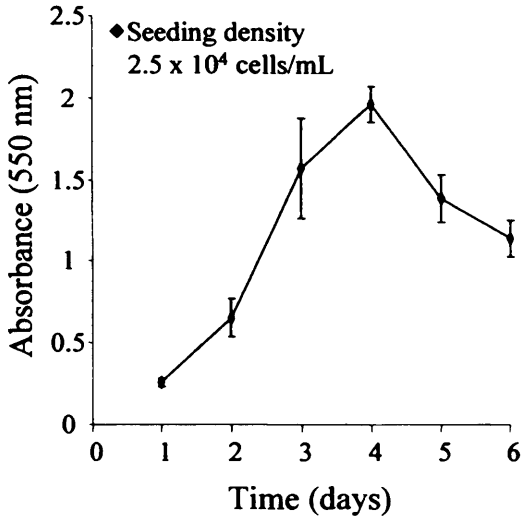

Figure 2.6 MTT assay of cell viability. Panel (a) reduction of MTT (A) to formazan crystals (B) by mitochondrial enzymes, and panel (b) a typical growth curve for B16F10 murine melanoma cells over 6 days. Cells were seeded at a density of 2.5 x 10^4 cells/mL. Data shown represents the mean (n=18) ± SD.

Chapter 3

Synthesis and characterisation of dextrin-trypsin conjugates and evaluation of enzyme activity

3.1 Introduction

The main aim of this research was to test the feasibility of protein masking, with subsequent reinstatement of enzyme activity, as outlined in Chapter 1 (section 1.6). Unlike traditional polymer-protein conjugation, this approach sought to hide the activity of the conjugated protein until triggered degradation of the masking polymer enables re-expression of protein activity. Initially, to investigate this concept, a simple system was chosen, utilising an established biodegradable polymer, dextrin, and a well characterised enzyme, trypsin. Conventional conjugation chemistry was chosen to prepare the conjugate.

3.1.1 Rationale for the selection of dextrin as a model polymer

Dextrin (α-1,4 poly(glucose)) was selected as the model polymer for conjugation for the reasons discussed in Chapter 1 (section 1.7.1.1). Dextrin is also FDA approved for use as a peritoneal dialysis solution (Icodextrin) (Mistry and Gokal, 1994). Initial experiments were conducted to study the effect of dextrin molecular weight on the efficiency of trypsin masking and unmasking. LMW ≈ 7,700 g/mol and HMW ≈ 47,200 g/mol (Mw) dextrins, were used to determine the optimum molecular weight and degree of polymer succinoylation required to enable enzyme activity masking. The molecular weights chosen also reflected the molecular weight of PEG used to prepare protein conjugates that are on the pharmaceutical market. For example, Adagen™ (Levy et al., 1988) uses PEG of 5,000 g/mol and Pegasys® (Reddy et al., 2001) is made using a branched PEG with a molecular weight of up to 40,000 g/mol.

3.1.2 Rationale for the selection of trypsin as a model protein

Trypsin was chosen as the model protein for these initial proof of principle studies. In addition to being well characterised, described in Chapter 1 (section 1.7.2.1), trypsin has also been used as a model enzyme for polymer conjugation by several other researchers (Abuchowski and Davis, 1979; Murphy and Fagain, 1996; Zhang et al., 2001) (Table 1.2). In particular, trypsin has been conjugated to the polysaccharides carboxymethylcellulose (Villalonga et al., 2000) and cyclodextrin (Fernandez et al., 2003) summarised in Table 3.1 (previously discussed in section 1.7.2.1). Several preliminary studies carried out within the Centre for Polymer Therapeutics, Cardiff University (Lewis, 2003; Meier, 2002; White, 2002) had shown

Table 3.1 Biodegradable polymer-trypsin conjugates

Polymer	Enzyme activity			Reference
	Free	Conjugated	Units	
β-cyclodextrin	60 ± 3	378 ± 16	Half life (h)	Fernandez et al., 2004
β-cyclodextrin modified carboxymethylcellulose (n=2)	100	95 110	Esterolytic activity (%)	Villalonga et al., 2003
	36	23	Km (affinity) (μM)	Villalonga et al., 2003
Cyclodextrin, monoamine derivatives (n=3)	36		Specific activity U/mg (%)	Fernandez et al., 2002
αCDNH^2		50 (140)		
βCDNH^2		52 (145)		
γCDNH^2		58 (160)		
Amino β-cyclodextrin (n=3)	36		Esterolytic activity (U/mg)	Fernandez et al., 2003
CDNH^2,		34		
CDPN,		31		
CDBN derivative		44		
	39		Km (μM)	Fernandez et al., 2003
CDNH^2,		27		
CDPN,		45		
CDBN derivative		23		
Cyclodextrin containing dicarboxylic acid (n=2)	36	70 51	Specific activity (U/mg)	Fernandez et al., 2004
	100	245 185	Catalytic efficiency	Fernandez et al., 2004
Carboxymethylcellulose (n=2)	100		Specific activity (%)	Villalonga et al., 2000
		42	- Casein substrate	
		62	- BAEE[†]	
	39×10^{-6}	18×10^{-6}	Km (BAEE[†])	Villalonga et al., 2000

[†] BAEE is defined as N-α-benzoyl-L-arginine-ethyl ester

that it was possible to prepare dextrin-trypsin conjugates by first succinoylating the dextrin to incorporate carboxyl groups onto the polymer backbone. These were subsequently conjugated to the amino groups of trypsin as described below.

3.1.3 Polymer-protein conjugation chemistry

A wide variety of conjugation chemistries have been used to prepare PEGylated proteins (see General Introduction section 1.3). Historically, polymer-protein conjugation was achieved *via* a hydroxyl, amine or carboxylic acid group present on the polymer (reviewed by Harris and Chess, 2003). If none of these groups is present however, polymer functionalisation is first required (Veronese and Morpurgo, 1999). Typically, the polymer is functionalised to enable conjugation to a primary amine on the protein, frequently either an N-terminal amine or a lysine group (Harris et al., 2001). As PEGylation chemistry has developed, a growing number of methods to enable site-specific protein conjugation (1 polymer : 1 protein) have been developed (discussed in Chapter 1, section 1.3.3, reviewed in Roberts et al., 2002). Despite the advantages of this advanced PEGylation chemistry (mainly the ability to avoid conjugation to the active site of the protein, and the formation of a well defined product), however, for these studies it was decided to utilise a multifunctional dextrin and random conjugation to amino groups in trypsin. Random conjugation was chosen because it enabled:

1. The number of conjugation sites to be varied. This was required to test the feasibility of masking protein activity by wrapping the polymer around the protein.
2. Simple conjugation chemistry to be applied.
3. No alteration of protein sequence was required, modifications may affect the native protein activity.

3.1.4 Methods used for polysaccharide functionalisation

Numerous methods of polysaccharide functionalisation have been used to create an active intermediate suitable for conjugation to proteins. These include reaction of amino-β-cyclodextrins with mono-6-O-tosyl derivative (Fernandez et al., 2003). Activation of pullulan using 4-nitrophenyl chloroformate (Bruneel and Schacht, 1993b) or cyanogen bromide activation (Figure 3.1) (reviewed by Kost and Goldbart,

(a) Chloroformate activation

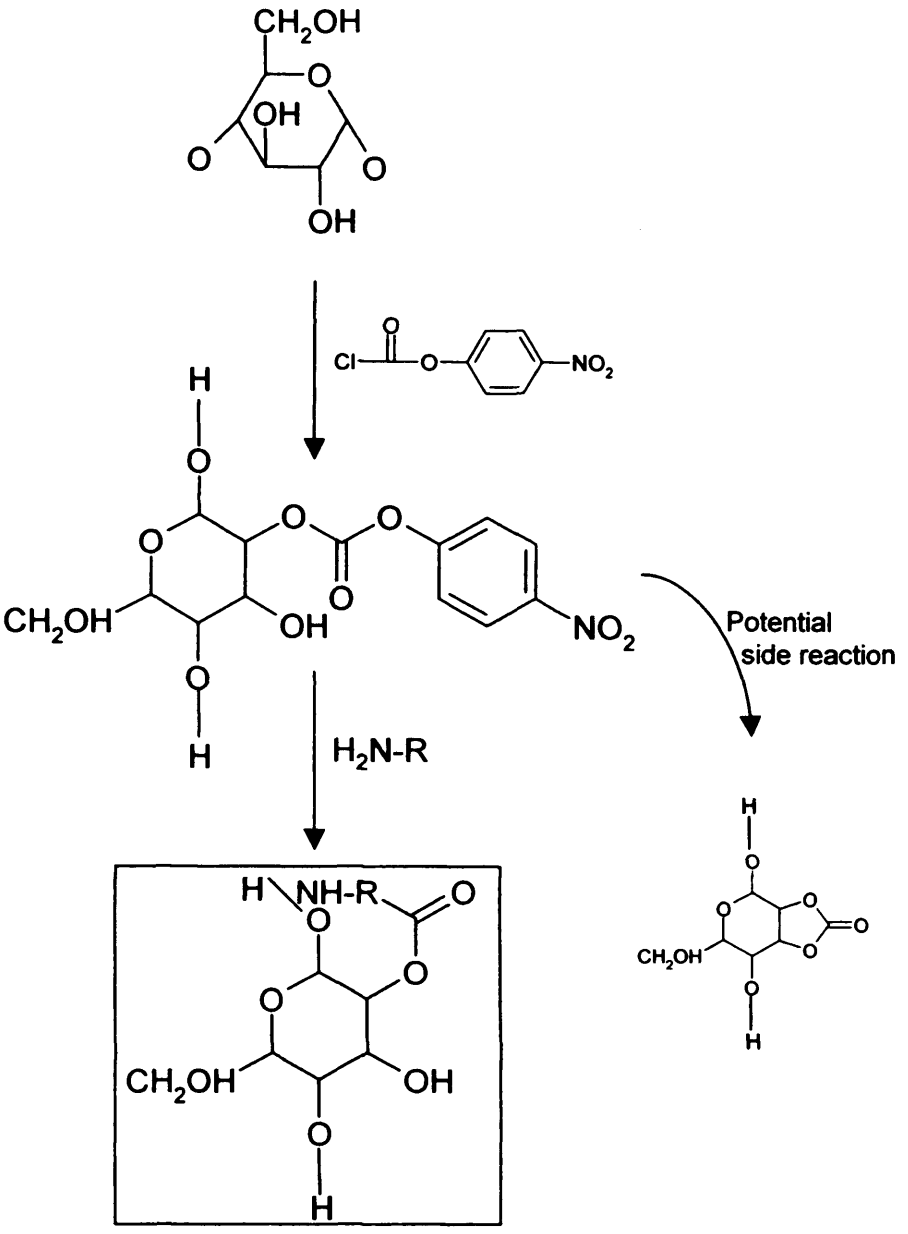

Figure 3.1 Potential methods used for polysaccharide functionalisation. Panel (a) chloroformate activation (German, 2001).

(b) Cyanogen bromide

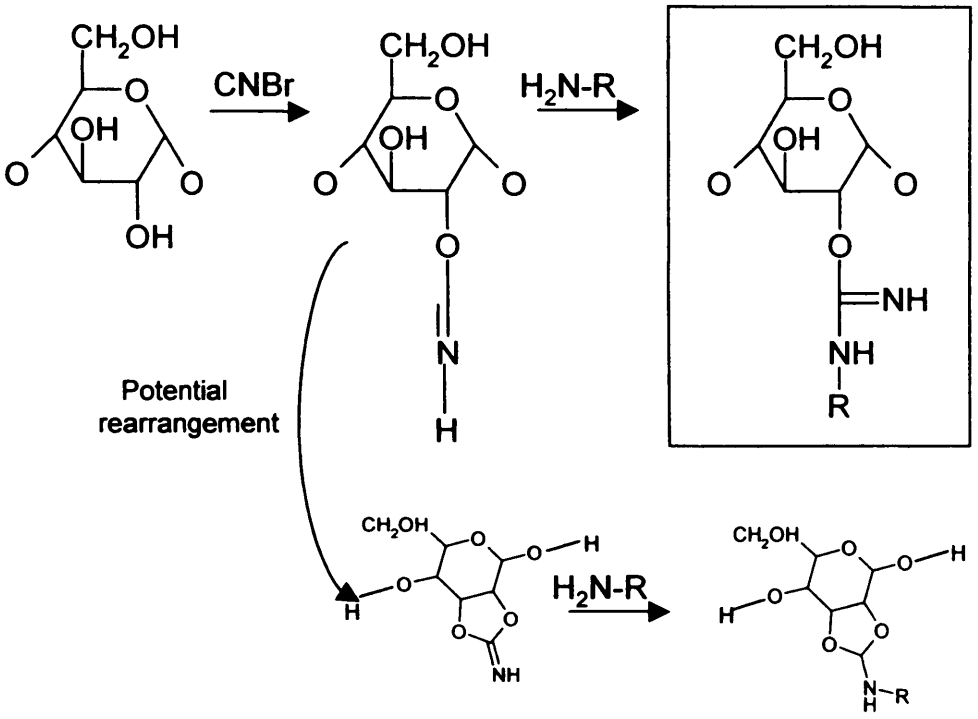

(c) Periodate oxidation

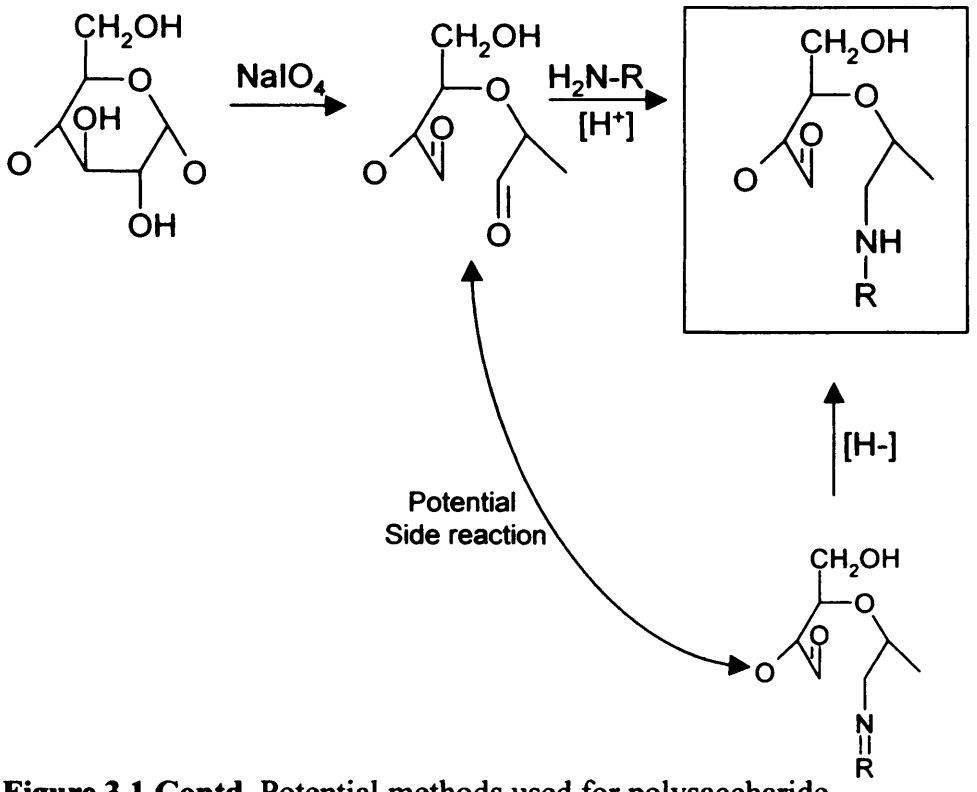

Figure 3.1 Contd. Potential methods used for polysaccharide functionalisation. Panel (b) cyanogen bromide activation, and (c) periodate oxidation (German, 2001).

(d) Succinoylation

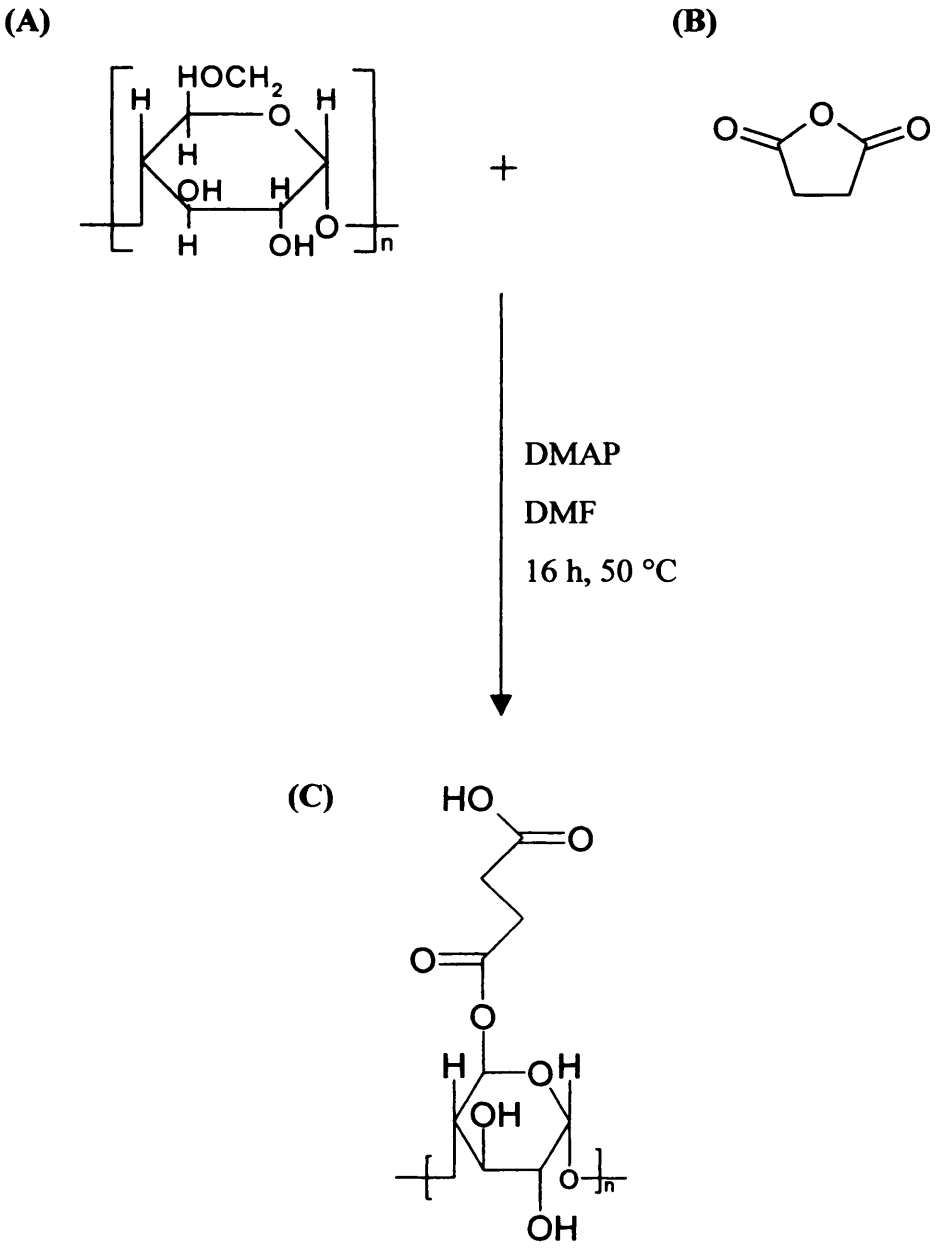

Figure 3.1 Contd. Potential methods used for polysaccharide functionalisation. Reaction scheme for the succinoylation of dextrin. Compounds: (A) dextrin, (B) succinic anhydride and (C) succinoylated dextrin (German, 2001).

1997; Schnaar et al., 1977). The succinoylation of pullulan and dextran, using succinic anhydride, has also been applied to incorporate ester groups (Bruneel and Schacht, 1994; Groff et al., 1982). Pullulan, dextran and chitosan have been functionalised using sodium periodate activation (Bruneel and Schacht, 1993a; Cheung et al., 2005; Vold and Christensen, 2005).

Cyanuric chloride has been used to conjugate BSA to PEG, despite the speculation that it causes toxicity and reduced enzyme activity on conjugation (Abuchowski et al., 1977). Quantification of the degree of functionalisation, when chloroformate activation was applied to the modification of pullulan, was found to be problematic. Typically, the degree of functionalisation was underestimated by UV analysis and was attributed to the presence of aliphatic carbonates (Bruneel and Schacht, 1993b). Conjugation of a protein to a succinimidyl carbonate derivative produces a selective urethane linker, which has been shown to have a reduced reactivity requiring prolonged reaction times (reviewed in Nucci et al., 1991) (Table 1.4).

Succinoylation (Figure 3.1d) was chosen as the method of dextrin functionalisation in this study because i) it introduces carboxyl groups suitable for conjugation to a protein's amino groups, ii) it is non-toxic, iii) the linker is relatively stable (Bruneel and Schacht, 1994; Groff et al., 1982), and iv) it has previously been the method of choice for the conjugation of dextrin to trypsin (discussed in section 3.1.2). There is also a history of use of succinoylated dextrin within the Centre for Polymer Therapeutics, Cardiff University. Hreczuk-Hirst and colleagues, (Hreczuk-Hirst et al., 2001b) optimised the reaction conditions needed for the reproducible succinoylation of dextrin to varying extents of modification. Additionally, Hreczuk-Hirst et al., (2001a) also conducted systematic studies on the degradation of succinoylated dextrin by amylase. Amylase (∝) randomly hydrolyses the ∝-1-4 $_D$-glucosidic linkages of dextrin producing degradation products of glucose and ∝-maltose (Kost and Goldbart, 1997). Hreczuk-Hirst et al., (2001a) concluded that increasing the extent of modification reduced the rate of degradation.

3.1.5 Method used to determine trypsin activity

Following the synthesis of the dextrin-trypsin conjugates, it was necessary to determine trypsin activity of the conjugate before and after exposure to amylase, and to compare conjugate activity to that of the free enzyme.

To measure the activity of free and bound trypsin, a direct continuous assay was used with BAPNA as a substrate (described in 3.2.6). The assay measures the release of p-nitroanilide (NAp) over time, and it is possible to determine the initial linear rate of substrate degradation.

Interpretation of the raw data obtained can be used to determine the affinity constant (Km), the turnover rate (Kcat) and maximum velocity (Vmax) of an enzyme substrate interaction. These parameters can then be used to make comparisons between different enzymes and different conditions, or in this case to compare the activity of free and polymer-bound trypsin. Several different mathematical models have been explored as tools to calculate these parameters and they are reviewed very well in Cornish-Bowden (2004). The models include the:-

- Double reciprocal plot
- Direct linear plot
- Lineweaver-Burk plot
- Eadie-Hofstee plot
- Hanes-Woolfe plot

All are derived using the Michaelis-Menten equation:

$$v = (V_{max} S)/(K_m + S)$$

where, v = velocity

Vmax = maximum velocity

S = substrate concentration

Km = affinity constant

For this equation to hold true, three assumptions are made. Firstly, that any reverse reaction occurring is negligible. Secondly, the measurement of the rate of reaction is made under conditions of steady state. Finally, the formation of the enzyme-substrate complex will not significantly affect the concentration of free substrate. These assumptions are validated experimentally if the initial rate is linear with time and linearly proportional to enzyme concentration, i.e. zero order kinetics (Cornish-Bowden, 2004).

3.1.6 Summary of the aims of these studies

1. To optimise the synthesis of dextrin-trypsin conjugates, and determine purification and analytical techniques that could be used to prepare pure and well characterised conjugates.

2. To test the hypothesis that it would be possible to mask the activity of a conjugated enzyme, and to reinstate it following amylase degradation of the polymer.
3. To evaluate the effect of dextrin molecular weight and degree of succinoylation on the ability to mask trypsin activity and upon the reinstatement of trypsin activity after exposure to amylase.
4. To choose the optimal parameters (molecular weight, degree of succinoylation) that could be used in the subsequent polymer-protein conjugate experiments.

3.2 Methods

The general methods used to characterise both functionalised polymer and polymer-protein conjugates were described in Chapter 2. These include FT-IR (section 2.2.2.2), titration (section 2.2.2.1), GPC (section 2.2.2.3), FPLC (section 2.2.3.4), BCA assay (section 2.2.3.2) and SDS-PAGE (section 2.2.3.3). The following sections will describe other specific methods used here such as NMR (section 3.2.2) and specific modifications to the general methods used to characterise dextrin-trypsin conjugates.

Synthesis and characterisation of succinoylated dextrin

3.2.1 Succinoylation of dextrin

Dextrin succinoylation was first conducted using the method of Hreczuk-Hirst and colleagues (Hreczuk-Hirst et al., 2001b) (Figure 3.1d), using dextrin of ~ 50,000 g/mol molecular weight. Subsequently, a dextrin of 7,700 g/mol molecular weight was used. In both cases different degrees of succinoylation (1 – 34 mol %) were sought. Adjustment of the molar ratio of dextrin to succinic anhydride used (taking into account polymer molecular weight) was used to control the degree of succinoylation.

Typical reaction conditions used to derive 16 mol % succinoylation was as follows:

Dextrin (Mw ~ 7,700 g/mol, 1 g, 1.96×10^{-5} mol) and DMAP (30 mg, 2.41×10^{-4} mol) were weighed into a 100 mL round bottom flask. The flask was sealed and purged with N_2 to ensure anhydrous conditions were maintained. Anhydrous DMF (15 mL) was withdrawn under N_2 and added to the flask. A second volume of DMF (5 mL) was then withdrawn and used to dissolve the succinic anhydride (90 mg, 9×10^{-4}

mol). The dissolved succinic anhydride was then added to the flask and the stirred reaction allowed to proceed overnight (50 °C, 16 h).

To terminate the reaction, excess DMF was removed using a vacuum pump and the reaction mixture added drop-wise to rapidly stirring diethyl ether (250 mL). This precipitated out the succinoylated dextrin, and removed any remaining DMF by dissolving it in the diethyl ether. The purification process was allowed to continue for 4 h. The succinoylated dextrin was then extracted by filtration (4 μm pore size) under vacuum and dissolved in ddH_2O (10 mL). Dialysis (Spectra/Por membrane; MWCO 15,000 g/mol) in ddH_2O (6 x 5 L) over 48 h was used to remove water-soluble impurities and unreacted succinic anhydride. The dialysed product was filtered and frozen with liquid N_2 (5 min) and lyophilised (48 h). The succinoylated dextrin produced was characterised by titration to measure the number of COOH groups (section 2.2.2.1), FT-IR (section 2.2.2.2) and ^1H NMR (section 3.2.2) to confirm product identity and GPC (section 2.2.2.3) to estimate molecular weight. The methods used are briefly described below.

3.2.2 Confirmation of the succinoylation of dextrin by nuclear magnetic resonance (NMR) spectroscopy

Dextrin and succinoylated dextrin were dissolved in deuterated water (D_2O) to a final concentration of 30 mg/mL and samples (1 mL) pipetted into NMR sample tubes for analysis. Selected samples were analysed by ^1H NMR spectroscopy. The NMR spectra peaks occurring between 2.86 - 2.81 ppm in ^1H spectra for succinoylated dextrin but not unmodified dextrin, were attributable to the presence of succinoyl ester groups (Hreczuk-Hirst et al., 2001b). Following preparation, samples were run on the NMR by Ms. L. Dieudonne (Centre for Polymer Therapeutics, Cardiff University).

Synthesis and characterisation of dextrin-trypsin conjugates

3.2.3 *Synthesis and purification of dextrin-trypsin conjugates*

The succinoylated dextrin intermediates were conjugated (Figure 3.2) to trypsin using EDC and Sulfo-NHS. An excess of these reagents was used to ensure maximum activation of succinoyl ester groups for conjugation.

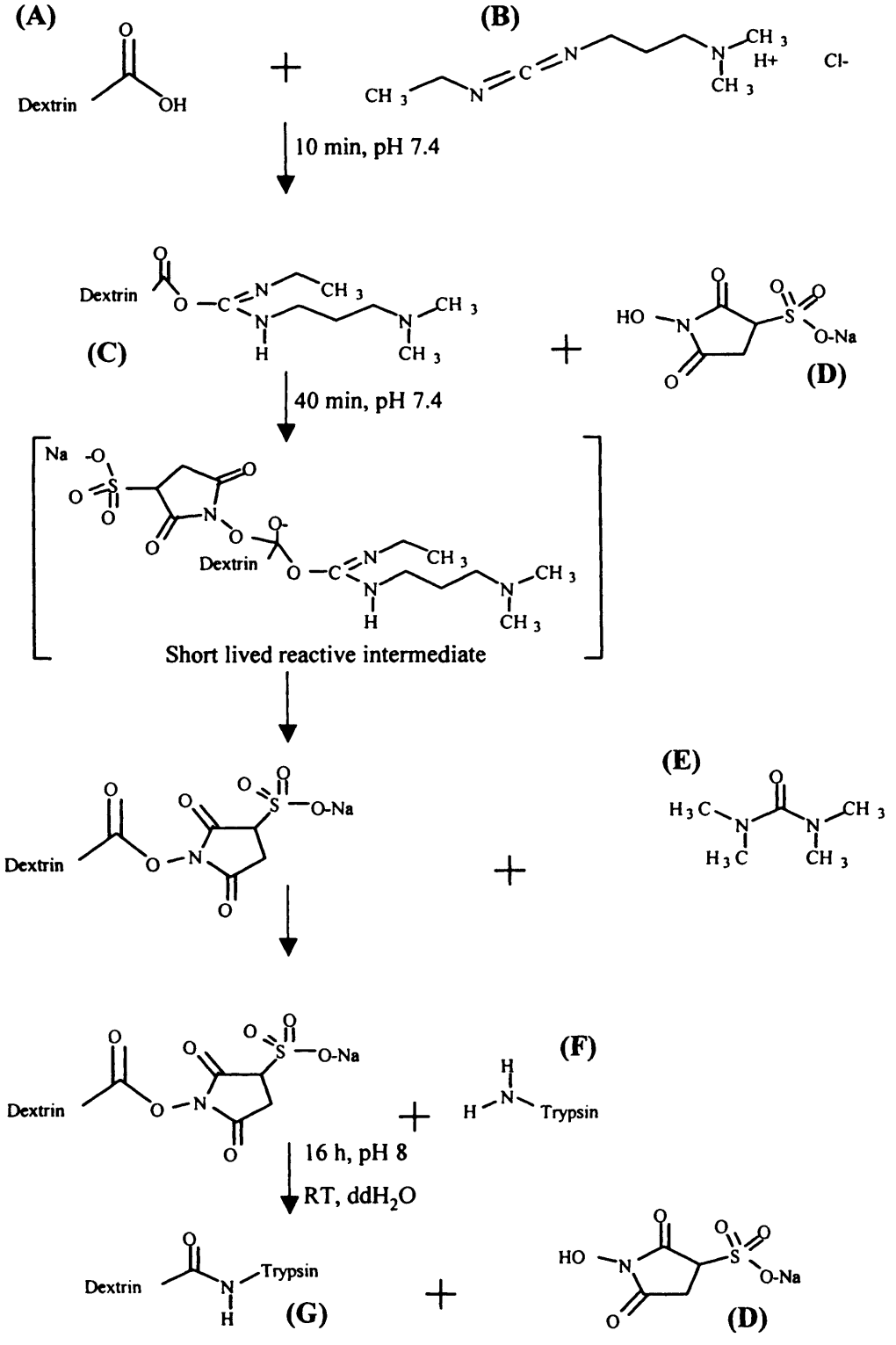

Figure 3.2 Conjugation of succinoylated dextrin to trypsin. Compounds: (A) succinoylated dextrin and (B) EDC, (C) O-Acylisourea, (D) sulfo-NHS, (E) urea, (F) trypsin, (G) dextrin-protein conjugate.

To optimise the reaction conditions the following parameters were varied:

(i) Molar ratio of dextrin : trypsin
- STE method; ratio of amines to carboxyl groups is in excess (1 COOH : 150 NH_2 groups excess)
- SFR method; fixed ratio of dextrin and trypsin quantities, but mol % succinoylation of dextrin was varied, altering the ratio of COOH : NH_2 groups
  1 : 40 : 1, 50 : 1 and 100 : 1 NH_2 : COOH

(ii) Dextrin molecular weight: 7,700 g/mol or 47,200 g/mol

(iii) mol % succinoylation of dextrin: from 2 to 32 mol %

To monitor the reaction, samples (100 µL) of the reaction mixture were taken throughout (0, 1, 2, 3, 4, 5, 6 and 16 h) a conjugation reaction, and subsequently analysed by SDS-PAGE as described in section 2.2.3.3.

Typical reaction conditions for conjugation of trypsin to succinoylated dextrin were as follows:

Succinoylated dextrin (26 mol %, 100 mg, 5.5×10^{-7} mol dextrin with COOH groups incorporated) was weighed into a round bottom flask (100 mL), dissolved in ddH_2O (10 mL) and sealed. Then, EDC (62 mg, 3.23×10^{-4} mol) was added and the solution stirred for 10 min at RT to ensure complete and uniform dissolution. Sulfo-NHS (88 mg, 4.04×10^{-4} mol) was then added, and the reaction stirred for a further 40 min at RT. The degree of dextrin succinoylation (as determined by titration) was used to calculate the quantity of trypsin required for the reaction, by estimating the molar ratio as follows:

- COOH (1 mol) : trypsin (15 mol) (STE method)
  e.g. trypsin (198 mg, 8.29×10^{-6} mol)
- COOH (1 mol) : trypsin (40 mol) (SFR method)
  e.g. trypsin (49.5 mg, 2.07×10^{-6} mol)

Trypsin was dissolved in ddH_2O (5 mL), added drop-wise to the reaction mixture, the pH adjusted to 8 and then the reaction was left to proceed for 16 h at RT, stirred. The product conjugate was filtered and purified by dialysis (Spectra/Por Membrane;

MWCO 25,000 g/mol) against ddH_2O (6 x 5 L) over 48 h, before freezing in liquid N_2 (5 min), and lyophilisation (48 h).

There are challenges in effectively purifying a polymer-protein conjugate, whilst maintaining maximum protein activity. Dextrin-trypsin conjugates were purified by dialysis using a Spectra/Por dialysis membrane (MWCO 25,000 and 50,000 g/mol). The purity of the product (in respect of free trypsin) was determined by SDS-PAGE (section 2.2.3.3).

3.2.4 Evaluation of dextrin and dextrin-trypsin conjugate degradation by amylase

The rate and extent of degradation of dextrin, succinoylated dextrin and dextrin-trypsin conjugates by α-amylase was assessed using a GPC method adapted from Hreczuk-Hirst et al., (2001a). Dextrin (Mw = 7,700 g/mol and 47,200 g/mol), succinoylated dextrin (~15 and ~30 mol % succinoylation) or dextrin-trypsin conjugate, was dissolved in PBS (4 mL, pH 7.4) at a concentration of 3.75 mg/mL. Amylase (400 µL; 2.5 ui/mL) was added and the mixture incubated at 37 °C for 5 h. At time points samples (100 µL) were taken, immediately snap frozen in liquid N_2 to stop the reaction and then stored at –20 °C until analysis by GPC.

Before GPC analysis, samples were placed for 5 min in a boiling water bath to denature the enzymatic activity of the amylase and stop polymer degradation. The supernatant was then analysed by GPC (section 2.2.2.3) to determine the change in molecular weight of the sample over time.

Assessment of free and conjugated trypsin activity

3.2.5 UV-vis spectrophotometric assay of controls for trypsin activity studies

To determine if there would be any interference with the measurement of trypsin activity at 400 nm, the UV-vis absorbance of dextrin, succinoylated dextrin or dextrin-trypsin conjugates (1 mg/mL), trypsin (0.01 – 5 mg/mL), tris buffer (pH 8.2, 40 mM tris, 16 mM CaCl) and BAPNA (0.021 % w/v, 4.83 x 10^{-4} M) was measured over 200 – 500 nm (scanning rate 100 nm/min, path length 1 cm), against a reference sample of tris buffer (pH 8.2). Unless otherwise stated, tris buffer refers to 40 mM tris, 16 mM CaCl, pH 8.2.

3.2.6 Measurement of trypsin activity

The activity of trypsin (8.54×10^{-5} and 8.54×10^{-6} mM) in tris buffer (pH 8.2) at 37 °C was measured using the trypsin specific substrate BAPNA (stock solution of 0.7 % w/v in DMSO). Trypsin cleaves BAPNA on the carboxyl side of arginine, releasing NAp, which may be measured at 400 nm. Throughout, trypsin stock solutions were kept on ice. The required volume of substrate (10 - 60 µL) was pipetted into a quartz cuvette (1 mL) and made up to 980 µL with tris buffer (pH 8.2). A reference cell of tris buffer (pH 8.2) and BAPNA (0.007 % w/v, 1.61×10^{-4} M in DMSO) was used as blank. To start the assay, trypsin (20 µL of 0.00001 or 0.000001 % w/v) was added to the cuvette and the rate of NAp release was measured at 400 nm over 20 min at 37 °C.

In order to characterise the kinetic rate constants, trypsin activity was determined against a range of substrate concentrations (BAPNA 1.61×10^{-4} – 9.66×10^{-4} M) as described above. Substrate concentration was calculated using the molar extinction coefficient of 8800 L/mol per cm for NAp at 400 nm (Johnson et al., 2002). From the raw data obtained, plots were drawn according to Hanes-Woolfe, Eadie-Hofstee and Lineweaver-Burk plot and used to calculate the kinetic rate constants Km, Vmax and Kcat (Figure 3.3).

3.2.7 Measurement of dextrin-trypsin conjugate activity

Using the trypsin content of the conjugate, determined by the BCA protein assay (section 2.2.3.2), the volume of conjugate solution containing 200 ng of trypsin could be calculated. The activity of the 200 ng trypsin equivalent (equiv.) concentration was then assessed against the substrate BAPNA (1.61×10^{-4} – 9.66×10^{-4} M) as described in section 3.2.6. To estimate any change in trypsin activity following conjugation, the NAp released by the conjugate at 20 min was expressed as a percentage of the NAp released by free trypsin. Furthermore, the kinetics rate constants were determined as described in section 3.2.6.

3.2.8 Assessment of trypsin activity following amylase degradation of dextrin-trypsin conjugates

Dextrin-trypsin conjugate (0.01 mg/mL) and amylase (0.004 mg/mL, 3.33 ui/mL) were incubated in tris buffer (pH 8.2) for 16 h at 37 °C to degrade the conjugate. The activity of the degraded conjugate was then assayed as previously described in section 3.2.7. The volume of conjugate solution containing 200 ng trypsin

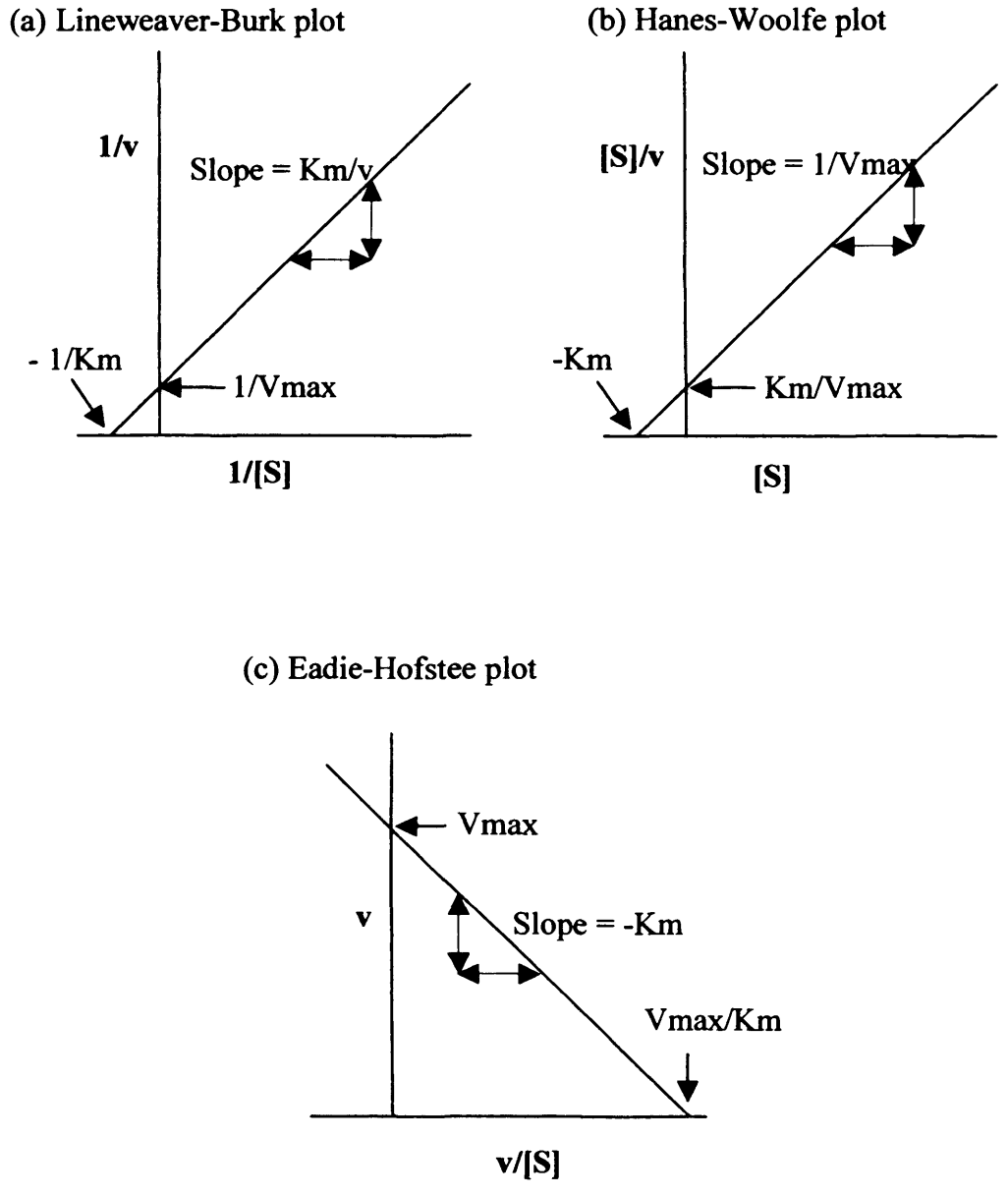

Figure 3.3 Enzyme kinetics models for data interpretation, based on the Michaelis-Menten equation. Panel (a) Lineweaver-Burk plot, (b) Hanes-Woolfe plot, and (c) Eadie-Hofstee plot.

equiv. was calculated from the known trypsin loading of the conjugate and pipetted into the cuvette for analysis. To estimate any change in trypsin activity following degradation of the conjugate, the NAp released by the degraded conjugate at 20 min was expressed as a percentage of the NAp released by free trypsin. The kinetics rate constants were also determined as described in section 3.2.6.

3.3 Results

3.3.1 Succinoylation of dextrin

Dextrins (Mw = 7,700 and 47,200 g/mol) were functionalised by succinoylation to produce a range of modifications (1 - 36 mol %), as summarised in Table 3.2.

Initially, the HMW dextrin was modified to a theoretical level of 30 mol % succinoylation. ^{1}H NMR qualitatively confirmed the incorporation of succinoyl groups (Figure 3.4). These were indicated by peaks at 2.6 – 2.8 ppm for ^{1}H NMR. FT-IR also showed succinoyl group incorporation (Figure 3.5a). The peak seen at 1720 cm^{-1} was not present in unmodified dextrin (Figure 3.5b). Furthermore, an increase in peak intensity at 1720 cm^{-1} was seen with increasing degree of succinoylation for both LMW and HMW succinoylated dextrins (Figure 3.5c).

Titration also confirmed presence of carboxyl groups and gave a degree of dextrin modification of up to 45 mol % (Figure 3.6, Table 3.2). Typically the conversion efficiency for the succinoylation reaction was in the range of 70 - 90 % of the theoretical maximum for both the HMW and the LMW dextrins (Table 3.2).

3.3.2 Characterisation of dextrin-trypsin conjugates

The characteristics of those succinoylated dextrins used to prepare trypsin conjugates are summarised in Table 3.3.

Both GPC and FPLC analysis confirmed the synthesis of dextrin-trypsin conjugates and showed that there was no free trypsin present in either the LMW or HMW dextrin-trypsin conjugates succinoylated up to 26 mol % (Figure 3.7). This was also confirmed by SDS-PAGE analysis (Figure 3.8). Control experiments carried out to define the limit of detection of free trypsin, showed this to be between 0.01 and 0.1 mg/mL for GPC and FPLC, and 0.5 – 0.1 mg/mL for SDS-PAGE (data not shown). The conjugation efficiency ranged from 50 - 100 % and was higher for the LMW dextrins (data not shown). SDS-PAGE analysis of a control sample of a mixture of

Table 3.2 Efficiency of incorporation of succinoyl moieties into dextrin; LMW (7,700 g/mol) and HMW (47,200 g/mol)

Dextrin molecular weight (g/mol)	Theoretical mol %	Actual mol % ± (SD of titration)*	Number of samples	% conversion
7,700	10	10 ± 2	3	101
7,700	21	14 ± 2	2	67
7,700	23	22 ± 1	1	94
7,700	29	24 ± 1	2	84
47,200	5	2 ± 0	1	49
47,200	11	9 ± 1	1	77
47,200	12	10 ± 1	1	83
47,200	20	18 ± 0	1	90
47,200	23	16 ± 1	1	69
47,200	30	26 ± 1	1	87
47,200	41	39 ± 2	1	95
47,200	61	45 ± 2	1	73

* Each sample of succinoylated dextrin was titrated three times

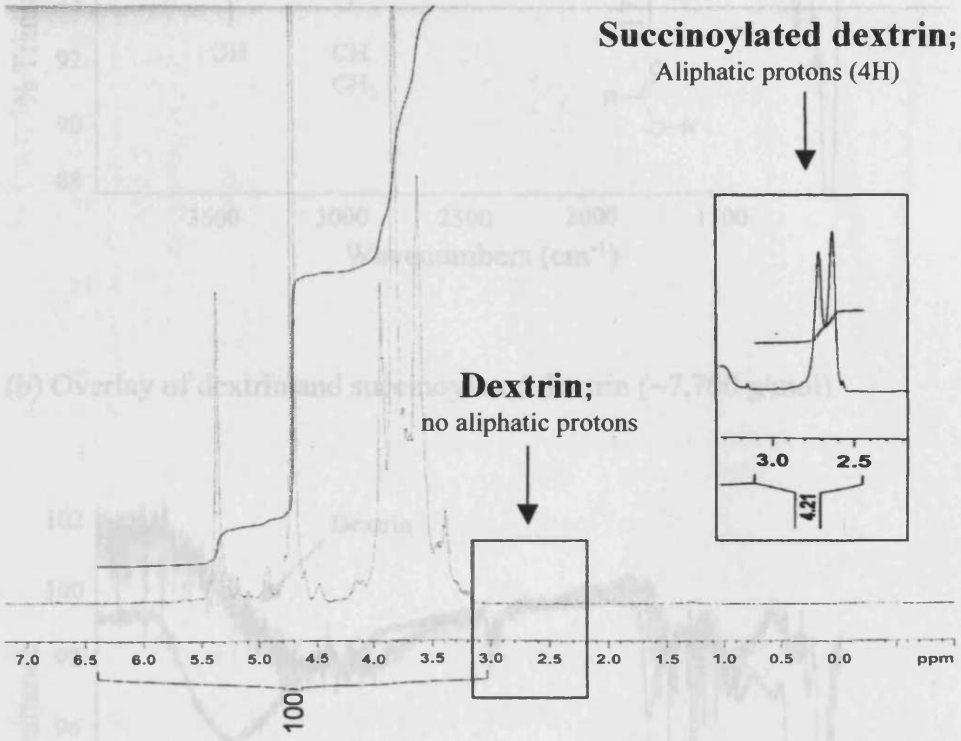

Figure 3.4 ^{1}H NMR spectra of dextrin (~7,700 g/mol) and succinoylated dextrin (inserted panel).

(a) Succinoylated dextrin (~7,700 g/mol)

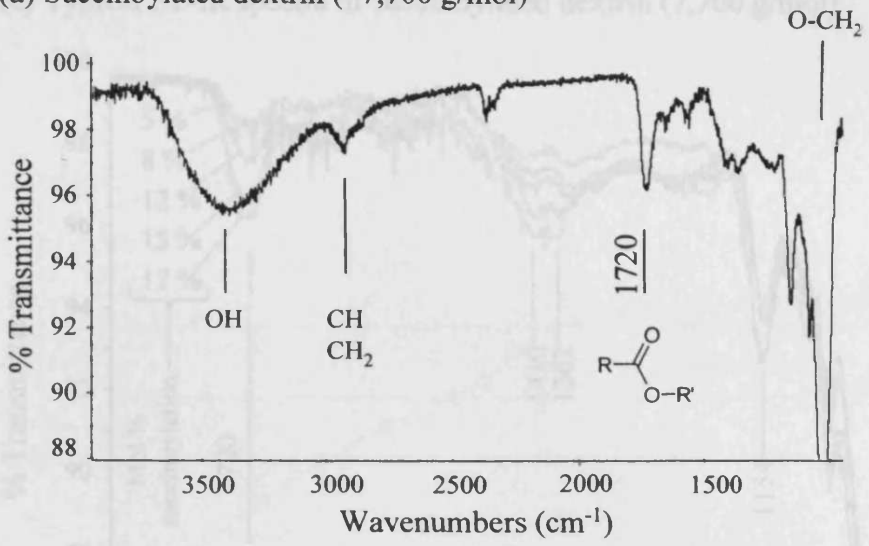

(b) Overlay of dextrin and succinoylated dextrin (~7,700 g/mol)

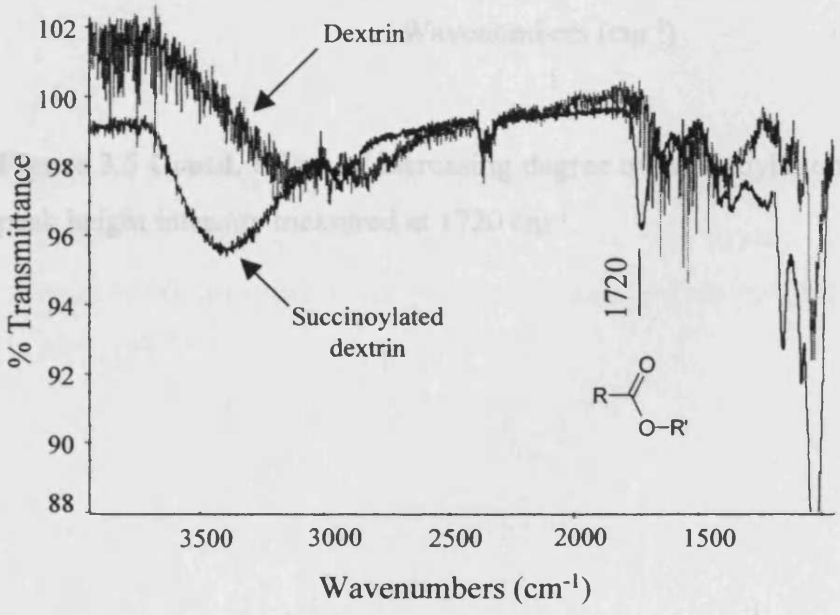

Figure 3.5 FT-IR spectra illustrating the increase in peak intensity at 1720 cm^{-1} when succinoyl ester groups are incorporated into dextrin.

(c) Typical FT-IR spectra of succinoylated dextrin (7,700 g/mol)

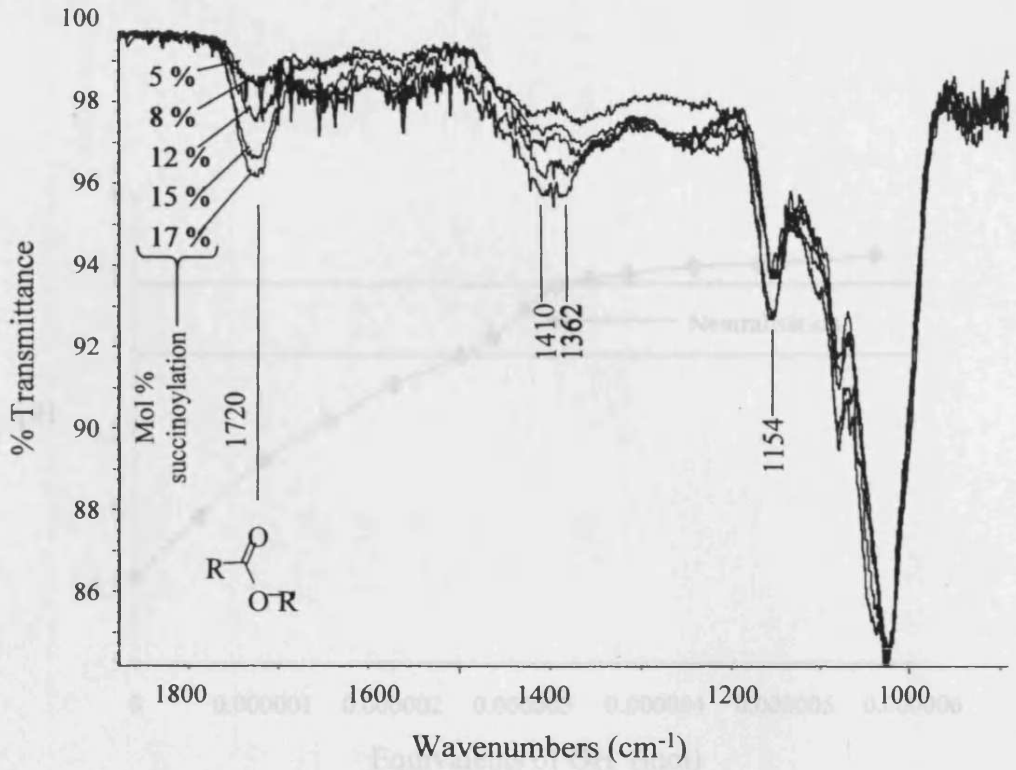

Figure 3.5 Contd. Effect of increasing degree of succinoylation on FT-IR peak height intensity measured at 1720 cm^{-1}.

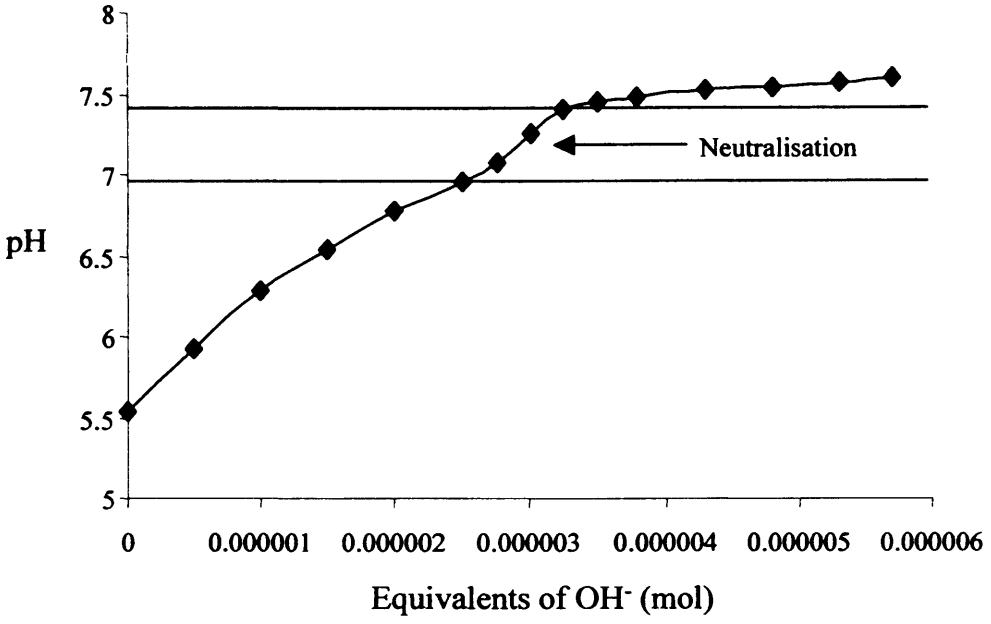

Figure 3.6 Quantification of succinoyl group incorporation by titration of succinoylated dextrin (9 mol %) against NaOH. Bromothymol blue used as an indicator, changing from yellow (pH 6) to blue (pH 7.6).

Table 3.3 Characteristics of succinoylated dextrins carried forward to conjugation reactions with trypsin

Dextrin molecular weight (g/mol)	Actual (mol %)	Number of samples	Mn † (g/mol)	Mw †† (g/mol)	PDI ††† (Mw/Mn)	Batch code
7,700	15	2	10,900	14,600	1.3	SD4(8)
7,700	23	2	9,500	13,500	1.4	SD2(8)
7,700	32	1	11,300	15,500	1.4	SD6(8)
7,700	36	1	9,200	12,100	1.3	SD1(8)
47,200	9	1	42,700	61,300	1.4	SD2(47)
47,200	18	1	41,400	57,800	1.4	SD3(47)
47,200	26	1	39,300	56,500	1.4	SD4(47)

† Mn defines number average molecular weight*

†† Mw defines weight average molecular weight*

††† PDI defines polydispersity index*

*Mn, Mw and PDI were calculated by GPC using pullulan molecular weight standards

(a) GPC chromatogram of dextrin (Mw = 7,700 g/mol)-trypsin conjugates

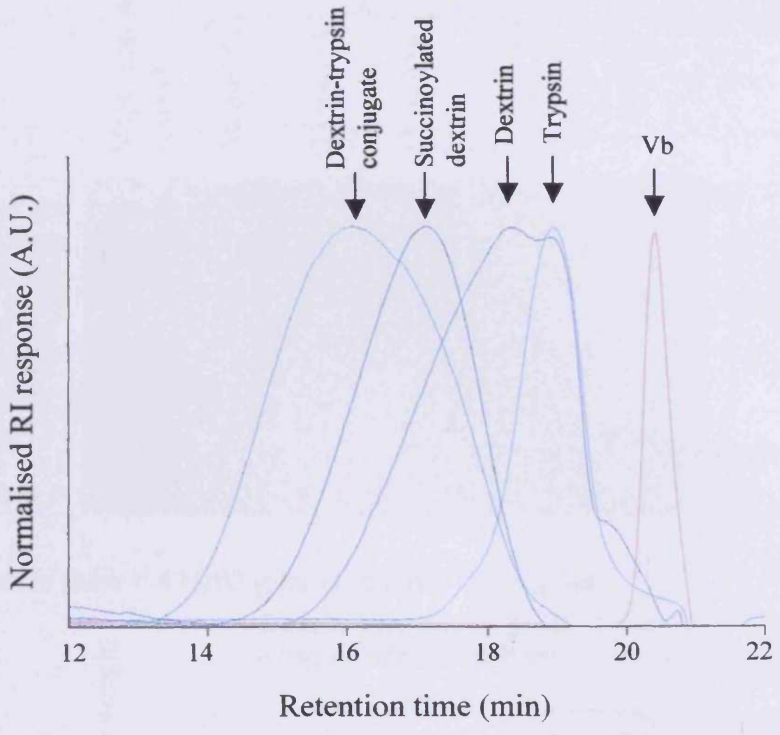

(b) Typical FPLC trace of dextrin (Mw = 7,700 g/mol)-trypsin conjugates

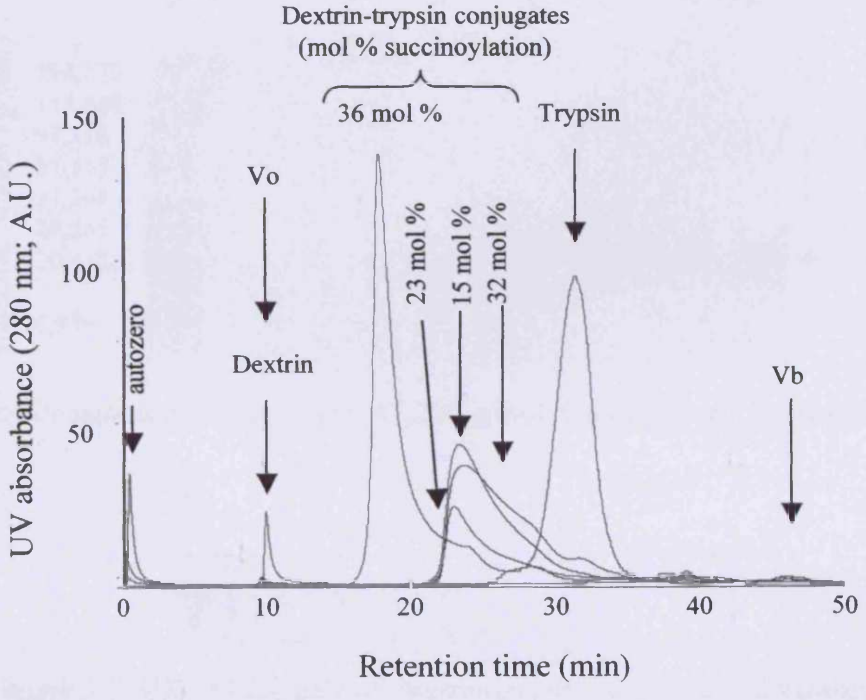

Figure 3.7 Characterisation of typical dextrin-trypsin conjugates by (a) GPC, and (b) FPLC.

(a) Dextrin (Mw = 7,700 g/mol) -trypsin conjugates

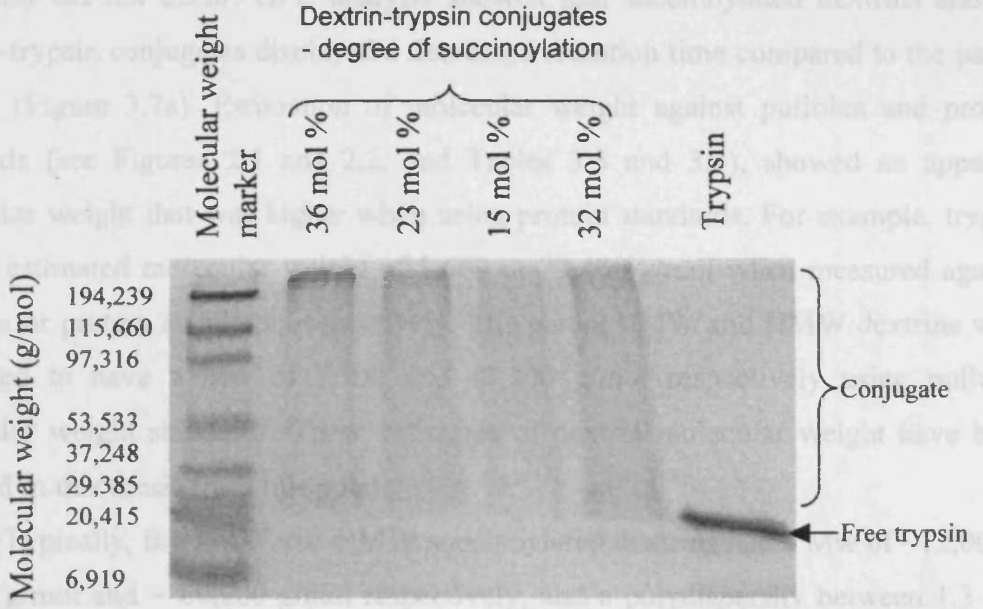

(b) Dextrin (Mw = 47,200 g/mol) -trypsin conjugates

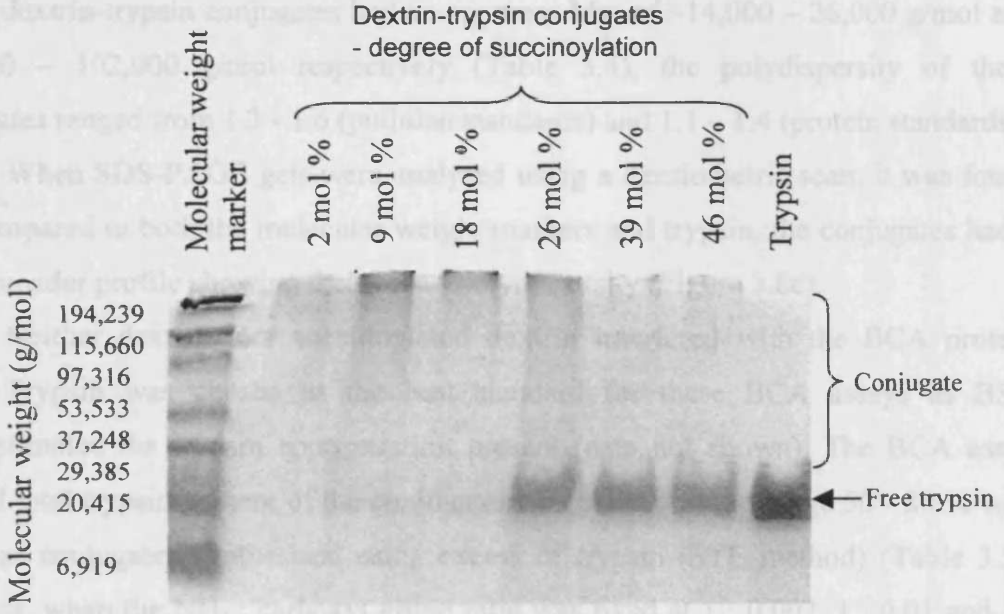

(c) Densiometric scan (Mw = 47,200 g/mol, 9 mol %) -trypsin conjugate

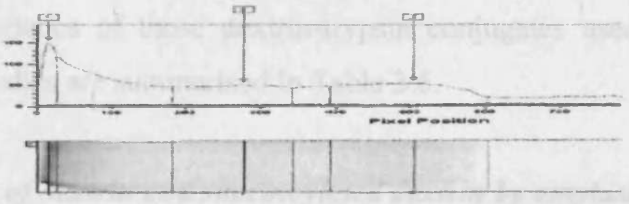

Figure 3.8 SDS-PAGE gels of dextrin-trypsin conjugates illustrating the free and conjugated trypsin. Panel (a) LMW dextrin-trypsin conjugates, (b) HMW dextrin-trypsin conjugates, and (c) a densiometric scan.

succinoylated dextrin and trypsin (data not shown) also confirmed that complex formation did not occur. GPC analysis showed that succinoylated dextrins and the dextrin-trypsin conjugates displayed a decreased retention time compared to the parent dextrin (Figure 3.7a). Estimation of molecular weight against pullulan and protein standards (see Figures 2.1 and 2.2, and Tables 3.3 and 3.4), showed an apparent molecular weight that was higher when using protein standards. For example, trypsin had an estimated molecular weight of 3,660 or 23,400 g/mol when measured against pullulan or protein standards respectively. The parent LMW and HMW dextrins were estimated to have a Mw of 7,700 and 47,200 g/mol respectively using pullulan molecular weight standards. These estimates of dextrin molecular weight have been reported in this thesis from this point.

Typically, the LMW and HMW succinoylated dextrins had a Mw of ~12,000 – 16,000 g/mol and ~ 60,000 g/mol respectively, and a polydispersity between 1.3 and 1.5 using the pullulan molecular weight standards (Table 3.3). Whereas, the LMW and HMW dextrin-trypsin conjugates had an apparent Mw of ~14,000 – 26,000 g/mol and ~49,000 – 102,000 g/mol respectively (Table 3.4), the polydispersity of these conjugates ranged from 1.3 - 1.6 (pullulan standards) and 1.1 – 1.4 (protein standards).

When SDS-PAGE gels were analysed using a densiometric scan, it was found that compared to both the molecular weight markers and trypsin, the conjugates had a much broader profile showing their broad polydispersity (Figure 3.8c).

Neither dextrin, nor succinoylated dextrin interfered with the BCA protein assay. Trypsin was chosen as the best standard for these BCA assays as BSA underestimated the trypsin concentration present (data not shown). The BCA assay showed total trypsin content of the conjugates was usually in the range 50 - 80 % w/w for those conjugates synthesised using excess of trypsin (STE method) (Table 3.5). However, when the NH_2 : carboxyl group ratio was fixed at 1 : 0.002, 1 : 0.01 and 1 : 0.02 (SFR method), the typical protein loading was between 10 and 32 % w/w.

The characteristics of those dextrin-trypsin conjugates used for the enzyme activity (kinetics) studies are summarised in Table 3.5.

3.3.3 Degradation of dextrin and succinoylated dextrin by amylase

A typical GPC elution profile of dextrin incubated with α-amylase is shown in Figure 3.9a, and it can be seen that a decrease in dextrin molecular weight occurred

Table 3.4 Estimation of conjugate molecular weight by GPC, against protein (PR) and pullulan (PS) molecular weight standards

Dextrin molecular weight (g/mol)	Degree of dextrin succinoylation (mol %)	Mn[†] (g/mol)		Mw[††] (g/mol)		PDI[†††] (Mw/Mn)	
		PS[‡]	PR[‡‡]	PS[‡]	PR[‡‡]	PS[‡]	PR[‡‡]
7,700	0	5,200	23,900	7,700	27,400	1.5	1.2
7,700	36	7,800	30,400	10,800	34,000	1.4	1.1
7,700	23	9,500	34,400	14,000	39,300	1.5	1.1
7,700	15	15,600	46,300	25,700	55,000	1.7	1.2
7,700	32	12,900	41,200	19,800	47,700	1.5	1.2
47,200	0	31,200	68,500	47,200	79,000	1.5	1.2
47,200	9	53,600	94,500	84,400	110,600	1.6	1.2
47,200	18	62,400	103,700	101,800	122,900	1.6	1.2
47,200	26	37,500	33,300	49,800	48,200	1.3	1.5
47,200	34	34,200	21,400	46,000	28,400	1.4	1.3
Trypsin	0	3,300	ND[‡‡‡]	3,700	23,400	1.1	ND[‡‡‡]

[†] Mn defines number average molecular weight [††] Mw defines weight average molecular weight [†††] PDI defines polydispersity index

[‡] PS; pullulan molecular weight standards [‡‡] PR; protein molecular weight standards [‡‡‡] ND defines not determined

Table 3.5 Summary of the characteristics of the dextrin-trypsin conjugates used to determine enzyme activity / kinetics

Dextrin molecular weight (g/mol)	Degree of dextrin succinoylation (mol %)	Synthesis code	Mw† (g/mol)	PDI†† (Mw/Mn)	Trypsin content** (% w/w)
7,700	15	STE‡‡	14,600	1.3	72
7,700	23	STE‡‡	13,500	1.4	67
7,700	32	STE‡‡	15,500	1.4	75
7,700	36	STE‡‡	12,100	1.3	81
47,200	9	STE‡‡	61,300	1.4	51
47,200	18	STE‡‡	57,800	1.4	78
47,200	26	STE‡‡	56,500	1.4	76
47,200	2	SFR#	ND‡	ND‡	10
47,200	9	SFR#	ND‡	ND‡	25
47,200	18	SFR#	ND‡	ND‡	32

† Mw defines weight average molecular weight*

†† PDI defines polydispersity index*

* Mw and PDI were calculated by GPC using pullulan molecular weight standards

‡ ND defines not determined

‡‡ STE synthesised using a trypsin excess (1 COOH : 2000 NH_2)

SFR synthesised using a fixed quantity of trypsin (1 NH_2 : 40, 50 and 100 COOH for 2, 9 and 18 mol % succinoylation respectively)

** determined by BCA assay

(a) GPC chromatogram; LMW dextrin degradation

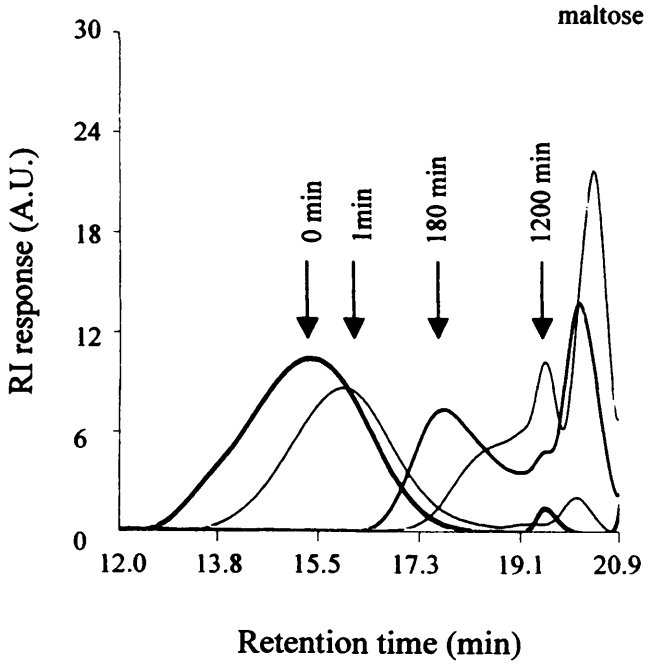

(b) LMW dextrin and succinoylated dextrin degradation

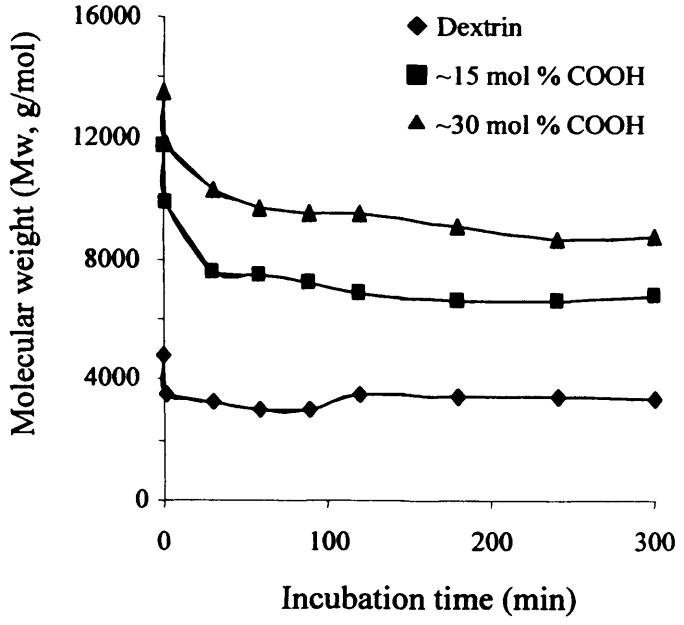

Figure 3.9 Degradation of dextrin and succinoylated dextrin over time, when incubated with the dextrin degrading enzyme amylase. Panel (a) illustrates the change in molecular weight fractions as dextrin is degraded, and (b) shows the change in molecular weight of the main peak fraction over time. Data shown represents n=1.

(c) HMW dextrin and succinoylated dextrin degradation

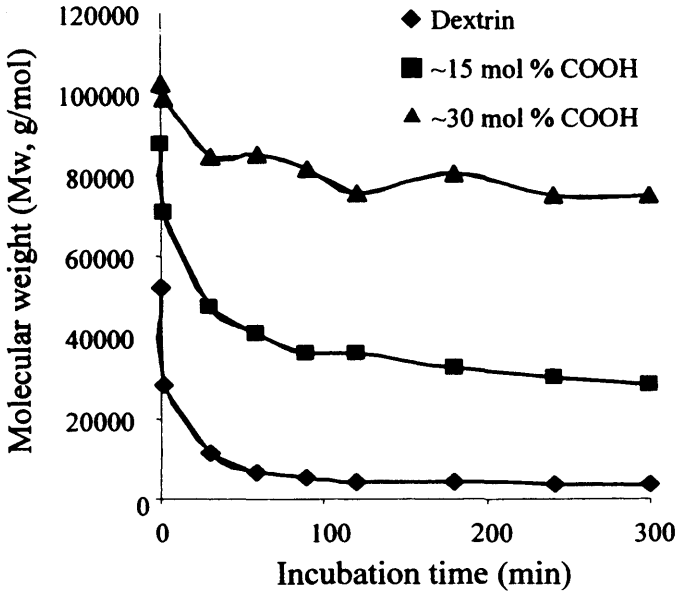

Figure 3.9 Contd. Degradation of dextrin and succinoylated dextrin over time, when incubated with the dextrin degrading enzyme amylase. Panel (c) shows the change in molecular weight of the main peak fraction over time for HMW dextrin and its succinoylated intermediates. Data shown represents n=1.

with time. This was coupled with the appearance of the degradation products (probably maltose and glucose). The molecular weight of the main peak of each sample was estimated against a pullulan standard calibration curve (Figure 2.1), and the decrease in molecular weight with incubation time plotted (Figures 3.9b and 3.9c).

For the parent dextrins molecular weight of 47,200 and 7,700 g/mol, the extent of degradation at 5 h was 95 and 30 % respectively. In contrast, the succinoylated dextrins (~15 mol % and ~ 30 mol %) were degraded more slowly. HMW and LMW dextrins succinoylated to a degree of ~15 mol % showed a decrease in molecular weight of 72 and 46 % respectively over 5 h. Increasing the degree of succinoylation further to ~30 mol % slowed degradation further, and the extent of degradation after 5 h had decreased to 32 and 41 % respectively (Figure 3.9b and c). However, these data should only be considered in terms of a degradation trend, as accurate Mw values are not easy to calculate.

3.3.4 Trypsin activity of free enzyme and dextrin-trypsin conjugates

The UV-vis absorbance spectra of dextrin, succinoylated dextrin, tris buffer, BAPNA and a typical dextrin-trypsin conjugate (spectra not shown) revealed that no absorbance occurred at the wavelength chosen (400 nm) for measuring the production of NAp cleaved from BAPNA. Hence, a control blank cell of tris buffer containing BAPNA (0.007 % w/v, 1.61 x 10^{-4} M in DMSO) was chosen to enable adjustment for background absorbance.

Activity of free trypsin

The rate of NAp released from BAPNA incubated with free trypsin increased as substrate concentration was increased (Figure 3.10a). Two trypsin concentrations were tested, 8.54 x 10^{-6} mol and 8.54 x 10^{-5} mol (Figure 3.10b) using a BAPNA concentration of 0.021 % w/v (4.83 x 10^{-4} M). An initial linear rate of NAp release with time was seen using a trypsin concentration of 8.54 x 10^{-6} mM and BAPNA concentration of 0.021 % w/v (4.83 x 10^{-4} M). Therefore, these conditions were used to measure the activity of the free trypsin control. Greater trypsin activity was observed at 37 °C than 25 °C and a tris buffer pH of 7, although the difference in pH did not have a significant effect on the trypsin activity over the 5 min tested (Figure 3.11).

(a) Varying substrate (BAPNA) concentration

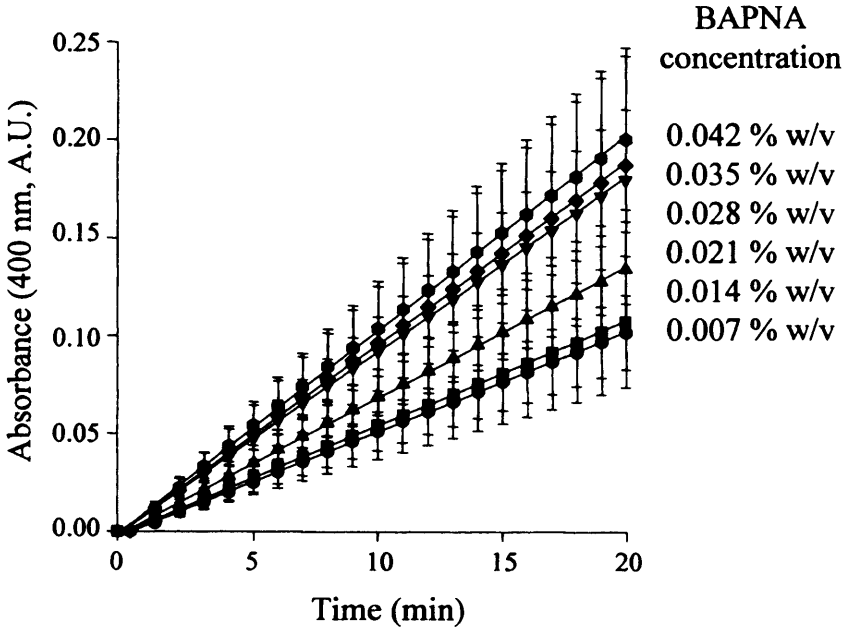

(b) Varying enzyme concentration

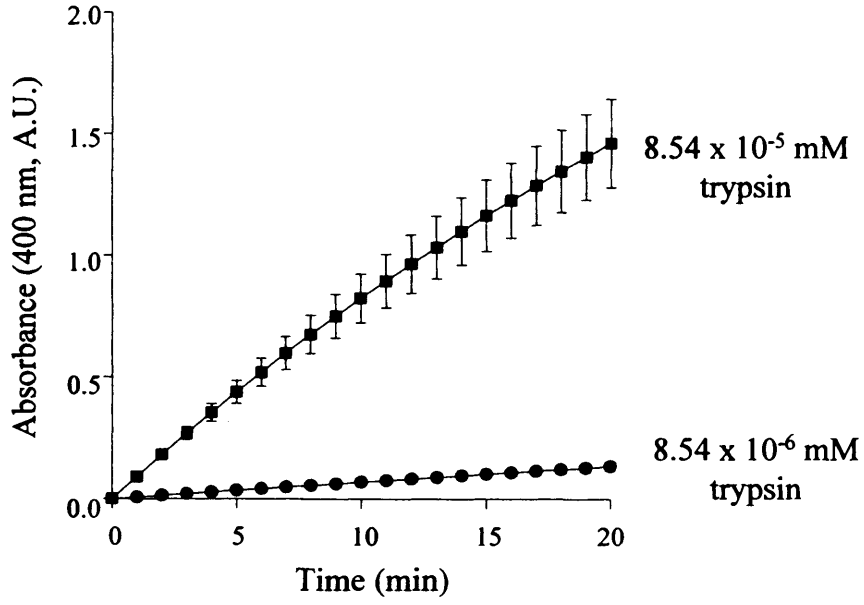

Figure 3.10 Trypsin activity measured using BAPNA. Progress curves show the UV-vis absorbance (400 nm) of NAp cleaved from (a) increasing concentrations of BAPNA by trypsin 8.54 x 10^{-6} mM, and (b) 0.021 % w/v BAPNA by trypsin; 8.54 x 10^{-6} mM (•) and 8.54 x 10^{-5} mM (■), over 20 min. Data shown represents the mean (n=3) ± SD. Where error bars are not visible, error is within the data point.

(a) Varying temperature

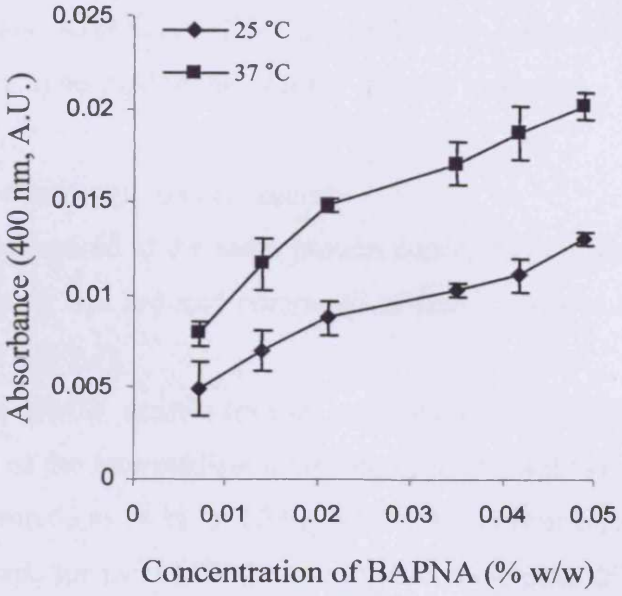

(b) Varying tris buffer pH

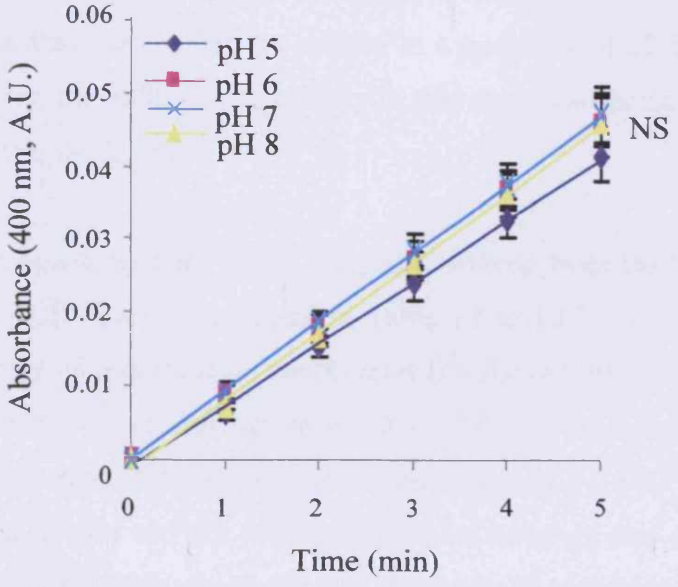

Figure 3.11 Effect of temperature (a) and pH (b) on the cleavage of NAp from BAPNA by trypsin (200 ng, 8.54 x 10^{-6} mM). Absorbance (400 nm) of NAp measured (a) at 5 min, (b) over 5 min. Data shown represents the mean (n=3) ± SD. NS defines no significant difference ($p>0.05$), calculated using ANOVA.

The kinetics of trypsin activity was analysed by the Michaelis-Menten equation using a Hanes-Woolfe plot, Lineweaver-Burk plot and an Eadie-Hofstee plot (Figure 3.12). All three of the Michaelis-Menten derived plots displayed poor linearity. Typically, Km was ~ 0.4 derived from the Hanes-Woolfe plot, Vmax varied with trypsin concentration and Kcat was ~ 2.3 – 2.9 molecules / second (s^{-1}). The Hanes-Woolfe plot was chosen to be used for any further kinetics analysis.

Activity of the dextrin-trypsin conjugates

When compared at the same protein concentration, the activity of the dextrin-trypsin conjugates was reduced compared to free trypsin in all cases (Figure 3.13 – 3.15, Table 3.6 and 3.7).

For the HMW dextrin-trypsin conjugates (STE method), as the degree of succinoylation of the intermediate increased (9 to 26 mol %), the enzyme activity fell significantly from 63 to 34 % ($p < 0.01$, ANOVA and Bonferroni *post hoc* test) (Figure 3.14). In contrast, for the LMW dextrin-trypsin conjugates (STE method), the degree of succinoylation did not influence the remaining enzyme activity, and this was always in the range 51 - 69 % (Figure 3.13).

For the HMW dextrin-trypsin conjugates synthesised using the SFR method, there was also a reduction in enzyme activity to a minimum of 22 % remaining trypsin activity. However, the reduction in activity in this case was unrelated to the degree of succinoylation (Figure 3.15a).

The rate constants Km, Vmax and Kcat, derived from the Hanes-Woolfe plots (Figures 3.13b - 3.15b) are summarised in Table 3.6 and 3.7. The Hanes-Woolfe plots displayed linearity with correlation coefficients (r^2) above 0.98. Conjugation of trypsin to dextrin typically did not alter Km from ~0.3 – 0.4, but the Vmax was reduced ~ 10 fold. The Kcat values calculated remained in the region of 2 – 3 s^{-1}. Kcat did correlate to the expressed trypsin activity, when the slowest turnover rate of 1.1 s^{-1} occurred where the maximal masking of activity was achieved (22 % remaining trypsin activity) (Table 3.6 and 3.7).

(a) Hanes-Woolfe plot

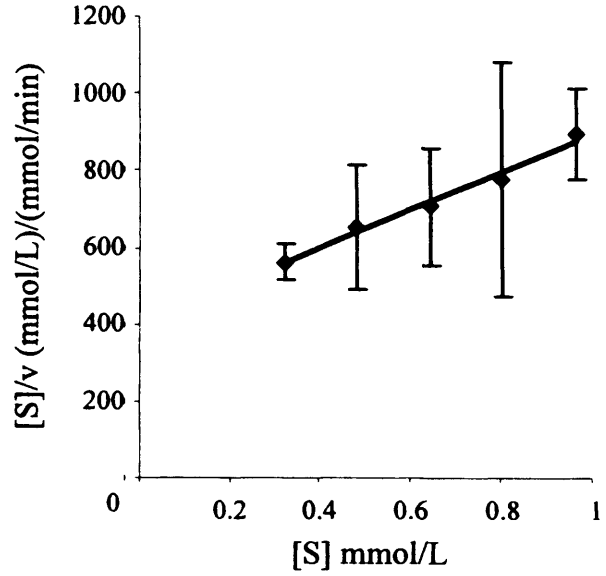

(b) Lineweaver-Burk plot

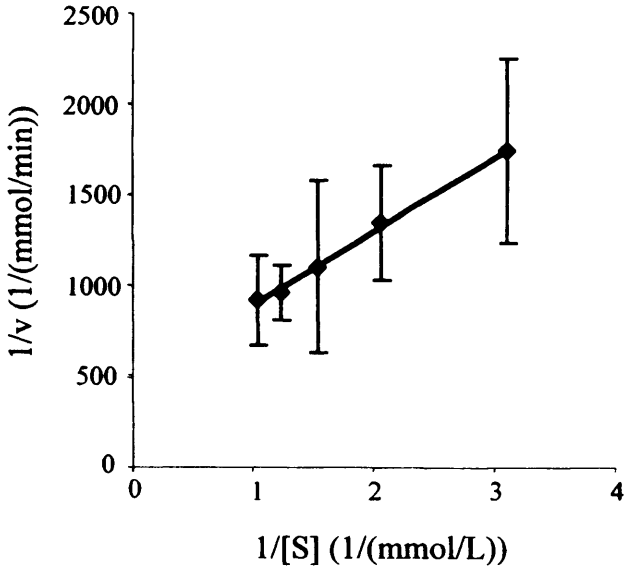

Figure 3.12 Trypsin (8.54 x 10^{-6} mM) activity against the substrate BAPNA (0.014 - 0.042 % w/v in DMSO), releasing NAp. Comparison of Michaelis-Menten plots to determine trypsin kinetics rate constants, where v and S define velocity and substrate concentration respectively. Data shown represents mean (n=3) ± SD.

(c) Eadie-Hofstee plot

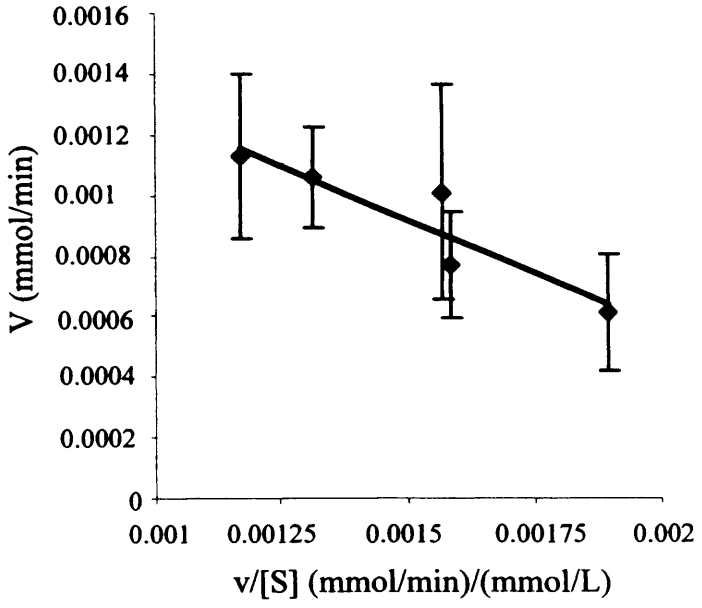

Figure 3.12 Contd. Trypsin (8.54 x 10^{-6} mM) activity against the substrate BAPNA (0.014 - 0.042 % w/v in DMSO), releasing NAp. Comparison of Michaelis-Menten plots to determine trypsin kinetics rate constants. Data shown represents mean (n=3) ± SD.

(a) Trypsin activity; substrate degradation with time

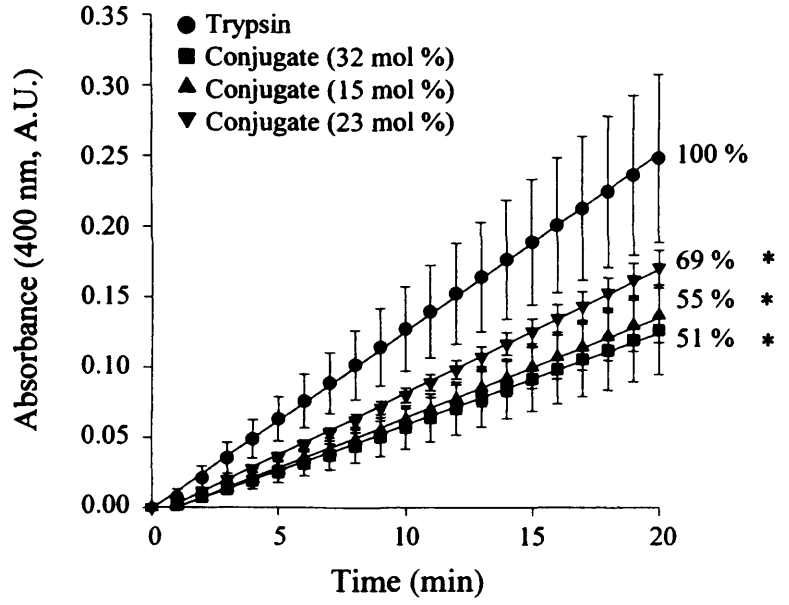

(b) Typical Hanes-Woolfe plot

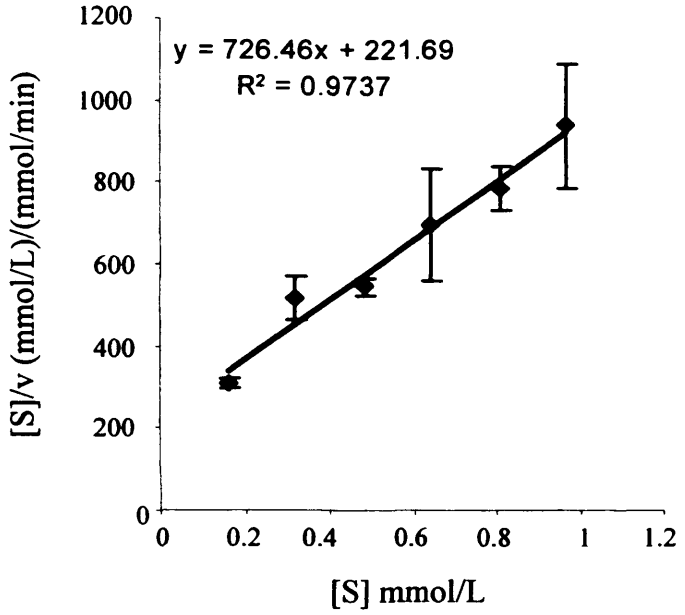

Figure 3.13 Activity of LMW dextrin-trypsin conjugates (STE method) against the substrate BAPNA. Panel (a) Progress curve for absorbance (400 nm) of NAp cleaved from 0.021 % w/v BAPNA by trypsin and dextrin-trypsin conjugates (8.54 x 10^{-6} mM trypsin equiv.) and (b) a typical Hanes-Woolfe plot to determine kinetics rate constants of the dextrin-trypsin conjugates. Data shown represents the mean (n=3) ± SD. * indicates significance compared to free trypsin control, where $p<0.05$ (ANOVA and Bonferroni *post hoc* test).

(a) Trypsin activity; substrate degradation with time

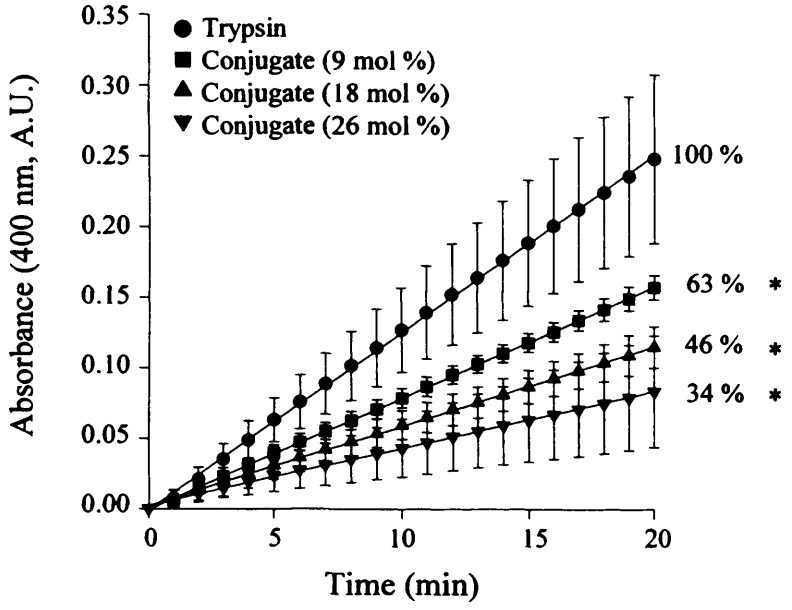

(b) Typical Hanes-Woolfe plot

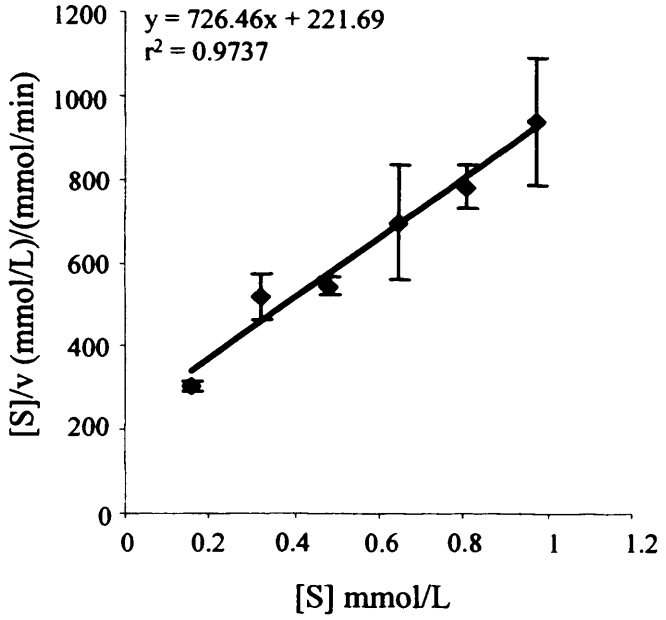

Figure 3.14 Activity of HMW dextrin-trypsin conjugates (STE method) against the substrate BAPNA. Panel (a) Progress curve for absorbance (400 nm) of NAp cleaved from 0.021 % w/v BAPNA by trypsin and dextrin-trypsin conjugates (8.54 x 10^{-6} mM trypsin equiv.) and (b) a typical Hanes-Woolfe plot to determine kinetics rate constants of the dextrin-trypsin conjugates. Data shown represents the mean (n=3) ± SD. * indicates significance compared to free trypsin control, where $p < 0.05$ (ANOVA and Boferroni *post hoc* test).

(a) Trypsin activity; substrate degradation with time

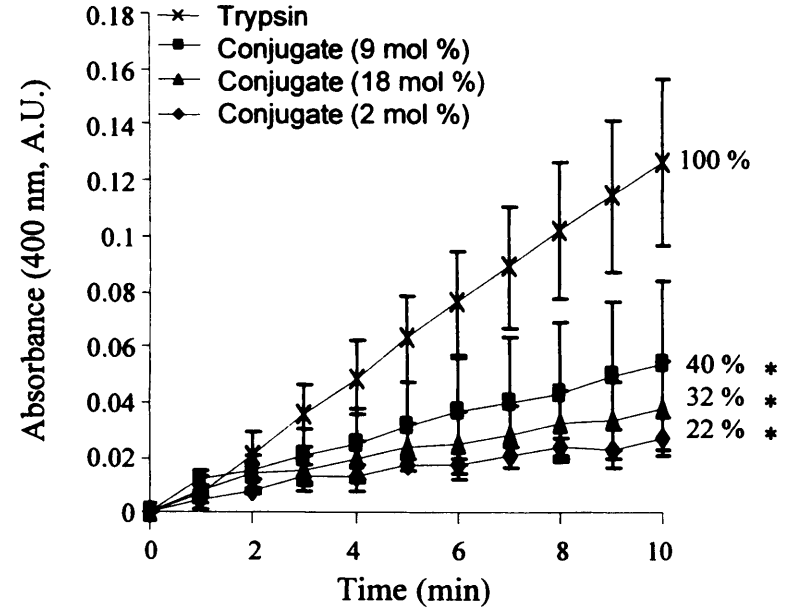

(b) Typical Hanes-Woolfe plot

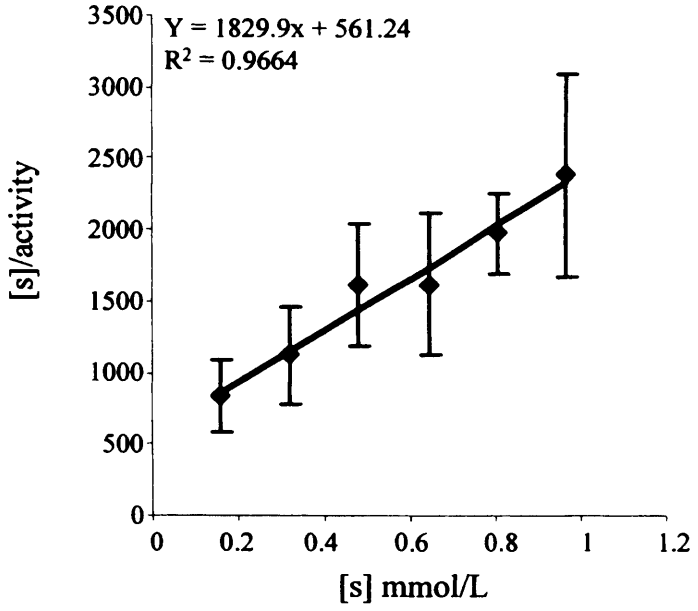

Figure 3.15 Activity of HMW dextrin-trypsin conjugates (SFR method) against the substrate BAPNA. Panel (a) Progress curve for absorbance (400 nm) of NAp cleaved from 0.021 % w/v BAPNA by trypsin and dextrin-trypsin conjugates (8.54 x 10^{-6} mM trypsin equiv.) and (b) a typical Hanes-Woolfe plot to determine kinetics rate constants of the dextrin-trypsin conjugates. Data shown represents the mean (n=3) ± SD. * indicates significance compared to free trypsin, where $p<0.5$ (ANOVA and Bonferroni *post hoc* test).

Table 3.6 Summary of the dextrin-trypsin conjugate activity, and the kinetics rate constants determined for those conjugates synthesised using STE method[‡‡]

Dextrin molecular weight (g/mol)	Degree of dextrin succinoylation (mol %)	% activity remaining	Km[††]	Vmax[†††]	Kcat (s^{-1})[‡]
7,700	15	55	0.33 ± 0.34	0.002 ± 1.1 x 10^{-3}	4.09 ± 2.19
7,700	23	69	0.32 ± 0.15	0.001 ± 9 x 10^{-4}	2.54 ± 1.78
7,700	32	51	0.10 ± 0.18	0.001 ± 3 x 10^{-4}	2.59 ± 0.66
47,200	9	63	0.31 ± 0.09	0.001 ± 1 x 10^{-4}	2.69 ± 0.25
47,200	18	46	0.40 ± 0.29	0.001 ± 4 x 10^{-4}	2.23 ± 0.78
47,200	26	34	0.39 ± 0.04	0.001 ± 2 x 10^{-4}	1.25 ± 0.38

[†] Mw defines weight average molecular weight determined by GPC using pullulan molecular weight standards

[††] Km defines the affinity constant

[†††] Vmax defines maximum velocity

[‡] Kcat defines turnover rate

[‡‡] STE method; synthesised using a trypsin excess (1 COOH : 150 NH_2)

Table 3.7 Summary of the dextrin-trypsin conjugate activity and the kinetics rate constants estimated for those conjugates synthesised using SFR method[‡‡]

Dextrin molecular weight (g/mol)	Degree of dextrin succinoylation (mol %)	% trypsin activity remaining	Km[††]	Vmax[†††]	Kcat[‡] (s^{-1})
47,200	2	22	0.31 ± 0.28	$0.001 \pm 1.8 \times 10^{-4}$	1.07 ± 0.32
47,200	9	40	0.59 ± 0.50	$0.001 \pm 1.9 \times 10^{-3}$	2.52 ± 1.32
47,200	18	32	0.26 ± 0.32	$0.001 \pm 4.8 \times 10^{-4}$	1.33 ± 0.32

[†] Mw defines weight average molecular weight determined by GPC using pullulan molecular weight standards

[††] Km defines the affinity constant

[†††] Vmax defines maximum velocity

[‡] Kcat defines turnover rate

[‡‡] SFR method; synthesised using a fixed quantity of trypsin (1 NH_2 : 40, 50 and 100 COOH for 2, 9 and 18 mol % succinoylation respectively

(a) Trypsin activity

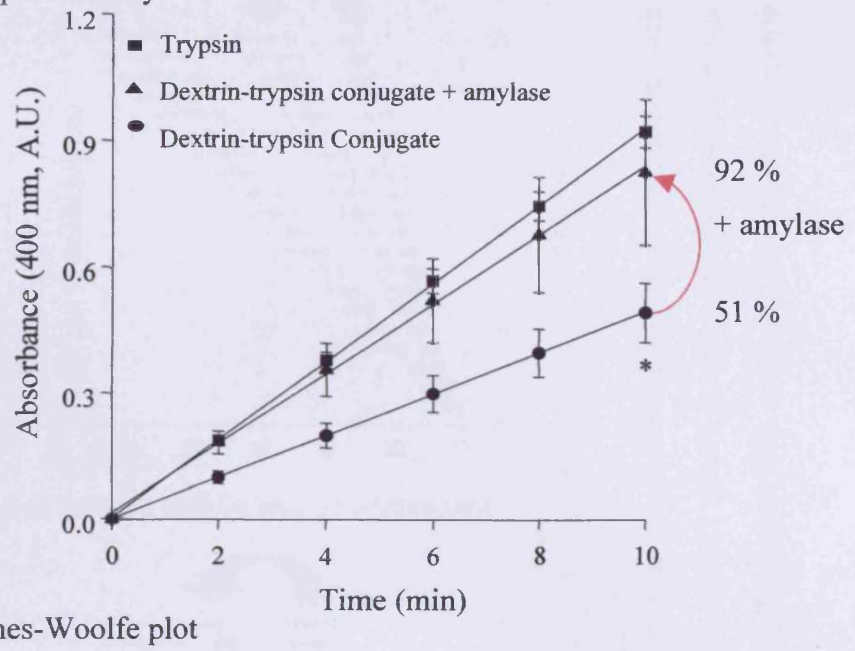

(b) Hanes-Woolfe plot

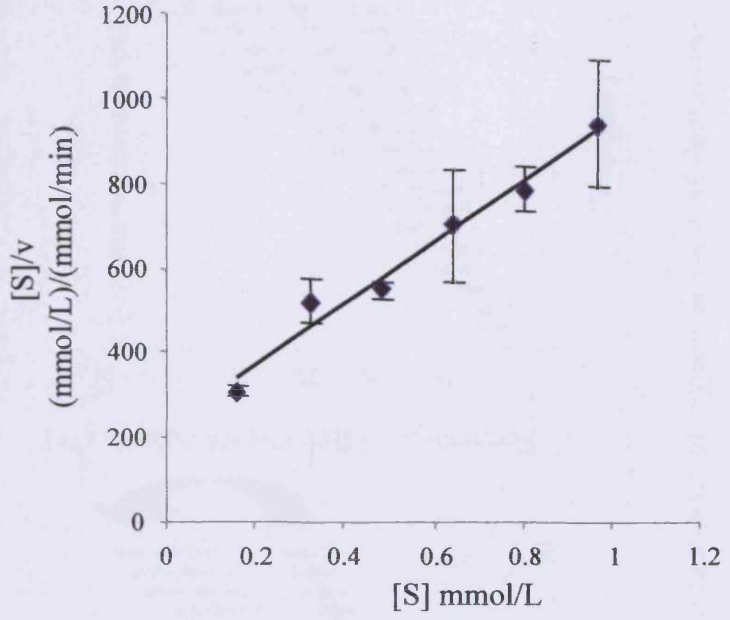

Figure 3.16 Typical reinstatement of trypsin activity of dextrin-trypsin conjugates following overnight incubation with amylase. Panel (a) progress curve for absorbance (400 nm) of NAp cleaved from 0.021 % w/v BAPNA by trypsin and LMW dextrin-trypsin conjugate (8.54×10^{-5} mM trypsin equiv.; 7,700 g/mol conjugate, ~32 mol % succinoylation). Panel (b) a typical Hanes-Woolfe plot to determine kinetics rate constants of trypsin activity following incubation with amylase. Data shown represents the mean (n=3) ± SD. * indicates significance ($p<0.05$) compared to trypsin control, calculated by ANOVA and Bonferroni *post hoc* test.

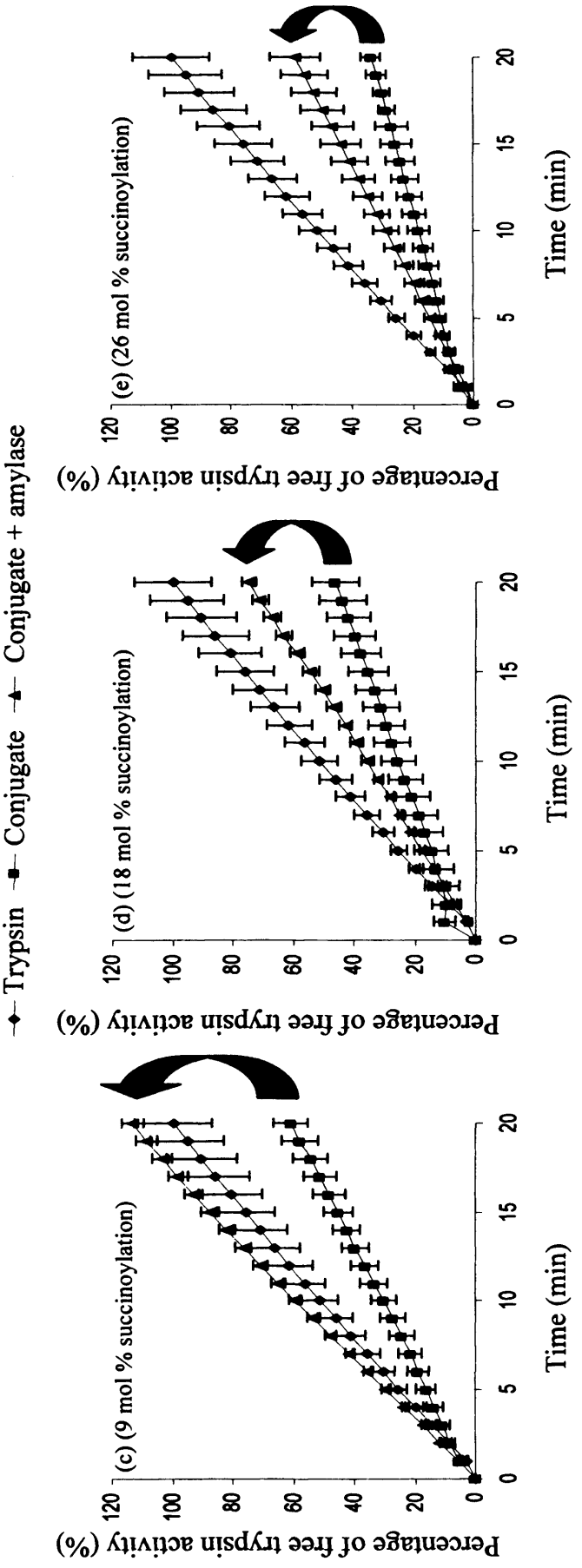

Figure 3.16 Contd. Typical reinstatement of trypsin activity of dextrin-trypsin conjugates following overnight incubation with amylase. Panel (c-e) Progress curves for the absorbance (400 nm) of NAp cleaved from 0.021 % w/v BAPNA by trypsin and dextrin-trypsin conjugates (47,200 g/mol, 9 - 26 mol % succinoylation) prior to and following incubation with amylase. Data shown represents the mean (n=3) ± SD.

Table 3.8 Summary of dextrin-trypsin conjugate activity and the kinetic constants obtained for dextrin-trypsin conjugates (STE method)[‡‡] following degradation of dextrin by amylase

Dextrin molecular weight (g/mol)	Degree of dextrin succinoylation (mol %)	% trypsin activity remaining	% activity following polymer degradation	Km[††]	Vmax[†††]	Kcat[‡] (s^{-1})
7,700	15	55	67	0.29 ± 0.07	$0.007 \pm 2 \times 10^{-4}$	1.27 ± 0.05
7,700	23	69	52	0.25 ± 0.27	$0.007 \pm 2.9 \times 10^{-3}$	1.26 ± 0.57
7,700	32	51	92	0.36 ± 0.07	$0.012 \pm 2.8 \times 10^{-3}$	2.30 ± 0.54
47,200	9	63	115	0.20 ± 0.07	$0.013 \pm 1.6 \times 10^{-3}$	2.49 ± 0.31
47,200	18	46	64	0.53 ± 0.23	$0.012 \pm 3.6 \times 10^{-3}$	2.40 ± 0.71
47,200	26	34	58	0.96 ± 0.34	$0.013 \pm 1.7 \times 10^{-3}$	2.49 ± 0.33

[†] Mw defines weight average molecular weight determined by GPC using pullulan molecular weight standards

[††] Km defines the affinity constant

[†††] Vmax defines maximum velocity

[‡] Kcat defines turnover rate

[‡‡]STE method; synthesised using a trypsin excess (1 : 15 molar ratio of COOH : trypsin)

3.3.5 Effect of amylase on the activity of dextrin-trypsin conjugates

Addition of amylase to the dextrin-trypsin conjugates led to an increase in trypsin activity (Figure 3.16, Table 3.8). In this case the optimum conjugate for the LMW dextrin (STE method) was modified to 32 mol % and reduced trypsin activity to 51 % on conjugation, with an increase to 92 % of trypsin activity on addition of amylase.

Similarly, HMW dextrin (26 mol % succinoylation, STE method) conjugation led to a reduction in trypsin activity to 34 % measured over 20 min, and on addition of amylase, reinstated trypsin activity to 58 % of the free trypsin control. All conjugate activity was found to be significantly different from the native trypsin ($p < 0.05$, ANOVA and Bonferroni *post hoc* test) indicating an incomplete reinstatement of activity.

Unfortunately, dextrin-trypsin conjugate activity studies following polymer degradation were only conducted on conjugates synthesised using the STE method, owing to limited time available.

Kcat was typically in the range of 1.2 – 2.5 s^{-1}. Both Km and Vmax were consistently higher for conjugated trypsin following polymer degradation (Table 3.8).

3.4 Discussion

The overall aim of these first studies was to synthesise dextrin-trypsin conjugates using dextrins of different molecular weight and degrees of succinoylation (up to 34 mol %), in order to (i) establish whether triggered degradation by amylase could reinstate enzyme activity, and (ii) give some indication of the optimum synthetic conditions.

A library of both succinoylated dextrins (LMW and HMW) and dextrin-trypsin conjugates were synthesised (Table 3.3 and 3.5), and used to assess the masking / unmasking hypothesis. The overall efficiency of the succinoylation reaction for the HMW dextrins was 70 - 90 % (as determined by titrimetric analysis). This was greater than the 50 % conversion efficiency reported by Hreczuk-Hirst et al., (2001b) (Table 3.2 and 3.9). As Brunneel and Schacht (1994) found that titration and NMR gave consistent quantification of the degree of succinoylation of pullulan, so the reason for this difference is not clear. Succinoylation of the LMW dextrin was achieved with a near 100 % conversion efficiency, implying that dextrin molecular weight, and or

Table 3.9 Comparison of reaction yield for dextrin succinoylation reported by Hreczuk-Hirst et el., (2001b) and in this work

Dextrin Mw† (g/mol)	Reaction time (h)	Theoretical mol % modification	Actual mol % modification ± SD (n=3)	Number of batches	% conversion	Reference
~50,000	8	30	16 ± 1	3	52	Hreczuk-Hirst et al (2001b)
~47,200	8*	30	14 ± 1	1	46	This research
~47,200	16	30	26 ± 1	1	87	This research

† Mw defines weight average molecular weight determined by GPC using pullulan molecular weight standards

* pilot reaction to repeat succinoylation reaction carried out by Hreczuk-Hirst et al., 2001b

steric hindrance may be factors affecting the efficiency of the succinoylation reaction for the HMW dextrin. Succinoylated dextrins of Mw 7,700 or 47,200 g/mol were subsequently synthesised to give a library with modifications of 2 - 32 mol % succinoylation (Table 3.2).

GPC analysis of the dextrins (Mw ~7,700 and 47,200 g/mol) and their succinoylated dextrin intermediates (0 - 32 mol %) revealed a decrease in retention time for the succinoylated intermediates related to the parent dextrin (Figure 3.7). This might be explained due to the incorporation of carboxyl groups into the polymer backbone, which would be expected to increase the hydrodynamic radius. This observation was consistent with the earlier studies that showed a higher than expected molecular weight for dextrins with a higher degree of modification (Hreczuk-Hirst et al., 2001b).

It should be noted that the dextrin and dextrin-trypsin conjugate molecular weights estimated using GPC are not absolute values. When protein and pullulan standards were used to estimate the molecular weight, the differences seen between the values estimated using the two standards was significant. This is illustrated by the values estimated for dextrin; Mw of 7,700 g/mol and 27,400 g/mol, and trypsin; Mw of 23,400 g/mol and 3,660 g/mol, when the GPC profiles were analysed using either protein or pullulan standards respectively.

Pullulan is a typical polysaccharide and would be expected to display a random coil in solution. This would be closest to the structure expected for dextrin. The globular structure of proteins makes them unsuitable to estimate the molecular weight of such linear polysaccharides, but of course would be most appropriate to analyse trypsin. Pullulan was chosen as the most appropriate standard, however, it is clear that the molecular weights of the dextrin-trypsin conjugates are most difficult to estimate. This is due to the difference in solution conformation of polymer standards, the protein standards and the protein conjugate which is a mixture.

Those dextrin-trypsin conjugates carried forward to enzyme activity and kinetics studies are summarised in Table 3.5.

Trypsin activity

Trypsin activity was assessed using assay conditions (40 mM tris HCl, pH 8.2 and 16 mM Ca^{2+}) previously described by John (1998), and at 37 °C. These conditions

are almost identical to those used in another study that compared ovine and porcine trypsin (Johnson et al., 2002) using BAPNA as the substrate and a temperature range of 25 - 55 °C. These assay conditions contrast experiments that use BAEE as the substrate. BAEE has been used more frequently (Fernandez et al., 2002; Fernandez et al., 2003; Fernandez et al., 2004a; Fernandez et al., 2004b; Villalonga et al., 2000) to study trypsin activity, but is less trypsin-specific. In the study of Johnson et al., (2002) 10 mM $CaCl_2$ was used in the tris buffer instead of the 16 mM $CaCl_2$ used in this work, added to the buffer to prevent autolysis and maintain trypsin stability in solution (SIGMA, 1995). This may explain the slight variation detected (Table 3.10).

Trypsin was also analysed in tris buffer within its optimum pH range (7 – 9) (Buck et al., 1962). The difference in immediate activity between pH 6 - 8 was negligible (Figure 3.11) and so tris buffer pH 8 was chosen to reflect the optimum pH specified in the literature (Johnson et al., 2002; Stevens, 1998).

Dextrin-trypsin conjugate activity

Assay conditions that gave an initial linear rate of substrate degradation were established and then used to determine the effect of dextrin molecular weight and degree of succinoylation in the conjugates on trypsin activity. As might have been expected, significant masking of activity ($p < 0.01$, ANOVA and Bonferroni *post hoc* test) was better achieved using the HMW dextrin (22 – 34 %) compared to the LMW dextrin (51 %). This was likely to be due to the greater steric hindrance caused by the larger, bulkier polymer (molecular weight 47,200 g/mol), blocking the trypsin active site.

Increasing extent of dextrin succinoylation was also found to reduce the remaining trypsin activity of the HMW dextrin-trypsin conjugates prepared using the STE method (Figure 3.14). The degree of succinoylation did not however affect either the activity of LMW dextrin-trypsin conjugates prepared using STE method, or for the HMW dextrin-trypsin conjugates prepared using the SFR method (Figures 3.13 and 3.15). This may be because the larger polymer may have the potential to cause more steric hindrance.

Secondly, protein loading may have been a factor in the ability of HMW dextrin to mask trypsin activity of conjugates. The dextrin-trypsin conjugates prepared using the STE method, typically contained ~ 80 % w/w trypsin loading. Whereas,

Table 3.10 Comparison of enzyme kinetic parameters derived from non-linear regression analysis and kinetics software

Trypsin (mM / units)	Substrate in DMSO	Kinetics constant	Hanes-Woolfe plot	Lineweaver-Burk plot	Eadie-Hofstee plot	Literature: LUCENZ III*
8.54×10^{-6}	BAPNA‡	Km†	0.41 ± 0.55	0.18 ± 0.01	0.20 ± 0.03	ND#
		Vmax††	$0.002 \pm 6 \times 10^{-4}$	$0.001 \pm 2 \times 10^{-4}$	$0.001 \pm 3 \times 10^{-4}$	ND#
		Kcat†††	2.93 ± 1.24	2.19 ± 0.46	2.34 ± 0.52	ND#
8.54×10^{-5}	BAPNA‡	Km†	0.38 ± 0.04	0.33 ± 0.05	0.27 ± 0.09	ND#
		Vmax††	$0.013 \pm 8 \times 10^{-4}$	$0.012 \pm 8 \times 10^{-4}$	$0.012 \pm 1.2 \times 10^{-3}$	ND#
		Kcat†††	2.52 ± 0.15	2.39 ± 0.16	2.30 ± 0.24	ND#
80-450 units‡‡	BAPNA‡	Km†	ND#	ND#	ND#	$*0.002 \pm 2 \times 10^{-4}$
		Vmax††	ND#	ND#	ND#	ND#
		Kcat†††	ND#	ND#	ND#	$*2.89 \pm 0.16$

† Km defines the affinity constant

†† Vmax defines maximum velocity

††† Kcat defines turnover rate

‡ BAPNA defines N-benzoyl-L-arginine-p-nitroanilide

‡‡ Units of activity against the substrate BAEE; Na-benzoyl-arginine-ethyl-ester

* literature values taken from Johnson et al., (2002)

ND; not determined

when the degree of succinoylation of dextrin was increased but the quantity of trypsin kept constant (SFR method of synthesis), a much lower trypsin loading was achieved (19 - 53 % w/w). Nevertheless, there was no clear relationship between molecular weight, degree of polymer functionalisation and the trypsin content of the resultant conjugates and their subsequent ability to mask protein activity. Ideally, the activity of the enzyme payload would be masked completely (100 %). Although this was not achieved here, the best conjugate would mask trypsin activity to the greatest extent and still enable some reinstatement of activity.

Michaelis-Menten kinetics

It was considered important not only to describe enzyme activity but to try and establish kinetic parameters. Many graphical analysis methods are used to analyse enzyme kinetics. All are based on the assumption that the Michaelis-Menten equation applies (Cornish-Bowden, 2004; Tipton, 1998). Most frequently used are the Lineweaver-Burk, Hanes-Woolfe and Eadie-Hofstee plots (Samoshina and Samoshin, 2005). Despite the popularity of the Lineweaver-Burk plot, it has been proven to be the most statistically unreliable (Cornish-Bowden, 2004; Samoshina and Samoshin, 2005). Similarly, the Eadie-Hofstee plot has been critisised for introducing error to both axes. Although the Hanes-Woolfe plot is not statistically ideal, the errors shown by this type of plot are believed to be lowest if a reasonable range of substrate concentrations are used in the experimental design (Cornish-Bowden, 2004). Hence, the Hanes-Woolfe plot was chosen for data analysis in this study. The main requirements of a linear reaction rate velocity with both time, and enzyme concentration, and a correction made for blank absorbance (Cornish-Bowden, 2004) were met to enable application of Michaelis-Menten based data analysis.

Although Km and Vmax were determined, it is known that experimental conditions, such as temperature and pH, and the method of measurement can cause variability in the Km values obtained. This is discussed further in Samoshina and Samoshin (2005). Vmax can also vary with enzyme purity and enzyme concentration (Cornish-Bowden, 2004; Samoshina and Samoshin, 2005). However, the constant Kcat is not subject to the same variability as Km and Vmax. The Kcat values determined for the dextrin-trypsin conjugates synthesised in this study were comparable to both the value determined for free trypsin in this study (Kcat 2.5 – 2.9 s^{-1}), and the published value reported for porcine trypsin (analysed under almost identical conditions using the

substrate BAPNA) i.e. Kcat = 2.89 s^{-1} (Table 3.10) (Johnson et al., 2002). Furthermore, there was no obvious relationship between increasing degree of dextrin succinoylation and either the Kcat of the conjugate or the degree of enzyme activity expressed following the degradation of dextrin.

Amylase triggered activation of dextrin-trypsin conjugate activity

Hreczuk-Hirst et al., (2001a) previously showed that increasing degree of succinoylation (to 34 mol %) decreased the rate of degradation of dextrin of molecular weight ~50,000 g/mol by amylase. Dextran has also been shown to have a reduced rate of degradation when chemically modified by methods including periodate oxidation and succinoylation (Vercauteren et al., 1990; Vercauteren et al., 1992). Furthermore, it was shown that the degradability of a dextrin conjugate was linked to the extent of drug loading (up to 12 % w/w) (Hreczuk-Hirst et al., 2001a). In these experiments, this was also the case, and dextrin maintained degradability up to the 32 mol % succinoylation tested. The dextrin-trypsin conjugates incubated with amylase for 16 h demonstrated protein release from the conjugates with concurrent reinstatement of trypsin activity. The greater trypsin activity was masked by dextrin conjugation, the less its activity was restored following dextrin degradation by amylase. For example, the greatest reduction in trypsin activity seen was to 34 % of the free trypsin control, but addition of amylase only reinstated activity to 58 % of the control. This might be because a part of the conjugation linkage or glucose oligomer still remains attached to the trypsin active site. With a longer incubation time with amylase it would be possible to test whether enzyme activity could have been restored to a greater extent.

3.5 Conclusions

Dextrin-trypsin conjugates were successfully synthesised using both the LMW and HMW dextrins. Dextrin conjugation to trypsin was able to mask enzyme activity within the range of 22 - 34 % of native trypsin activity. This activity could subsequently be regenerated using amylase-triggered polymer degradation.

Overall, the HMW dextrin with a high degree of succinoylation (26 mol %) and high protein loading (~80 % w/w), showed the most effective reduction and reinstatement of trypsin activity.

Chapter 4

Amylase triggered activation of dextrin-MSH conjugates: conjugate synthesis and biological characterisation

4.1 Introduction

Having shown that the unmasking concept could be applied to a model enzyme, trypsin, the study was extended to investigate its ability to modify the properties of a peptidyl ligand that acts by binding to a specific receptor (Figure 4.1). For this purpose, the peptide hormone MSH was chosen as a model ligand.

4.1.1 Rationale for choosing MSH as a model peptide

MSH has been used to target daunomycin (by direct conjugation) (Varga et al., 1977), to target microspheres and macrospheres (Sharma et al., 1996), and for targeting of HPMA copolymer-doxorubicin conjugates (O'Hare et al., 1993). A summary of MSH delivery systems are listed in Table 4.1.

The aim of these studies was the site-specific delivery of anti-cancer agents to melanoma cells. *In vivo* studies in mice with s.c. B16F10 tumours, showed that MSH-HPMA copolymer-doxorubicin, administered IP, was more effective as an anti-tumour agent than doxorubicin without MSH. The work was supported by preliminary pharmacokinetic studies demonstrating the selective targeting of the labelled conjugates to B16F10 cells.

Before describing the main objectives of this study, the MSH receptor and the assays available to test MSH activity will be briefly discussed. The structure and physiological function of MSH were previously described in Chapter 1 (section 1.7.2.2).

4.1.2 The MSH receptor

The MSH receptor is present on human melanocytes and keratinocytes as well as on melanoma cells (Sharma et al., 1996). There is currently debate regarding the effect of cell cycle on MSH receptor expression. In one case, non-synchronised cells incubated with MSH for 30 min demonstrated complete binding, suggesting expression was independent of cell cycle (Sharma et al., 1996), but earlier studies (Varga et al., 1974) found that when Cloudman cells had been synchronised, MSH was only effective in the G2 phase of the cell cycle. Additionally, O'Hare et al., (1993) using B16F10 cells showed that MSH activation of melanin production was lost with an increasing number of days in culture. Similarly, McQuade et al., (2005) showed that culture media affected MC-R1 expression, reducing it from 8009 ± 1606 receptors /

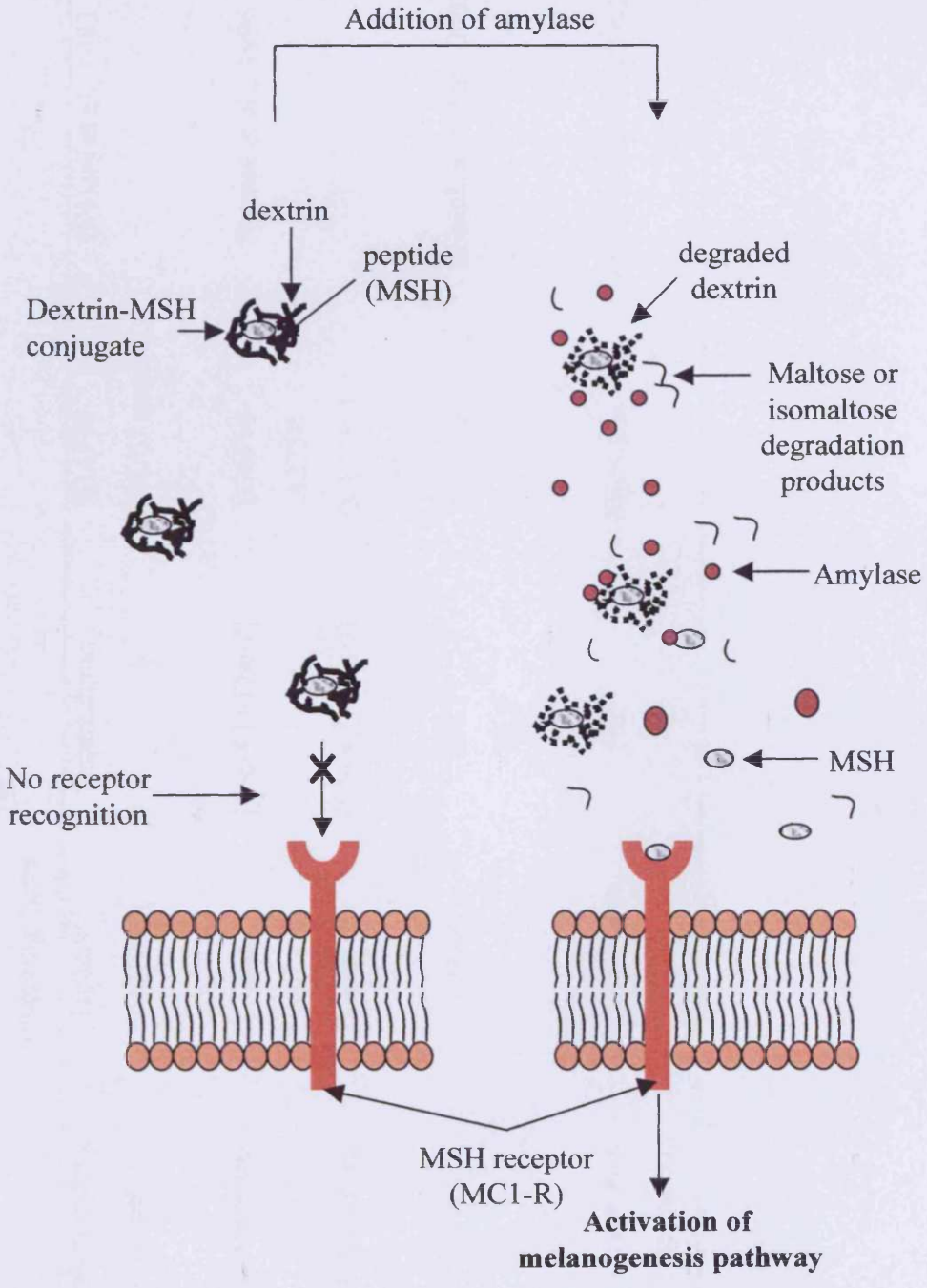

Figure 4.1 Hypothesised concept of masked peptide activity and reinstatement of activity following amylase triggered degradation of dextrin; application to extracellular targeting of the MSH membrane bound receptor MC1-R. Dextrin ( ) is degraded by amylase ( ) in the extracellular space, to release conjugated MSH ( ).

Table 4.1 Application of MSH and its derivatives in drug delivery systems

Peptide	Delivery system	Polymer / conjugating agent	Other agents	Cell line / model	Reference
α-MSH	Polymer-drug conjugates	HPMA[‡‡] copolymer	Doxorubicin	B16F10 C57BL/6J mice	O'Hare et al., 1993
α-MSH	Microsphere	Latex	[Nle-4,D-Phe-7]	B16F10 A375P	Sharma et al.,, 1996
	Macrosphere	Polyamide	[Nle-4,D-Phe-7]	NCI-N592 MCF-7	
α-MSH	Plasmid	Plasmid	MRT[†] HLP[†] PS[†]	B16F10	Rosenkranz et al., 2003
α-MSH	Biodegradable polymer matrix	Nitrocellulose	NS[††]	Microglia	Zhang and Bellamkonda, 2005

Contd.

Table 4.1 Application of MSH and its derivatives in drug delivery systems (Contd).

Peptide	Delivery system	Polymer / conjugating agent	Other agents	Cell line / model	Reference
α-MSH	Peptide conjugates	PVA	FITC	B16F10 A375P NCI-N592 MCF-7	Sharma et al., 1994
Melanotan-I (MT-1)	Biodegradable polymer matrix	Poloxamer 407 (Pluronic F127)	PVP MC HPMC	Guinea pig (IP)	Bharowaj et al., 1996
Melanotan-I (MT-1)	Biodegradable polymer matrix	PLGA (50:50)‡	NS††	NS††	Bhardwaj and Blanchard, 1998
Melanotan-II	Gelfoam biodegradable disk	Unknown	Unknown	NS††	Pinsuwan et al., 1997

† MRT; modular recombinant transporter, HLP defines hemoglobin like protein, PS defines photosensitiser

†† NS is an abbreviation for not stated

‡ PLGA; poly(DL-lactide-co-glycolide)

‡‡ HPMA copolymer is an abbreviation for N-'(2-hydroxypropyl)methacrylamide

cell to 3191 ± 139 receptors / cell, when B16F10 cells were cultured in DMEM-HG or RPMI 1640 respectively (McQuade et al., 2005).

The MSH receptor aggregates prior to internalisation. Free MSH will competitively inhibit MSH conjugated to microspheres (Sharma et al., 1996). In other experiments, MSH receptor recognition was found to be unaffected by its conjugation to melphalan (Ghanem et al., 1991) and in this case synthesis of conjugates improved receptor affinity.

4.1.3 Assays of MSH activity

There are several well established MSH assays (Eberle, 1988; O'Hare et al., 1993) (summarised in Table 4.2), determining either melanin production or tyrosinase activity. Two main cell types are used in these *in vitro* assays; B16F10 and Cloudman S91 cells. B16F10 cells were chosen for this study because they have been used to assess HPMA copolymer-MSH conjugates in this laboratory in the past (O'Hare et al., 1993). B16F10 cells have both a greater sensitivity to MSH than Cloudman S91 melanoma cells, and a lower EC_{50} (the effective concentration needed to achieve 50 % response) (Table 4.2). Assay of melanin release was preferred to the tyrosinase assay due to its reproducibility and simplicity (Eberle, 1988). As this was a modification of the O'Hare et al., (1993) protocol, the effects of media supplementation with tyrosine (0.3 – 0.4 mM) were investigated here. These conditions were recommended to ensure that melanin production is independent of available tyrosinase substrate (Eberle, 1988). It should be noted that B16F10 cells have also been widely used as a screening model for anticancer polymer-drug conjugates both *in vitro* and *in vivo*. Moreover, they have been extensively characterised in this research group (Centre for Polymer Therapeutics, Cardiff University) in terms of endocytosis and intracellular trafficking of polymer-anticancer conjugates and polycations used for gene delivery (Seib et al., 2007; Xyloyiannis, 2004).

As a small peptide, MSH has been shown to be susceptible to degradation by serum enzymes (discussed in Sawyer et al., 1980), the melanin assays were conducted using heat inactivated serum (56 °C, 30 min) (Al-Obeidi et al., 1992; Sawyer et al., 1980) to assess the effects of serum on the stability and activity of dextrin-MSH conjugates.

Table 4.2 *In vitro* bioassays used to determine MSH activity (adapted from Eberle, 1988)

Assay name	Basis of assay	Detection limit (mol/mL)	EC_{50}[†] (mol/L)
Rana pipiens	NS[††]	2.5×10^{-15}	2.5×10^{-11}
Hyla arborea	NS[††]	4×10^{-15}	-
Anolis carolinensis:	Photometric / visual		
	Rate	5×10^{-14}	2×10^{-10}
		5×10^{-14}	1×10^{-10}
Xenopus laevis tadpoles	Microscopic		
	Photometric	3×10^{-13}	5×10^{-10}
		4.5×10^{-13}	7×10^{-10}
Bufo arenarum	NS[††]	1×10^{-15}	6×10^{-12}
Ctenopharyngodon idellus	NS[††]	4×10^{-13}	1×10^{-9}
B16F10 murine melanoma cells	Tyrosinase		
	Melanin production	3×10^{-14}	1.6×10^{-10}
		$0.5 - 1 \times 10^{-14}$	2.7×10^{-11}
Cloudman S91 melanoma cells	Tyrosinase		
		3×10^{-13}	2.5×10^{-9}

[†] EC_{50} signifies the concentration required to achieve 50 % efficacy [††] NS; not specified

4.1.4 Optimisation of the conjugation of dextrin to the peptide MSH

The method used in Chapter 3 for the conjugation of dextrin (26 mol % succinoylation) to trypsin was used again to conjugate MSH to succinoylated dextrin using the coupling agents EDC and sulfo-NHS (Figure 4.2). Others have shown that conjugation of MSH to biotin, using the coupling agents N,N'carbonyldiimidazole and N-hydroxysuccinimide, can be directed to the N-terminal of MSH without subsequent reduction in MSH activity (Chaturvedi et al., 1984). This was attributed to the fact that the terminal SER-TYR-SER sequence is not required for receptor recognition, whereas the tetrapeptide sequence 'HIS-PHE-ARG-TRP' has been identified as being required for receptor recognition (Hruby et al., 1987). When conjugating MSH (source not specified) to daunomycin using a 1 : 2.2 molar ratio, Varga et al., (1977) found that conjugation occurred via lysines in positions 6 and 17, and also the terminal aspartic acid residue (position 1). Thus they had identified three potential binding sites. The pKa values of those amino acids in MSH that may be potential conjugation sites for succinoylated dextrin are shown in Figure 4.2.

4.1.5 Aims and objectives of this chapter

In summary, the main aims of these studies were:

- To adapt the dextrin conjugation and purification method of Chapter 3 to synthesise the peptide conjugate 'dextrin-MSH', utilising dextrin of HMW 47,200 g/mol with 26 mol % succinoylation. Variables assessed:
  - Ratio of reactants
  - Purification method
- Tailoring of the polymer-protein conjugate characterisation methods employed to assess the peptide MSH.
- To optimise the melanin assay (O'Hare et al., 1993) to enable measurement of MSH activity in the dextrin-MSH conjugate. The following variables were assessed:
  - Time MSH was added
  - Time when melanin production is measured
  - Concentration of MSH
  - Media composition
    - FBS or heat inactivated FBS
    - Presence / absence of tyrosine

(i) Conjugation of succinoylated dextrin (26 mol %) to MSH

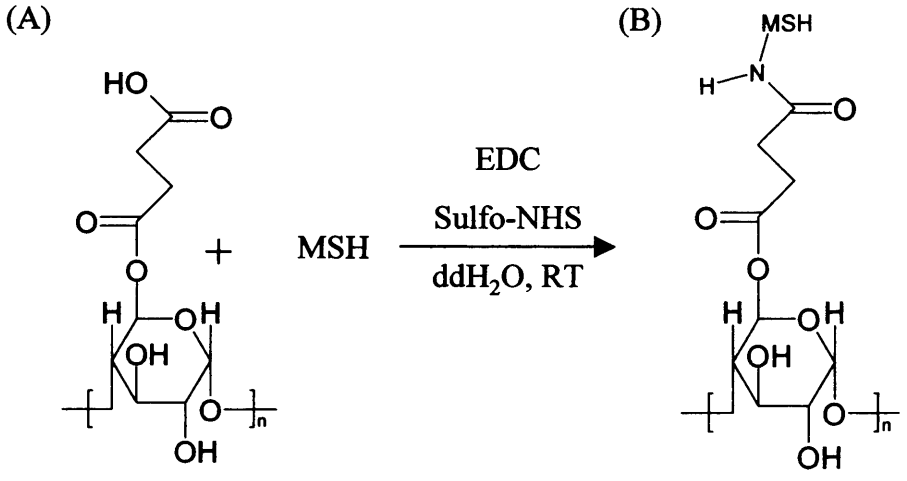

(ii) MSH amino acid sequence

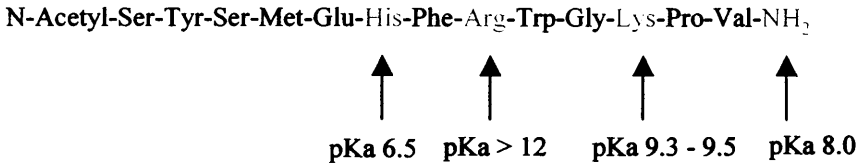

Figure 4.2 Conjugation of succinoylated dextrin to MSH. Panel (i) reaction scheme and (ii) amino acid sequence of MSH, identifying potential amine groups for conjugation. Compounds: (A) succinoylated dextrin and (B) dextrin-MSH conjugate.

- To determine the biological activity of MSH and the dextrin-MSH conjugates by measuring melanin production in B16F10 cells.
- To adapt the melanin assay to enable measurement of dextrin-MSH conjugate activity following polymer degradation. In order to do this two factors needed to be determined, (i) the degradation of dextrin-MSH conjugates in the two possible media, and (ii) the effect of amylase on B16F10 cell viability.

4.2 Methods

Dextrin (47,200 g/mol) was succinoylated to 26 mol % COOH incorporation, as described in Chapter 3, section 3.2.1 (Figure 3.1d). The methods used to characterise both the succinoylated dextrin and the dextrin-MSH conjugates were previously described in Chapter 2. For succinoylated dextrin, these included FT-IR (section 2.2.2.2), titration (section 2.2.2.1) and GPC (section 2.2.2.3). Whereas, to characterise the dextrin-MSH conjugate, the basic methods for GPC (section 2.2.2.3), FPLC (section 2.2.3.4), BCA assay (section 2.2.3.2) and SDS-PAGE (section 2.2.3.3) previously described in Chapter 2, were tailored to the assessment of the peptide MSH, described in section 4.2.2.

General cell culture techniques, including maintenance and seeding of B16F10 cells and the MTT assay of cell viability have also been described in Chapter 2 (section 2.2.4.6).

Synthesis and characterisation of dextrin-MSH conjugates

4.2.1 Conjugation of succinoylated dextrin to the peptide MSH

The typical conjugation reaction, described in Chapter 3 (section 3.2.3), was adapted to enable the conjugation of HMW succinoylated dextrin (26 mol %) to the peptide MSH using the coupling agents EDC and Sulfo-NHS (Figure 4.2). Two key changes were made to the reaction conditions when conjugating MSH to succinoylated dextrin. Firstly, the ratio of carboxylic acid groups (COOH) on the succinoylated dextrin to peptide was changed to 1 COOH : 5 MSH (i.e. 1 COOH : 20 NH_2). For example; 30 mg (5.15×10^{-7} mol) succinoylated dextrin was reacted with 5 mg (2.6×10^{-6} mol) MSH. The reaction was then run over 16 h at RT.

Secondly, the dextrin-MSH conjugates were purified by FPLC fractionation, described in section 2.2.1.2. The isolated conjugate fraction was then desalted using a

Vivaspin centrifugal filter (section 2.2.1.4), and the resulting conjugate frozen in liquid N_2 and lyophilised (48 h).

4.2.2 Characterisation of dextrin-MSH conjugates

Dextrin-MSH conjugates were characterised by GPC using TSK-gel columns G4000PW_{XL} and G3000 PW_{XL} in series as described in section 2.2.2.3, with dextrin and succinoylated dextrin as reference samples. FPLC was also utilised, using a Superdex HR 10/30 size exclusion column, to determine whether any free MSH was left in the conjugate. A reference sample of free MSH was used (section 2.2.3.4). Conjugate formation and purity was further assessed using SDS-PAGE (section 2.2.3.3) using samples of free MSH and molecular weight markers to calibrate the assay. Finally, the MSH content of the purified dextrin-MSH conjugates was quantified using a BCA assay (section 2.2.3.2) against an MSH standard curve.

4.2.3 Maintenance and characterisation of B16F10 murine melanoma cells

B16F10 cells were maintained in RPMI 1640 (+ Glutamax) media + 10 % FBS and split twice weekly at a ratio of 1 : 9, as described in section 2.2.4.2 (Table 2.3). For experiments, B16F10 cells were counted and seeded into 96 well flat-bottomed plates at the required seeding density, and then allowed to adhere for 24 h (as described in section 2.2.4.3).

To establish the optimum seeding density of B16F10 cells and their doubling time, growth curves were constructed using the MTT assay (section 2.2.4.6) for initial seeding densities of 2.5 x 10^4, 5 x 10^4 and 1 x 10^5 cells/mL. B16F10 cell proliferation was also investigated in the presence of RPMI containing 10 % heat inactivated FBS, to determine the effect of using heat inactivated serum on the cell growth and viability. Bright-field microscopy was used to visualise cell morphology, and in some studies bright-field images of the cells were acquired using an inverted Leica DM IRB fluorescence microscope (section 2.2.4.5).

4.2.4 MSH-induced melanin release as an indirect method to monitor MSH receptor expression over time

Previously, O'Hare et al., (1993) demonstrated that MSH receptor expression by B16F10 cells decreased over time after subculture. It was also observed that following the addition of MSH, melanin production reached a plateau at 72 h. In order

to confirm these observations, and to optimise the melanin assay for this work, the following were determined;

- The optimum time to add MSH after subculturing the B16F10 cells
- The optimum time to measure melanin production after addition of MSH

B16F10 cells were seeded in 96 well plates to a density of 2.5 x 10^4 cells/mL. After 24 h, the incubation media was removed and MSH dissolved in complete media (RPMI + 10 % FBS) was added to the wells (100 µL) to give a final concentration of 10^{-10} M. The cells were then incubated (37 °C) for a further 72 h, after which the absorbance of the samples in the 96 well plate were read at 405 nm using a Tecan plate reader to quantify the total melanin produced in both the cells and cell culture media. This assay was repeated varying both the final concentration of MSH added (10^{-4} M – 10^{-10} M), and the time after subculture that the MSH was added (24 - 148 h) (Figure 4.3). After the addition of MSH, the production of melanin was measured (405 nm) every 24 h for 6 days. Following these experiments, melanin assays were typically carried out with addition of MSH 24 h post subculture of B16F10 cells, and measurement of melanin production (at 405 nm) at 72 h after the addition of MSH.

4.2.5 Experiments conducted to optimise MSH-induced melanin production

A series of experiments were conducted to study variables described in the literature (O'Hare et al., 1993; Eberle, 1988; Meier, 2002) that might have an impact on the MSH stimulated melanin production by B16F10 cells. The variables were tested using the above method (section 4.2.4) and were:

(i) Solvent used to dissolve MSH; media or PBS / media (1 : 1)
(ii) Presence of tyrosine (0.3 mM) in the cell culture medium
(iii) B16F10 cell seeding density from 2.5 x 10^4, 5 x 10^4 and 1 x 10^5 cells/mL
(iv) MSH concentration from 10^{-4} - 10^{-10} M

4.2.6 Effect of tissue culture media composition on the degradation of dextrin-MSH conjugates

The molecular weight distribution of dextrin-MSH conjugate, dextrin and succinoylated dextrin was monitored during incubation in tissue culture media (RPMI + 10 % FBS or RPMI + 10 % heat inactivated FBS diluted 1 : 20 in PBS; pH 7.4) using GPC. A final sample concentration of polymer or conjugate of 1 mg/mL was

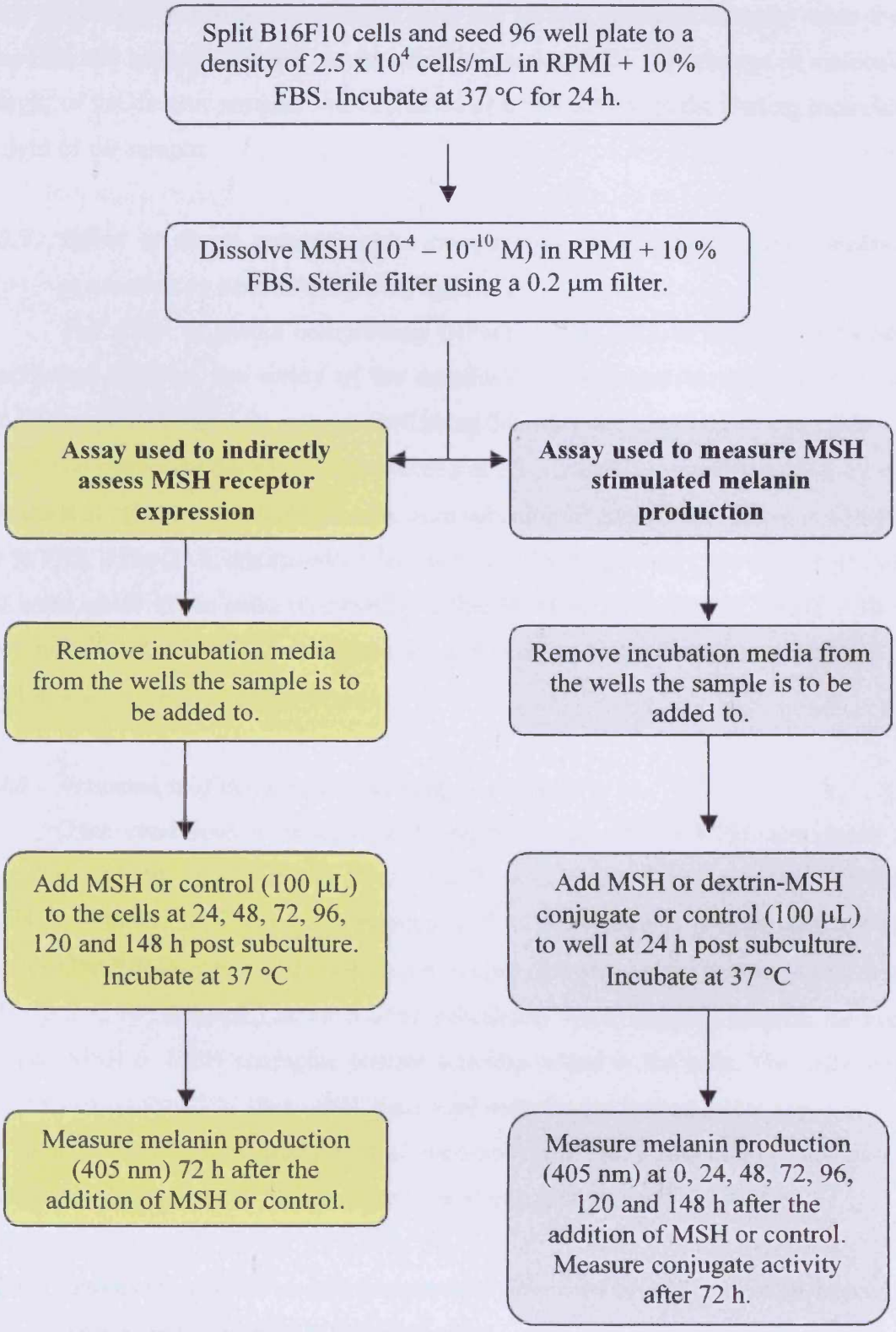

Figure 4.3 Schematic diagram showing the assays used to measure melanin release from B16F10 murine melanoma cells after addition of MSH, dextrin-MSH conjugates or media control.

used. Aliquots (200 μL) of incubation medium were withdrawn at t = 0 and 16 h, and they were snap frozen in liquid N_2 to stop any further reaction. Samples were then prepared and analysed by GPC as described in section 3.2.4. The change in molecular weight of the dextrin samples was expressed as a percentage of the starting molecular weight of the sample.

4.2.7 Effect of tissue culture media composition on MSH stimulated melanin production by dextrin-MSH conjugates

The effect of media composition (RPMI +10 % FBS or RPMI +10 % heat inactivated FBS) on the ability of the dextrin-MSH conjugate to stimulate melanin production in B16F10 cells was assessed using the assay described in section 4.2.8.

To inactivate the FBS, it was heated at 56 °C for 30 min as described by Al-Obeidi et al., (1992). The B16F10 cells were subcultured into 96 well plates in RPMI + 10 % FBS. After 24 h, dextrin-MSH conjugate (10^{-4} M MSH equiv.) or free MSH (10^{-4} M) were added to the cells, dissolved in either RPMI + 10 % FBS or RPMI + 10 % heat inactivated FBS. The remainder of the assay was conducted as described in section 4.2.8.

4.2.8 Assessment of dextrin-MSH conjugate activity

Once conditions were optimised, the ability of dextrin-MSH conjugates to stimulate melanin production in B16F10 cells was analysed and compared to free MSH as follows: MSH (both conjugated 10^{-4} M MSH equiv. or free MSH) were dissolved in RPMI + 10 % FBS and sterile filtered (0.2 μm) before addition to B16F10 cells (2.5 x 10^4 cells/mL) at 24 h after subculture. As a negative control, medium without MSH or MSH conjugate present was also added to the cells. The cells were then incubated for 72 h, after which time total melanin production was assayed at 405 nm using a Tecan pate reader, as described above. Melanin production induced by dextrin-MSH conjugate or MSH was expressed as a percentage of the control.

4.2.9 Optimisation of the media composition and amylase concentration required to degrade the dextrin-MSH conjugates

In order to try and optimise the conditions required for the assessment of dextrin-MSH conjugate activity, following amylase-mediated polymer degradation, preliminary experiments were conducted:

(a) Maximum no effect dose of amylase on B16F10 cell viability. An MTT assay was used to determine B16F10 cell viability in the presence of amylase as described below. B16F10 cells were seeded at a density of 2.5 x 10^4 cells/mL. The effect of the addition of amylase, PEI and dextran (0.001 – 1 mg/mL) dissolved in either RPMI + 10 % FBS or RPMI +10 % heat inactivated FBS, on B16F10 cell viability was then measured. Cell viability measured in the presence of test compounds was expressed as a percentage of the control cells exposed only to the respective media controls. Cell viability was subsequently calculated and expressed as the mean ± SD.

(b) The effect of the addition of amylase dissolved in both media compositions on the MSH stimulated melanin production by B16F10 cells. To study the effect of amylase and media composition on MSH-induced melanin production, the following media and amylase compositions were used:

(a) RPMI + 10 % FBS
(b) RPMI + 10 % heat inactivated FBS
(c) RPMI + 10 % FBS + amylase 0.2 mg/mL
(d) RPMI + 10 % heat inactivated FBS + 0.2 mg/mL amylase

B16F10 cells were seeded into 96 well plates (2.5 x 10^4 cells/mL) and incubated for a further 24 – 148 h at 37 °C. At each time point, the incubation medium was removed, and MSH (final concentration of 10^{-6} M) dissolved in the media compositions (a-d) was added (100 μL) to each well. The cells were then incubated for a further 72 h. The absorbance of melanin synthesised by the cells was read at 405 nm using a Tecan plate reader and the melanin produced expressed as the mean ± SD.

4.2.10 Determination of melanin induction by dextrin-MSH conjugates in the presence of amylase

The optimum conditions for the assessment of dextrin-MSH conjugate activity in the presence of amylase were shown to be:

- Amylase 0.2 mg/mL (10 ui/mL)
- RPMI + 10 % heat inactivated FBS
- MSH added 24 h post subculture

In order to study the effect of conjugate unmasking by amylase on biological activity, these conditions were applied, as follows.

A dextrin-MSH conjugate (10^{-4} M MSH equiv.) was dissolved in RPMI + 10 % heat inactivated FBS and sterile filtered (0.2 μm). This solution was then incubated with amylase (10 ui/mL) for 16 h. The incubation media was removed from a 96 well plate containing B16F10 cells (2.5 x 10^4 cells/mL incubated for 24 h after subculture). The samples; dextrin-MSH conjugate (10^{-4} M MSH equiv.) ± amylase, free MSH (10^{-4} M) or media alone (100 μL) were added. The plates were incubated (37 °C) for a further 72 h. The absorbance of total melanin synthesised by the cells (both located in the cells and cell culture medium) was read at 405 nm using a Tecan plate reader. The melanin levels determined were then expressed as a percentage of melanin seen in the free MSH control.

4.3 Results

4.3.1 Synthesis and characterisation of dextrin-MSH conjugates

The characteristics of the dextrin-MSH conjugates synthesised are summarised in Table 4.3. Dextrin-MSH conjugates when purified by FPLC fractionation (Figure 4.4) eluted in fractions 6 – 10 (mL), whereas the free MSH was eluted as three peaks in fractions ~ 16, 19 and 22 (mL). After FPLC fractionation, GPC analysis of the pooled fractions confirmed conjugate formation (Figure 4.5). The absence of free MSH was also confirmed by FPLC and SDS-PAGE (data not shown). The first conjugates synthesised had an MSH content in the range of ~ 14 % w/w. However, when the initial pilot reactions were scaled-up, the reaction efficiency improved, resulting in conjugates that contained 37 % w/w MSH loading.

4.3.2 Effect of media composition and the presence of amylase on B16F10 cell growth and viability

Measurement of B16F10 growth using the MTT assay (Figure 4.6a-c) showed that as the seeding density was increased (2.5 x10^4, 5 x 10^4 and 1 x 10^5 cells/mL), cell growth remained rapid in the first 2 days after subculture. The B16F10 doubling times were 19, 22, and 22 h for cell seeding densities of 2.5 x10^4, 5 x 10^4 and 1 x 10^5 cells/mL respectively. However, cell death occurred earlier when cells were initially seeded at a higher density. A seeding density of 2.5 x10^4 cells/mL led to continuous cell growth over the 4 days after subculture, hence it was chosen for subsequent experiments, where the melanin assay is conducted over 4 days.

Table 4.3 Characteristics of dextrin-MSH conjugates synthesised

Batch code	Dextrin Mw† (g/mol)	Succinoylation (mol %)	Synthetic ratio, COOH : MSH (mol)	MSH content (% w/w)	Free MSH detectable
SDMSH1	47,200	26	1 : 2.5	1.2	None
SDMSH2	47,200	26	1 : 5	13.5	None
SDMSH3	47,200	26	1 : 5	14.1	None
SDMSH4††	47,200	26	1 : 5	37.0	None

† Mw defines weight average molecular weight determined against pullulan standards

†† Scaled up reaction

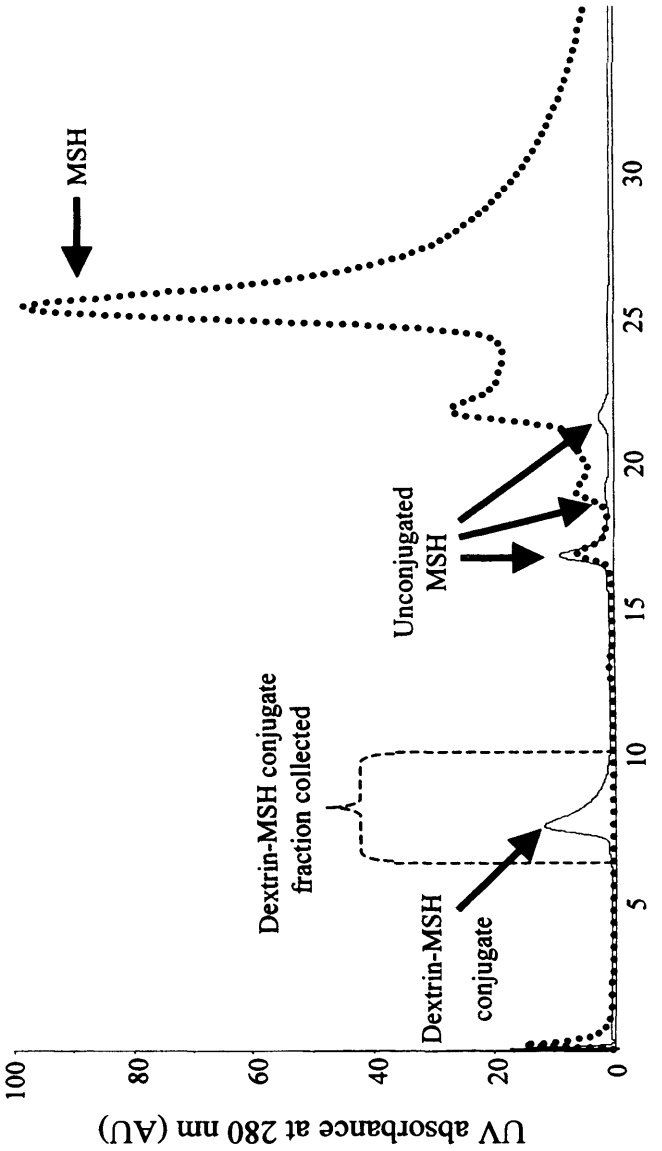

Figure 4.4 FPLC characterisation of free MSH and the reaction mixture of a typical dextrin-MSH conjugate using a superdex HR 10/30 size exclusion column. The dextrin-MSH conjugate fraction was subsequently collected as indicated, in order to isolate it from the free MSH in the reaction mixture.

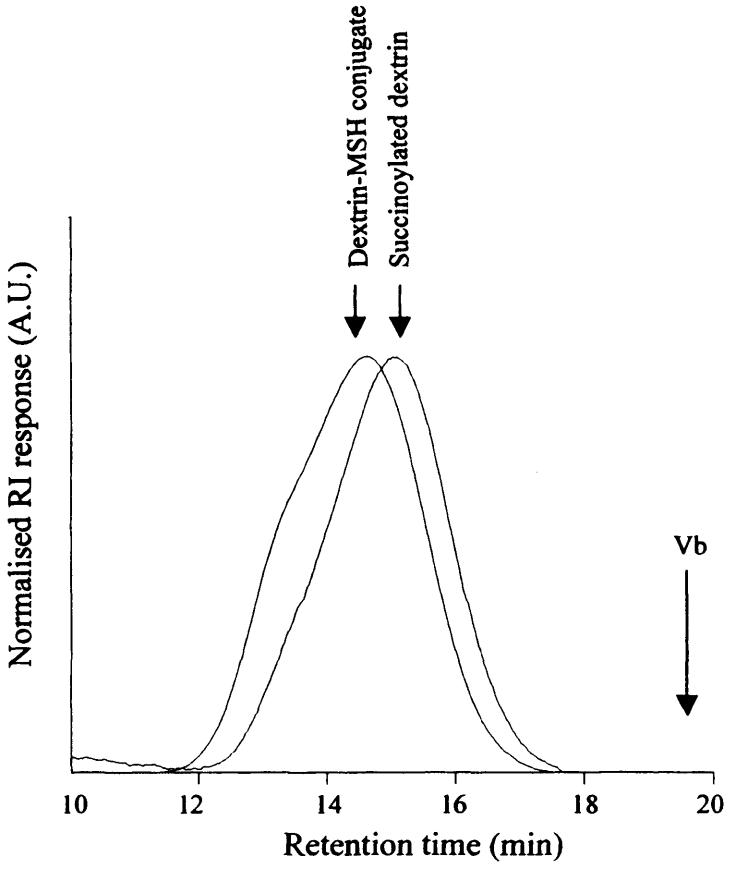

Figure 4.5 Characterisation of a typical dextrin-MSH conjugate by GPC using TSK-gel columns G4000 PW_{XL} and G3000 PW_{XL} in series. Succinoylated dextrin (26 mol %, 47,200 g/mol) was conjugated to MSH (1,640 g/mol) resulting in a 37 % w/w MSH loading, illustrated above. Vb represents the bed volume of the column.

(a) Seeding density
2.5 x 10^4 cells/mL

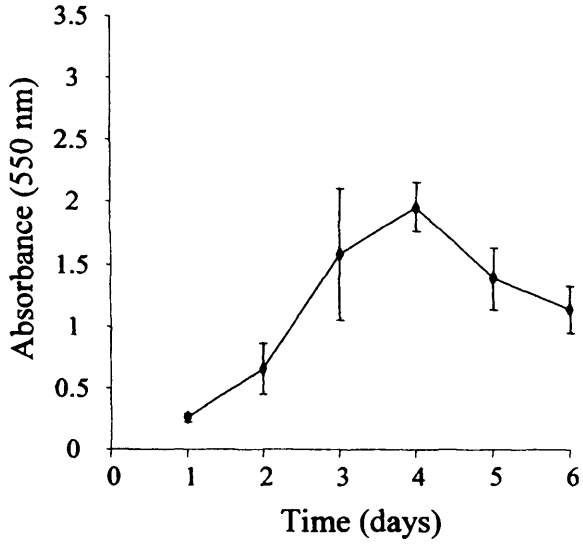

(b) Seeding density
5 x 10^4 cells/mL

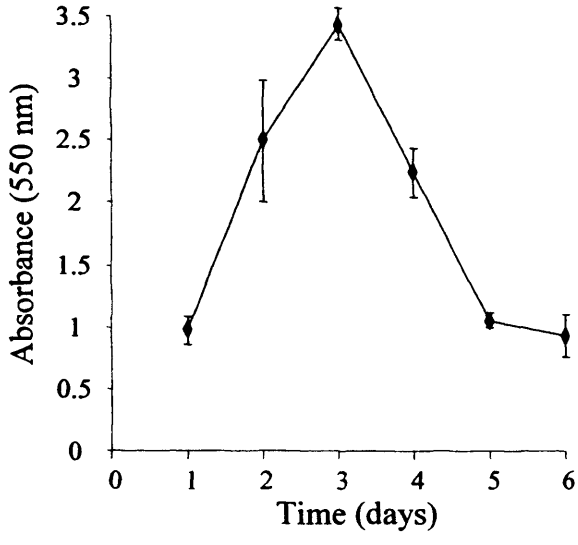

(c) Seeding densty
1 x 10^5 cells/mL

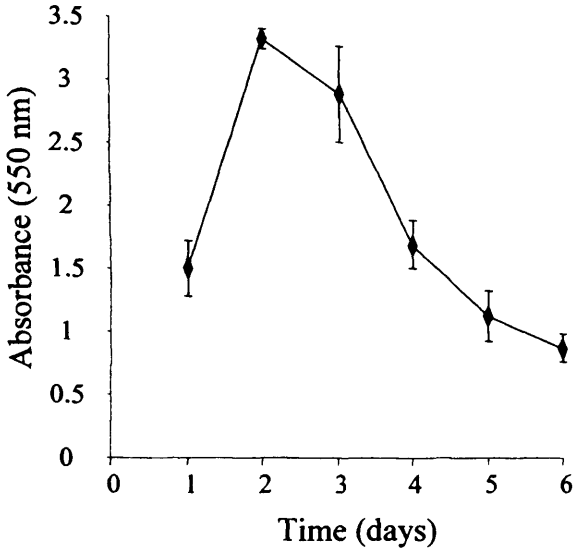

Figure 4.6 Growth curves for B16F10 murine melanoma cells seeded at different density in RPMI + 10 % FBS, measured using the MTT assay. Data represents the mean (n=18) ± SD.

When B16F10 cell viability (seeding density of 2.5 x 10^4 cells/mL) was measured in RPMI containing 10 % heat inactivated FBS over 4 days using the MTT assay, the doubling time was much slower (41 h) compared to that seen in RPMI containing 10 % FBS (Figure 4.7). After the lag, the growth rate rapidly increased, and the doubling time was similar to that seen previously (15 h).

Evaluation of cell viability when B16F10 cells (seeding density 2.5 x 10^4 cells/mL) were cultured in RPMI + 10 % FBS or RPMI + 10 % heat inactivated FBS in the presence of dextran, PEI or amylase (0.001 – 1 mg/mL) (Figure 4.8), showed that as expected, dextran was not toxic in either cell culture media composition. In contrast, PEI was toxic at concentrations greater than 0.01 mg/mL reducing cell viability by up to ~ 90 % when dissolved in either of the media compositions. Like dextran, amylase was generally not toxic, but a reduction in cell viability to 79 % was measured when B16F10 cells cultured in RPMI + 10 % heat inactivated FBS were exposed to an amylase concentration of 0.5 mg/mL (Figure 4.8b).

4.3.3 Optimisation of the melanin assay parameters to maximise melanin production

The degree of melanin production induced by addition of MSH (10^{-7} – 10^{-9} M) at 24 – 148 h post subculture, decreased by ~ 12 % when MSH was not added until 148 h after subculture. In fact, the highest melanin production was seen when MSH was added 24 h post subculture of the B16F10 cells (Figure 4.9a). When MSH was added up to 72 h post subculture of the cells, melanin production was rapidly induced, but thereafter melanin production plateaued. This indicated that the optimum time to measure melanin production was 72 h after the addition of MSH (Figure 4.9b).

Addition of MSH (10^{-7} – 10^{-10} M) did not significantly increase the melanin production compared to the media control (Figure 4.10). When higher concentrations of MSH (10^{-5} M and 10^{-6} M) were added to cells seeded at various densities (2.5 x10^4, 5 x 10^4 and 1 x 10^5 cells/mL) (Figure 4.11) however, increased melanin production was seen. Thus, a cell density of 2.5 x 10^4 cells/mL and an MSH concentration of 10^{-5} M were chosen for future melanin assays.

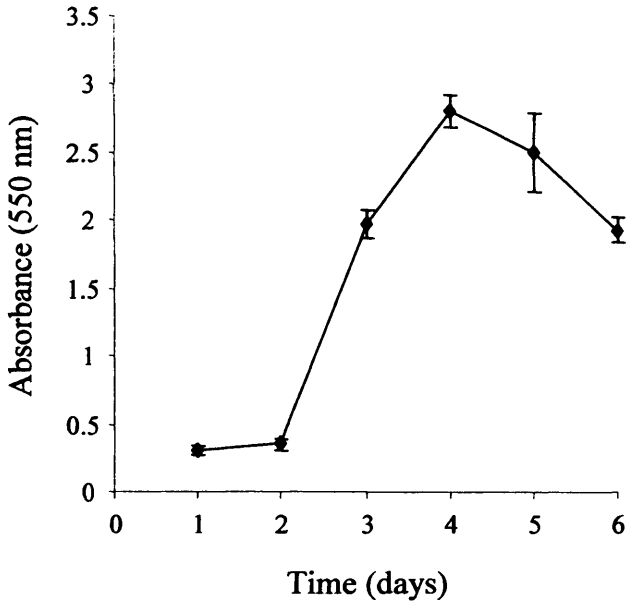

Figure 4.7 Growth curve for B16F10 murine melanoma cells seeded at a density of 2.5 x 10^4 cells/mL in RPMI + 10 % heat inactivated FBS, measured using the MTT assay. Data represents the mean (n=6) ± SD.

(a) RPMI + 10 % FBS

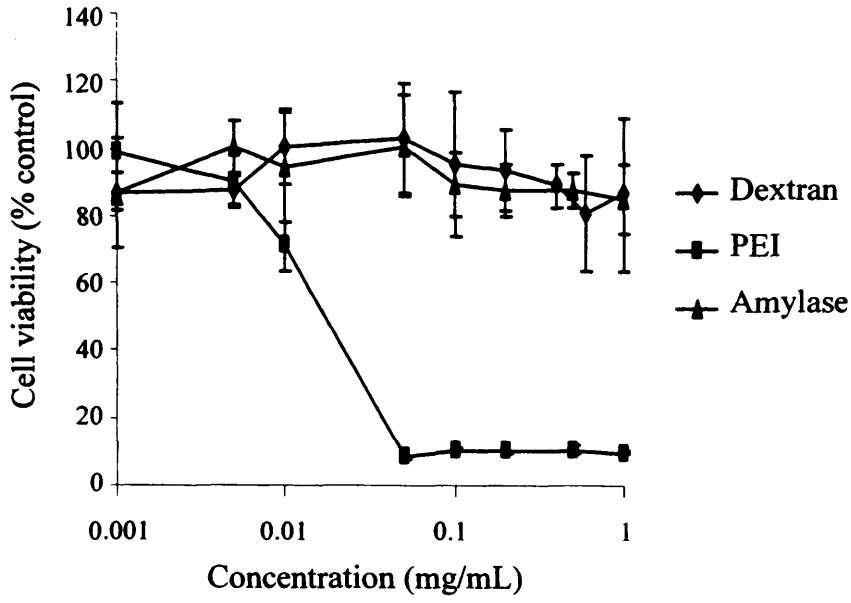

(b) RPMI + 10 % heat Inactivated FBS

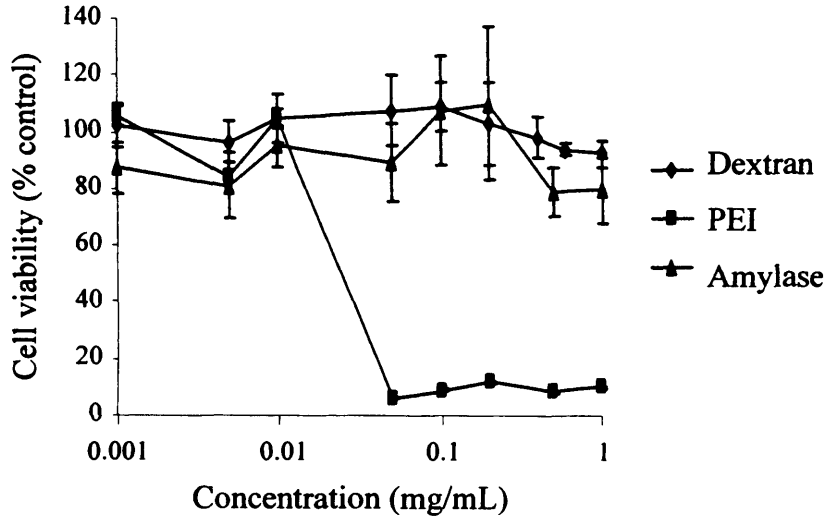

Figure 4.8 Effect of amylase, dextran (-ve control) and PEI (+ve control), incubated over 72 h in (a) RPMI + 10 % FBS, and (b) RPMI + 10 % heat inactivated FBS, on the cell viability of B16F10 cells. Cells seeded at a density of 2.5 x 10^4 cells/mL. Data shown represents the mean (n=5) ± SD.

(a) Effect of the time that MSH is added after subculture of B16F10 cells on the subsequent melanin production

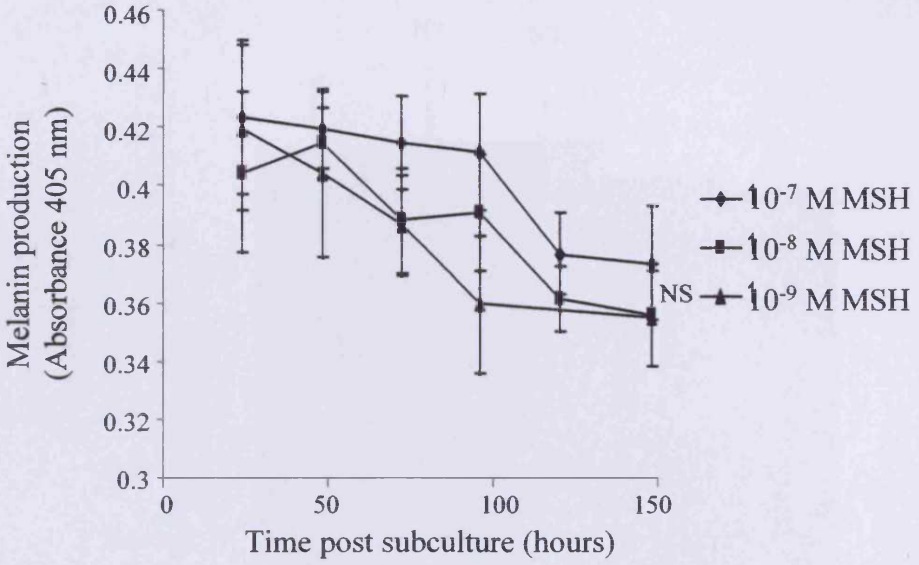

(b) Melanin production over time

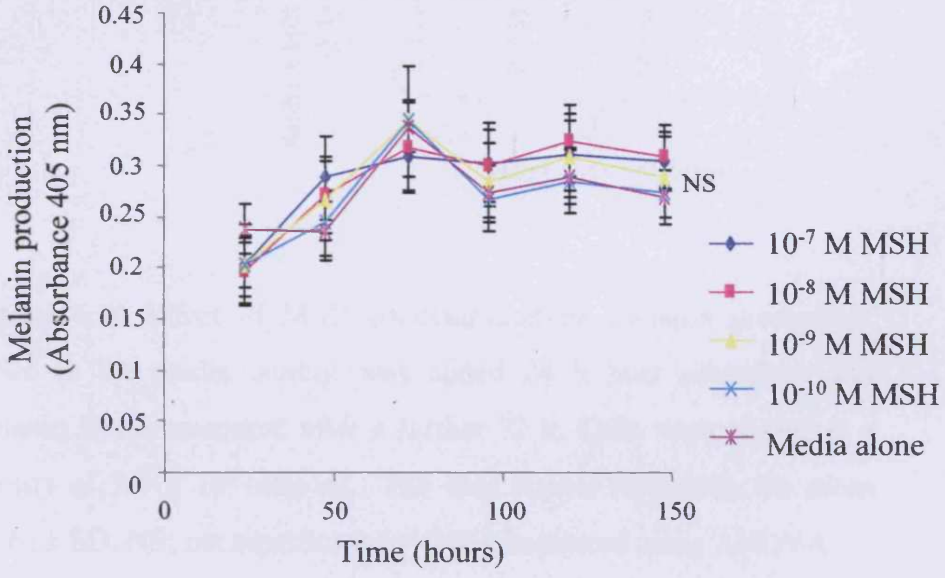

Figure 4.9 Effect of time MSH (10^{-7} – 10^{-9} M) is added to the B16F10 cells following subculture (panel a), and the effect of increasing the duration of time (24 – 144 h) that B16F10 cells were stimulated with MSH (10^{-7} – 10^{-10} M) (panel b), on the subsequent melanin production. MSH was added 24 h post subculture for panel (b) and cells were seeding at a density of 2.5 x 10^4 cells/mL. Data shown represents the mean (n=6) ± SD. NS; not significant ($p>0.05$), measured using ANOVA.

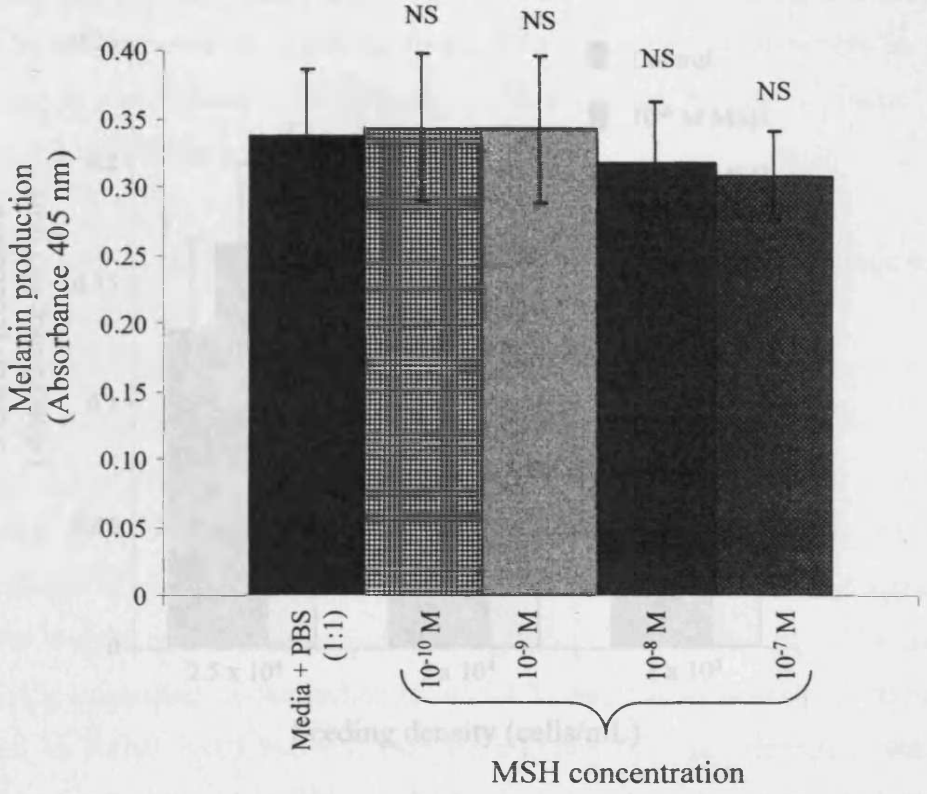

Figure 4.10 Effect of MSH concentration on melanin production. MSH or the media control was added 24 h post subculture and melanin levels measured after a further 72 h. Cells were seeded at a density of 2.5 x 10^4 cells/mL. The data shown represents the mean (n=6) ± SD. NS; not significant ($p>0.05$), measured using ANOVA.

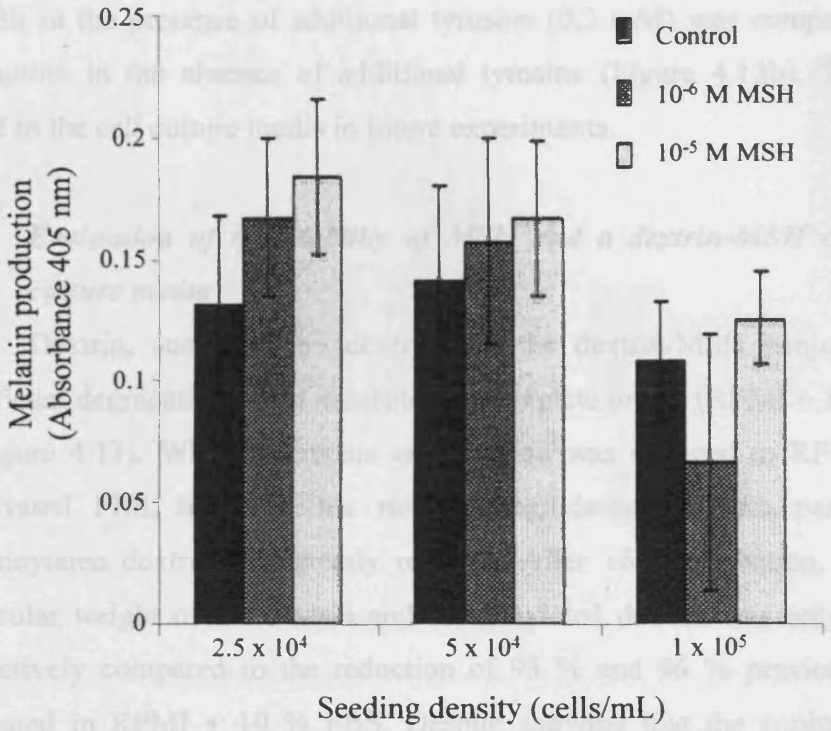

Figure 4.11 Effect of B16F10 cell seeding density (2.5 x 10^4, 5 x 10^4 and 1 x 10^5 cells/mL) on MSH induced melanin production. MSH or media control were added 24 h after cell subculture and melanin production measured after a further 72 h. Data represent the mean (n=6) ± SD.

MSH (5 x 10^{-5} M) added to B16F10 cells in media was more effective ($p < 0.05$) at stimulating melanin production, than MSH added in PBS + RPMI + 10 % FBS (1 : 1) (Figure 4.12a). Future experiments were thus carried out using MSH dissolved in complete media only. Melanin production by B16F10 cells cultured in RPMI + 10 % FBS in the presence of additional tyrosine (0.3 mM) was comparable to melanin production in the absence of additional tyrosine (Figure 4.12b). Tyrosine was not added to the cell culture media in future experiments.

4.3.4 Evaluation of the stability of MSH and a dextrin-MSH conjugate in cell culture media

Dextrin, succinoylated dextrin and the dextrin-MSH conjugate all showed significant degradation when incubated in complete media (RPMI + 10 % FBS) for 16 h (Figure 4.13). When the media composition was changed to RPMI + 10 % heat inactivated FBS, however, the rate of degradation of both parent dextrin and succinoylated dextrin was greatly reduced. After 16 h incubation, the reduction in molecular weight of the dextrin and succinoylated dextrin was only 2 % and 39 % respectively compared to the reduction of 93 % and 96 % previously found when incubated in RPMI + 10 % FBS. Despite showing that the conjugate was readily degraded when incubated in RPMI + 10 % FBS for 16 h, the effect of changing the media composition to RPMI + 10 % heat inactivated FBS did not hinder conjugate degradation (Figure 4.13).

MSH (5 x 10^{-5} M in PBS / RPMI + 10 % FBS) stimulated melanin production was shown to be significant compared to media control ($p < 0.05$, ANOVA and Bonferroni *post hoc* test). Whereas, when MSH (5 x 10^{-5} M) was stored in PBS / RPMI + 10 % FBS in the fridge for 72 h, the melanin production measured previously (Figure 4.14a) was reduced by 18 - 29 % relative to media control (Figure 4.14b).

4.3.5 Effect of media composition and amylase on melanin production

The ability of MSH to stimulate the production of melanin decreased when added after increasing periods of time post subculture (Figure 4.15a). B16F10 cells cultured in RPMI + 10 % heat inactivated FBS typically produced more melanin over 72 h than the other conditions analysed. Overall, the MSH stimulated melanin production (when added 24 h after subculture) was significantly greater

(a) Effect of MSH vehicle (media + PBS 1:1 or media alone) on melanin production

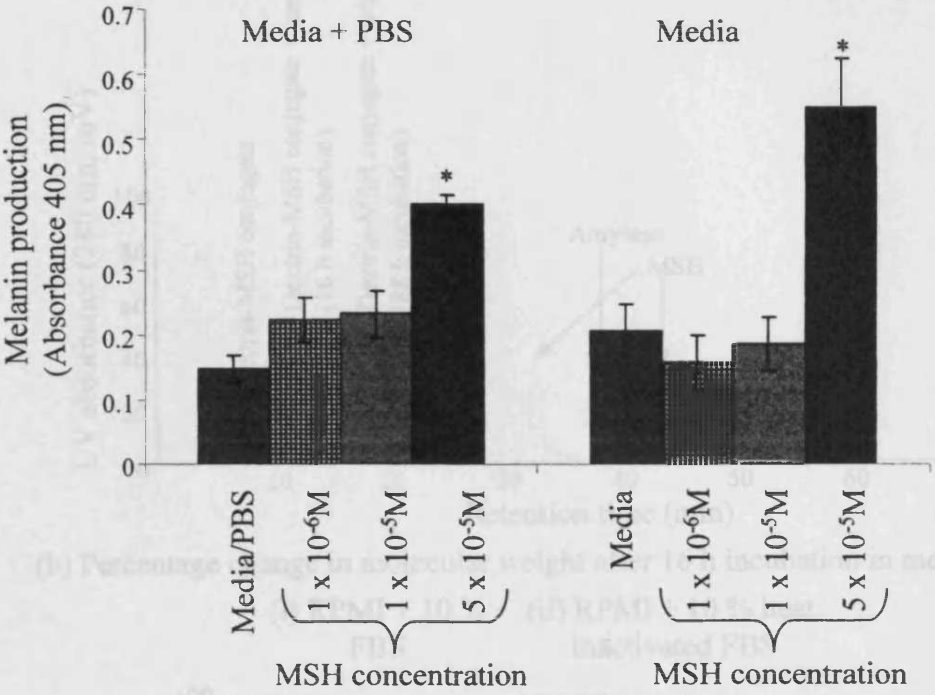

(b) Effect of the presence of tyrosine on melanin production

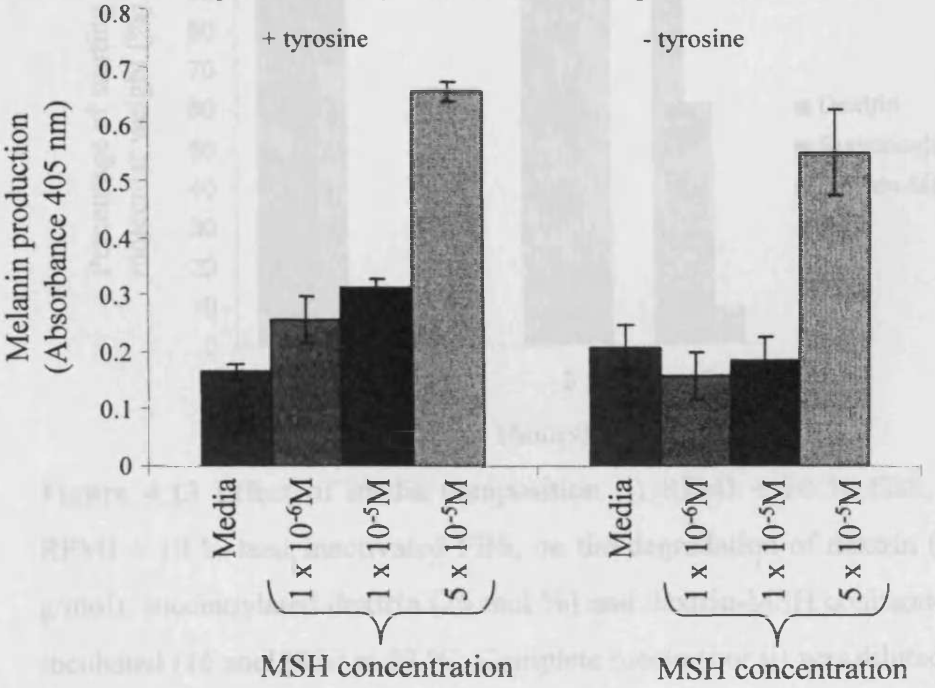

Figure 4.12 Effect of MSH vehicle and tyrosine on melanin production by B16F10 cells. Cells were seeded at a density of 2.5 x 10^4 cells/mL. Data shown represent mean (n=6) ± SD. Statistical significance (*) indicates $p<0.05$ vs media control (ANOVA and Bonferroni *post hoc* test).

(a) GPC degradation profile

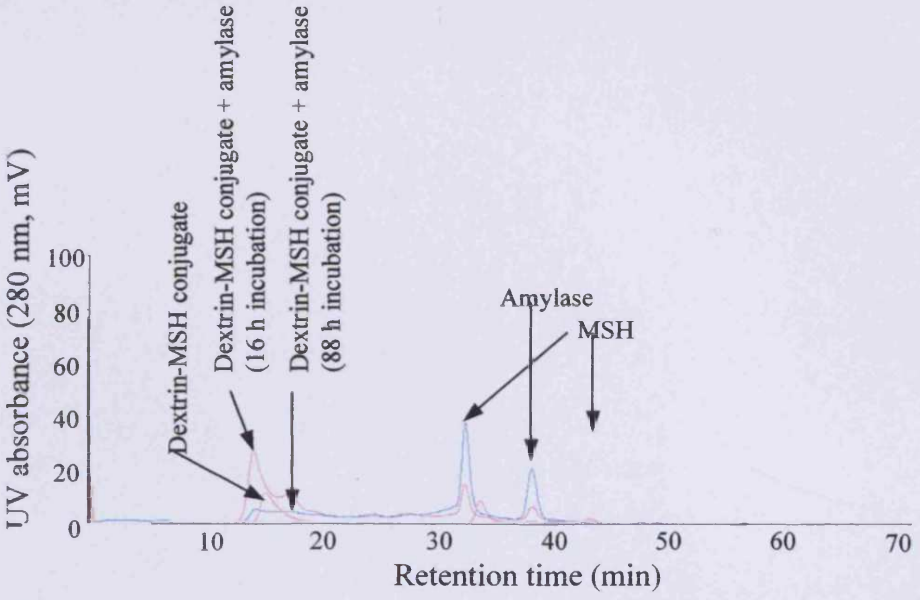

(b) Percentage change in molecular weight after 16 h incubation in media

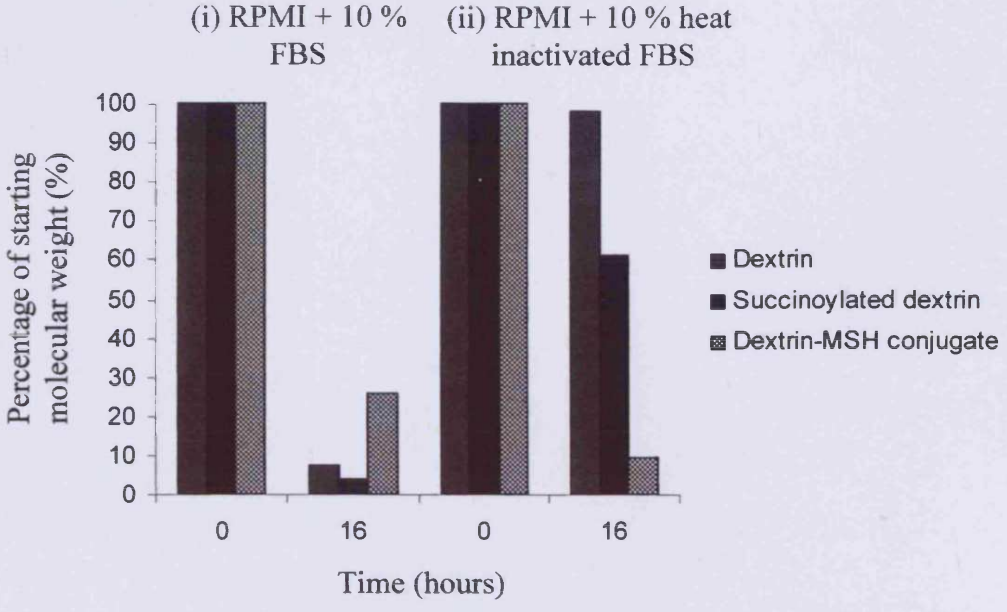

Figure 4.13 Effect of media composition (i) RPMI + 10 % FBS, or (ii) RPMI + 10 % heat inactivated FBS, on the degradation of dextrin (47,200 g/mol), succinoylated dextrin (26 mol %) and dextrin-MSH conjugate when incubated (16 and 88 h) at 37 °C. Complete media (i or ii) was diluted 1 : 20 with PBS (pH 7.4) and analysed by GPC and FPLC (panel a). The change in molecular weight of dextrin, succinoylated dextrin and conjugate was then estimated using a pullulan molecular weight standards calibration curve and appears in panel (b).

(a) MSH dilutions freshly prepared

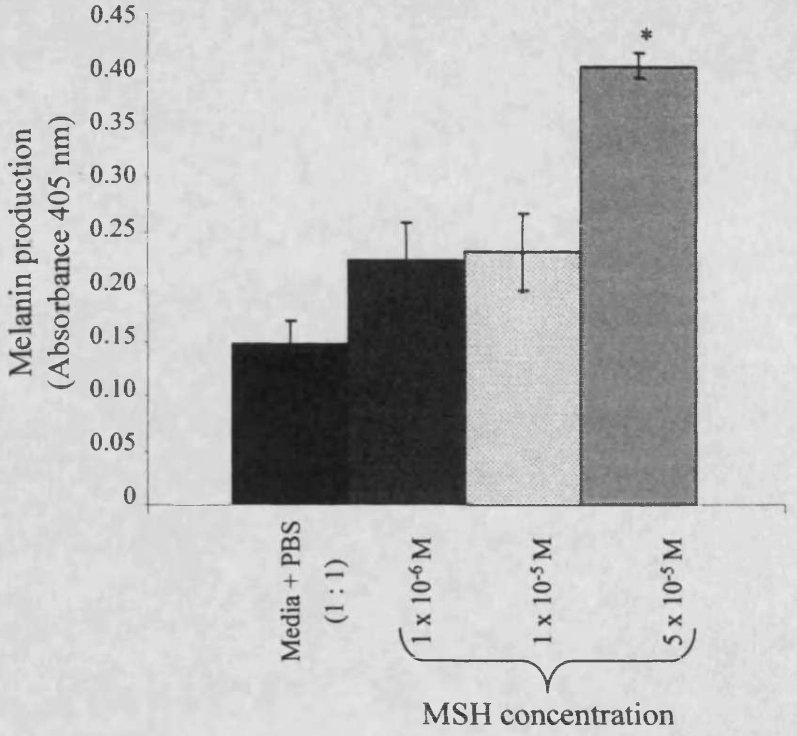

(b) MSH dilutions stored in the fridge for 72 h

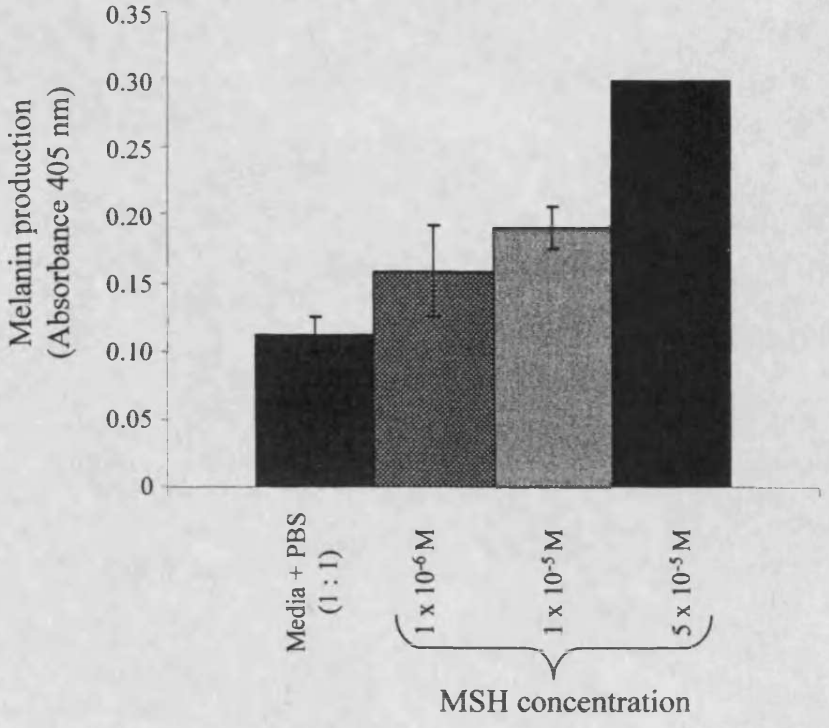

Figure 4.14 Ability of MSH to stimulate melanin production in B16F10 cells following 72 h storage at 2 – 8 °C in RPMI + 10 % FBS. Cells were seeded to a density of 2.5 x 10^4 cells/mL. Data represents the mean (n=6) ± SD. Where error bars are not visible, the SEM was below the limit representable.

(a) Varying time after subculture

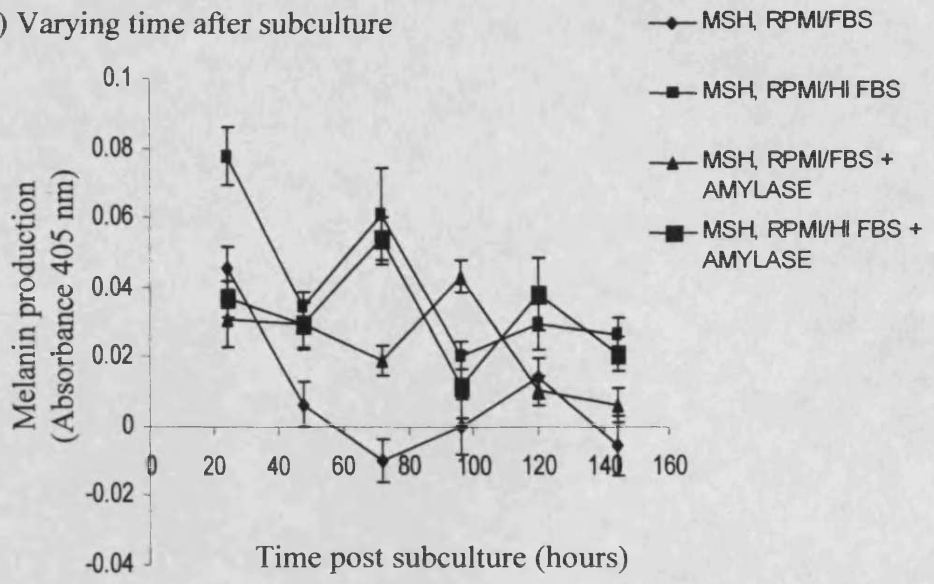

(b) 24 h post subculture

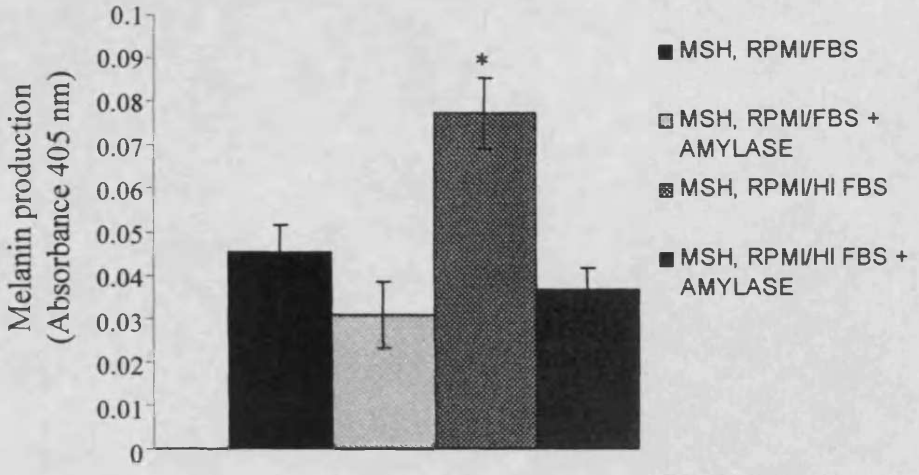

Figure 4.15 Evaluation of the effect of media composition and amylase on MSH (10^{-6} M) stimulated melanin production in B16F10 cells. MSH was dissolved in either RPMI + 10 % FBS or RPMI + 10 % heat inactivated (HI) FBS ± amylase. Cells were seeded at a density of 2.5 x 10^4 cells/mL and data expressed as mean (n=12) ± SEM. Statistical significance (* indicates $p<0.05$) was measured using ANOVA and Bonferroni *post hoc* test.

($p < 0.05$, ANOVA and Bonferroni *post hoc* test) than all other conditions tested when directly compared at 72 h (Figure 4.15b).

The production of melanin was not significantly affected by the presence or absence of amylase when cells were cultured in RPMI + 10 % FBS. However, when heat inactivated FBS was used, the presence of amylase reduced the previously raised melanin synthesis by 53 %, so that it was not significantly different from when cells were cultured in RPMI + 10 % FBS ($p > 0.05$, ANOVA and Bonferroni *post hoc* test).

4.3.6 Ability of the dextrin-MSH conjugate to stimulate melanin production

Melanin production caused by dextrin-MSH conjugate (10^{-5} M MSH equiv. (SDMSH2 13.5 % w/w MSH)) was 57 % that seen for the MSH control, when assayed in RPMI + 10 % FBS (Figure 4.16). When the media composition was changed to RPMI + 10 % heat inactivated FBS (to reduce undesired conjugate degradation), however, the dextrin-MSH conjugate stimulated melanin production was further reduced to 37 % of MSH control ($p < 0.05$, ANOVA and Bonferroni *post hoc* test).

Conjugation of MSH to succinoylated dextrin (SDMSH4 37 % w/w MSH) reduced melanin production to 11 % of free MSH control, when analysed using the optimised melanin assay in RPMI + 10 % heat inactivated FBS. Following incubation of the dextrin-MSH conjugate with amylase (0.2 mg/mL), it was possible to increase the stimulation of melanin production to 33 %, thus modulating activity between 11 and 33 % compared to MSH control (Figure 4.17). This was shown to be a significant masking and unmasking of activity ($p < 0.05$, ANOVA and Bonferroni *post hoc* test).

4.4 Discussion

Here the aims were primarily to synthesise dextrin-MSH conjugates to determine if it was possible to apply the concept of masked and reinstated protein activity to a small peptide for activation of a receptor.

Lessons learned on the synthesis and characterisation of dextrin-MSH conjugates

The synthesis of dextrin-MSH conjugates was successfully achieved. The molar ratio of COOH : MSH was optimised to 1 : 5 (i.e. 1 COOH : 20 NH_2) and this gave conjugates with loading of 37 % w/w MSH. The MSH loading was typically less than 50 % the loading achieved for the trypsin conjugates (Chapter 3). This may have been due to the much lower quantity of MSH used in the conjugation reactions (owing

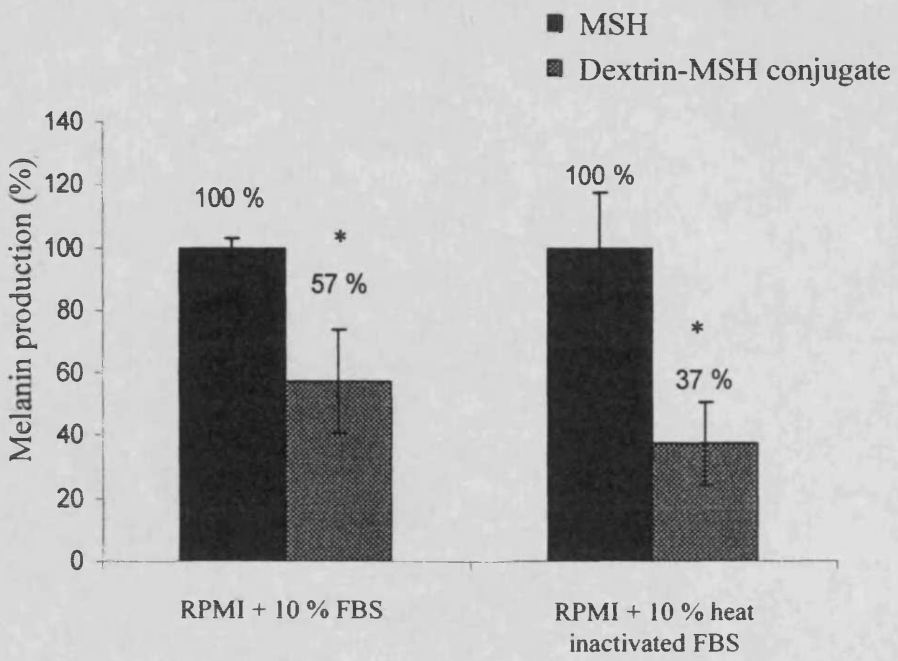

Figure 4.16 Effect of media composition (RPMI + 10 % FBS or RPMI + 10 % heat inactivated FBS) on MSH stimulated melanin production in B16F10 cells. Cells, seeded at a density of 2.5 x 10^4 cells/mL, were either incubated with free MSH (10^{-5} M) or dextrin-MSH conjugate (10^{-5} M MSH equiv. (SDMSH2; 13.5 % w/w MSH)) over 72 h. Data shown represents the mean (n=6) ± SD. Statistical significance (*) is indicated where $p<0.05$ vs free MSH control (ANOVA and Bonferroni *post hoc* test).

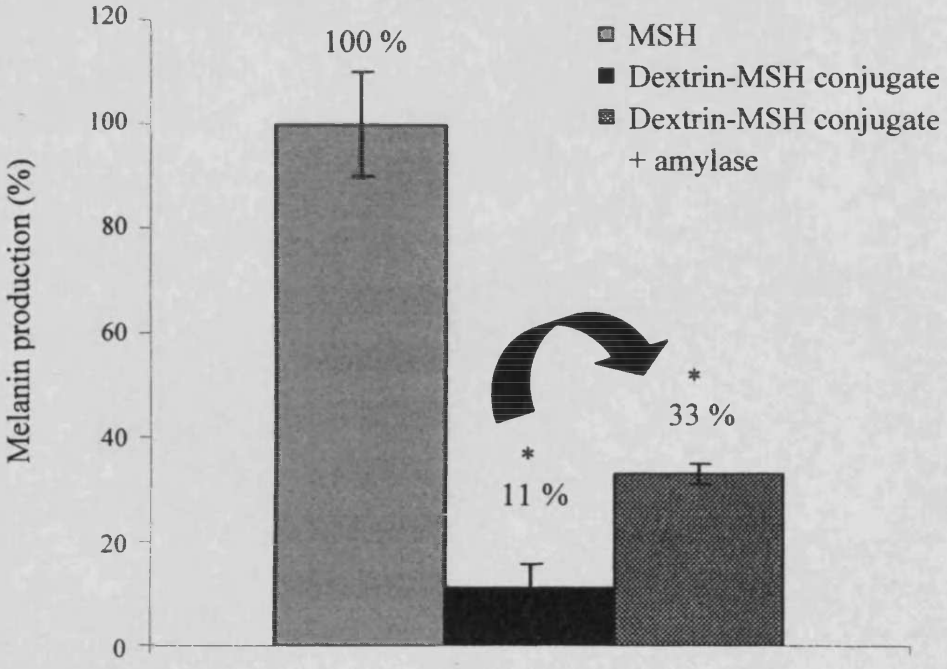

Figure 4.17 Production of melanin, after 72 h, by B16F10 cells when incubated with free MSH (10^{-5} M) or dextrin-MSH conjugate (10^{-5} M MSH equiv. (SDMSH4; 37 %w/w MSH)), prior to and following incubation with amylase (0.2 mg/mL), in RPMI + 10 % heat inactivated FBS. Cells were seeded at a density of 2.5 x 10^4 cells/mL. Data shown represents the mean (n=12 - 18) ± SEM. Statistical significance (*) indicates $p<0.05$ vs free MSH control (measured using ANOVA and Bonferroni *post hoc* test).

to the expense of MSH) as it was not possible to reproduce the molar excess used for trypsin conjugation (STE method). The MSH loading achieved was however still much greater than typical polymer-protein conjugates (~10 % w/w) described in the literature (reviewed in Harris and Chess, 2003).

As free trypsin was still present in the dextrin-trypsin conjugates purified by dialysis or centrifugation, the dextrin-MSH conjugate was purified by fractionation (SDMSH1, Figure 4.4) and characterised by GPC, SDS-PAGE and FPLC. This showed that no free MSH remained. FPLC fractionation was subsequently used to purify all future polymer-protein conjugates that were synthesised.

Optimisation of the B16F10 melanin assay

The initial experiments reproduced the work of O'Hare et al., (1993), confirming that the MSH-stimulated melanin production decreased after increasing days of B16F10 cell subculture. The optimum time to add MSH after subculture was found to be 24 h. In accordance with Eberle (1988), melanin production also increased the longer the cells were exposed to MSH (Figure 4.9), reaching a plateau after 72 h. This may be due to receptor down regulation with increasing time in culture or medium depletion of the substrate tyrosine, required for tyrosinase mediated conversion to melanin (Eberle, 1988).

The melanin assay was optimised according to the B16F10 cell seeding density, the MSH concentration used and by characterising the MSH stability, MSH dissolution and the effect of the presence of the substrate tyrosine (Figure 4.9 - 4.12). MSH dissolved in RPMI + 10 % FBS + PBS (1 : 1) showed improved solubility, but melanin production caused by MSH dissolved in RPMI + 10 % FBS was highest. When MSH was stored in RPMI + 10 % FBS for 72 h (2 - 8 °C), ability to induce melanin production decreased (Figure 4.14). This may be explained as MSH degradation by serum enzymes (Sawyer et al., 1980). Addition of tyrosine increased melanin production as also shown by Eberle (1988), although in this study it was not significant (Figure 4.12). It is not commonly added to the media in melanin assays (O'Hare et al., 1993), hence tyrosine was not added to any further experiments.

Degradation and reinstatement of activity of dextrin-MSH conjugates

Dextrin and the dextrin-MSH conjugates were degraded over time when incubated in RPMI + 10 % FBS. Use of heat inactivated FBS reduced the rate of degradation of dextrin and succinoylated dextrin (Figure 4.13). This was important to investigate as the melanin assay is conducted in culture media for 72 h, when significant conjugate degradation may occur.

There is inconsistency in the general literature over the necessity to culture melanoma cells in a composition of RPMI + 10 % heat inactivated FBS (56 °C, 30 min). It is possible that the alternative media conditions affect the MSH receptor expression on the B16F10 cells, thus decreasing the maximum potential melanin production. This effect was previously discussed in the introduction to this chapter and also by McQuade et al., (2005). It has also been suggested that MSH is susceptible to degradation by serum enzymes (reviewed in Sawyer et al., 1980). Thus it may be that the ability of the MSH to stimulate melanin production has been decreased in O'Hare et al., (1993). For this reason, there are several examples which have chosen to utilise heat inactivated serum in their media composition (Al-Obeidi et al., 1992; Sawyer et al., 1980).

Use of heat inactivated FBS made it possible to estimate the masked activity of the conjugate better, reducing the dextrin-MSH stimulated melanin production from 57 % (RPMI + 10 % FBS) to 37 % (RPMI + 10 % heat inactivated FBS) compared to MSH control (Figure 4.16). The modulation of activity shown, controlled by serum enzymes, provided both proof of principle for a receptor activation model, and also for a controlled release model.

To improve on the modulation of MSH activity already shown (37 to 57 %), the conjugate was incubated with amylase to promote degradation, as in Chapter 3. However, it was important to determine the effect of the addition of amylase to the culture media on the viability of B16F10 cells and also on the MSH receptor expression. There was no effect on cell viability when amylase was added at concentrations of 0.5 mg/mL in RPMI + 10 % heat inactivated FBS (Figure 4.15). Hence, a concentration of 0.2 mg/mL amylase was chosen for the remaining experiments. MSH receptor expression, indirectly assessed through melanin production, was found to decrease with time post subculture (Figure 4.15a). When a single time point was analysed (72 h after addition of MSH, MSH added 24 h post

subculture), there was a significantly greater MSH stimulated melanin production by cells cultured in RPMI + 10 % heat inactivated FBS (Figure 4.15b). Interestingly, melanin production in the presence of amylase (RPMI / heat inactivated FBS) was not significantly different to melanin production in cells cultured in RPMI + 10 % FBS (± amylase). This may suggest that there is an enzyme present in the FBS that either degrades the MSH receptor (glycoprotein) or the melanin that is synthesised.

To conclude this work and establish proof of principle for modulation of peptide activity in a receptor activation model, the optimum dextrin-MSH conjugate (SDMSH4, 37 % w/w MSH loading) was tested in the optimised melanin assay.
It was shown that it was possible to reduce MSH stimulated melanin production to 11 % on conjugation to dextrin. Following incubation with amylase, melanin production was reinstated to 33 % of MSH control. This assay was carried out under conditions of RPMI + 10 % heat inactivated FBS, which would negatively bias both the masked and unmasked activity measured due to the reduction in melanin production noted above. Under the conditions that the masked activity of the conjugate is measured, MSH stimulation of the cells has shown significantly increased melanin production than the same conditions in the presence of amylase, thus giving a higher activity for the masked activity and a lower activity for the unmasked conjugate.

The reinstatement of MSH activity to only 33 % of MSH control may be explained by irreversible inactivation of the MSH. The lysine in the structure of MSH is separated from the active site sequence by only one amino acid. This presents the potential for steric hindrance of the active site if conjugation to lysine occurs and may be partially responsible for the lower activity measured.

4.5 Conclusion

The most effective dextrin-MSH conjugate was synthesised using a molar ratio of 1 COOH : 5 MSH. Subsequently, purification of the reaction mixtures by FPLC fractionation produced pure conjugates with an absence of free peptide and polymer. The melanin assay was tailored to the assessment of dextrin-MSH conjugate activity. However, the use of heat inactivated FBS played a key role in the MSH receptor expression and was one of the main solutions identified to improve the characterisation of dextrin-MSH conjugate activity.

The optimum dextrin-MSH conjugate displayed the ability to mask and reinstate MSH activity (11 – 33 % of free MSH activity), however, to a lesser extent than the previous dextrin-trypsin conjugates (Chapter 3). Although it is possible to modulate activity of a peptide, this concept may be better suited to the conjugation of a protein, where multiple conjugation sites exist.

Chapter 5

Hyaluronidase triggered activation of hyaluronic acid-trypsin conjugates: conjugate synthesis and biological characterisation

5.1 Introduction

In Chapters 3 and 4 it was shown that dextrin-trypsin and dextrin-MSH conjugates could be reactivated by an amylase-triggered degradation of the polymer to unmask the activity of the conjugated protein or peptide. The HA-trypsin conjugates synthesised in this part of the study were prepared based on experiences gained and to see whether the "masking", "unmasking" concept could be applied to another system, i.e. HA and HAase.

Building on the conclusions of Chapters 3 and 4, HA-trypsin conjugates were synthesised utilising an HA polymer (~130,000 g/mol), with approximately 30 mol % of conjugating bonds in the hope that this would enable the conjugate to still be degraded. The protein trypsin was a simple cheap model for these studies and the conjugated trypsin had shown better modulation through conjugation than had MSH.

5.1.1 Rationale for choosing HA as the polymeric backbone

HA was considered an interesting model because it is a natural polysaccharide widely distributed in the body and degraded by the enzyme HAase. It has an established safety profile and it is FDA approved for therapeutic use, as in the form of sodium hyaluronate used for IA injection into the osteoarthritic joint Synvisc® and Hyalgan® (Table 1.6) (Bobic, 2005; reviewed by Hamburger et al., 2003).

Commercially available HA is derived from a range of sources (summarised in Table 5.1) being either extracted from mammalian tissues such as rooster comb, bovine vitreous humor and human umbilical cord, or derived by bacterial fermentation. The source affects its salt form, purity and solubility. Typically, HA is used as either a sodium or potassium salt, containing varying levels of protein (1 – 5 %) and chondroitin sulphate (up to 25 %) contamination.

Rooster comb HA (Rc HA) was chosen for this study because it is better characterised, with a low level of protein impurity (≤ 2 %), contains no chondroitin sulphate, and it has reasonable solubility (3 mg/mL) (Table 5.1). It is used for IA injections such as Orthovisc® and is also used to support intra-ocular lens implantation (Anika, 2004) (Table 1.6). The sodium hyaluronates used for IA injection have molecular weights in the range of the HAs found naturally in the synovial fluid (4 x 10^6 - 6 x 10^6 g/mol) (Table 1.6). Other uses of HA as drug / gene delivery systems, and the chemistry used for drug conjugation are described briefly in the following sections.

Table 5.1 Characteristics of commercially available hyaluronic acid (alternating poly(β-glucuronic acid-[1,3]-β-N-acetylglucosamine-[1,4]).

Source	Molecular formula	Salt form (%)	Impurities (%)	Solubility	Supplier	Product code
Rooster comb	$(C_{14}H_{20}NaNO_{11})n$	Sodium (3-7 %)	Protein (≤ 2 %)	3 mg/mL (sodium phosphate buffer)	Sigma	H5388
Human umbilical cord	$(C_{14}H_{20}KNO_{11})n$	Potassium (~10 %)	Chondroitin sulfate (NS) Protein (≤ 5 %)	NS†	Sigma	H1504
Human umbilical cord	$(C_{14}H_{20}KNO_{11})n$	Potassium (NS†)	Chondroitin sulfate (≤ 3%) Protein (≤ 3 %)	5 mg/mL (H_2O)	Fluka	53730
Human umbilical cord	$(C_{14}H_{20}KNO_{11})n$	Potassium (NS†)	Chondroitin sulfate (≤ 25 %) Protein (≤ 10 %)	5 mg/mL (H_2O)	Fluka	53750
Bovine vitreous humor	$(C_{14}H_{21}KNO_{11})n$	Sodium and Potassium (NS†)	NS†	0.3 mg/mL (sodium phosphate buffer)	Sigma	H7630
Streptococcus equi.	NS†	Sodium (NS†)	Protein (≤ 1 %)	5 mg/mL (H_2O)	Fluka	53747
Streptococcus zooepidemicus	NS†	Sodium (NS†)	NS†	20 mg/mL (H_2O)	Sigma	H9390

†NS; not specified

5.1.2 Pharmaceutical use of HA and the chemistry of HA-drug conjugation

In addition to the use of HA as an IA preparation for the treatment of osteoarthritis, as described above, HA has been studied for gene (Yun et al., 2004) and cytokine delivery (Fernandez-Botran et al., 1999). It has been explored as a carrier for tyramine (Kurisawa et al., 2005), 1,4-diaminobutane (Bulpitt and Aeschlimann, 1999) and bupivacaine (Gianolio et al., 2005), and has been widely used as a hydrogel for controlled release (Bulpitt and Aeschlimann, 1999). For example, the cytokine Interferon gamma interacts ionically with HA without reduction in cytokine activity (Fernandez-Botran et al., 1999). To synthesise HA conjugates, the coupling agents EDC and HOBt have frequently been used, i.e. in the conjugation of HA to tyramine (Kurisawa et al., 2005), to 1,4-diaminobutane (Bulpitt and Aeschlimann, 1999) and to bupivacaine (Gianolio et al., 2005). In some cases, however, the carboxyl group of glucuronic acid has been directly conjugated to an amine or an amine-derivative, e.g. using 1,4-diaminobutane and tyramine without first functionalising the HA (Bulpitt and Aeschlimann, 1999; Kurisawa et al., 2005). In other experiments a hydrolysable linker has been incorporated onto the HA polymeric backbone before conjugation to the local anaesthetic bupivacaine (Gianolio et al., 2005).

Two options were considered here for conjugation of HA to trypsin. These are outlined in Figure 5.1. They were either direct conjugation of trypsin to the carboxyl group of the glucuronic acid HA monomer, or succinoylation of HA following the procedure adopted earlier in Chapter 3 for the succinoylation of dextrin, and then trypsin conjugation.

A method involving direct conjugation of HA to trypsin was chosen because:

(i) HA already has a carboxyl group on each glucuronic acid monomer making polymer activation by succinoylation unnecessary.

(ii) The number of carboxyl groups involved in the reaction may be controlled by the ratio of EDC and sulfo-NHS used in the reaction.

(iii) If HA were first succinoylated, there would be two potentially different conjugation reactions, resulting in heterogeneous HA-trypsin conjugates.

(a) Conjugation of succinoylated HA to trypsin

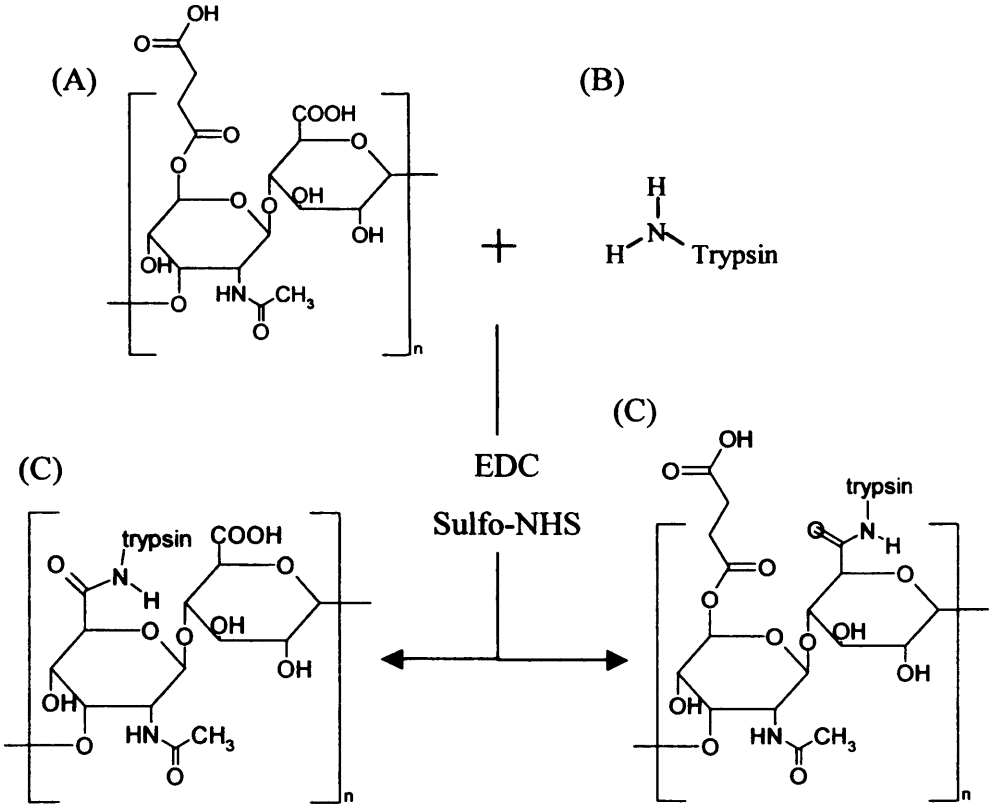

(b) Direct conjugation of HA to trypsin

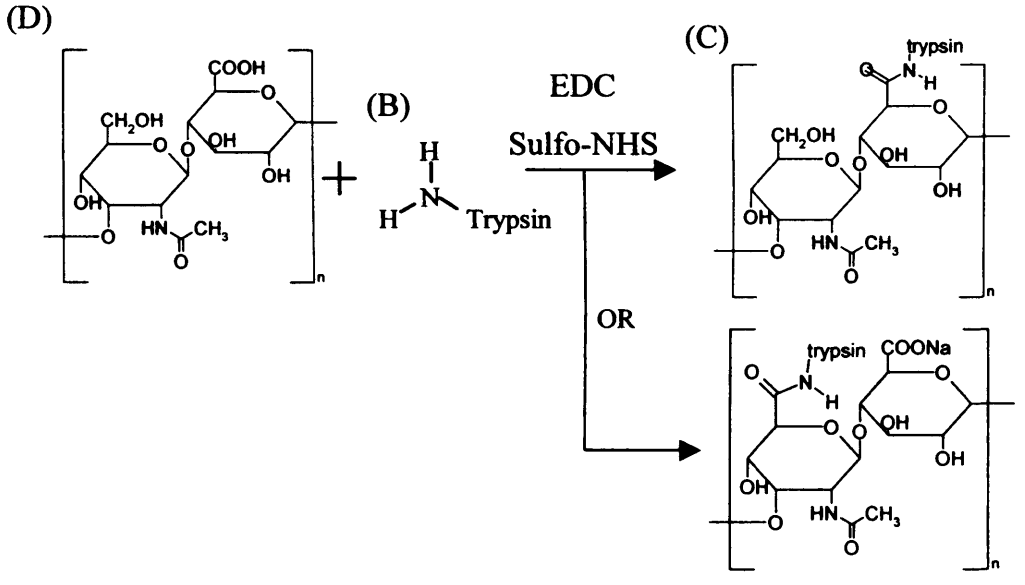

Figure 5.1 Possible reaction schemes for the synthesis of (a) succinoylated HA-trypsin conjugates and (b) HA-trypsin conjugates. Compounds (A) succinoylated HA, (B) trypsin, (C) possible HA-trypsin conjugates, and (D) HA.

(iv) If HA were succinoylated, then distinguishing between the succinoyl carboxyl groups introduced and the glucuronic acid carboxyl groups already present in the polymer would make it difficult to quantify the degree of succinoylation.

Bulpitt and Aeschlimann (1999) synthesised HA containing aldehyde and amine groups which were then crosslinked with amines to enable subsequent incorporation of HA into hydrogels. They used three methods of HA activation, (i) EDC / HOBt, pH 6.8, (ii) EDC, pH 4.75, and (iii) EDC / Sulfo-NHS, pH 7.5. The latter method used reaction parameters that are very similar to those described here for the conjugation of dextrin to trypsin (Chapter 3), i.e. a combination of EDC and sulfo-NHS with pH adjustment to pH 8. For this reason, the HA-trypsin conjugates (Figure 5.1) were prepared using the method previously described for the synthesis of dextrin-trypsin conjugates (Figure 3.2).

If HA was to function as a biodegradable polymer for protein masking-unmasking, it was essential that the HA would ultimately degrade in the body. It was important therefore to consider the physiological mechanisms of HA degradation. These are briefly described in the following sections.

5.1.3 CD44 mediated uptake and trafficking of HA

There are three main classes of HA receptor; (i) lectins, (ii) intracellular HA-binding proteins (IHABP) and (iii) link proteins. Removal of HA from the circulation occurs mainly through the action of the lectin-type receptors; ASGP-R and HARE, located in the lymph nodes, liver and spleen. IHABPs are involved in the trafficking of kinases into cells and so will not be discussed any further here. The remaining receptor type link-proteins, fall into two sub classes:

- Receptors membrane-bound to lymphatic tissue, which remove HA from the circulation, subesquently eliminated by the liver (Torsteinsdottir et al., 1999)
- CD44 receptor, the primary receptor involved in the turnover and organisation of the ECM of the joint cavity.

The CD44 receptor is distributed throughout the body, primarily on liver sinusoidal endothelial cells, chondrocytes and macrophages. It is a cell-surface glycoprotein (85,000 - 100,000 g/mol) able to bind HA to the cell surface through an NH_2 extracellular domain (Culty et al., 1992; reviewed by Lee and Spicer, 2000). Subsequently, it mediates the endocytosis of HA, enabling lysosomal degradation by acid hydrolases, specifically HAase. The receptor itself however, has no HAase activity (Aguiar et al., 1999), and there are no enzymes capable of degrading HA present in the synovial cavity, cartilage or synovial fluid (Aguiar et al., 1999).

5.1.4 Physiological and chemical degradation of HA

HA is degraded by the enzyme HAase which is located in the lysosomal compartment of cells. Following HA endocytosis (mediated by the CD44 receptor as discussed above) it is transported to the lysosome (Aguiar et al., 1999) where HAase hydrolyses the 1-4 linkage of HA between N-acetyl-beta-D-glucosamine and D-glucuronate (ExPASy, 2004). Furthermore, HA is removed from the body and degraded very rapidly. Because HA has such a short degradation half-life, it was considered important to slow down the degradability of HA, as has been done previously for dextrin by succinoylation. This increases the potential circulation time in the body should its conjugates find clinical use.

For this study it was decided to use HA of similar molecular weight to the HMW dextrin used earlier (Chapter 3). The Rc HA supplied had a Mw of ~ 900,000 g/mol, so it was first important to prepare a lower molecular weight fraction suitable for trypsin conjugation. In theory, degradation of HA to produce LMW fragments or oligosaccharides could have been achieved by enzymatic degradation (Tawada et al., 2002; Volpi, 2003), however, this has the disadvantage that the reaction mixture requires complex purification following HA degradation to remove the HAase. Acid or alkaline degradation methods are routinely used to degrade polysaccharides (e.g. alginate; Al-Shamkhani, (1993) and HA; Blundell and Almond, (2006)) and acid hydrolysis has the advantage of speed and also the degraded polymers do not need further purification. Both techniques were explored to prepare the HA for the these studies.

The HAase available commercially comes from three main sources: bovine testes, sheep testes or streptomyces hyalurolyticus, and they vary in activity and specificity (summarised in Table 5.2). Bovine testes HAase was used here because it is known to degrade Rc HA (Tawada et al., 2002; Volpi, 2003). This HAase has a molecular weight of ~55,000 g/mol, and randomly cleaves β-N-acetylhexosamine-[1,4] glycosidic bonds. Its substrates include the glycosaminoglycans HA, chondroitin and chondroitin sulphates.

In order to assay HAase degradation of HA and the HA-trypsin conjugate, it was necessary to optimise the incubation conditions in respect of the buffer type and pH optimum. HAase-mediated degradation of HA is usually conducted in PBS (Tawada et al., 2002), an acetate-based buffer, such as ammonium acetate (Asteriou et al., 2006) or sodium acetate (Blundell and Almond, 2006; Volpi, 2003). The buffer pH is typically ~pH 5 (Asteriou et al., 2006; Tawada et al., 2002). The pH optimum for bovine testes HAase activity is pH 4.5 to 6.0 (SIGMA, 2002), although the enzyme has significant activity at pH 7.5 (reviewed in Menzel and Farr, 1998).

Established methods used to assess HAase activity include colorimetric (Asteriou et al., 2006), turbidimetric (SIGMA, 2002) and combination assays (Asteriou et al., 2001), and they have been reviewed by Menzel and Farr (1998). The complex experimental design needed to assay the reinstatement of trypsin activity in HA-trypsin conjugates is described in section 5.2.5.

5.1.5 Summary of the aims of Chapter 5:

- To degrade Rc HA (~900,000 g/mol) to give a HA fraction suitable for conjugation to trypsin.
- To ensure that the HA fraction was still degradable by HAase.
- To establish a method for the conjugation of trypsin to HA, considering the following factors:
    - Could trypsin be conjugated directly to the glucuronic acid monomer of HA? (Figure 5.1).
    - Would direct conjugation of HA to trypsin affect the rate of degradation of the conjugate and subsequently its ability to mask trypsin activity?
    - Could the method of conjugation of succinoylated dextrin to trypsin be adapted to HA-trypsin conjugation?

Table 5.2 Properties of commercially available sources of HAase

Source	Activity (units/mg)	Specificity	Substrates	Molecular weight (g/mol)	Supplier	Product code
Bovine testes	400 - 1000	Random hydrolysis of glycosidic bonds (1,4 linkage)	HA Chondroitin Chondroitin sulfate	55,000	Sigma	H3506
Sheep testes	≥ 1,500	Random hydrolysis of glycosidic bonds (1,4 linkage)	HA Chondroitin Chondroitin sulfate	55,000	Sigma	H6254
Streptomyces hyalurolyticus	NS[†]	Random hydrolysis of glycosidic bonds (1,4 linkage)	HA	NS[†]	Sigma	H1136

[†]NS defines not specified

- To assess the suitability of the purification and characterisation methods used previously, to be applied to the HA-trypsin conjugates synthesised.
- To tailor the UV-vis spectrophotometric method used to measure HA-conjugated trypsin activity, considering the following factors:
  - Buffer pH and composition
  - Incubation time
  - Enzyme concentration
- To determine if HA can be used to mask trypsin activity with reinstatement following HAase triggered degradation of the conjugate.

5.2 Methods

The methods used to characterise both polymer and polymer-protein conjugates have already been described in Chapter 2. These include GPC (section 2.2.2.3), FPLC (section 2.2.3.4), BCA assay (section 2.2.3.2) and SDS-PAGE (section 2.2.3.3).

Synthesis and characterisation of HA-trypsin conjugates

5.2.1 Preparation of HA fractions

Rc HA (~900,000 g/mol) was degraded by acid hydrolysis and by the enzyme HAase to find an optimal method that could be scaled-up to produce a stock of HA for the conjugation experiments.

5.2.1.1 Acid hydrolysis

Typically, HA (30 mg) was dissolved in HCl (10 mL, 1 M), to a final concentration of 3 mg/mL. The solution was neutralised (pH 7) with NaOH (1 M) after 1 h and then purified by dialysis (Spectra/Por membrane, MWCO 50,000 g/mol) against ddH_2O (6 x 5 L) to remove NaCl. The resulting solution was frozen in liquid N_2 (5 min) and then lyophilised (48 h). The Mw of the HA fraction produced was determined by GPC using pullulan molecular weight standards (section 2.2.2.3). Acid hydrolysis was repeated using HCl (1 – 5 M) and exposure times of 1 – 12 h to optimise the conditions required to degrade Rc HA to a HA fraction ~100,000 g/mol.

5.2.1.2 Enzymatic degradation

HA (9 mg) was dissolved in PBS (0.1 M) and HAase added to produce a final enzyme concentration of 3 mg/mL HA i.e. 0.125 - 500 ui/mL HAase. The mixture was

incubated at 37 °C for 2 h, and 100 μL samples were withdrawn at 0, 30, 60, 90 and 120 min. They were snap frozen in liquid N_2 (1 min) to stop the reaction, and stored at –20 °C. The samples were then prepared (section 3.2.4) and analysed by GPC (section 2.2.2.3) as described previously. The data were expressed as the change in HA molecular weight over time.

5.2.2 Conjugation of HA to trypsin

The reaction protocol used for dextrin-trypsin conjugation (section 3.2.3) was adjusted to optimise HA conjugation to trypsin (Figure 5.1), by investigating the effect of duration of reaction and ratio of HA to trypsin. The ratio of HA to EDC to Sulfo-NHS was adjusted to control the number of conjugating bonds formed (30 or 50 mol %). The ratio of HA to trypsin used was either 1 to 0.5, 1 to 1 or 1 to 2, to minimise the presence of free trypsin in the resulting conjugate. HA-trypsin conjugates were synthesised using the method described in section 3.2.3 with the above variables of ratio and duration of reaction (16 – 20 h). To remove free trypsin, the conjugates were purified by FPLC fractionation and desalting, as described in section 2.2.1.2. The final product was then freeze-dried and characterised by GPC (section 2.2.2.3), SDS-PAGE (section 2.2.3.3) and BCA protein assay (section 2.2.3.2), to determine conjugate molecular weight, purity and protein content respectively.

5.2.3 Degradation of HA and HA-trypsin conjugates by HAase

The sample (HA or HA-trypsin conjugate) was dissolved in PBS to a final concentration of 3 mg/mL. HAase was then added to a final concentration of 50 – 500 ui/mL and the solution incubated (37 °C, 2 h). Samples (100 μL) were removed during the course of the incubation (t = 0, 30, 60, 90 and 120 min), snap frozen in liquid N_2 and stored at –20 °C, until analysed by GPC. Samples were prepared for GPC analysis as described in section 2.2.2.3.

5.2.4 Evaluation of free and conjugated trypsin activity

UV-vis absorbance spectra as controls for kinetics studies

The absorbance spectra (200 – 700 nm) of HA, HAase and HA-trypsin conjugates was analysed in tris buffer (pH 5 – 9) to exclude their contribution to any absorbance detected at 400 nm in the kinetics studies. The effect of incubation time (0, 1 and 22 h) on the absorbance and potential absorbance of subsequent degradation

products was also analysed. Other controls studies measuring the UV-vis absorbance of samples such as tris buffer and BAPNA were previously carried out in Chapter 3.

Assessment of HA-trypsin conjugate activity in tris buffer

The trypsin content of the conjugates (determined by BCA assay) was used to calculate the volume of HA-trypsin conjugate (0.1 mg/mL) containing 200 ng trypsin equiv.. The remaining trypsin activity of HA-trypsin conjugates was then measured at 37 °C as previously described for dextrin-trypsin conjugates in section 3.2.6 – 3.2.8.

5.2.5 Assessment of HA-trypsin conjugate activity following incubation with HAase

The primary method used to measure reinstatement of trypsin activity involved use of a single buffer system (tris buffer pH 8.2) previously selected as optimal for measuring trypsin activity.

To try and optimise further HAase activity alternative buffer systems were explored (Figure 5.2). These methods used a multi-buffer system, combining the optimum buffer for HAase activity with the optimum buffer for trypsin activity measurement. This multi-buffer system was piloted in this study, and it is described in more detail in the following sections.

5.2.5.1 Direct measurement of trypsin activity using a single buffer system

To determine the effect of HAase concentration on the degradation of HA-trypsin conjugates, the conjugates were prepared as a 0.1 mg/mL (conjugate) solution in tris buffer (pH 8.2). Tris buffer (up to 1000 μL), HAase (0.5 – 25 ui / 1 – 50 μL) and BAPNA (30 μL of 0.7 % w/v in DMSO) were then mixed in a 1 mL quartz cuvette. The UV-vis absorbance was zeroed and 54 μL (200 ng trypsin equiv.) of conjugate solution added. The production of NAp cleaved from BAPNA was measured at 400 nm over 5 min.

The effect of buffer pH and incubation time on trypsin activity were then assessed. HA-trypsin conjugates were prepared as a 0.1 mg/mL (conjugate) solution in tris buffer (pH 5.2, 6.2, 7.2 and 8.2) and HAase (178 ui/mL) added. The solutions were incubated at 37 °C overnight (22 h) and then analysed as described in the above paragraph.

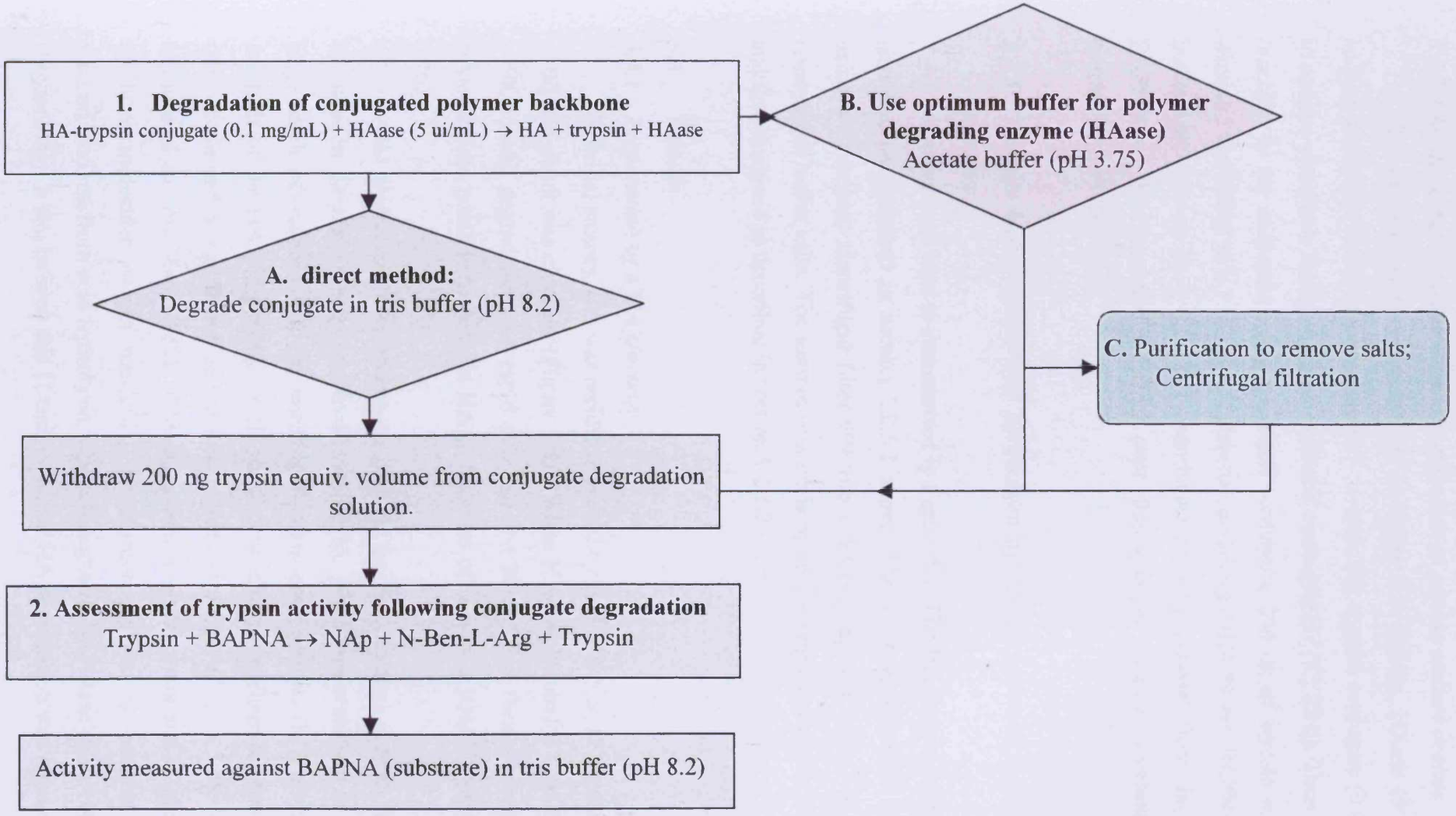

Figure 5.2 Schematic illustrating the three possible methods of assessment of degraded conjugate activity; optimising buffer type and pH.

5.2.5.2 Multiple buffer system without purification to remove sodium acetate

This protocol used is summarised in Figure 5.3. Briefly, HAase (5 ui/mL in sodium phosphate buffer (a)) was mixed 1 : 1 with HA-trypsin conjugate (0.03 % w/v in sodium phosphate buffer (b)) and incubated overnight (37 °C, 22 h). Then a volume (specific to the conjugate being analysed) containing 200 ng of trypsin equiv. was removed and added to a 1 mL quartz cuvette containing 0.021 % w/v BAPNA and tris buffer (pH 8.2) up to 1 mL. The absorbance of NAp cleaved from the substrate BAPNA was then measured at 400 nm over 10 min, as per Chapter 3 (section 3.2.7) to estimate trypsin activity.

5.2.5.3 Multiple buffer system with purification by centrifugation to remove sodium actetate

The protocol used is summarised in Figure 5.3. The HA-trypsin conjugate was degraded as described in section 5.2.5.2 above. The solution was then centrifuged using a Centriprep centrifugal filter (10 min x 4000 g) against ddH_2O (4 times) to remove the buffer salts. The sample was made up to the original volume with ddH_2O and then analysed as described in section 5.2.5.2.

5.3 Results

5.3.1 Preparation of a HA fraction

In initial studies, HA was rapidly degraded by HCl (5 M), at 12 h a fraction of ~100,000 g/mol was obtained (Figure 5.4a). When HA was incubated with HAase (15 – 500 ui/mL) degradation was rapid over the first 30 min and then decreased. Using HAase it was possible to degrade HA to fractions of less than 100,000 g/mol (Figure 5.4b).

Acid hydrolysis was chosen to prepare the HA fraction needed for trypsin conjugation. Degradation by acid hydrolysis (5 M, 12 h) was scaled-up to prepare a large batch of material and the resulting fraction compared to the parent Rc HA. Analysis of the HA samples by FT-IR showed no change in chemical structure, but GPC confirmed a significant decrease in molecular weight (Figure 5.5), to give an estimate of the Mn, Mw and PDI of 99,600 g/mol, 128,900 g/mol and 1.3 respectively (pullulan molecular weight standards). Furthermore, it was shown that this HA fraction, derived from acid hydrolysis, was still degraded by HAase (50 – 1000 ui/mL) (Figure 5.6a). It can be seen that HAase mediated HA degradation was rapid over the

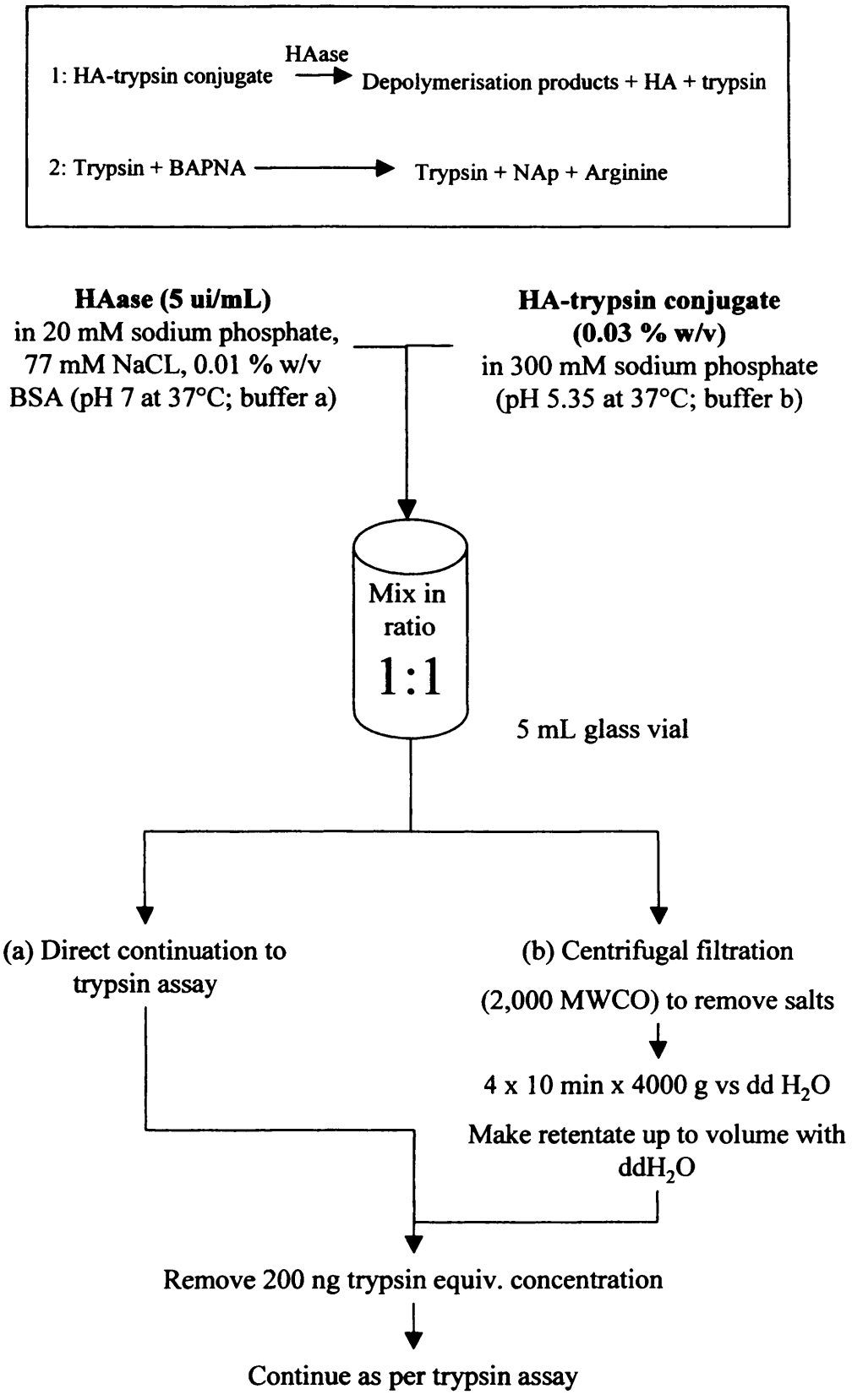

Figure 5.3 UV-vis spectrophotometric assay of trypsin activity following HA-trypsin degradation; multiple buffer protocol (Figure 5.2).

(a) pH-mediated degradation

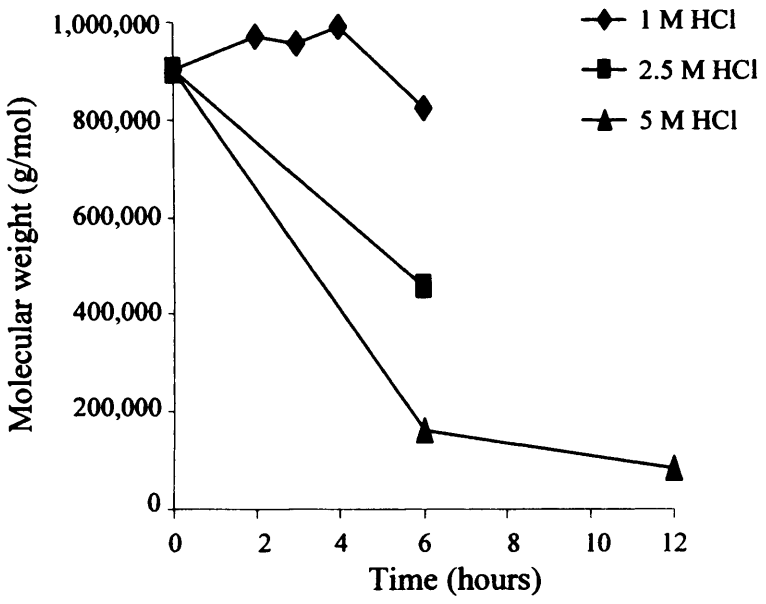

(b) Enzymatic degradation

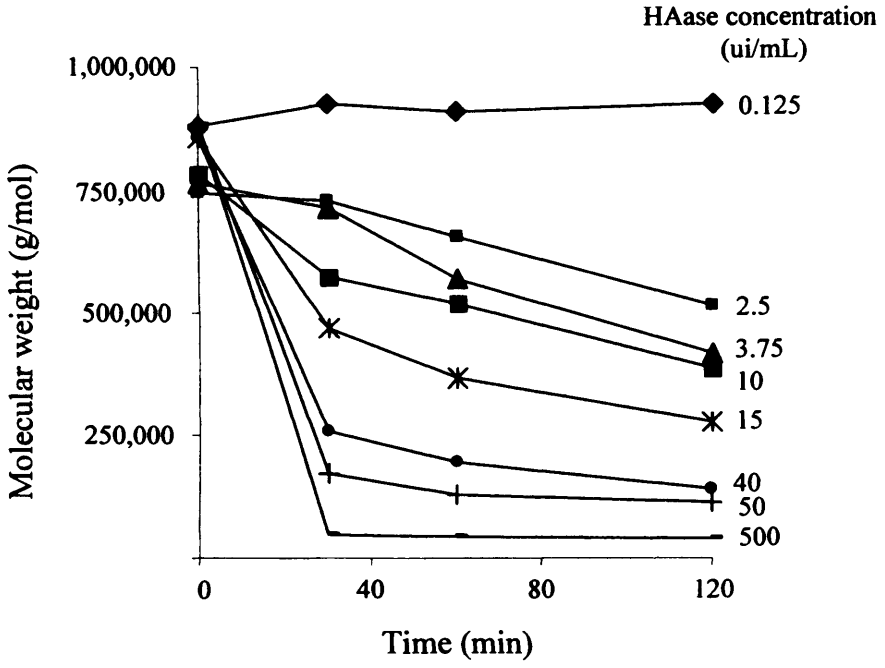

Figure 5.4 Degradation of Rc HA by (a) acid hydrolysis, (b) HAase. Samples were run on a GPC using TSk G4000PW$_{XL}$ followed by G3000 PW$_{XL}$ columns and analysed against pullulan molecular weight standards, to estimate approximate molecular weights (Mw).

(a) FT-IR spectra

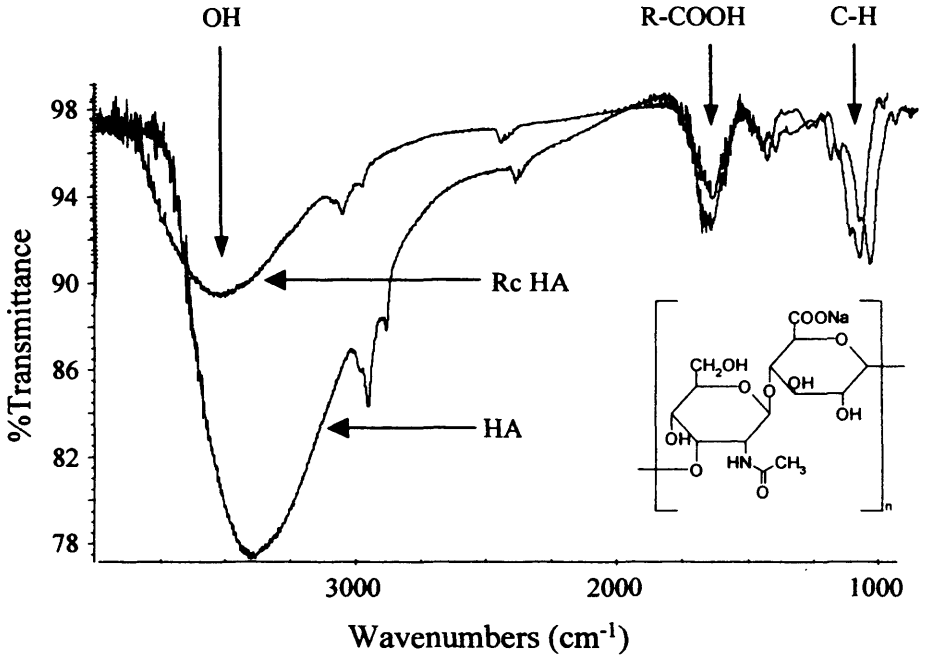

(b) GPC chromatogram

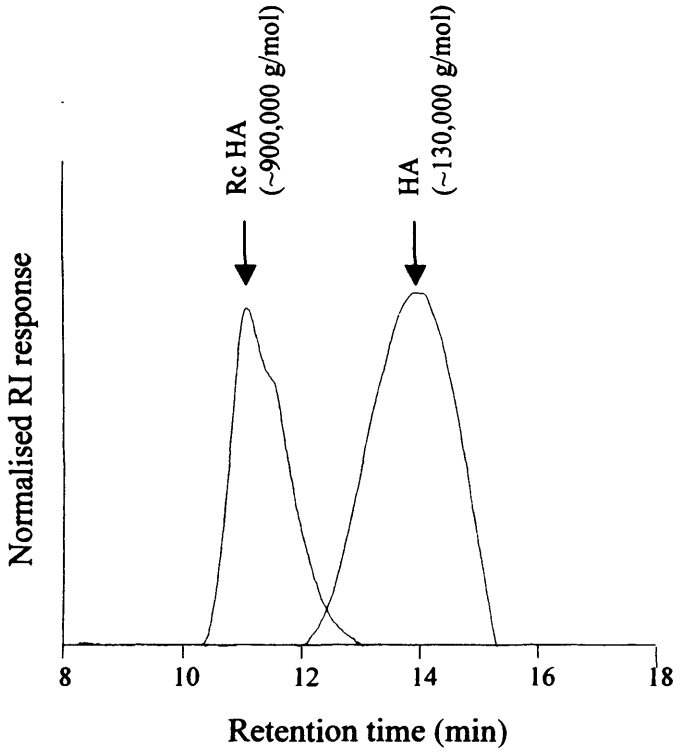

Figure 5.5 Characterisation of the structure, molecular weight and polydispersity of HA from rooster comb (RcHA) (supplied by sigma) and HA (derived from the degradation of HA in HCl (12h, 5M)). Panel (a) FT-IR spectra, and panel (b) GPC chromatogram.

(a) HAase-mediated degradation of HA

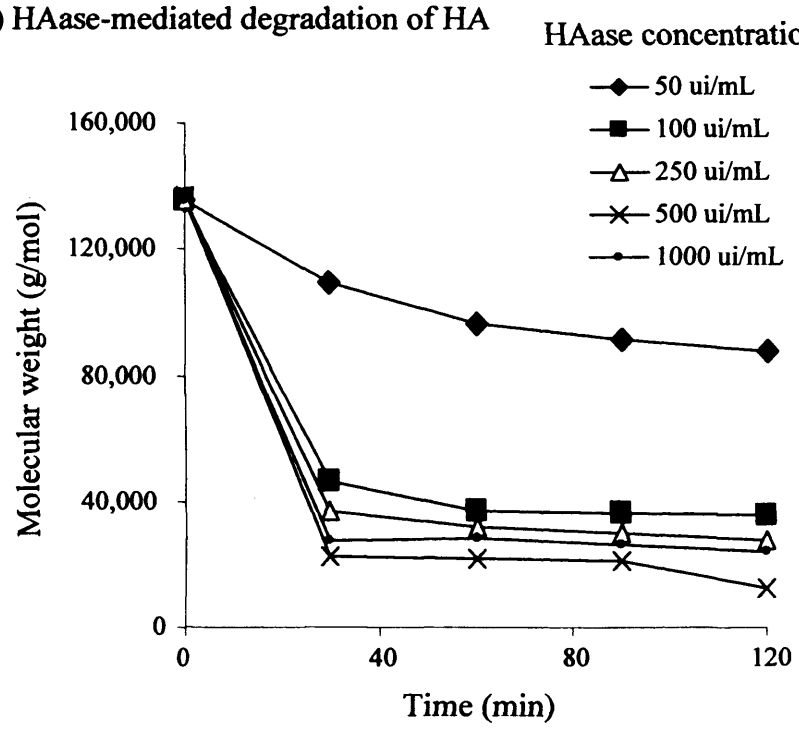

(b) HAase-mediated degradation of HA and HA-trypsin conjugates

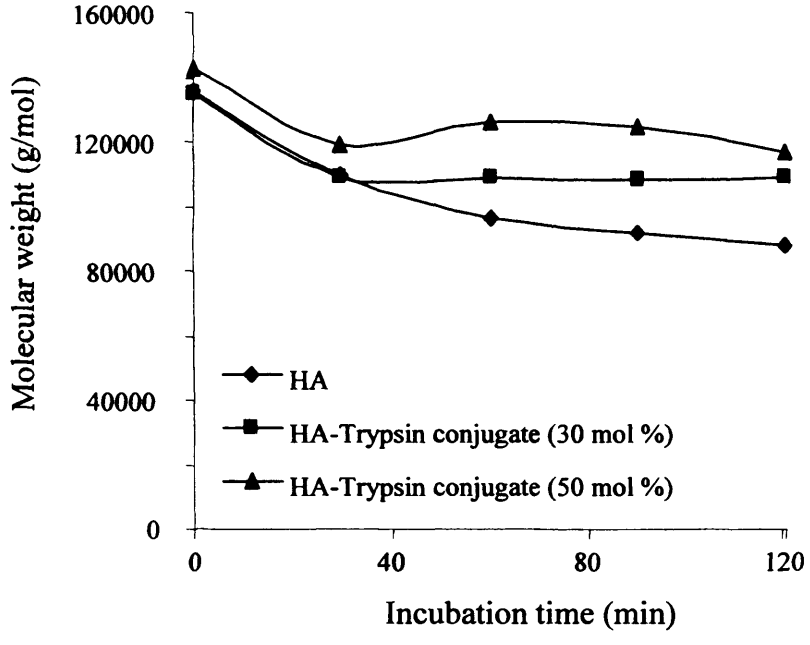

Figure 5.6 Degradation of HA and typical HA-trypsin conjugates by HAase. Panel (a) degradation of HA by increasing concentrations of HAase over 2h, (b) the relationship between mol % activation and rate of change in molecular weight over time, when incubated with HAase (50 ui/mL).

first 30 min and the lowest HA molecular weight obtained under these conditions was ~12,500 g/mol.

5.3.2 Synthesis, purification and characterisation of HA-trypsin conjugates

A library of HA-trypsin conjugates were synthesised by varying (i) the molar ratio of HA : trypsin and (ii) duration of reaction. Typically, the conjugates had a Mw of ~ 80,000 – 115,000 g/mol and a PDI of ~1.4 – 1.7. The total protein content of the conjugates was typically up to 30 % w/w, determined by BCA assay. Characterisation of some of these HA-trypsin conjugates by GPC, SDS-PAGE and FPLC revealed the presence of free trypsin (Table 5.3, Figure 5.7). Consequently, FPLC fractionation was subsequently used to isolate a pure HA-trypsin conjugate (Figure 5.8). The trypsin content of the fractionated conjugate was 3.7 % w/w, and the conjugate Mw and PDI were ~61,000 g/mol and 1.2 respectively. The fractionated HA-trypsin conjugate showed negligible free trypsin and both a reduced molecular weight and polydispersity compared to unfractionated conjugates (Figure 5.9, Table 5.3).

Incubation of HA and typical HA-trypsin conjugates (30 and 50 mol %) with HAase (50 ui/mL, 120 min) caused an increase in their respective GPC retention time, indicating a decrease in molecular weight. As expected, HA was degraded fastest and the 50 mol % modified HA was the least degraded (Figure 5.6b).

5.3.3 Evaluation of free and HA conjugated trypsin activity

The UV-vis absorbance spectra (200 – 700 nm) of HA in tris buffer (pH 5 – 9) showed that HA has no absorbance at the wavelength (400 nm) used to measure NAp production (data not shown). HA also caused no degradation of the substrate BAPNA under the conditions used for trypsin assay (Figure 5.10a). Furthermore, the presence of HA (1 – 10 μg/mL) did not alter trypsin activity against the substrate BAPNA (Figure 5.10b).

HA-trypsin conjugate activity was reduced to 6.4 % of the free trypsin ($p < 0.05$, ANOVA with Bonferroni *post hoc* test) (Figure 5.11a). When the substrate (BAPNA) concentration was increased there was generally an increase in NAp release with time (Figure 5.11b). This was not however a typical linear relationship, preventing the determination of the Michealis-Menten rate constants (Figure 5.12).

Table 5.3 Characteristics of HA-trypsin conjugates synthesised

Batch	Mol % COOH	Molar reaction ratio of HA : trypsin	Duration of reaction (h)	Total trypsin content (% w/w)	Free trypsin detected by SDS-PAGE	Mn† (g/mol)	Mw†† (g/mol)	PDI††† (Mw/Mn)
HAT1	30	1 : 0.5	16	4.5	x	76,900	115,300	1.5
HAT2	30	1 : 1	16	29.1	✓	70,800	113,800	1.6
HAT3	30	1 : 2	16	27.8	✓	60,900	93,800	1.5
HAT4	50	1 : 0.5	20	8.5	✓	108,300	143,000	1.3
HAT5*	30	1 : 0.5	20	3.7	x	51,100	61,200	1.2

† Mn defines the number average molecular weight determined against pullulan standards

†† Mw defines the weight average molecular weight determined against pullulan standards

††† PDI defines the polydispersity index determined against pullulan standards

* HAT5 was fractionated by FPLC to remove free trypsin present in the reaction mixture. Data represents characterisation post fractionation.

(a) GPC chromatogram of typical HA-trypsin conjugates, post dialysis

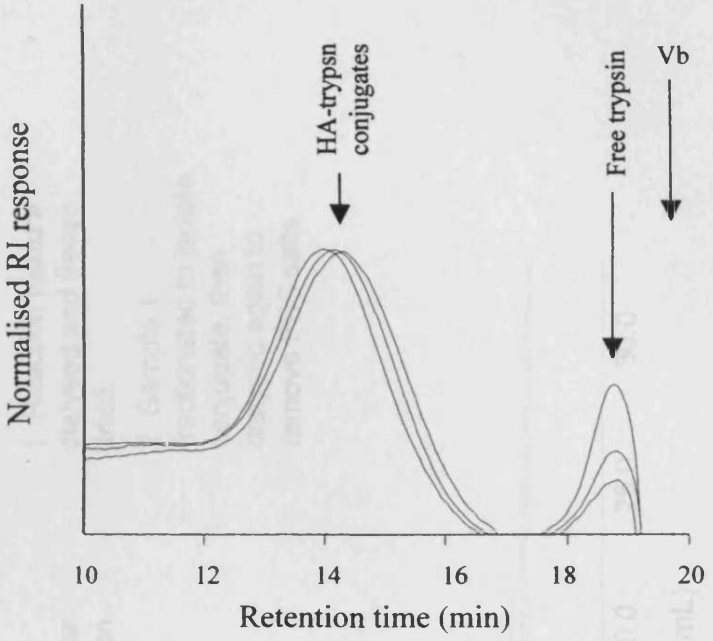

(b) SDS-PAGE of typical HA-trypsin conjugates, post dialysis

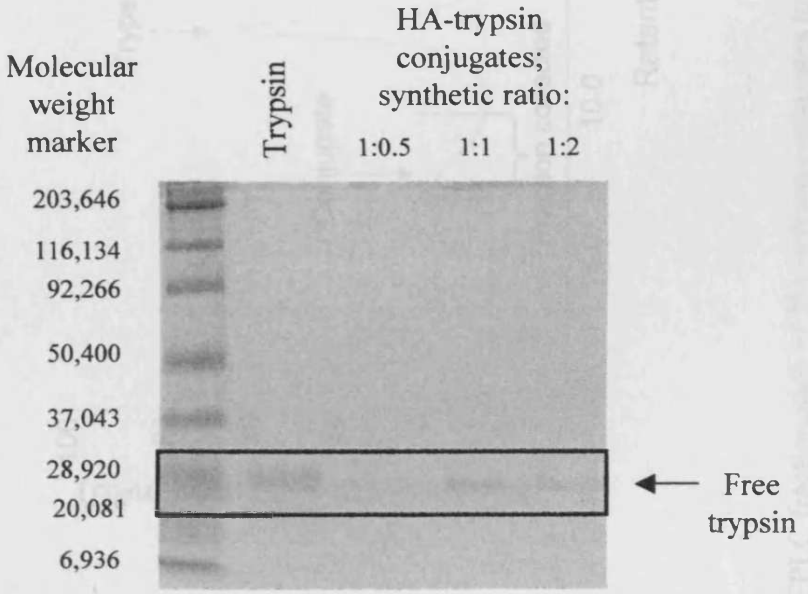

Figure 5.7 Characterisation of the presence of free trypsin present in the HA-trypsin conjugates, following purification by dialysis, by Panel (a) GPC, and (b) SDS-PAGE.

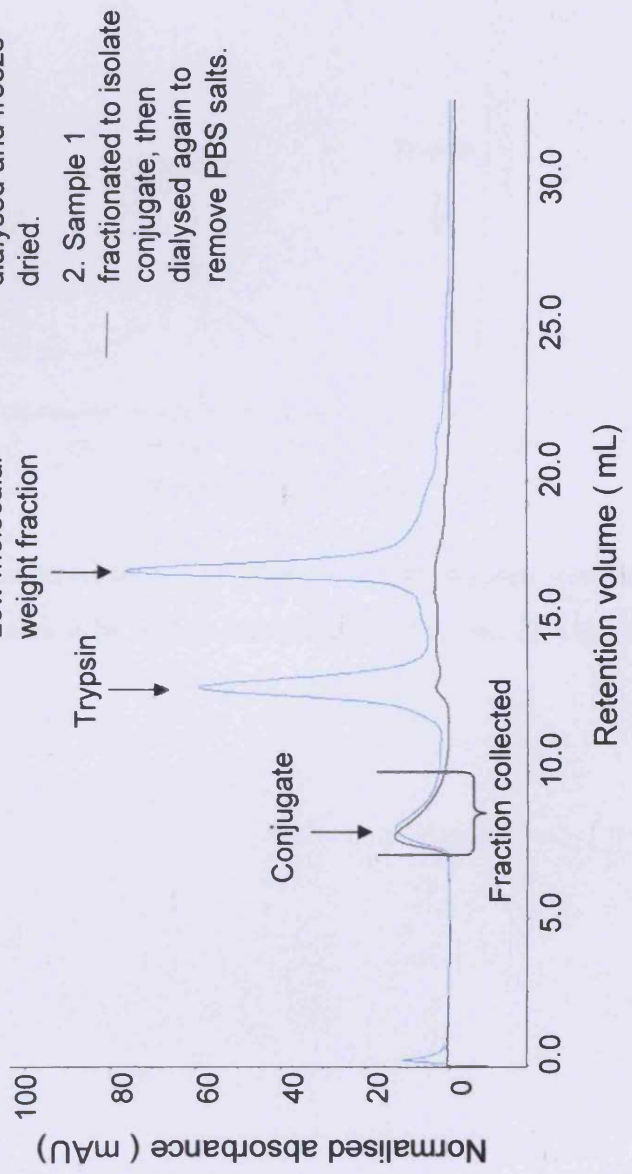

Figure 5.8 FPLC fractionation of HA-trypsin conjugates to remove free, unconjugated trypsin.

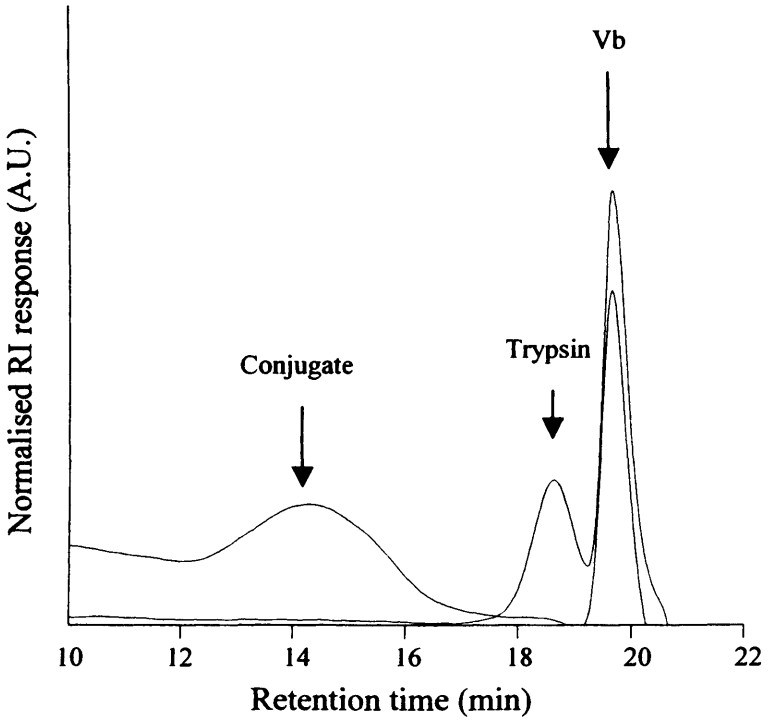

Figure 5.9 Characterisation of a typical HA-trypsin conjugate by GPC following purification by FPLC fractionation. Trypsin (0.1 mg/mL) used as a positive control.

(a) Activity of HA against BAPNA

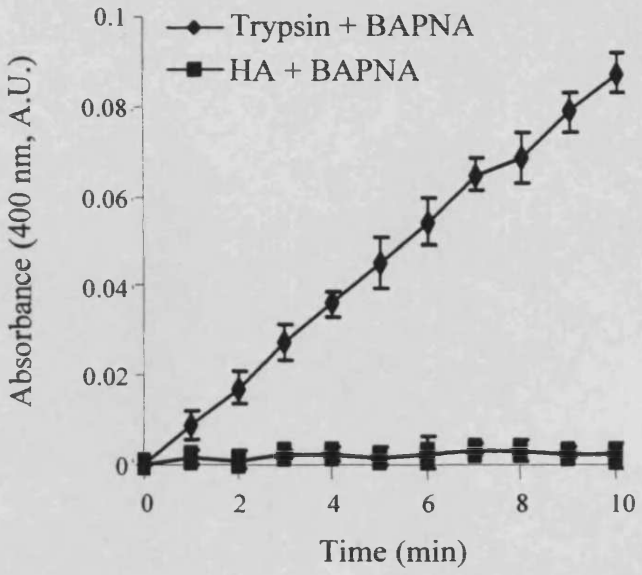

(b) Effect of increasing concentration of HA

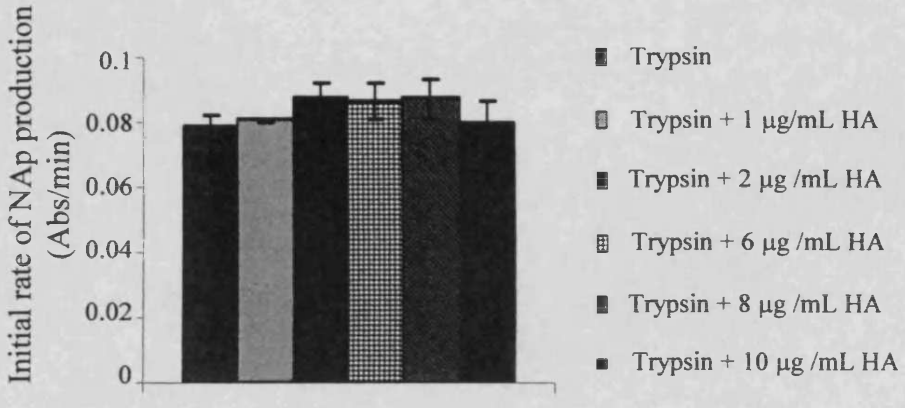

Figure 5.10 Effect of HA on trypsin activity. Panel (a) release of NAp cleaved from BAPNA (0.021 % w/v) by trypsin (8.54 x 10^{-5} mM) or HA (1 mg/mL) over 10 min, (b) effect of HA concentration (1 – 10 µg/mL) on the cleavage of BAPNA (0.021 % w/v) by trypsin (8.54 x 10^{-5} mM) over 10 min. Data represent mean (n=3) ± SD.

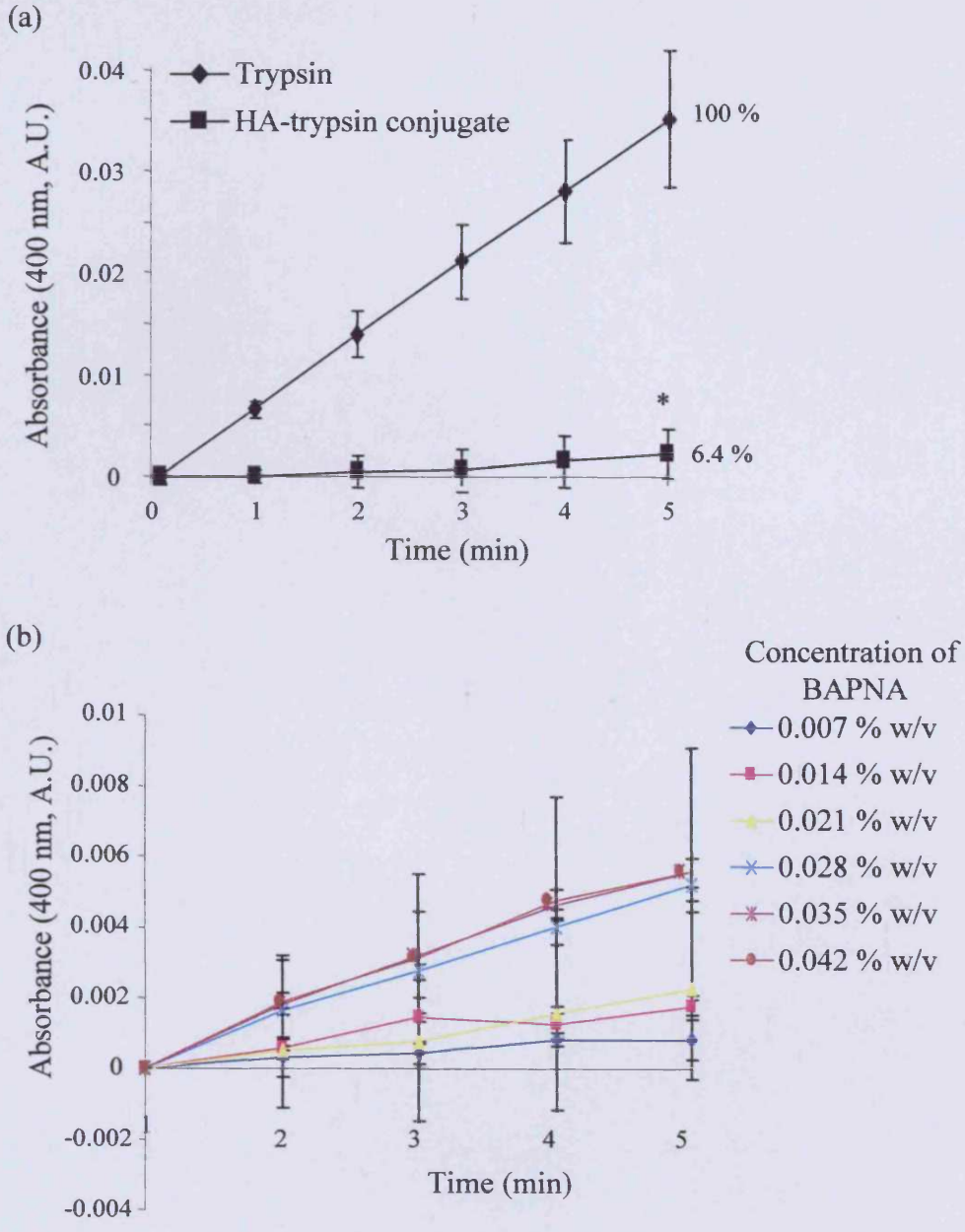

Figure 5.11 Activity of trypsin and HA-trypsin and the effect of substrate concentration on the release of NAp (400 nm) cleaved from BAPNA over 5 min. Panel (a) activity of trypsin (8.54×10^{-5} mM) and HA-trypsin conjugate (8.54×10^{-5} mM trypsin equiv.) against BAPNA (0.021 % w/v), (b) activity of HA-trypsin conjugate with increasing BAPNA concentration. Data shows the mean (n=3) ± SD. Significance (*) indicates $p<0.05$ analysed by ANOVA and Bonferroni *post hoc* test.

(a) Hanes-Woolfe plot

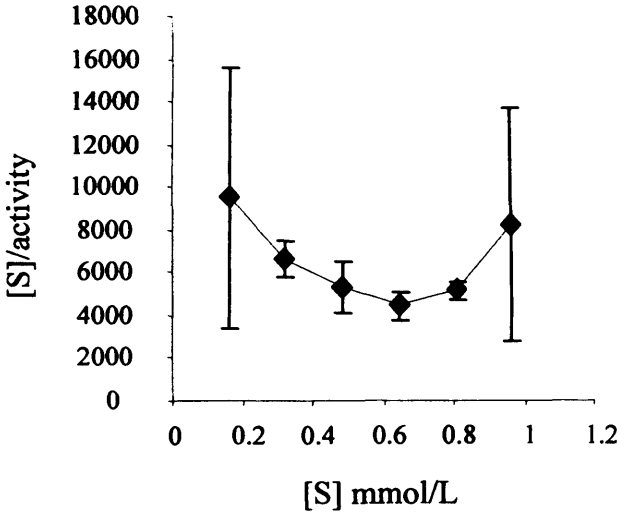

(b) Lineweaver-Burk plot

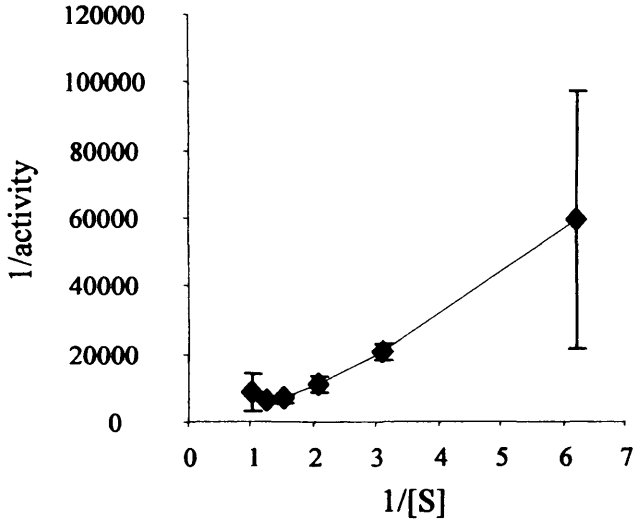

(c) Eadie-Hofstee plot

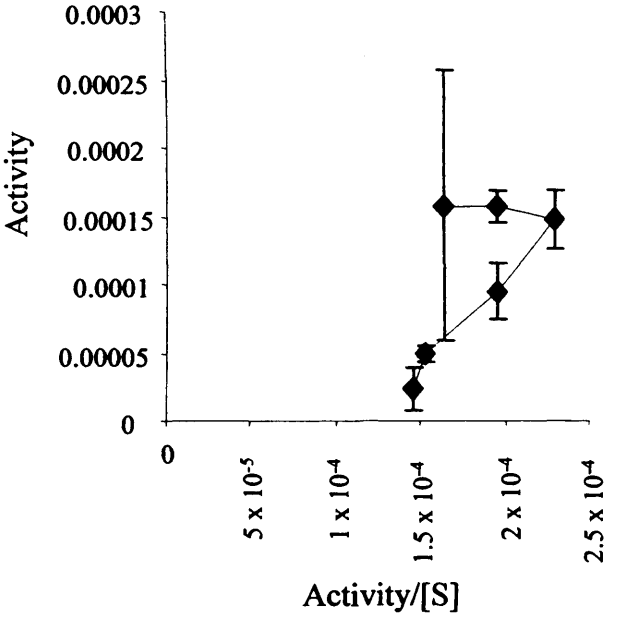

Figure 5.12 Analysis of HA conjugated trypsin activity using Michaelis-Menten derived plots, to determine kinetics rate constants. Data shows mean (n=3) ± SD.

It was necessary to conduct a number of control experiments to determine HA-trypsin activity during incubation with HAase. The UV-vis absorbance (400 nm) of mixtures of BAPNA with either HA or HAase and of mixtures of trypsin with either HA or HAase were assessed (Figure 5.13). Overall, it could be concluded that combinations of trypsin and BAPNA with HA and HAase did not significantly increase or decrease trypsin activity. HAase in tris buffer (pH 5 – 9) did not show any absorbance at 400 nm, and both HA and HAase, incubated in tris (pH 8) overnight, did not produce degradation products which would absorb at 400 nm (data not shown).

5.3.4 Evaluation of HA-trypsin activity in the presence of HAase

After addition of HAase (5 ui/mL) to the HA-trypsin conjugate, there was an immediate increase in trypsin activity. This was maximal when 10 ui/mL HAase was added (Figure 5.14), leading to ~ a four fold increase in trypsin activity compared to activity of the conjugate (Figure 5.15). Addition of increasing concentrations of HAase (0.5 – 25 ui/mL) did not produce a linear increase in trypsin activity and HAase concentrations greater than 10 ui/mL appeared to have an inhibitory effect (Figure 5.14b).

When trypsin activity was measured in tris buffers of different pH (5 – 8) (Figure 5.16), maximum activity was seen at pH 8. However, trypsin activity decreased over the 22 h incubation in all buffers tested. The activity of the HA-trypsin conjugate was not greatly increased by incubation with HAase up to 22 h. Similarly, incubating the conjugate for 22 h with higher concentrations of HAase (100 – 500 ui) was also unable to significantly increase conjugate activity (data not shown).

5.3.5 Evaluation of a multi-buffer system used to study HAase unmasking of HA-trypsin conjugate

The absorbance of HA degraded by HAase was measured at 600 nm in sodium acetate buffer of pH 3.75. However, when the sodium acetate buffer was adjusted to pH 4.75, there was no absorbance detected (Figure 5.17a).

When an HA-trypsin conjugate was co-incubated with HAase (22 h) in sodium acetate buffer (pH 3.75) and then transferred directly into tris buffer to measure activity, a cloudy white precipitate was formed. This was reflected by a negative absorbance, which occurred for 4 min after the addition of the substrate BAPNA (Figure 5.17b). After 4 min, a positive increase in absorbance was measured.

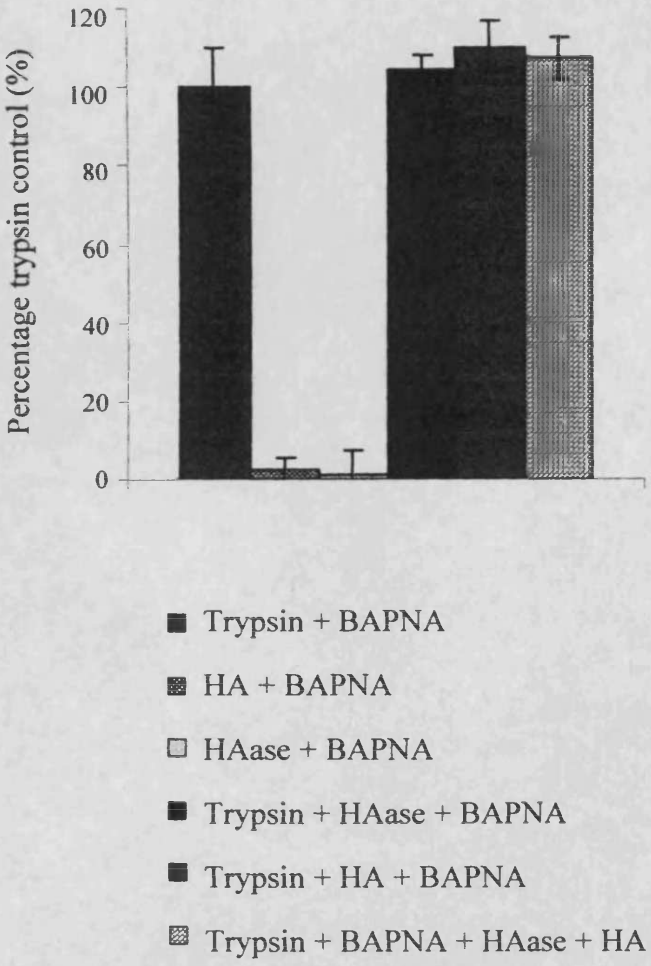

Figure 5.13 Release of NAp cleaved from BAPNA (0.021 % w/v) over 10 min by mixtures of trypsin, HA and HAase (listed above). Data expressed as percentage of free trypsin (8.54×10^{-5} mM) activity. Data shows mean (n=3) ± SD.

(a) Effect of addition of HAase to mixture of HA-trypsin conjugate and BAPNA

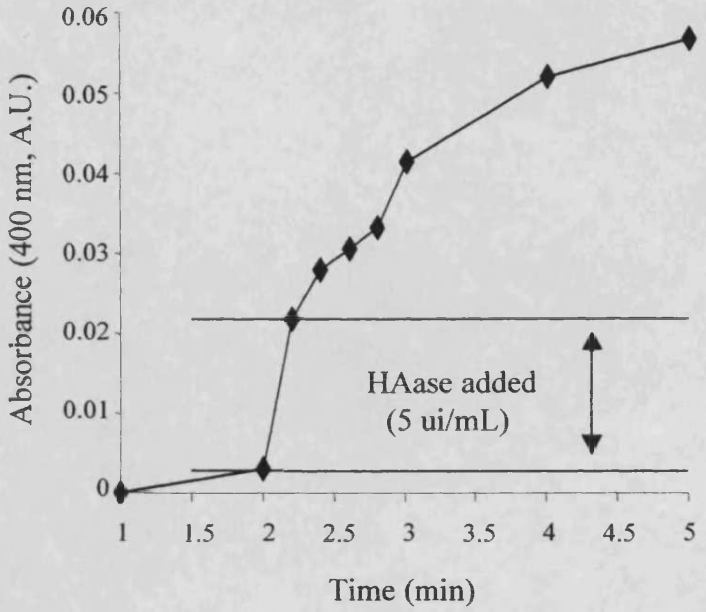

(b) Addition of HAase (varying concentration)

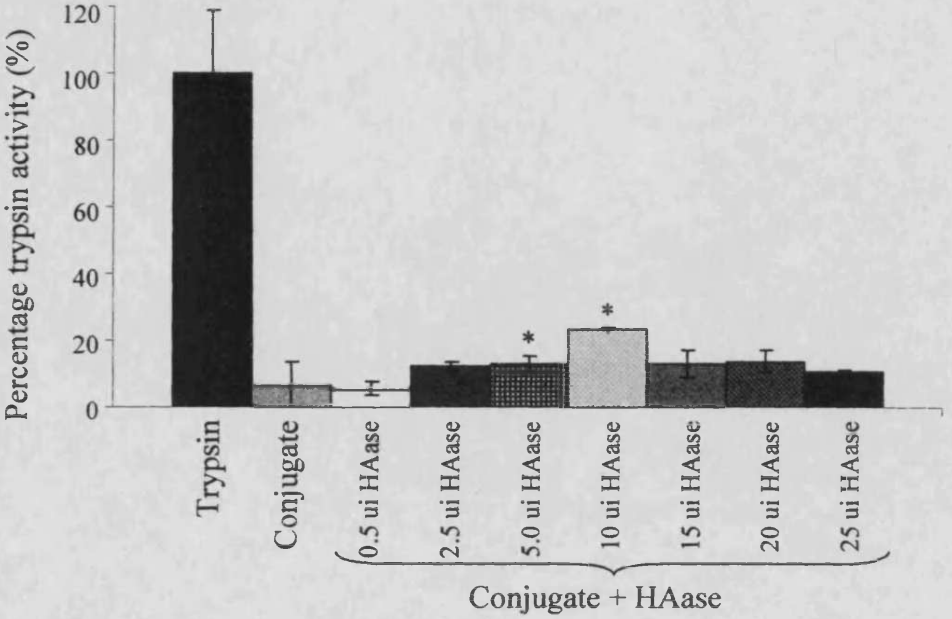

Figure 5.14 Release of NAp (400 nm) cleaved from BAPNA (0.021 % w/v) by HA-trypsin conjugate. Panel (a) HAase added at 2 min to degrade the conjugate, and (b) free and conjugated trypsin activity in the presence and absence of HAase (0.5 – 25 ui/mL) over 10 min. HAase added to the cuvette at onset of the experiment. Data shows mean (n=3) ± SD. * indicates $p<0.05$ (ANOVA and Bonferroni *post hoc* test) compared to the remaining HA-trypsin conjugate activity.

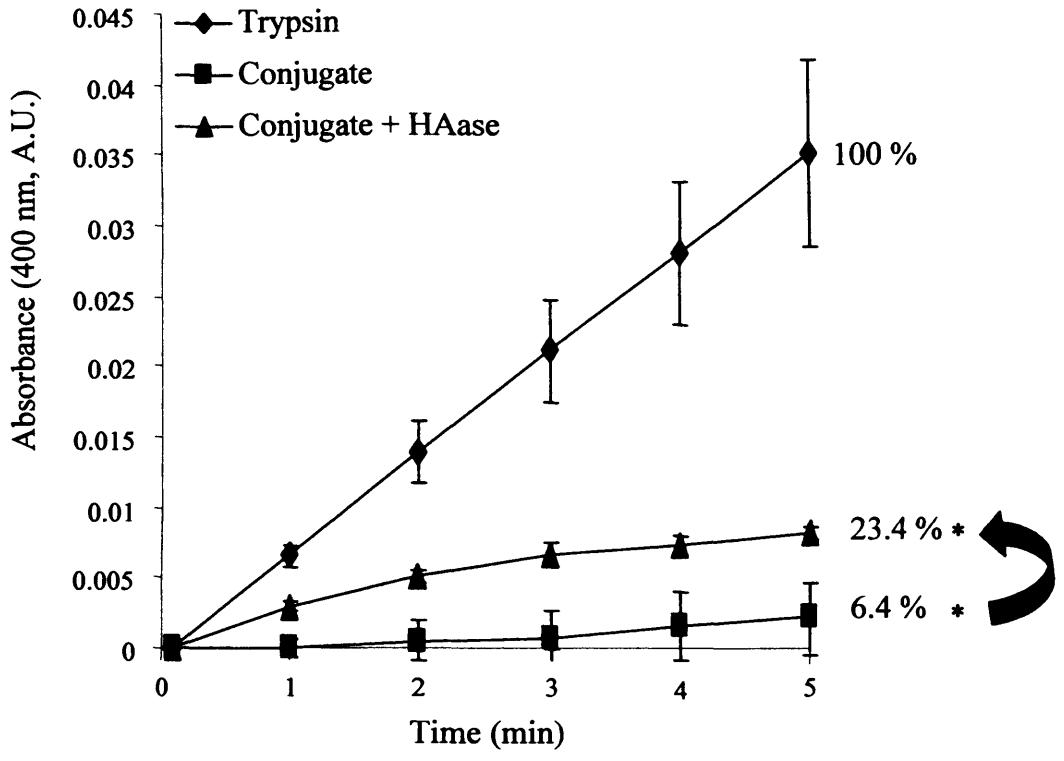

Figure 5.15 Release of NAp (400 nm) cleaved from BAPNA (0.021 % w/v) by trypsin and HA-trypsin conjugate (8.54 x 10^{-5} mM trypsin equiv.) , prior to and following addition of HAase (10 ui/mL). Data shown represents the mean (n=3) ± SD. Significance (*) indicates $p<0.05$ determined by ANOVA and Bonferroni *post hoc* test.

(a) Effect of pH on trypsin activity over 22 hours

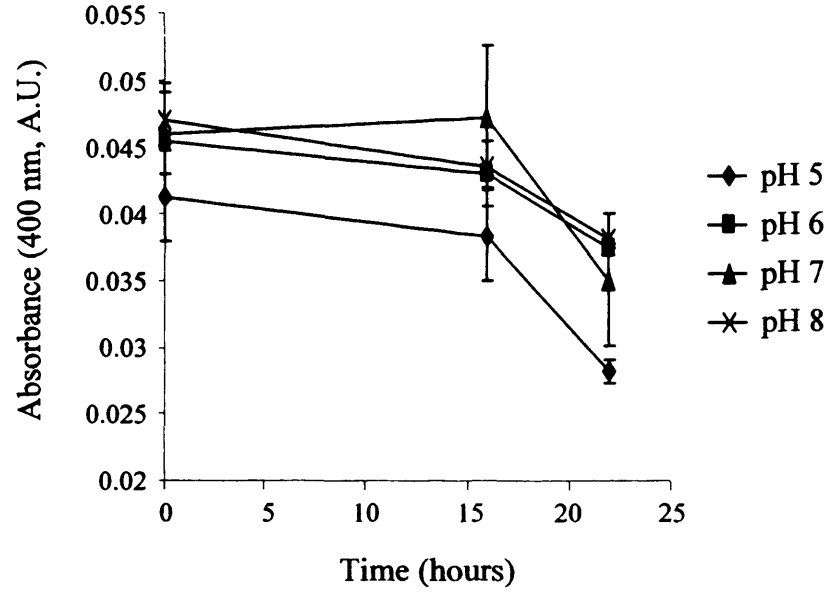

(b) Effect of pH on trypsin activity after 22 h incubation at 37 °C

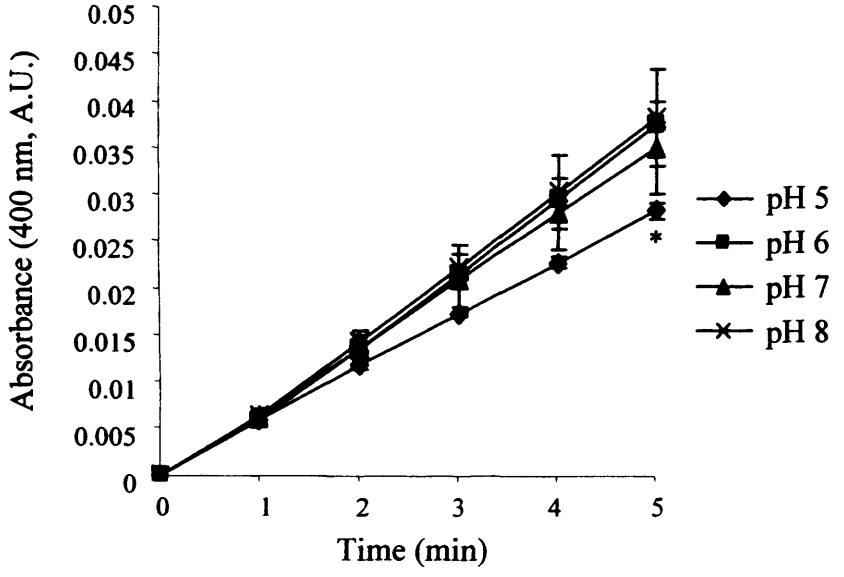

Figure 5.16 Effect of pH on the release of NAp from BAPNA (0.021 % w/v) cleaved by trypsin (8.54 x 10^{-5} mM trypsin equiv.). Panel (a) trypsin activity tested at 0, 16 and 22 h, and (b) trypsin activity tested following 22 h incubation at 37 °C. Data represents mean (n=3) ± SD. * indicates significance ($p<0.05$) determined using ANOVA and Bonferroni *post hoc* test.

(a) Degradation of HA

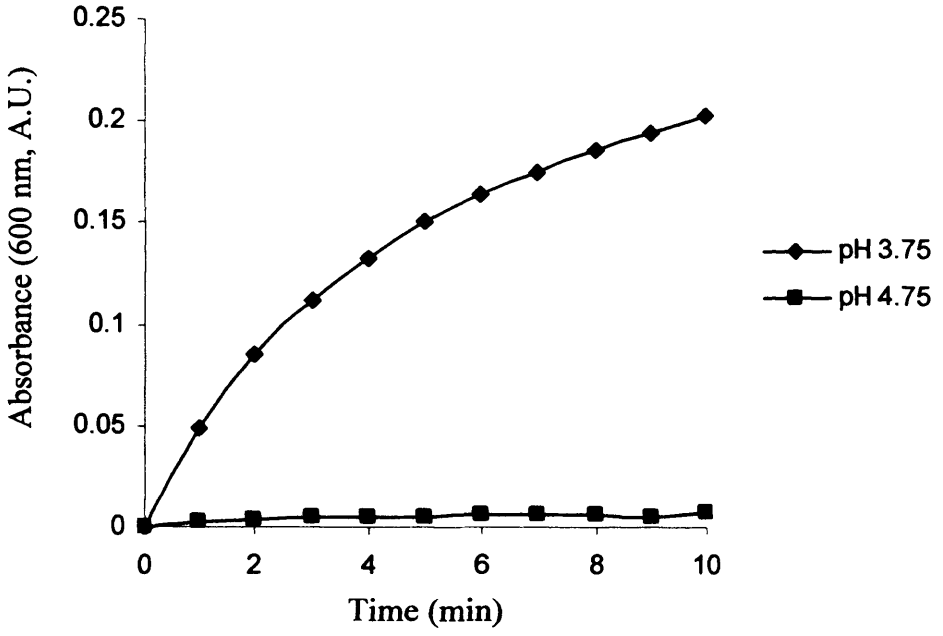

(b) HA-trypsin conjugate + HAase (multi-buffer system)

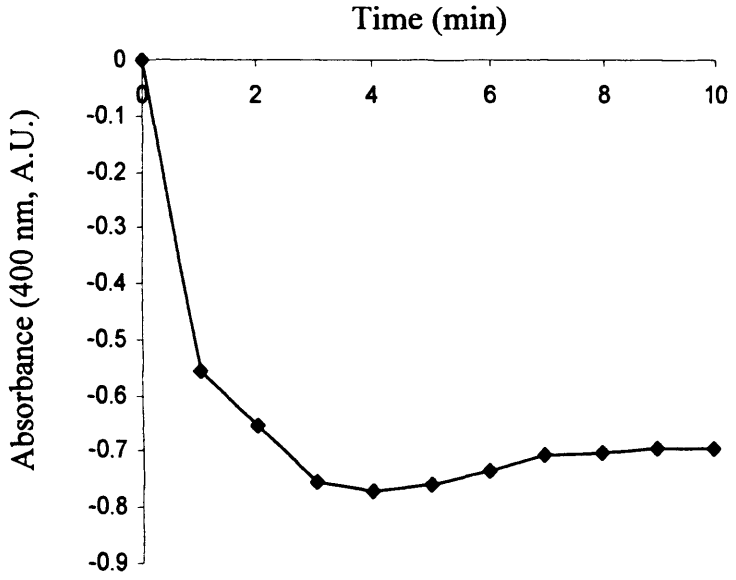

Figure 5.17 Pilot study on the use of a multibuffer system to measure HA-trypsin conjugate activity following polymer degradation. Panel (a) degradation of HA by HAase (5 ui/mL) in sodium acetate buffer, method adapted from SIGMA. Panel (b) UV-vis absorbance (400 nm) of NAp cleaved from the substrate BAPNA, following incubation of a HA-trypsin conjugate with HAase (5 ui/mL) in sodium acetate buffer. Method adapted from Sigma protocol. Not possible to make corrections for blank absorbance.

Unfortunately, it was not possible to subtract the absorbance of the control blank as it had also undergone precipitation.

Purification of the HA-trypsin conjugate and HAase mixture by centrifugation was used to remove sodium acetate from the sample. Trypsin activity was then measured in tris buffer and found to be comparable to the previous conjugate activity experiments that used tris buffer alone. Conjugate activity was reinstated to 24 % of trypsin control (Figure 5.18). However, there was a much greater degree of fluctuation detected for the progress curve (Figure 5.18b).

5.4 Discussion

This study assessed HA as a potential polymeric backbone for masking trypsin activity and the ability of HAase to trigger unmasking. To prepare a suitable HA fraction for conjugation, Rc HA was degraded (enzymatically and by hydrolysis) to give a HA fraction of molecular weight ~100,000 g/mol (Figure 5.4). The target molecular weight for HA of 100,000 g/mol was chosen with the hope that this would both optimise masking of conjugated protein activity, whilst also allow subsequent HA degradation to a size below the renal threshold (~40,000 g/mol), to ensure ultimate elimination if used in a therapeutic conjugate. HAase degradation of the HA fraction confirmed it was possible to degrade the polymer to ~12,500 g/mol within 2 h (Figure 5.6).

A potential concern when using such a lower molecular weight HA fraction than native HA, however, is that molecular weights of $2.8 \times 10^5 - 4.7 \times 10^5$ g/mol have been shown to promote inflammation through stimulation of CD44 on macrophages. Nonetheless, these HAs have also shown beneficial effects, such as protection of eosinophils through stimulation of GCSF production (reviewed in Ghosh and Guidolin, 2002).

The HA-trypsin conjugates initially synthesised contained unconjugated trypsin. Unlike the previous studies using dextrin, where an excess of trypsin (Chapter 3) or a 1 : 5 ratio of COOH : MSH (Chapter 4) could be used without problems of conjugate purity, here, the ratio of HA : trypsin that could be used was much lower (1 : 0.5 – 1 : 2). Even, with the lowest synthetic ratio (1 : 0.5) and purification by dialysis, there was still unconjugated trypsin detectable by FPLC. This may be due to the

(a) Multibuffer system

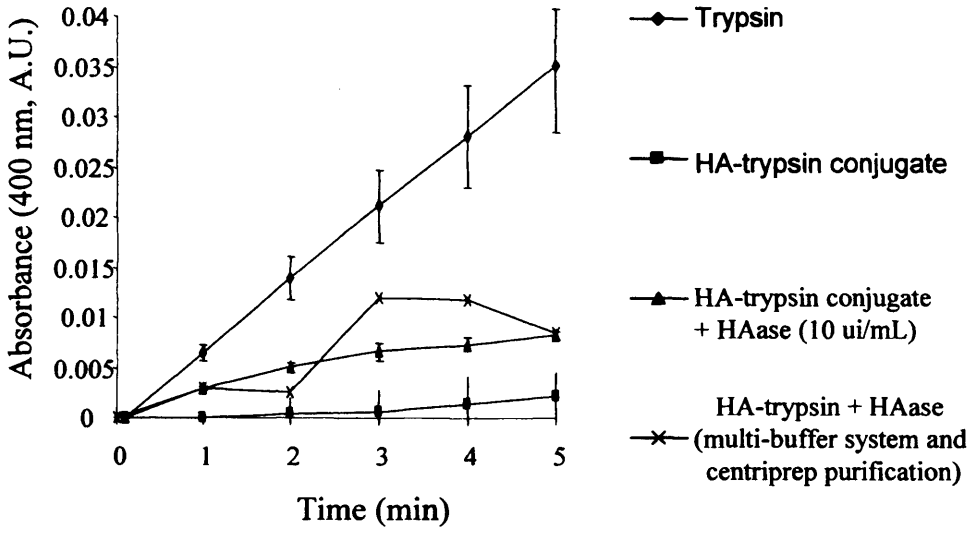

(b) Multibuffer system with purification to remove sodium acetate

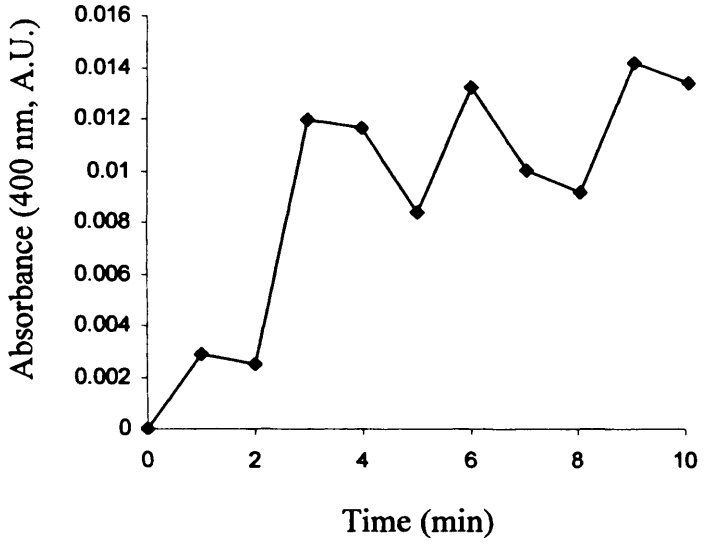

Figure 5.18 Absorbance of NAp (400 nm) measured when cleaved from the substrate BAPNA (0.021 % w/v) by trypsin (8.54 x 10^{-5} mM) and HA-trypsin conjugate (8.54 x 10^{-5} mM trypsin equiv.), prior to and following degradation by HAase (10 ui/mL). Panel (b) multi-buffer system; conjugate degraded in acetate buffer pH 3.75, centrifuged to remove acetate salts and then analysed in tris buffer (protocol as detailed in Figure 5.3).

bulkiness of the HA or the formation of complexes between HA and trypsin. Isolation of a pure conjugate could only be achieved by FPLC fractionation (Figure 5.8).

A trend between the ratio of polymer : enzyme in the reaction mixture and the ultimate protein loading was observed across the three types of conjugates. Previously, in Chapter 3, an excess of trypsin was used in the reaction mixture. This produced conjugates of a much higher trypsin loading (~ 70 – 90 % w/w). Whereas, when the ratio of polymer : protein was lower (1 : 0.5 – 5), the protein loading was typically up to 30 % w/w. This held true for both the dextrin-MSH (Chapter 4) and HA-trypsin conjugates (Chapter 5).

It was also found that the mol % activation of both HA and typical HA-trypsin conjugates (prepared using HA with 30 and 50 mol % activation) demonstrated reduced degradability (Figure 5.6b) with increasing degree of modification of the polymer. This is consistent with the previous work on dextrin-trypsin conjugates, Chapter 3 (Figure 3.9).

Activity of the HA-trypsin conjugate

HA conjugation significantly masked trypsin activity ($p < 0.05$, ANOVA and Bonferroni *post hoc* test). The HA-trypsin conjugate (30 mol % activation, 3.7 % w/w trypsin loading) displayed 6.4 % activity of trypsin control (Figure 5.11a). This reduction in activity is greater than was seen for dextrin-trypsin (Chapters 3). The greater masking of trypsin activity by HA may have been due to the increased polymer molecular weight and / or the lower protein loading of the HA-trypsin conjugate (3.7 % w/w).

However, when the activity of the HA-trypsin conjugate was measured against a range of substrate concentrations (BAPNA 0.007 – 0.042 % w/v), the relationship did not follow typical Michaelis-Menten kinetics. It was therefore not possible to determine the kinetics rate constants (Figure 5.12). The non-linearity may be due to interference by HA (complexation of HA with free trypsin generated) but it is difficult to explain.

HA-trypsin conjugate activity in the presence of HAase

In preliminary experiments activity was determined after simply adding HAase. This assay showed that it was possible to cause degradation of the conjugate with immediate increase in trypsin activity (Figure 5.14). HAase was subsequently added at

time zero (Figure 5.14b). In these initial experiments it was shown that HAase (10 ui/mL) incubated with the HA-trypsin conjugate could increase activity 4 fold over 5 min. Nevertheless, the total increase seen (% control) was relatively modest when more HAase was added, such that as the concentration of HAase was increased above 10 ui HAase, the trypsin activity began to decrease. This may be explained by the work of Asteriou et al., (2001) where addition of increasing HAase concentration was believed to result in increasing turbidity and increased formation of HA-protein complexes. In the case of the HA-trypsin conjugates, there could be complex formation between HAase added and either trypsin released from the conjugate or with the conjugate itself.

The complexity of this assay is also increased by the fact that two enzymes are required to function simultaneously and they require different assay conditions. Firstly, HAase is needed to degrade the HA backbone of the conjugate, and secondly, trypsin activity is required to degrade the substrate BAPNA. The optimal trypsin assay conditions (tris buffer, pH 8.2; Buck et al., 1962) are not optimised for HAase (pH 4.5 – 6.0; SIGMA, 2002).

Initial experiments were conducted at the optimum pH for trypsin as it has been shown that HAase from bovine testes also has significant activity at pH 7.5 (reviewed by Menzel and Farr, 1998). However with the aim of improving the modulation of trypsin activity, the effect of incubation (37 °C) of trypsin in tris buffer (pH 5 – 8; 0 – 22 h) and HAase concentration were examined. Unfortunately it was not possible to further improve the unmasking of trypsin activity. Possible explanations may be that the combination of random conjugation and low protein loading (3.7 % w/w) may have caused a greater proportion of the protein payload to be irreversibly inactivated at the trypsin active site. Secondly, there may be trypsin inhibitors present in the HAase as impurities. Therefore as the concentration of HAase was increased there would also be an increase in the inhibition of trypsin activity (Zhuo et al., 2004; Jessen et al., 1994). Typically, HAase activity is measured in either PBS (Tawada et al., 2002) or acetate (Blundell and Almond, 2006) buffer, at a pH of ~5 (Asteriou et al., 2006), rather than the tris buffer (pH 8.2) used in this system. Despite the conditions used, the conjugate did show that it was degraded, as the activity of the conjugate was rejuvenated 4 fold in 5 min on addition of HAase (discussed earlier).

Preliminary studies on a multi-buffer system to optimise unmasking of trypsin conjugate activity

In the previous sections, it was noted that the method used to degrade the HA-trypsin conjugate and measure subsequent trypsin activity, could either be optimised to the conditions required for conjugate degradation, or for measurement of trypsin activity (Figure 5.2). All studies carried out so far on dextrin-trypsin (Chapter 3) and HA-trypsin (Chapter 5) conjugates, have optimised conditions solely for trypsin activity.

Preliminary assessment of the multi-buffer system utilised a sodium acetate buffer (pH 3.75) to degrade the HA-trypsin conjugate (Figure 5.3). Direct transfer of the 200 ng trypsin equiv. volume of conjugate from the sodium acetate buffer into tris buffer (pH 8.2) (Figure 5.17b) led to precipitate formation in the cuvette. To overcome the issue of precipitation, the conjugate solution was purified by centrifugation to remove sodium acetate and re-suspended in tris buffer for measurement of trypsin activity.

Despite, reinstating trypsin activity to a comparable level to when the conjugate was degraded in tris buffer, this method was considered inaccurate (Figure 5.18) as trypsin may be lost in the process of purification and the progress curve of the purified degraded sample was very variable (Figure 5.18b).

In summary, initial studies utilising a multiple buffer system were hindered by problems of reproducibility and precipitation and would require much further work to optimise a system that could be used reliably.

5.5 Conclusion

HA-trypsin conjugates were synthesised using a HA fraction (~130,000 g/mol), purified by FPLC fractionation and characterised, revealing a pure conjugate.

The optimum conjugate was shown to mask activity to 6.4 % and on addition of HAase, reinstate trypsin activity 4 fold in 5 min. This was a greater immediate re-expression of activity than observed for the previous dextrin-trypsin conjugates (Chapter 3).

However, further expression of trypsin activity was not achieved even when factors of HAase concentration, incubation time and buffer pH were varied. This may be attributed to an irreversible inactivation of the trypsin active site caused by random conjugation to HA.

A multi-buffer system was piloted, combining the optimum conditions for both HAase and trypsin activity. However, these methods require further study.

Chapter 6

Preliminary study on the synthesis and characterisation of HA-RNase A conjugates, cellular uptake and assessment of their cytotoxicity in CV-1 and B16F10 cells

6.1 Introduction

The preceding work demonstrated that enzyme and peptide activity may be decreased and subsequently reinstated by their conjugation either to dextrin and HA followed by enzymatic degradation of the polymer (Chapters 3 - 5). In this part of the study, it was considered important to conduct at least one preliminary experiment to evaluate a potentially therapeutic polymer-anti-cancer protein conjugate. For these, preliminary studies, it was decided to utilise the HA fraction of molecular weight 130,000 g/mol, with ~30 mol % activation of the carboxyl groups conjugated to the anti-tumour enzyme RNase A.

HA was chosen (rationale discussed in Chapter 5) as it has the potential to target the CD44 receptor which has been suggested to mediate tumour targeting. The rationale for choosing a ribonuclease as the therapeutic enzyme for this work is discussed in the following section.

6.1.1 Rationale for choosing bovine pancreatic RNase A as the therapeutic enzyme for conjugation to HA

Three ribonucleases are commonly used; bovine pancreatic (RNase A), bovine seminal (BS-RNase) and northern leopard frog (Onconase) (described in section 1.7.2.3).

It has been shown that BS-RNase and Onconase are cytotoxic to cell cultures of human cell lines (Monti and D'Alessio, 2004), and both seem able to evade RIs, unlike RNase A which can become tightly bound (reviewed in Matousek et al., 2003). The concentration of Onconase and BS-RNase required to achieve 50 % inhibition of cell growth of ML-2 cells (IC_{50} values) was 0.4 μg/mL and 2 μg/mL respectively (Matousek et al., 2003). Despite the poor or non-existent cytotoxicity of free RNase A *in vitro* (Matousek et al., 2003) however, an poly[HPMA] conjugate of RNase A administered IV route was found to be as effective as poly[HPMA]-BS-RNase conjugates (Pouckova et al., 2004). Moreover, when assessing the immunogenicity of a single dose of ribonuclease in mice, Matousek et al., (2003) found that RNase A (10 – 80 antibody titer) was less immunogenic than Onconase (80 – 320 antibody titer) and BS-RNase (1600 – 3200 antibody titer). Onconase was also found to cause dose limiting toxicity (renal) in Phase I and II clinical trials (reviewed by Erickson et al., 2006). For these reasons, RNase A was chosen to prepare the HA conjugate. It was hoped that conjugation to HA might promote increased RNase A tumour targeting by

the EPR effect and CD44-mediated cellular uptake of the conjugate. Additionally, to improve stability in transit, reduced exposure to the kidneys, and release of the ribonuclease into the cytosol where it may induce apoptosis.

6.1.2 Polymer-ribonuclease conjugates

Various studies have already compared the cytotoxicity of polymer conjugated ribonuclease (bovine pancreatic, bovine seminal and Onconase) to free ribonuclease *in vitro* and *in vivo*. *In vitro* polymer conjugation of ribonuclease produced reduced activity, whereas BS-RNase was cytotoxic in the UKF-NB-3 cell line with an IC_{50} of 2.18 ± 0.18 μg/mL (Table 6.1). PEG conjugated BS-RNase displayed no cytotoxicity in a UKF-NB-3 cell line (Evans stage 4 NB) up to a concentration of 100 μg/mL (BS-RNase equiv.) measured using an MTT assay over 5 days (Michaelis et al., 2002). Additionally, a poly[HPMA] conjugate of BS-RNase had poor activity when incubated with both an ML-2 cell line and with stimulated human lymphocytes. This was attributed in part to the huge size of the overall conjugate, which may have prevented penetration into the cell (Ulbrich et al., 2000).

In contrast, preliminary *in vivo* studies (Michaelis et al., 2002) showed that it was possible to significantly reduce neuroblastoma size in CD-1 athymic mice (UKF-NB-3 xenotransplantate), when the BS-RNase-PEG conjugate was administered systemically. An increase in efficacy of 16 - 17 fold was seen, compared to the native BS-RNase. Moreover, poly[HPMA]- and PEG (5,000 or 22,000 g/mol) conjugates of RNase A had significantly better anti-tumour effects and less side effects in mice bearing human melanoma, than the corresponding BS-RNase conjugates (Pouckova et al., 2004; Soucek et al., 2002; Ulbrich et al., 2000).

6.1.3 Choice of B16F10 and CV-1 cells for the biological assays

Several *in vitro* assays have been used to measure ribonuclease activity (summarised in Table 6.2). In the present study B16F10 and CV-1 cells were used in preliminary experiments to study the cytotoxicity of RNase A and the HA-RNase A conjugate. This was because they have been reported to have a high (B16F10) and low (CV-1) CD44 receptor expression respectively (Eliaz and Szoka, 2001). Eliaz and Szoka, (2001) used these two cell lines to study the CD44 receptor-mediated uptake of HA oligosaccharide-liposomes loaded with doxorubicin, and they found that

Table 6.1 Sources of ribonucleases and their activity in *in vitro* cell models

Ribonuclease source	Form	Cell line	Cytotoxic	IC_{50} (μg/mL)	Reference
BS-RNase‡	Dimeric homolog of RNase A	ML-2†	Yes	2	Matousek et al., 2003
				ND#	Ulbrich et al., 2000a
				ND#	Pouckova et al., 2004
BS-RNase‡	Dimeric homolog of RNase A	UKF-NB-3††	Yes	2.18 ± 0.18	Michaelis et al., 2002
BS-RNase‡	Dimeric homolog of RNase A	K-562†††	Yes	1.3 ± 0.1	Eugene Lee and Raines, 2005
RNase A‡‡	NA*	ML-2†	No	NA*	Pouckova et al., 2004
					Soucek et al., 2002
RNase A‡‡	NA*	K-562†††	No	NA*	Eugene Lee and Raines, 2003
Onconase‡‡‡	Homolog of RNase A	K-562†††	Yes	0.8	Eugene Lee and Raines, 2003
E. Coli‡‡‡‡	Homolog of RNase A	ML-2†	Yes	0.4	Matousek et al., 2003

† ML-2 defines human myeloid leukaemia cells

†† UKF-NB-3 defines cells derived from evans stage 4 NB

††† K-562 cells are derived from chronic myelogenous leukaemia (human)

ND; not determined

* NA; not applicable

‡ BS-RNase is ribonuclease of bovine seminal source

‡‡ RNase A; ribonuclease from bovine pancreas

‡‡‡ Onconase; northern leopard frog ribonuclease

‡‡‡‡ Recombinant Onconase grown using *E. Coli*

Table 6.2 *In vitro* assays used to measure ribonuclease activity

Assay type	Indicators measured	Other information	Cell line used (seeding density)	Reference
Fluorescence assay	Absorbance (490 and 515 nm)	Fluorescence spectroscopy using an RNA oligomer-fluorescein substrate	NA*	Daly et al., 2005
MTT cytotoxicity assay	Cell viability	Absorbance of formazan crystals	UKF-NB-3† cells (2×10^4 cells/mL)	Michaelis et al., 2002
Immunosuppressive activity	Cell viability	Radioactivity [6-^{3}H]-thymidine	Human lymphocytes in a MLC††	Ulbrich et al., 2000a Matousek et al., 2003
Anti-tumour activity	Cell uptake of radioactivity	Radioactivity [6-^{3}H]-thymidine	ML-2††† (2×10^5 cells/mL)	Matousek et al., 2003
Embryotoxic activity *in vitro*	Development stage	Embryos cultured in CZB media and monitored by stereomicroscopy	Embryos from C57/BL6 mice	Matousek et al., 2003 Pouckova et al., 2004

† UKF-NB-3 are cells derived from evans stage 4 NB

†† MLC defines a mixed lymphocyte culture

††† ML-2 cells are derived from human myeloid leukaemia

* NA indicates not applicable

HA-liposomes were rapidly bound to B16F10 cells in a concentration-dependent manner that could be competitively inhibited by addition of free HA. This indicated that binding and uptake was likely to be occurring *via* the CD44 receptor. Additionally, these workers also showed that the HA targeted liposomes were more toxic to B16F10 than CV-1 cells.

Here it was hypothesised that the HA-RNase A conjugate may bind to the CD44 receptor (hopefully in a tumour-specific manner). After endocytic uptake it was expected that the conjugate would be trafficked to the lysosome, and that lysosomal HAase would degrade the HA. To avoid premature degradation of RNase A it would be necessary for rapid cytosolic entry. To study the uptake of HA by B16F10 and CV-1 cells, it was therefore labelled with the fluorophore OG.

6.1.4 Conjugation of HA to RNase A

RNase A has a pKa of 8.93, molecular weight of 16,362 g/mol and contains 11 lysines that could be available for polymer conjugation (EXPASY, 2007).

A number of polymer-ribonuclease conjugates have already been described in the literature (reviewed in Table 6.3). N-terminal modification of RNase A was preferred by Daly et al., (2005) when conjugating RNase A to mPEG-propionaldehyde (~20,000 g/mol) using a ratio of 1 : 6 mole RNase A : mPEG respectively. The reaction was carried out over 17 h (4 °C) at pH 5.1 in a sodium phosphate / sodium cyanoborohydride buffer (100 mM / 20 mM respectively). The PEG-RNase A conjugate had a greater intrinsic activity than the corresponding native RNase A (4 x 10^7 vs 3 x 10^7 M^{-1} s^{-1} respectively).

Similarly, when BS-RNase was conjugated to poly[HPMA] (~3,000 – 670,000 g/mol), the polymer conjugates showed significant inhibition of tumour growth *in vivo* despite the non-selective binding to the lysines of BS-RNase (Soucek et al., 2002; Ulbrich et al., 2000). Michaelis et al., (2002) used N-methoxy-PEG-succinimidyl propionate bound (*via* an amide bond) to the lysine groups of BS-RNase. In this case, there was also significant inhibition of tumour growth *in vivo*. The method used to prepare HA-trypsin (Chapter 5) was therefore modified and used here to prepare HA-RNase A conjugates.

Table 6.3 Structure and composition of polymer-ribonuclease conjugates

Ribonuclease source	Polymer	Polymer molecular weight (g/mol)	Structure	Reference
RNase A‡‡	PEG	20,000	N-terminal conjugation of RNase A‡‡ with mPEG-propionaldehyde	Daly et al., 2005
BS-RNase‡	PEG	22,000	Amide linkage between mPEG-succinimidyl propionate and lysines of BS-RNase‡	Michaelis et al., 2002
BS-RNase‡	Poly[HPMA]-⊕†	(A) 2940 (B) 7250 (C) 19,470	Conjugation of terminal COOH of HPMA to lysines of BS-RNase‡	Oupicky et al., 1999
(1) BS-RNase‡ (2) RNase A‡‡	Poly[HPMA]-⊕†	(A) 60,000 (B) 670,000	(A) Conjugation of terminal COOH of HPMA to lysines of BS-RNase‡ (B) Multiple BS-RNase‡ conjugated to an HPMA copolymer backbone via biodegradable Gly-Phe-Leu-Gly spacers	Ulbrich et al., 2000 Pouckova et al., 2004 Soucek et al., 2002

† Poly[HPMA] defines poly[N-(2-hydroxypropyl)methacrylamide]

‡ BS-RNase is ribonuclease of bovine seminal source

‡‡ RNase A; ribonuclease from bovine pancreas

6.1.5 Summary of the aims of Chapter 6

The main aims of these studies were:

- To synthesise, purify, and characterise HA-RNase A prepared from the HA fraction of molecular weight ~130,000 g/mol, activated to a degree of 30 mol % (Chapter 5).
- To fluorescently label the HA fraction (~130,000 g/mol) with OG (1 mol %) in order to assess the cell associated fluorescence of HA-OG by B16F10 and CV-1 cells. Dextrin-OG and HPMA copolymer-OG were used as reference controls.
- To determine if HA-OG cell associated fluorescence could be reduced by co-incubation with HA.
- To compare the cytotoxicity of RNase A and the HA-RNase A conjugate in B16F10 and CV-1 cells using an MTT assay.

6.2 Methods

An HA fraction of molecular weight ~130,000 g/mol was prepared from Rc HA (900,000 g/mol) by acid hydrolysis as previously described (section 5.2.2.1). The HA-RNase A conjugate was also prepared as previously described (Chapter 5; section 5.2.2). The methods used to characterise HA included FT-IR (section 2.2.2.2) and GPC (section 2.2.2.3). FPLC (section 2.2.3.4), SDS-PAGE (section 2.2.3.3) and the BCA protein assay (section 2.2.3.2) were used to characterise the molecular weight distribution, purity and the protein content of the HA-RNase A respectively. UV-vis absorbance was used to determine the OG content of the HA-OG conjugates and PD10 chromatography used to determine purity (Chapter 2; section 2.2.1.3).

General cell culture techniques, and the MTT assay, have been previously described in Chapter 2 (section 2.2.4.6).

6.2.1 Synthesis and characterisation of HA-RNase A conjugate

HA-RNase A conjugates were synthesised using the method previously described in Chapter 5 (section 5.2.2). Using this method, the ratio of the coupling agents EDC and Sulfo-NHS used should theoretically activate 30 mol % of the HA COOH groups (Figure 6.1). Briefly, HA 0.0585 mmol (30 mg), EDC 0.01755 mmol (3.4 mg) and Sulfo-NHS 0.01755 mmol (3.8 mg) were added to the round bottomed

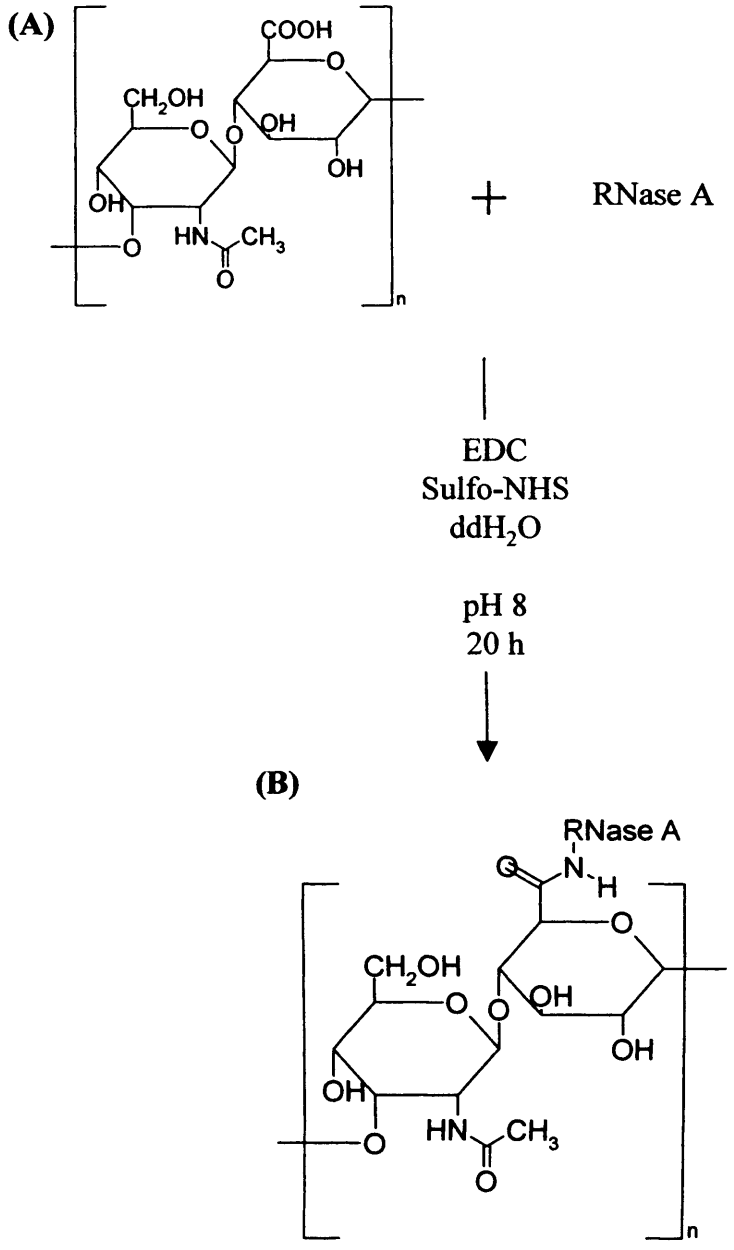

Figure 6.1 Reaction scheme for the conjugation of HA to the enzyme RNase A. Compounds (A) HA, and (B) HA-RNase A.

flask (25 mL) containing ddH_2O (10 mL) at 0, 10 and 20 min respectively. The reaction was left for a further 40 min (stirred, RT) then 1.2 x 10^{-3} mmol of RNase A (20 mg) in ddH_2O (2 mL) was added to the reaction mixture (10 mL ddH_2O) and the pH adjusted to pH 8 using NaOH (1 M). The reaction was allowed to proceed for 20 h (not 16 h as used previously) to maximise the efficiency of conjugation. The reaction mixture was then purified by fractionation using FPLC (section 2.2.3.4) to remove free RNase A. The pooled HA-RNase A fractions (5 - 10 mL) were centrifuged four times (4000g x 10 min) using a Vivaspin centrifugal filter (MWCO 30,000 g/mol; section 2.2.1.4) against ddH_2O (made up to 6 mL after each centrifugation), to remove PBS salts from the sample. This purified sample was then frozen in liquid N_2 and lyophilised (48 h) (section 2.2.1.5).

The HA-RNase A conjugate was characterised by GPC (TSK columns G4000 PW_{XL} and G3000 PW_{XL}; section 2.2.2.3), FPLC (Superdex HR 10/30 column; section 2.2.3.4) and SDS-PAGE (see section 2.2.3.3) to estimate the molecular weight, polydispersity and purity of the conjugate. Protein content was determined using a BCA protein assay (section 2.2.3.2) with RNase A as the protein standard.

6.2.2 Synthesis, purification and characterisation of HA-OG conjugates

The HA conjugation to OG was achieved using reaction conditions described previously (Chapter 5; section 5.2.2) but modified by using a 1 : 1 : 1 ratio of EDC : Sulfo-NHS : HA (Figure 6.2). Initially; HA 0.0195 mmol (10 mg) was dissolved in ddH_2O (10 mL) and EDC 0.0195 mmol (3.7 mg) and Sulfo-NHS 0.0195 mmol (4.2 mg) were added and stirred (RT). OG-Cadaverine ($OG\text{-}_{CAD}$) was added after 40 min (1 % i.e. 0.000195 mmol (0.1 mg)) with the aim of achieving a 1 mol % OG loading.

The conjugation reaction was optimised by varying the ratio of reactants, reaction time (16 – 22 h), or the pH of the reaction mixture prior to adding $OG\text{-}_{CAD}$ (pH 6 – 8) as summarised in Table 6.4. Binding of HA to $OG\text{-}_{CAD}$ was monitored during the reaction using TLC as follows. TLC plates (~5 x 7 cm; silica-covered, UV_{254} indicator) were prepared by drawing a baseline in pencil approximately 0.5 cm from the bottom. A small spot of the reaction mixture was then applied to the baseline using a capillary tube, and HA and free $OG\text{-}_{CAD}$ (1 mg/mL in ddH_2O) applied as controls. The spots were dried using a heat gun (low setting), and placed in the methanol (depth of ~3 mm) solvent. Once the solvent had travelled for ~4 cm the

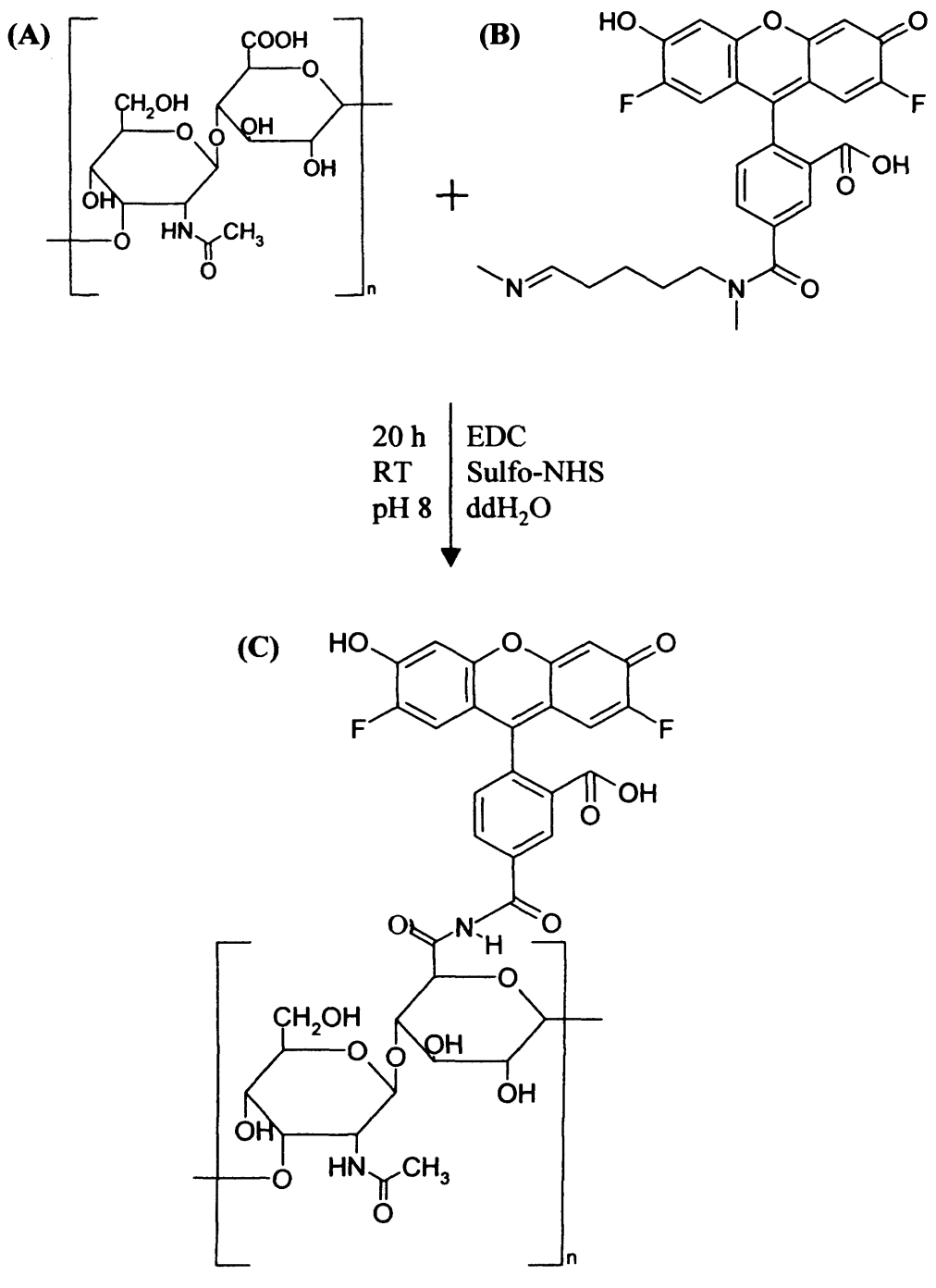

Figure 6.2 Reaction scheme for the conjugation of HA to the fluoropohore oregon green-cadaverine (OG-$_{CAD}$). Compounds (A) HA, (B) OG-$_{CAD}$ and (C) HA-OG.

Table 6.4 Parameters investigated during the optimisation of the synthesis of HA-OG conjugates

Batch code	HA (mmol)	EDC (mmol)	Sulfo-NHS (mmol)	OG (mmol)	Reaction time (h)	pH (at addition of $OG\text{-}_{CAD}$)
HA-OG1	0.0195	0.0195	0.0195	0.000195	12	NAD*
HA-OG2	0.0195	0.0975	0.0975	0.00039	24	NAD*
HA-OG3	0.0195	0.0975	0.0975	0.00039	20	8
HA-OG4	0.0195	0.0975	0.0975	0.00039	20	8

* NAD defines not adjusted

solvent front was marked, and the plate was dried using a heat gun (low setting). The spots were then viewed under a UV lamp, and outlined in pencil for comparison. Reactions were continued until the TLC plate showed that the majority of the OG-$_{CAD}$ was bound to HA, i.e. it remained at the origin and any free OG-$_{CAD}$ remaining in the reaction mixture could be clearly seen (Figure 6.3).

Initially the HA-OG conjugate was purified by dialysis against ddH_2O (6 x 5 L) using a spectra Por dialysis membrane (MWCO 2,000 g/mol), and the product was lyophilised. When the amount of bound and free OG was assessed by PD10 column chromatography it was found that dialysis did not remove all free OG. Subsequently the HA-OG conjugate was purified using the PD10 column to collect the conjugate. In this case, reaction mixture (1 mL) was loaded onto a PD10 column which was then eluted with 0.5 mL fractions of PBS. The conjugate was eluted from the PD10 column in fractions 2 – 5 mL. This was collected and dialysed against ddH_20 (6 x 5 L) to remove PBS salts from the sample before freeze drying (section 2.2.1.5).

Quantification of the OG content

The percentage of bound and free OG was estimated by diluting the reaction mixture (100 µL up to 1 mL with PBS) and loading onto a PD10 column (section 2.2.1.3). The column was eluted using PBS as the mobile phase and forty fractions (0.5 mL) were collected in Eppendorf tubes (1 mL). Samples (200 µL) were placed into a black 96 well plate, in duplicate, and the fluorescence determined at 520 nm using a Fluorostar Optima Plate Reader. The plot of fluorescence against elution volume was used to calculate the percentage of free (peak 2) and bound (peak 1) OG in the conjugate (Figure 6.4).

OG in PBS (pH 7.4) has an absorbance maximum of 494 nm (Figure 6.5a), and absorbance at 494 nm increased with increasing OG concentration (Figure 6.5b). Using this calibration curve the OG loading of the conjugates was determined. The total OG content of the purified HA-OG conjugate was therefore estimated by absorbance at 494 nm. The absorbance of the conjugate (1 mg/mL) in PBS (pH 7.4) was measured and the OG content extrapolated from the aforementioned calibration curve (Figure 6.5b). The calibration curve was consistent with earlier studies in the Centre for Polymer Therapeutics (Cardiff University).

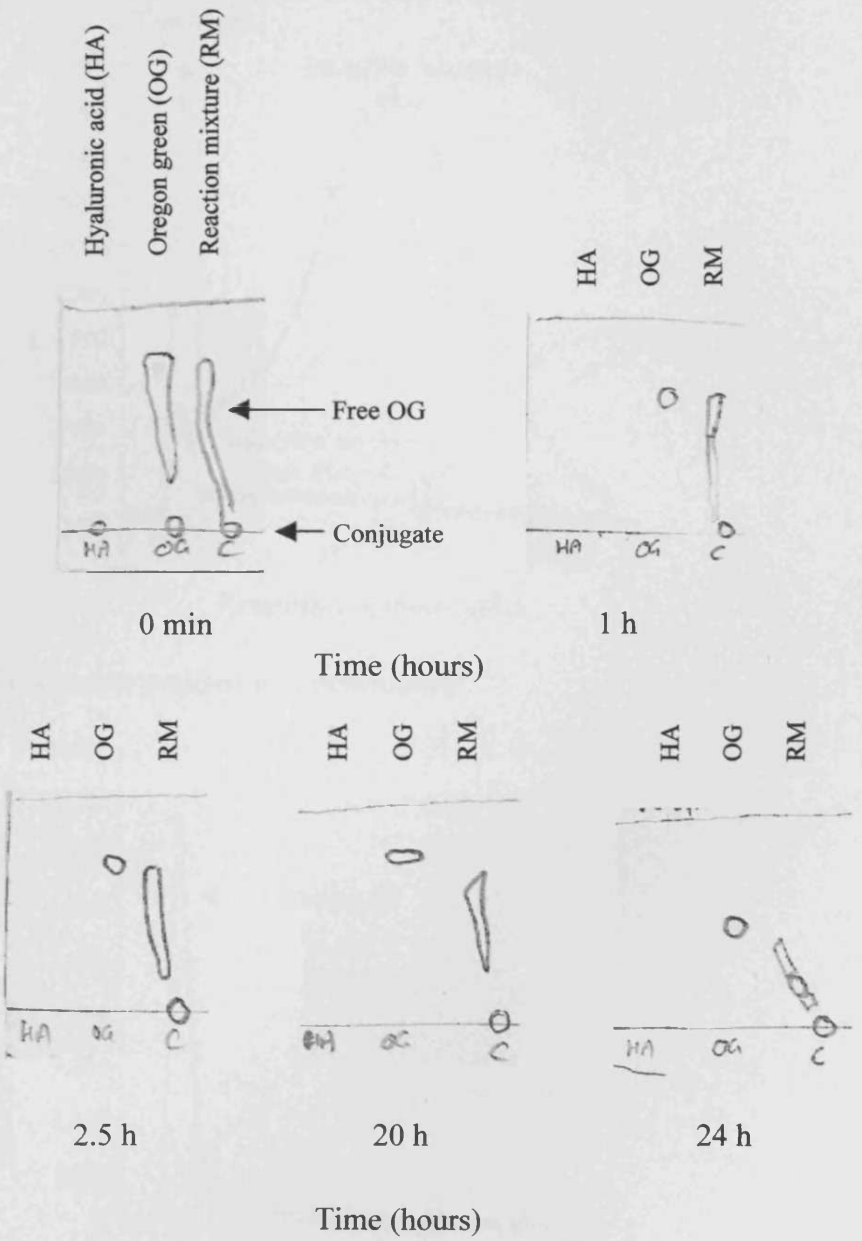

Figure 6.3 Monitoring the conjugation of HA to OG using TLC. The conjugate reaction mixture (RM) was analysed against controls of HA and OG.

(a) Reaction mixture prior to and following dialysis

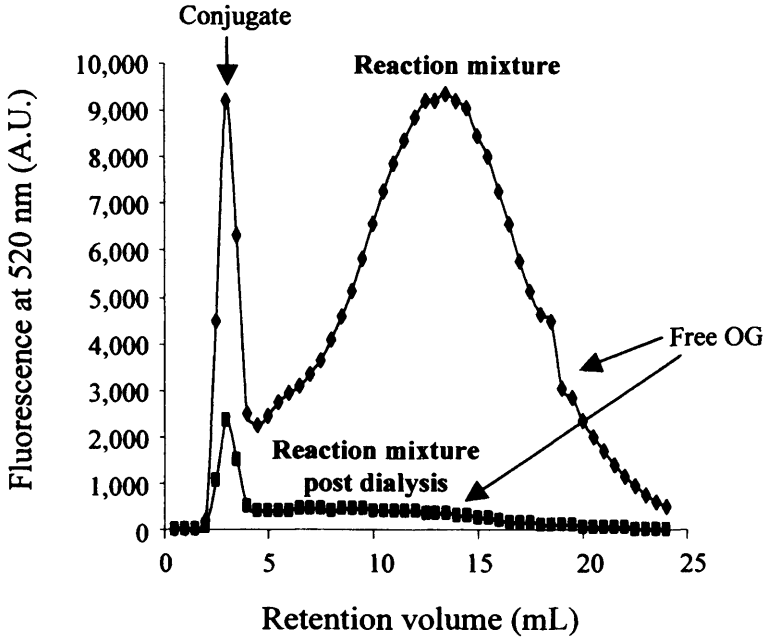

(b) HA-OG conjugate purified by fractionation

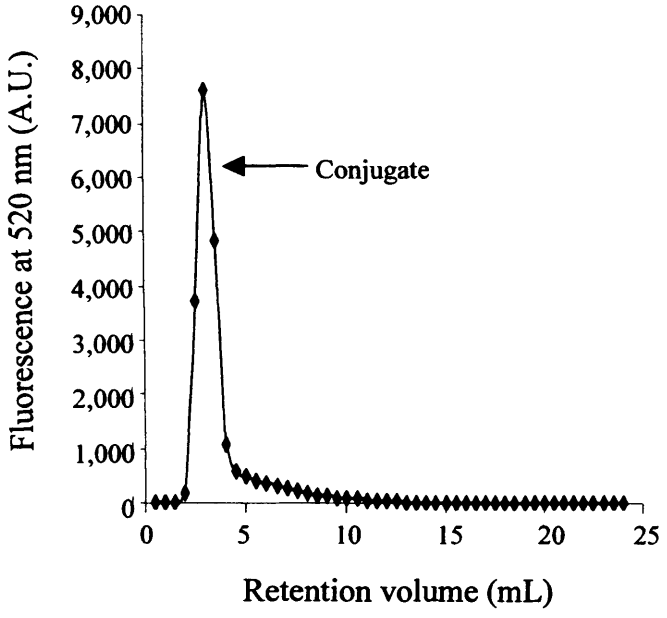

Figure 6.4 PD10 chromatography of HA-OG. Fractions (0.5 mL, PBS) were collected and the fluorescence measured at 520 nm. Panel (a) HA-OG conjugate before and after dialysis, and (b) HA-OG conjugate purified by fractionation using a PD10 column. Data represents mean (n=2).

(a)

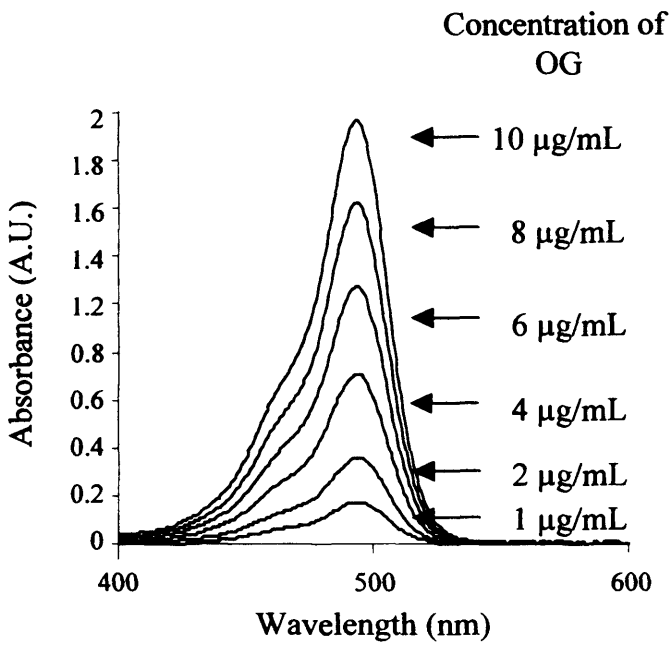

(b)

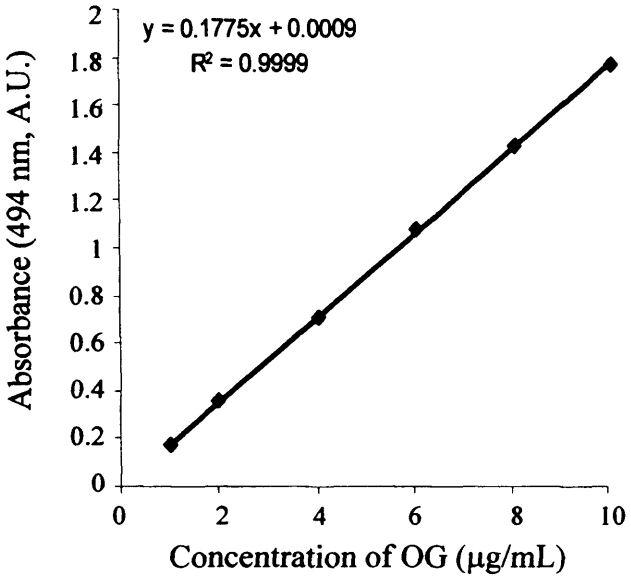

Figure 6.5 Absorbance of OG in PBS pH 7.4. Panel (a) effect of OG concentration (1 – 10 μg/mL) on the UV-vis absorbance spectra, (b) subsequent calibration curve used to determine the OG content of the HA-OG conjugates.

6.2.3 Uptake and binding of HA-OG conjugates by B16F10 and CV-1 cells

A doubling time of ~19 h for B16F10 cells seeded to a density of 2.5 x 10^4 cells/mL was previously determined in Chapter 4; section 4.3.2. A growth curve for CV-1 cells seeded to a density of 2.5 x 10^4 cells/mL was also prepared using the MTT assay to define number of viable cells (Figure 6.6). After the initial lag phase, the doubling time of CV-1 cells was calculated to be ~29 h.

FACS analysis

A range of concentrations (1 mL; 0.01 – 1 mg/mL HA-OG in RPMI) were initially tested to determine the minimum concentration of HA-OG required for measurement of binding and uptake (henceforward referred to as cell associated fluorescence). Following addition of HA-OG, the cells were incubated for 60 min at 37 °C.

To determine the binding and uptake of HA-OG with time, at 37 °C, by both B16F10 and CV-1 cells, conjugate was added (1 mL of 1 mg/mL conjugate in media (RPMI or DMEM)) and samples taken at 0, 1 or 3 h. In these experiments, aliquots of the media were additionally removed at 0, 1 and 3 h and snap frozen in liquid N_2 for future analysis to determine free and bound OG using a PD10 column as described above (also section 2.2.1.3).

To compare the uptake of HA-OG, HPMA copolymer-OG and dextrin-OG by B16F10 and CV-1 cells, the conjugates (1 mL of 0.9 μg/mL OG-equiv.) or media control (RPMI or DMEM) was added, and the cells then incubated at 37 °C for 3 h.

Following the initial experimental set up as above, cells were analysed by flow cytometry as described below. Each sample was analysed in triplicate and the mean ± SD determined.

Flow cytometry was used to study the extent of cellular uptake of HA-OG with time by B16F10 and CV-1 cells. Dextrin-OG and HPMA copolymer-OG conjugates (provided by A. Paul and K. Wallom, Centre for Polymer Therapeutics, Cardiff University) were used as reference controls.

B16F10 or CV-1 cells were seeded in 6 well plates to a density of 5 x 10^5 cells/mL and allowed to adhere for 24 h at 37 °C. The media was removed and

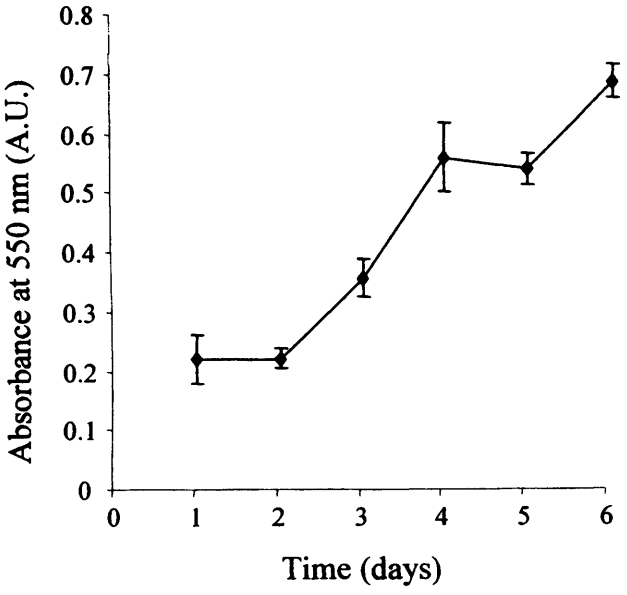

Figure 6.6 Growth curve for CV-1 cells. Cells were seeded at a density of 2.5 x 10^4 cells/mL and cell number measured using the MTT assay. Data shown represent the mean (n=6) ± SD.

HA-OG, dextrin-OG, HPMA copolymer-OG (1 mL of 0.9 μg/mL OG equiv.) or HA (dissolved in media alone) or media control was added (1 mL). The cells were incubated at 37 °C in the dark and at the end of the incubation period, the media was removed from the wells, replaced by ice-cold PBS (1 mL) and the 6 well plates were put on ice. The cell monolayers were washed three times with ice-cold PBS (1 mL) and detached from the wells using a scraper. After pipetting (1 mL) into FACS tubes, they were centrifuged at 500 g at 4 °C for 5 min to form a cell pellet. The supernatant was removed and the pellet re-suspended in PBS (ice-cold, 200 μL). Cells were incubated in media alone (RPMI or DMEM without FBS) from the start of the experiment.

Cell samples were analysed (20,000 total cell counts) using a FACScalibur flow cytometer with an argon laser (488 nm excitation). The cells were gated (forward and side scatter) using Cell Quest software, to discount non-viable cells, and fluorescence measured (FL1 channel) at 520 nm. The data may be expressed as (i) fluorescence of all cells (if 100 % uptake), (ii) percentage of positive cells fluorescing over time, and (iii) fluorescence adjusted for the proportion of viable cells to differentiate between cell autofluorescence and the fluorescence due to the polymer-OG probe, using the equation below:

Cell associated fluorescence = (% positive cells x geometric mean) / 100

In this work, the fluorescence measured was adjusted for the proportion of positive cells.

Competition studies using HA

The uptake of the HA-OG conjugate by B16F10 and CV-1 cells was also assessed in the presence of increasing concentrations of HA in order to determine if HA would be a competitor. In these experiments the incubation medium (1 mL) was removed at the start of the experiment and HA-OG conjugate (final concentration 1 mg/mL conjugate) was added ± HA (final concentrations in the range 0.25 – 1 mg/mL). Medium alone was used as a control. The cells were incubated at 37 °C for 3 h before analysis by FACS as described above.

6.2.4 Evaluation of cytotoxicity of HA-RNase A

B16F10 and CV-1 cells were seeded at a density of 2.5 x 10^4 cells/mL in 96 well plates. The incubation medium was removed and samples (dextran as a negative

control, PEI as a positive control, RNase A, HA, mixture of HA and RNase A, a media control or the HA-RNase A conjugate) were added (100 μL) to each well. Samples were added at concentrations between 0.001 – 1 mg/mL (n=6) and for the HA-RNase A conjugate and RNase A, a concentration range of 0.0001 – 0.1 mg/mL RNase A equiv. was used. The plates were incubated for 72 h, and cell viability assessed using the MTT assay as described in Chapter 2 (section 2.2.4.6). The experiments were repeated three times (n=6 in each experiment) and the mean and SEM were determined.

6.3 Results

6.3.1 HA-RNase A conjugates and their cytotoxicity

FPLC fractionation gave good purification of the HA-RNase A conjugate (no detectable free RNase A). The conjugate had an RNase A content of 16 % w/w, and further GPC and SDS-PAGE analysis confirmed the absence of free RNase A (Figure 6.7).

The reference control polymer PEI was cytotoxic in both B16F10 and CV-1 cell lines (Figure 6.8 and 6.9), whereas dextran was not. Moreover, RNase A was also non-toxic in either cell line up to a concentration of 1 mg/mL. HA and a mixture of HA and RNase A did not cause cytotoxicity in either cell line, although a mixture of the HA and RNase A did cause negligible cytotoxicity in the B16F10 cell line (Figure 6.8). Most importantly HA-RNase A conjugate significantly reduced cell viability to a maximum of ~50 % at a concentration of 0.1 mg/mL RNase A equivalent.

6.3.2 Synthesis and characterisation of HA-OG conjugates

Early HA-OG conjugates had very low conjugation efficiencies, with ~ 30 % yield. By increasing the reaction time from 12 h to 20 h however (Table 6.5), and also by adjusting the pH of the reaction mixture to pH 8 by addition of NaOH (1 M) prior to the addition of OG, the yield was increased to 85 %. The HA-OG conjugate was eluted from the PD10 column as a sharp peak (mobile phase of PBS) in the first 2 - 5 mL, whereas, free OG eluted later 5 – 20 mL. Typically, the free OG content of the reaction mixture after dialysis was still ~ 50 – 97 % (Figure 6.4). It was possible however to reduce this to < 1 % following purification using a PD10 column (Figure 6.4). All conjugates contained < 1 % free OG following purification (Figure 6.4, Table 6.5).

(a) GPC chromatogram

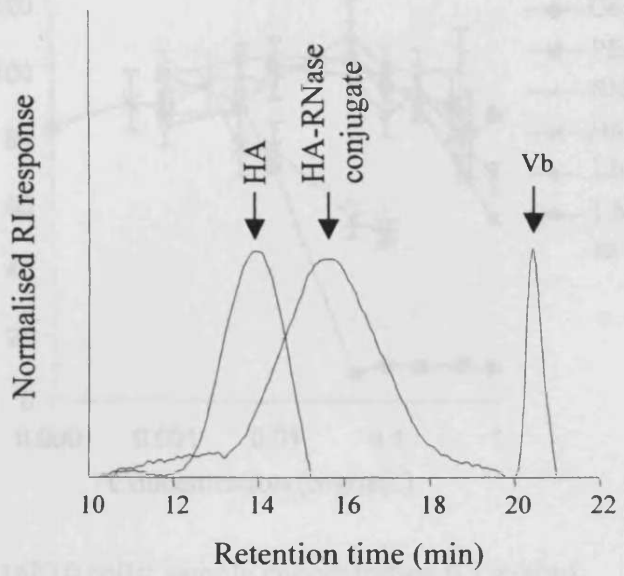

(a) SDS-PAGE of HA-RNase A conjugate

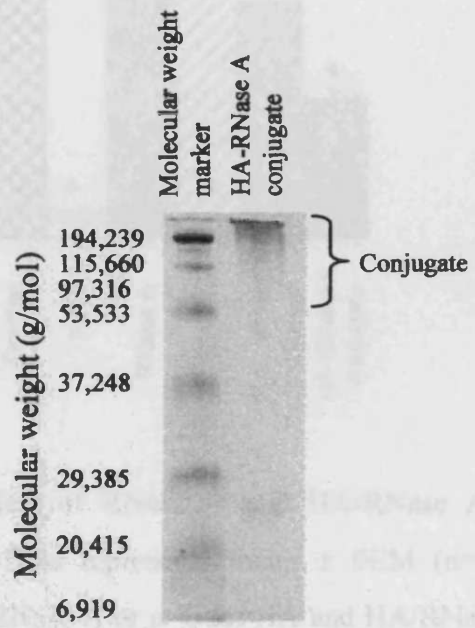

Figure 6.7 Characterisation of the HA-RNase A conjugate by (a) GPC and (b) SDS-PAGE.

(a) B16F10 cells; varying sample concentration

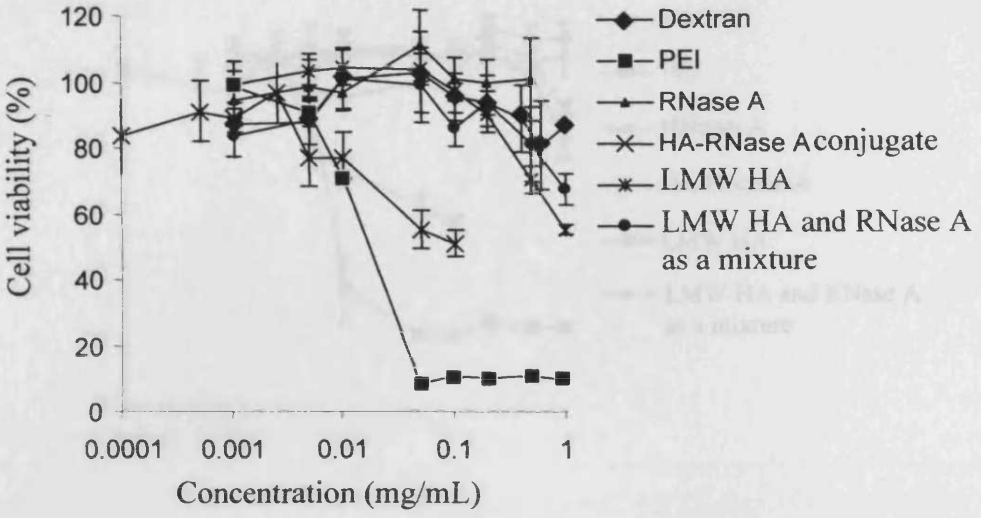

(b) B16F10 cells; sample concentration 0.1 mg/mL

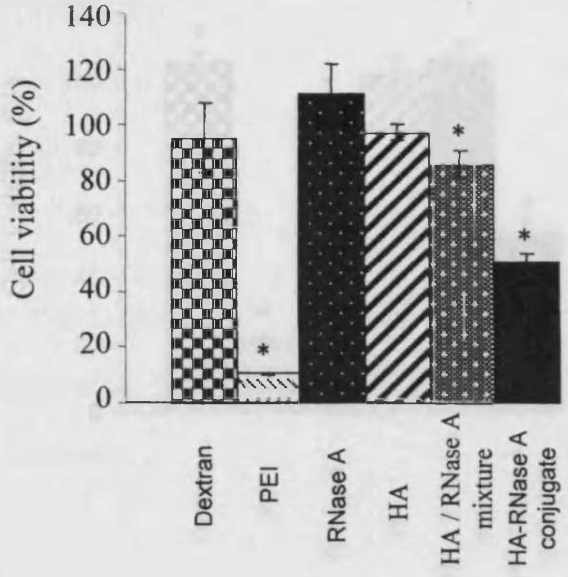

Figure 6.8 Effect of RNase A and HA-RNase A on the viability of B16F10 cells. Data represents mean ± SEM (n=18 for dextran, PEI, RNase A, HA-RNase A or n=6 for HA and HA/RNase A mixture). Where error bars are not visible, error is below the limit of representation.

* indicates $p<0.05$ relative to RNase A control, calculated using ANOVA and Bonferroni *post hoc* test.

(a) CV-1 cells; varying sample concentration

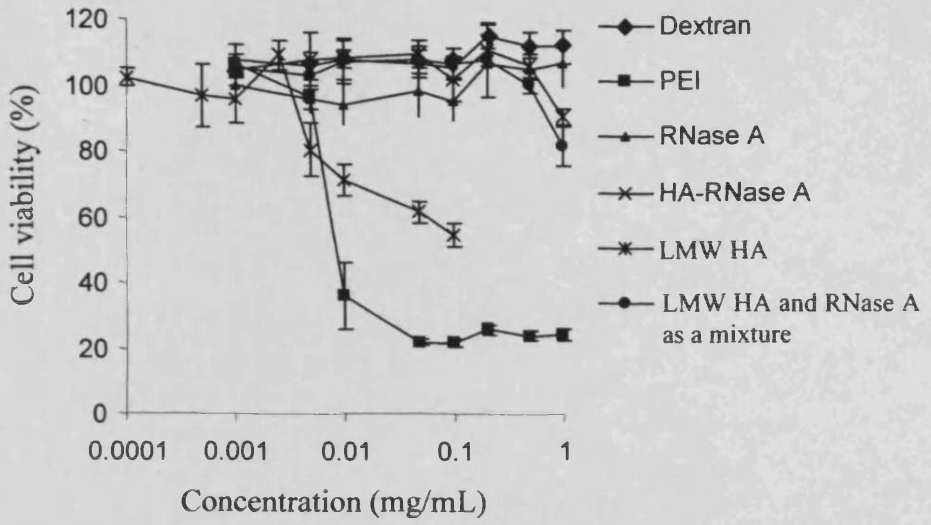

(b) CV-1 cells; sample concentration 0.1 mg/mL

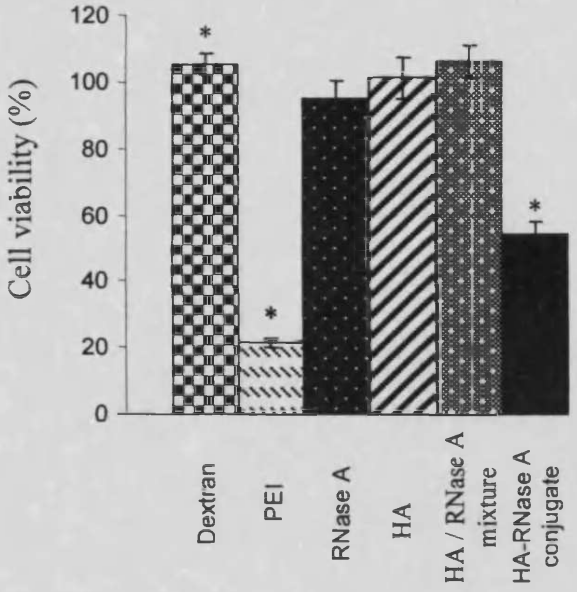

Figure 6.9 Effect of RNase A and HA-RNase A on the viability of CV-1 cells. Data represents mean ± SEM (n=18 for dextran, PEI, RNase A, HA-RNase A and n=6 for HA, HA/RNase A mixture). Where error bars are not visible, error is below the limit of representation. * indicates $p<0.05$ relative to RNase A control, calculated using ANOVA and Bonferroni *post hoc* test.

Table 6.5 Characteristics of HA-OG conjugates

Batch code	Batch size (mg)	Total OG content (% w/w)	Free OG after dialysis (%)	Free OG after fractionation (%)
HA-OG1	~ 3	1.5	53	NF[#]
HA-OG2	~ 32	0.8	47	NDE[†]
HA-OG3	~ 44	0.9	62	NDE[†]
HA-OG4	~ 68	0.9	NC[*]	NDE[†]

[#] NF; sample was not fractionated as there was not enough remaining

[*] NC; not characterised

[†] NDE; not detectable

6.3.3 Association of HA-OG with B16F10 and CV-1 cells and competition experiments

Only an HA-OG conjugate concentration of 1 mg/mL (0.9 μg/mL OG equiv.) was high enough to allow detection of B16F10 cell association over 60 min; significant ($p<0.05$, ANOVA and Bonferroni *post hoc* test) (Figure 6.10). Subsequent experiments conducted in both B16F10 and CV-1 cells over 3 h showed that the HA-OG (0.9 μg/mL OG equiv.) showed increasing cell association with time (Figure 6.11) and was only significantly greater in the B16F10 cell line after 3 h. There was some cell association already at t = 0 (more marked in the CV-1 cells), and this is probably due to rapid membrane binding. PD10 column chromatography of tissue culture medium after 3 h showed that the conjugates were stable and no increase of free OG was detected (Figure 6.12).

When the cell association of HA-OG, HPMA copolymer-OG and dextrin-OG was compared (Figures 6.13 and 6.14), the association of dextrin- and HPMA copolymer-OG was lower than seen for the HA-OG. In both B16F10 and CV-1 cells, there was a greater cell associated fluorescence when incubated with HPMA copolymer-OG rather than dextrin-OG conjugate but this was only significant in the B16F10 cells (Figure 6.13 and 6.14).

Addition of HA at concentrations of 1 mg/mL decreased the cell associated fluorescence of B16F10 cells when incubated with HA-OG. Similarly, in the case of the CV-1 cells, 0.75 mg/mL decreased the CV-1 cell associated fluorescence of HA-OG (Figure 6.15 – 6.16).

6.4 Discussion

The primary aim of these preliminary studies was to investigate whether a HA-RNase A conjugate might have potential as a therapeutic anti-cancer agent.

Synthesis, characterisation and cytotoxicity of the HA-RNase A conjugate

The optimum parameters determined in the preceding experimental chapters concluded that the HA-RNase A conjugate should be synthesised using the HA fraction (molecular weight ~130,000 g/mol, activated to 30 mol %) and RNase A, in order to obtain maximum protein loading.

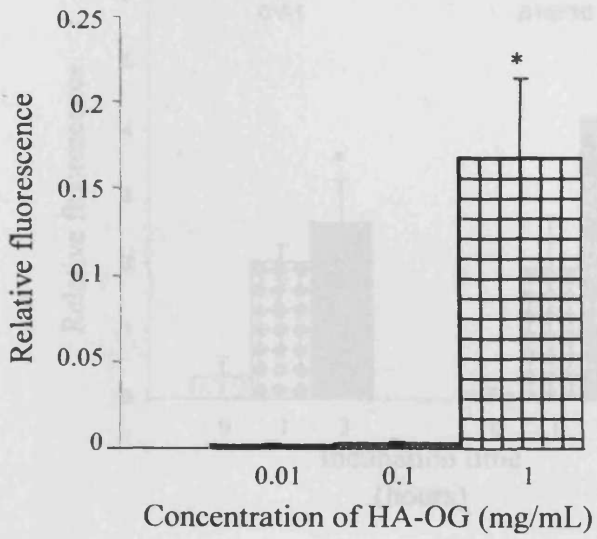

Figure 6.10 Effect of HA-OG concentration on its detection by flow cytometry in B16F10 cells (1 h, 37 °C). Cells were seeded at a density of 5 x 10^5 cells/mL. Data shown represents the mean (n=3) ± SD. * $p<0.05$ (ANOVA and Bonferroni *post hoc* test).

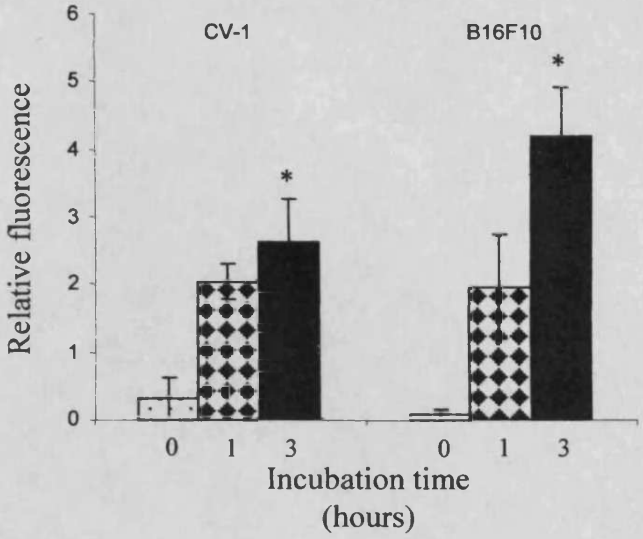

Figure 6.11 Effect of the incubation time on HA-OG association with CV-1 and B16F10 cells at 37 °C. Data shown represents the mean (n=3) ± SD. * $p<0.05$ (ANOVA and Bonferroni *post hoc* test).

(a) CV-1 cells

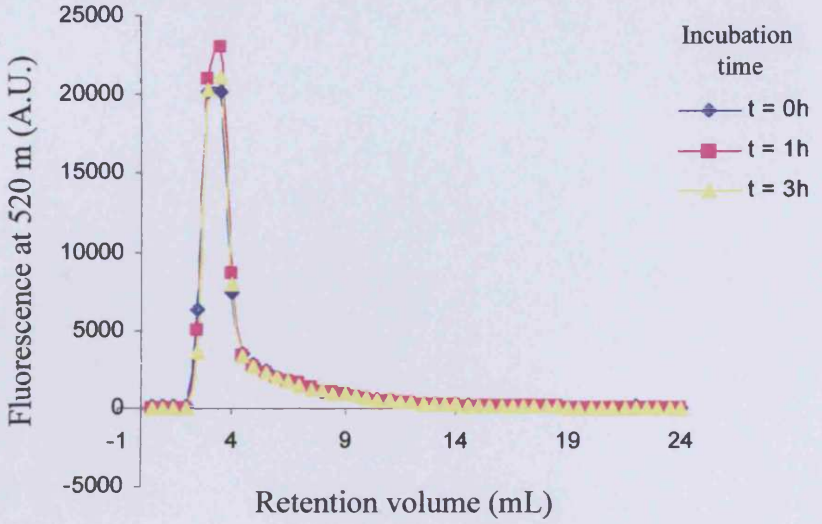

(b) B16F10 cells

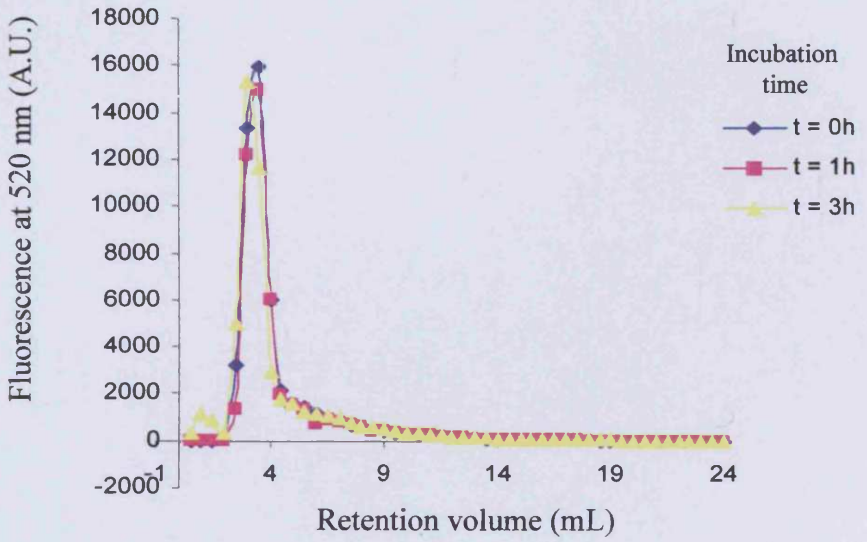

Figure 6.12 PD10 column chromatography of cell culture media containing HA-OG. Panel (a) CV-1 cells and panel (b) B16F10 cells. Data shown represents mean (n=2).

(a) Uptake of polymer-OG conjugate

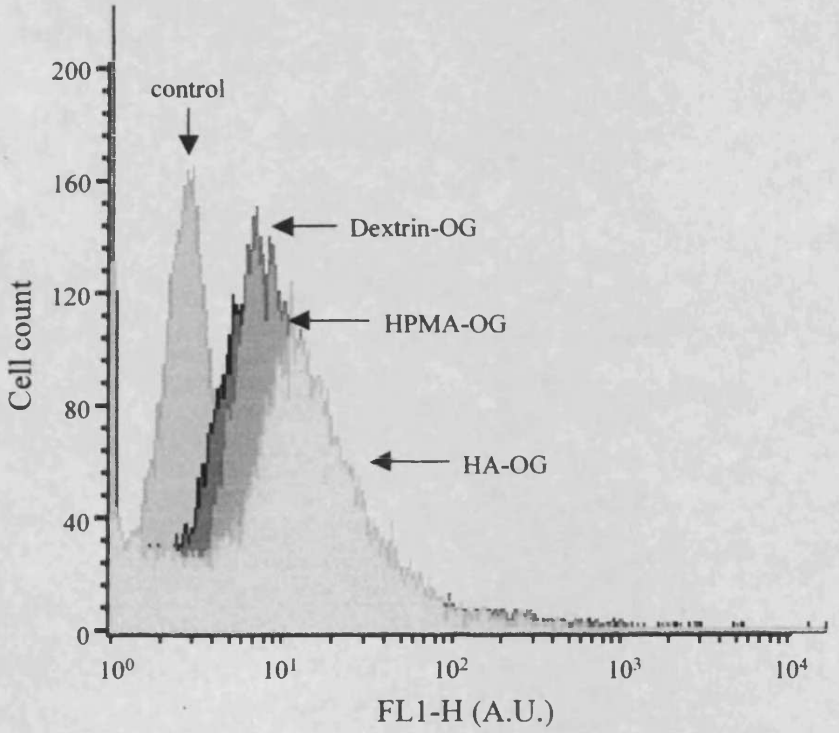

(b) Comparison of geometric mean

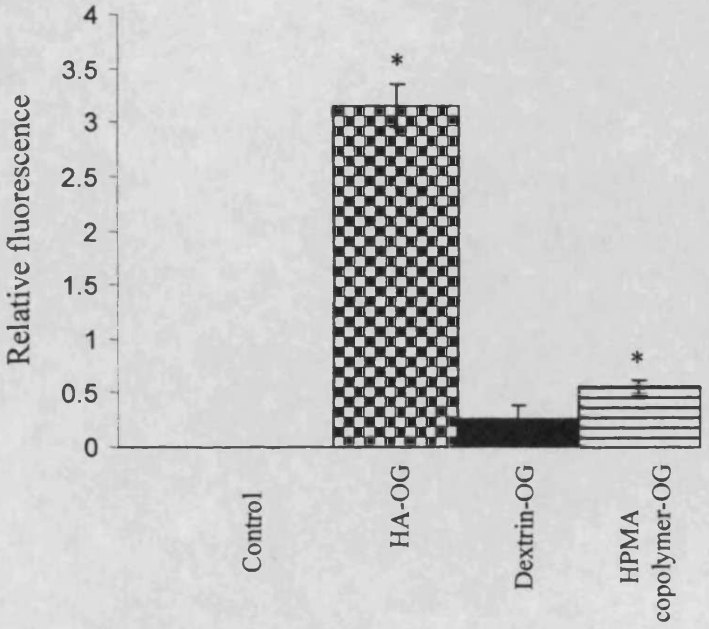

Figure 6.13 Comparison of the cellular association of HA-OG, dextrin-OG and HPMA copolymer-OG conjugates by B16F10 cells. Data represents mean (n=3) ± SD. Control is on the baseline.

* $p<0.05$ (ANOVA and Bonferroni *post hoc* test).

(a) Uptake of polymer-OG conjugate

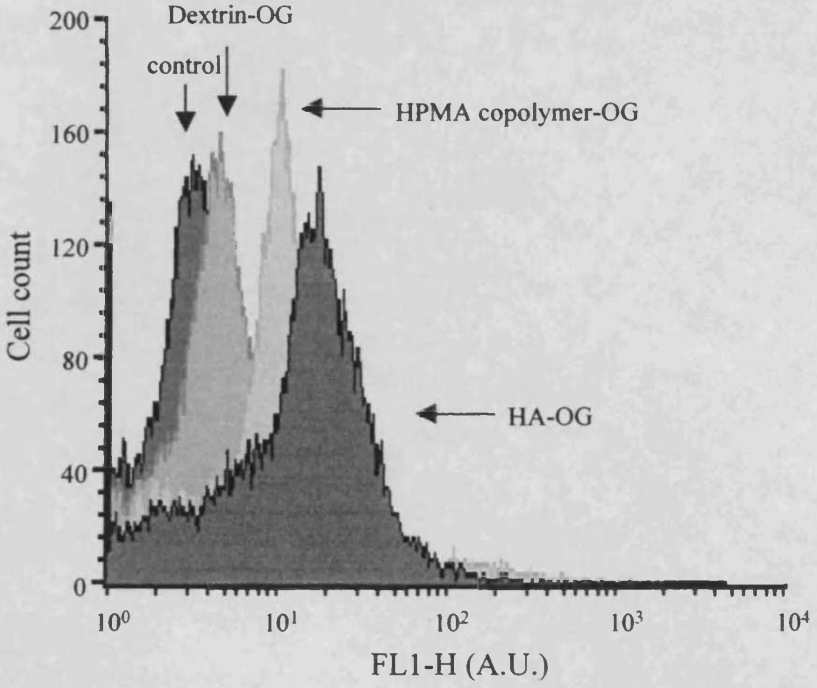

(b) Comparison of geometric mean

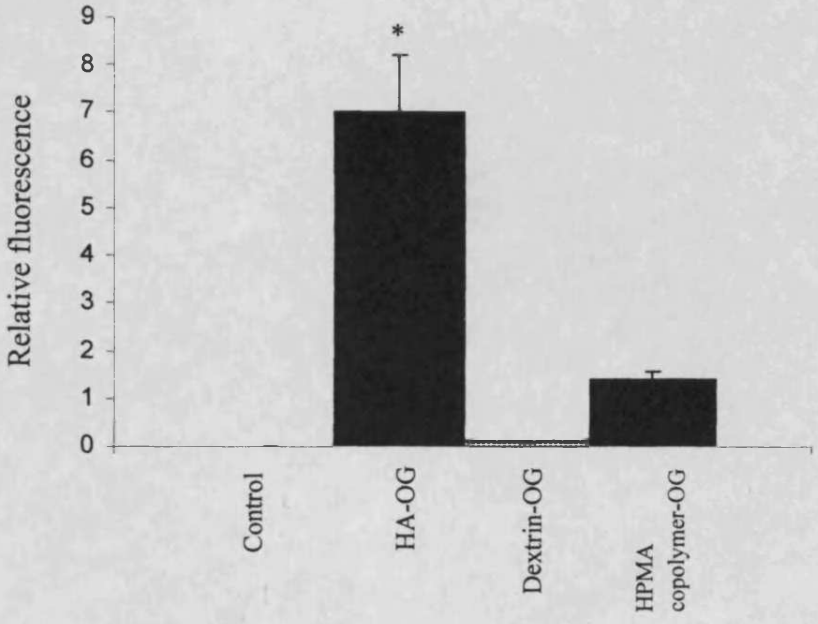

Figure 6.14 Comparison of the cellular association of HA-OG, dextrin-OG and HPMA copolymer-OG in CV-1 cells. Cells were seeded at a density of 5 x 10^5 cells/mL. Data shown represents mean (n=3) ± SD. Control is on the base line. * $p<0.05$ (ANOVA and Bonferroni *post hoc* test).

(a) Uptake of and competition of HA-OG conjugate

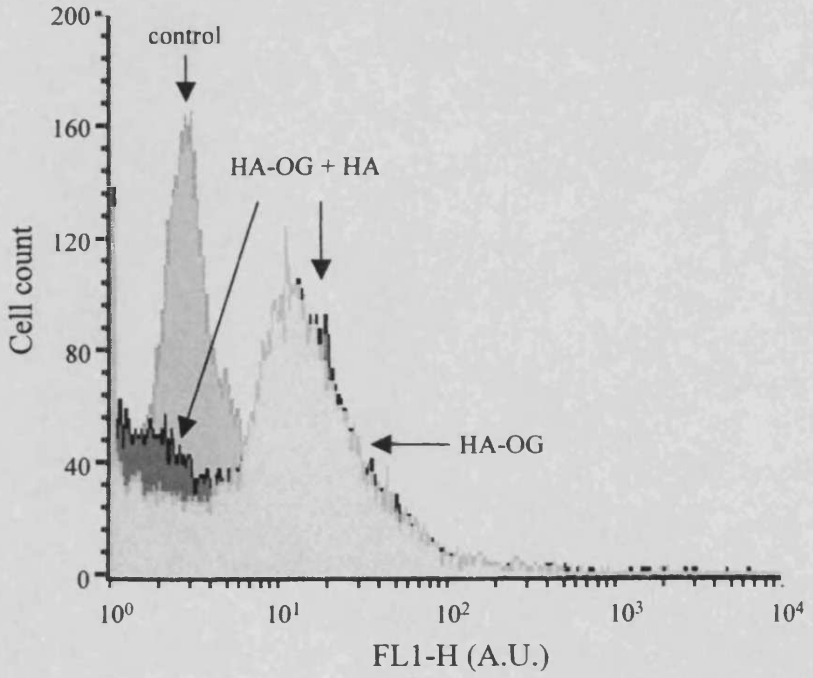

(b) Comparison of geometric mean

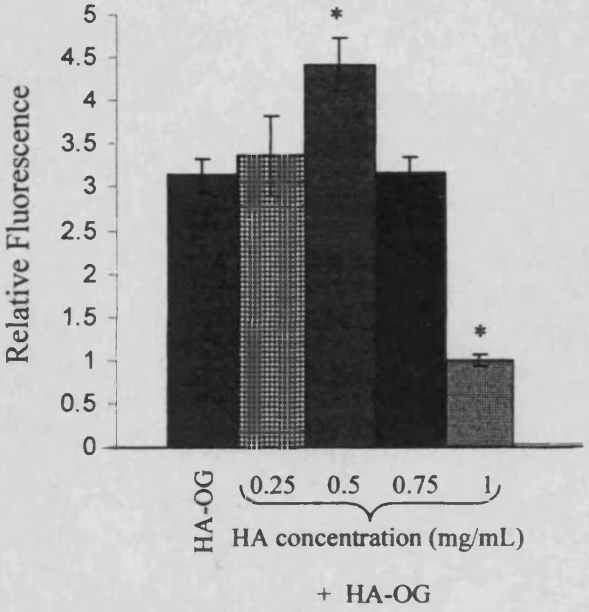

Figure 6.15 Effect of HA on the cell association of HA-OG in B16F10 cells. Data shown represents mean (n=3) ± SD.

* $p<0.05$ (ANOVA and Bonferroni *post hoc* test).

(a) Uptake of and competition of HA-OG conjugate

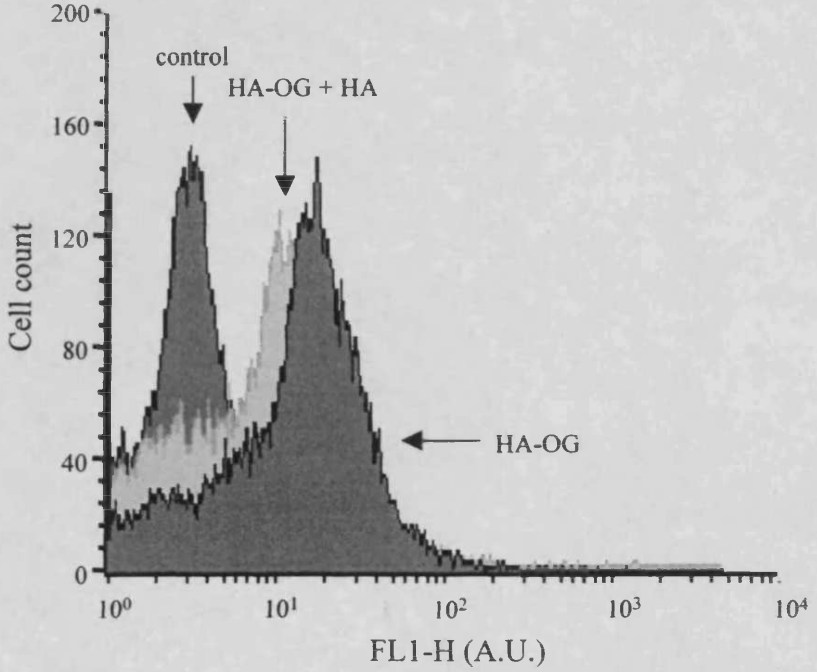

(b) Comparison of geometric mean

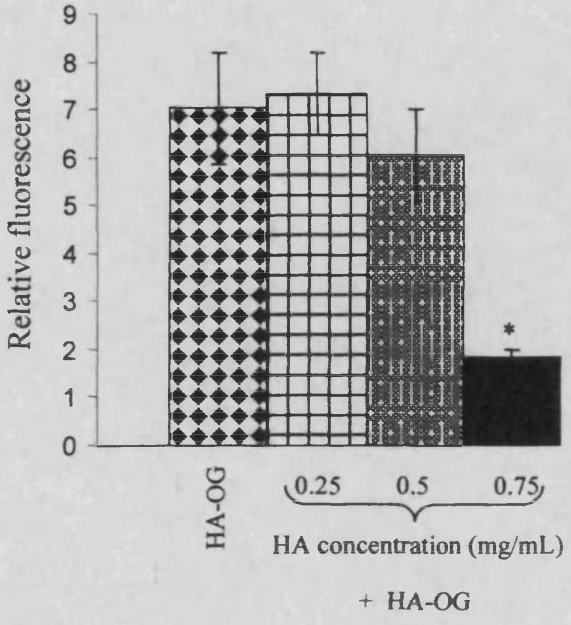

Figure 6.16 Effect of HA on the cell association of HA-OG in CV-1 cells. Data shown represents mean (n=3) ± SD. * $p<0.05$ (ANOVA and Bonferroni *post hoc* test).

A pure HA-RNase A conjugate was synthesised with a protein loading (16 % w/w RNase A) within the range previously attained for the HA-trypsin conjugates (4 - 30 % w/w trypsin; Chapter 5), but significantly less than the dextrin-trypsin conjugate loadings (~70 – 80 % w/w trypsin; Chapter 3). The HA-RNase A conjugate had a loading comparable to other polymer-ribonuclease conjugates studied. Such as, poly[HPMA]-RNase A (28 - 34 % w/w RNase A; Soucek et al., 2002), PEG-BS-RNase (30 % w/w BS-RNase; Michaelis et al., 2002) and poly[HPMA]-BS-RNase (33 % w/w BS-RNase; Ulbrich et al., 2000).

The previous work on HA-trypsin conjugates (Chapter 5) produced a conjugate that was masked to 6.4 % remaining trypsin activity, so it is possible that the HA-RNase A conjugate synthesised here was also able to mask activity. If there had been more time and conjugate available, then a ribonuclease fluorescence assay (Table 6.2) would have been carried out to measure the ribonuclease activity of the conjugate both prior to and following HAase mediated polymer degradation. It was however considered important to conduct preliminary experiments on the cytotoxicity of the HA-RNase A conjugate instead.

In this study, free RNase A did not cause cytotoxicity in either cell line. This may be because it was not taken up into the cell. Similarly, Pouckova et al., (2004) and Eugene Lee and Raines, (2003) also found that RNase A was not cytotoxic in either ML-2 or K-562 cells (summarised in Table 6.1). In comparison to other polymer-ribonuclease conjugates, the HA-RNase A conjugate achieved cell cytotoxicity (~50 % cell death after 72 h, 0.1 mg/mL RNase A equiv.) *in vitro*. Previously, the poly[HPMA]-BS RNase (Ulbrich et al., 2000) and poly[HPMA]-RNase A (Pouckova et al., 2004) conjugates were not cytotoxic in the human myeloid leukaemia cell line (ML-2). Similarly, a PEG-BS-RNase conjugate synthesised by Michaelis et al., (2002) was also shown not to be cytotoxic in a UKF-NB-3 evans stage 4 cell line (Table 6.6). As both free HA and a mixture of HA and RNase A only caused negligible cytotoxicity, it is possible that conjugation of RNase A to HA may have promoted cellular uptake and thus the subsequent cytotoxicity measured. Alternatively, it is possible that HA conjugation merely protected RNase A from being bound by RIs in the cytosol. This study did however demonstrate that polymer conjugated RNase A, rather than Onconase or BS-RNase, can be cytotoxic when delivered into two different cell lines, but also demonstrated cytotoxicity of a ribonuclease *in vitro*. All previously

Table 6.6 Cytotoxicity of polymer-ribonuclease conjugates in *in vitro* cellular models

Polymer-RNase conjugate	Cell line	Seeding density (cells/mL)	Cytotoxic	Reference
polyHPMA-BS RNase[‡]	ML-2[†]	2×10^5	No	Ulbrich et al., 2000
polyHPMA-RNase A[‡‡]	ML-2[†]	2×10^5	No	Pouckova et al., 2004 Soucek et al., 2002
PEG-BS-RNase[‡]	UKF-NB-3[††]	2×10^4	No	Michaelis et al., 2002
HA-RNase A[‡‡]	B16F10[†††]	2.5×10^4	Yes	Data shown here
HA-RNase A[‡‡]	CV-1*	2.5×10^4	Yes	Data shown here

[†] ML-2 defines human myeloid leukaemia cells

[††] UKF-NB-3 defines cells derived from evans stage 4 NB

[†††] B16F10 cells are murine melanoma

* CV-1 cells; African green monkey fibroblasts

[‡] BS-RNase is ribonuclease of bovine seminal source

[‡‡] RNase A; ribonuclease from bovine pancreas

successful ribonuclease activity studies have been proven in animal models, where the route of administration is also a contributary factor.

HA-OG conjugates; synthesis, characterisation and FACS uptake and binding studies

Following the preliminary HA-RNase A cytotoxicity studies, it was considered interesting to also conduct preliminary studies into the mechanism of action of the conjugate. The cell associated fluorescence (combined cellular uptake and binding) of the fluorescent probe HA-OG conjugate in both cell lines was measured using flow cytometry in order to (i) compare the binding and uptake in the two cell lines, and (ii) see if HA would reduce or inhibit the cell associated fluorescence of cells incubated with HA-OG.

HA-OG conjugates were synthesised using a method adapted from Phelps (2006) to give soluble conjugates ~ 1 mol % OG loading. The improved solubility noted may be due to differences in both the source and molecular weight of HA used. Alike the previous study on HA-trypsin conjugates (Chapter 5), it was found that the conjugate reaction mixture had to be fractionated by FPLC in order to achieve adequate purification.

The first flow cytometry studies were carried out to determine the concentration and incubation time of HA-OG conjugates required for significant cell associated fluorescence to occur in B16F10 and CV-1 cells. The experimental conditions determined for significant cell associated fluorescence (1 mg/mL; 0.9 μg/mL OG equiv., incubated for 3 h) were not sufficient for exocytosis of OG released from the HA-OG conjugate to occur and also revealed that the conjugate was stable over the course of the experiment. If time had permitted, the effect of pH on HA-OG fluorescence would have been characterised to mimic the change in pH that occurs during endocytosis. Xyloyiannis (2004) and Seib (2005) however had analysed the effect of PBS buffer pH (5.5 - 7.4) on the fluorescence of OG and polymer-OG conjugate and found no direct correlation was shown between decreasing pH and quenching of fluorescence. Similarly, no quenching of fluorescence was caused by conjugation of (PEG)-poly(ester) dendritic hybrids to OG (Xyloyiannis, 2004).

Cell associated fluorescence was significantly greater in both cell lines incubated with HA-OG conjugates than the HPMA copolymer-OG, and dextrin-OG conjugate controls. Where comparative studies using three different polymer-OG conjugates were conducted, the concentrations used were standardised to OG content. The greater cell associated fluorescence may have been in part due to the presence of CD44 receptors, known to endocytose HA (Culty et al., 1992). There was however also a significant uptake of both HPMA copolymer-OG, and dextrin-OG conjugates compared to inherent cellular fluorescence. This may be attributed to non-specific endocytosis, such as in the case of dendrimer labelled OG conjugates (Xyloyiannis, 2004).

To ascertain if binding and cellular uptake of the HA-OG conjugate may have occurred at least in part through CD44 receptor interaction, a competition experiment was carried out using the polymer HA. In both the B16F10 and CV-1 cell line used, there was a reduction in HA-OG induced cell associated fluorescence when co-incubated with HA (0.75 or 1 mg/mL). This was illustrated in the histogram as both a slight shift in the fluorescence units and a partial change from unimodal towards a bimodal distribution.

Following on from these preliminary studies, future work on this HA-RNase A conjugate should examine the uptake of HA-OG over a 72 h time frame, to better understand what happens over the duration of the MTT assay. Similarly, Onconase, has been shown to take between 48 and 72 h to induce apoptosis (reviewed in Ardelt et al., 2003). Conducting the MTT assay over 5 days may therefore better characterise the cytotoxicity of the HA-RNase A conjugate.

6.5 Conclusion

Although time did not enable the masked and reinstated RNase A activity to be measured, it did show that the protein RNase A alone was not cytotoxic. However, the HA-RNase A conjugate mediated the delivery of RNase A into the cell potentially *via* an HA / CD44 receptor interaction. Furthermore, it was possible to achieve an ~50 % cytotoxicity over 72 h in both B16F10 and CV-1 cells. Whereas other polymer-ribonuclease conjugates have previously not shown cytotoxicity in cellular models that used ML-2 and UKF-NB-3 cell lines.

Chapter 7

General Discussion

7.0 GENERAL DISCUSSION

Over recent years, the field of medicinal nanotechnology, specifically polymer therapeutics, has attracted increasing interest (reviewed by Wagner, 2007; Duncan, 2003 and 2006). There has also been a growing acknowledgement of the importance of 'nanomedicines' on a European level, with publication of reports such as the European Science Foundation's Forward Look on Nanomedicine (ESF, 2007) and the European Technology Platform on Nanomedicine (ETPN, 2007). The Royal Society and The Royal Academy of Engineering published a report in 2004, entitled "Nanoscience and Nanotechnologies: opportunities and uncertainties", which noted the potential for nanotechnology to be applied to drug delivery. In particular, it noted current applications to polymer delivery systems, including polymer-protein conjugates (The Royal Society and The Royal Academy of Engineering, 2004). PEGylation has remained popular, with recent reviews such as "Nanomedicine: clinical applications of polyethylene glycol conjugated proteins and drugs", which indicated that nanomedicines and PEGylation are two of the key branches of nanotechnology leading the way towards targeted delivery (Parveen and Sahoo, 2006).

Following on from the evolving field of PEGylation, the work described here aimed to evaluate a novel method for polymer-protein conjugation, for its potential to overcome the two key limitations of PEGylation; lack of polymer biodegradability and non-specific expression of protein activity (described in section 1.3).

7.1 Contribution of this thesis to nanotechnological medicine

The work carried out in this thesis has led to an exciting proof of principle for this novel type of protein delivery system. These studies have demonstrated the concept of masking and then reinstating enzyme and hormonal activity through the triggered degradation of the masking polymer (Gilbert et al., 2005; Gilbert and Duncan, 2006). The potential to apply this concept to an enzyme, a peptide that acts *via* interaction with a receptor and to aid the delivery of a protein that requires intracellular access for activity has also been demonstrated here (Duncan et al., 2007). In addition, this work has also highlighted the potential for application of the masking / unmasking concept by two different classes of polymer: dextrin and HA. Finally, and quite promising, are the preliminary cytotoxicity studies carried out using a HA-RNase A conjugate which have shown that polymer conjugated RNase A is cytotoxic in two

cell lines, where previously no cytotoxicity has been demonstrated for the native RNase A *in vitro* (Table 6.6).

Since the initial studies that provided proof of principle for both the masked and reinstatement of protein activity using dextrin-trypsin conjugates as a model (Gilbert et al., 2005), this laboratory has applied the concept to three potential therapeutic agents. The dextrin / amylase model has been used to explore the possibility of improving the delivery of the anti-tumour proteins phospholipase A_2 (for breast cancer (Ferguson et al., 2007)) and RNase A as an anti-cancer agent (Chapter 6). This system is being explored as a means of improving epidermal growth factor (EGF) delivery in the hope of improving wound healing (Hardwicke et al., 2007) (Figure 7.1). Results so far have supported those shown in this thesis, and most excitingly in the case of dextrin-phospholipase A_2, have shown a modulation of activity between 36 and 114 % (Ferguson et al., 2006 and 2007).

To place the observations of this thesis into context, the other advances in the field of polymer-protein conjugates that have occurred during the period of this study are briefly discussed in the following section.

7.2 Recent developments in the field of polymer-protein conjugates

Since the commencement of this study in 2003, polymer-protein conjugates have continued to enter clinical trials and moreover, enter the pharmaceutical market (Table 7.1). All conjugates however contain the non-biodegradable polymer PEG, even though limitations of PEG are well known (section 1.3.4). PEGylation chemistry is frequently reviewed as it remains a key area of developing nanomedicines (Veronese and Pasut, 2005).

Recent focus on the development of PEGylation and polymer conjugation chemistry has consisted of (i) site-specific conjugation, and (ii) biodegradable linkers. Most recently, Brocchini et al., (2006) developed a protocol that enables the conjugation of PEG to the disulfide bonds found naturally in proteins. This enables site-specific PEGylation of a protein without first having to alter the protein sequence (described in section 1.3.3.1). Importantly, the tertiary structure of the protein and biological activity remains unaffected by this new method of conjugation. Whereas, in other cases, protein sequences have been altered, such as the incorporation of a cysteine residue into recombinant ScFv, to enable thiol specific conjugation to PEG-maleimide (Natarajan et al., 2005). This is not however always the case for

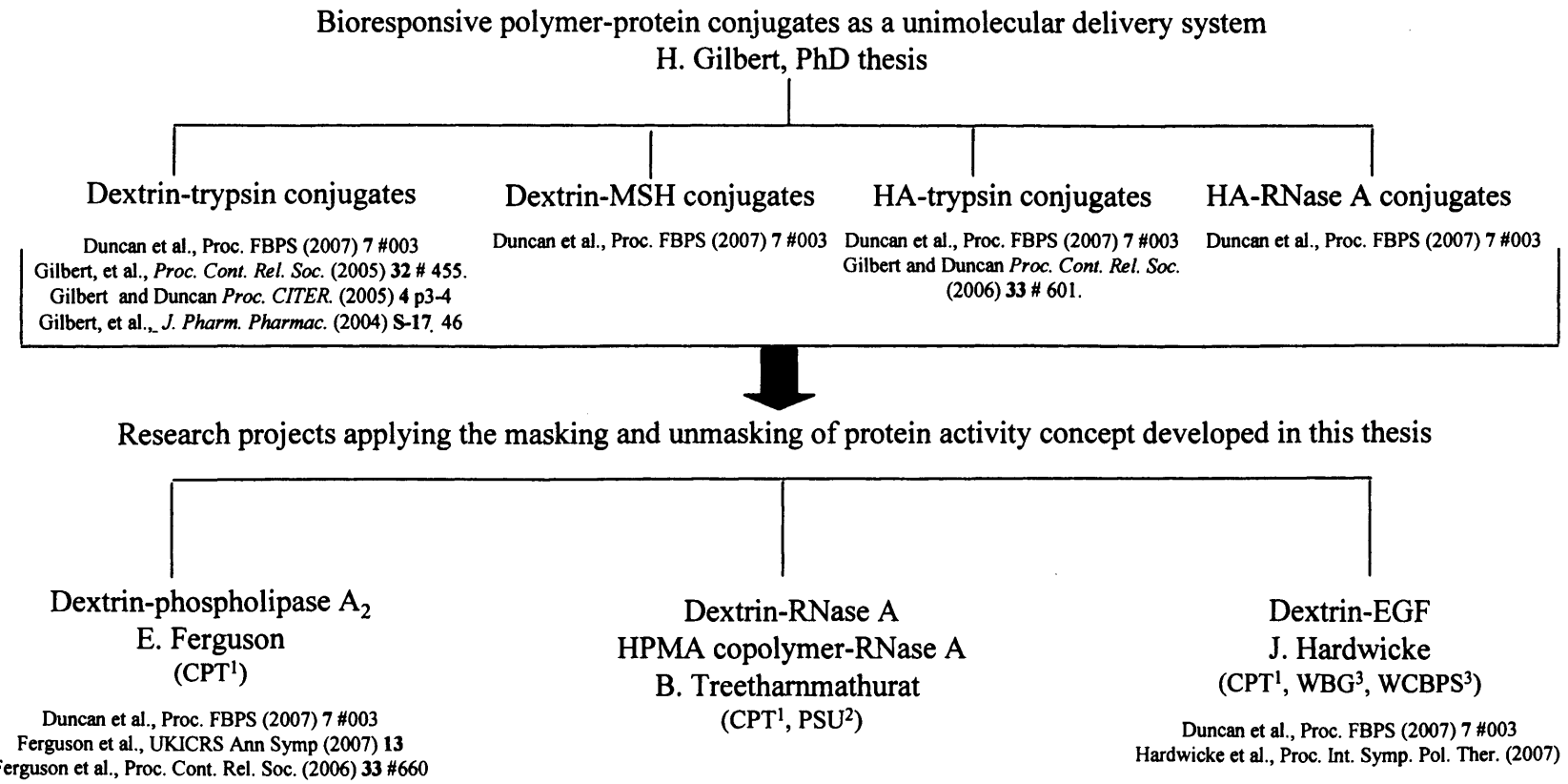

[1]Centre for Polymer Therapeutics, Welsh school of Pharmacy, Cardiff University. [2]Prince of Songkhla University, Thailand
[3]Wound Biology Group, CITER, Cardiff University. [4]Welsh Centre for Burns and Plastic Surgery, Morriston Hospital, Swansea

Figure 7.1 Contribution of this thesis to science; publications stemming from this study, and subsequent work conducted by other researchers.

Table 7.1 Polymer-protein conjugates entering clinical trials in the last 3 years

Year / status	Drug name	Polymer-protein combination	Indication	Reference
CT (P III)†	PEG Intron®	PEG-interferon alpha-2b	Renal cell carcinoma	Odaimi et al., 2004
			Advanced melanoma (stage IV)	Krown et al., 2004
CT (P II)†	PEG Intron®	PEG-interferon alpha-2b	Chronic myeloid leukaemia	NIH, 2006a
			Brain and CNS tumours	NIH, 2007a
			Plexiform Neurofibromas	NIH, 2006c
CT (P III)†	NS‡	PEG-interferon alpha-2a	Chronic hepatitis B and C	NIH, 2005a
CT (P I)†	NS‡	PEG-interferon alpha-2a	Non-melanomatous skin cancer	NIH, 2007b
CT (P II)†	CDP870 (certolizumab pegol)	PEG-Anti TNF FAB†††	Crohn's disease	NIH, 2006b
			Chronic plaque psoriasis	NIH, 2005b
CT (P II)†	pegsunercept	PEG-sTNF-a-R1†††	Rheumatoid Arthritis	PhRMA, 2004
CT (P II)†	PEG-Uricase	PEG-Uricase	Refractory Gout	NIH, 2004
CT (P I)†	LYSODASE	PEG-Glucocerebrosidase	Gaucher disease	Enzon, 2004

†CT is an abbreviation for clinical trials; PI, PII or PIII represents phase one, two or three

‡NS indicates not stated

††† TNF and R stand for tumour necrosis factor and receptor respectively

thiol-specific conjugation, as bovine haemoglobin has a naturally occurring very reactive cysteine at position 93, which has been targeted for site-specific conjugation to PEG-maleimide (Manjula et al., 2003). More notably, site-specific conjugation of PEG has also been achieved to the lysine at position 18 in salmon calcitonin, using a one-pot synthetic strategy protecting other susceptible amines with 9-fluorenylmethoxycarbonyl (FMOC) (Youn et al., 2007).

A second area of interest in the development of PEG chemistry has been within the area of biodegradable linkers. An established example is the tetrapeptide linker GLY-PHE-LEU-GLY, which is specifically cleaved in the lysosome by the enzyme cathepsin B (a thiol dependent lysosomal protease) (reviewed by Duncan, 2003). This mechanism of lysosomotropic delivery to release protein or drug payload through the cleavage of biodegradable linkers has been reviewed by Duncan (2007) and Haag and Kratz (2006). In the last few years, other examples of biodegradable linkers have included acid-labile imine linkers incorporated onto a PEI backbone (Kim et al., 2005), cathepsin B and D degradable sequences of peptides used to link radioimmunoconjugates (DeNardo et al., 2003), and a peptidyl linker susceptible to degradation by matrix metalloproteinases, which was utilised in a dextran-methotrexate conjugate (Chau et al., 2006). No new degradable linkers have however been described specifically for polymer-protein conjugation.

Despite the increasing popularity of incorporating bioresponsive elements into delivery systems to enable triggered or site-specific activation of the therapeutic, the greatest application of bioresponsive / stimuli-responsive polymers has remained within the field of *in situ* hydrogels. These are responsive polymer matrices which typically undergo a change in conformation when exposed to stimulus, releasing an entrapped or conjugated protein (reviewed by Alexander and Shakesheff, 2006). There has been very limited application of such responsive polymers to other types of polymeric delivery systems. Gopin et al., (2004) have however developed a self-destructing polymeric (dendrimer) conjugate, where breakdown occurs as a cascade, triggered through a chemical or biochemical reaction. This chemistry includes a self-immolating system, which is triggered to degrade through the use of pH, amidase and an antibody to expose a nucleophile which subsequently triggers the release of the

bound drug doxorubicin. This system has not however been applied to the delivery of proteins.

An interesting twist on the polymer-protein conjugate theme, two-step systems; PDEPT and PELT, involve triggered release of the protein or drug through degradation that is induced by the administration of a polymer-enzyme conjugate rather than by utilisation of a biochemical trigger (reviewed by Duncan, 2003). Although, this is not directly relevant to bioresponsive polymer-protein conjugates, it could be applied to the concept of this thesis, using a polymer-enzyme conjugate to trigger the degradation of the masked polymer-therapeutic protein conjugate.

In light of the limitations of PEG, there has been increasing interest in the use of polysaccharides for application as biodegradable polymers in drug delivery. Mehvar (2003) has reviewed the application of dextran, pullulan and mannan for drug delivery but not for protein delivery. The particular application of polysaccharides, including HA, for site-specific delivery to the colon has also been thoroughly reviewed by Jain et al., (2007). Furthermore, there remains interest in the potential application of dextran and HA as polymeric backbones for protein and drug delivery, with recent studies investigating the effects of their conjugation to BSA (Jung et al., 2006), bupivacaine (Gianolio et al., 2005) and lipids (Ruhela et al., 2006) respectively.

Although the field of PEGylation has continued to evolve, and advancements are also occurring in the related fields of bioresponsive polymers (typically hydrogels) and biodegradable linkers / biodegradable polymers, these have not as yet been applied to polymer-protein conjugates.

7.3 Summary of the key results of this thesis; successes, challenges and possible future studies

The overall aim of this thesis was to establish proof of principle for the concept of masking and then reinstating protein activity (Figure 1.3). Chapters 3 and 4 showed that dextrin-trypsin and dextrin-MSH conjugates, designed to be activated by an amylase trigger, could be synthesised to mask the activity of the conjugated protein or peptide. Subsequently, amylase-triggered degradation of both dextrin-trypsin and dextrin-MSH conjugates showed that it was possible to reinstate at least some of the activity of trypsin (Chapter 3) or MSH (Chapter 4). It was additionally shown that it

was possible to mask trypsin activity to 6 % of free trypsin control, by conjugation to the polymer HA. Unlike the aforementioned conjugates, on addition of the polymer degrading enzyme HAase, an immediate re-expression of trypsin activity was observed (Chapter 5).

The ability to reduce protein and peptide activity on conjugation, and reinstate activity following addition of the polymer degrading enzyme, was affected by (i) type of polymer, (ii) molecular weight of the polymer, and (iii) number of conjugating bonds. The initial intention of this work was to create a conjugate whereby the polymer would completely mask the protein, illustrated in Figure 7.2. In hindsight, however, the ratio of reactants used would be more likely to result in a conjugate composed of a single polymer with many proteins attached (Figure 7.2). Despite the high ratio of protein to polymer that was used, the results from all of the conjugates studied still demonstrated that it was possible to partially mask protein activity. Therefore, it is possible that the conjugate may have had an intermediary structure combining several polymers with several protein molecules. Further study on structure conformation and optimisation of the polymer : protein ratio of reactants would therefore be desirable. The difference between the two polymers utilised; dextrin and HA, was significant in terms of both structure and molecular weight. The degradability of succinoylated dextrin had been previously characterised (Hreczuk-Hirst et al., 2001a) and was consistent with the slow unmasking of trypsin and MSH activity observed. In the case of HA however, the ability to control the rate of HAase mediated degradation was unknown and so studied here. It was demonstrated that it was possible to control the number of functional groups activated using the coupling agents EDC and sulfo-NHS. This level of functionalisation, alike succinoylation, also correlated to the rate of degradation.

In addition to providing proof of principle for the concept of this thesis (Figure 3.18), the dextrin-trypsin conjugate also highlighted several interesting questions which would benefit from further study. In particular, there was an apparent trend between increasing the trypsin loading and masking of activity of the HMW dextrin conjugate. Similarly, another trend between high trypsin loading (80 % w/w vs ~30 % w/w) and better unmasking of trypsin activity was also noted. It would be desirable therefore to expand the library of conjugates synthesised, in order to further explore this possible link between protein loading and modulation of protein activity.

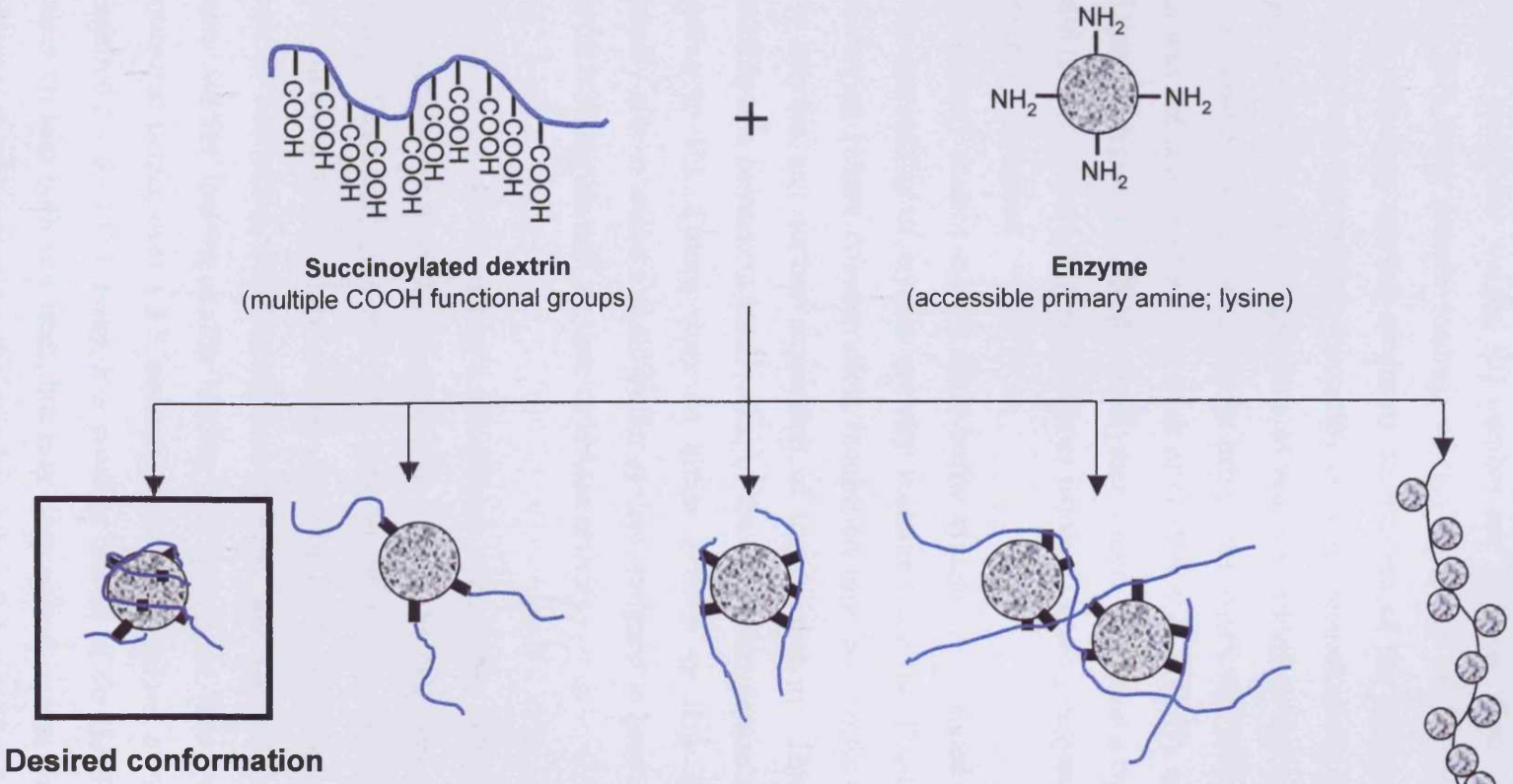

Figure 7.2 Possible polymer-protein conjugates that may have been synthesised

One of the main challenges in this work was to adapt the assay methods that were used to determine protein activity to include the "unmasking" step. This was a particular problem with both the dextrin-MSH conjugate and HA-trypsin conjugates.

It is unclear, whether the reduced modulation of MSH activity was contributed to by factors of (i) peptide molecular weight, (ii) number and location of amines for polymer conjugation, (iii) lower protein loading, or (iv) the assay method used to measure MSH activity following amylase-mediated degradation of the conjugate. In the case of dextrin-MSH, both the naturally occurring enzymes present in the FBS of the complete cell culture media and the presence of amylase added to the system, caused interference with the assay. The necessity for using heat inactivated FBS in the cell culture medium was not apparent from the work of O'Hare et al., (1993), as their studies had utilised the non-degradable HPMA copolymer. Future studies on a receptor / ligand system would ideally utilise a different polymer whose degrading enzyme does not interfere with receptor expression.

Secondly, preliminary studies using a multi-buffer system were carried out to try and improve the unmasking of trypsin activity measured for the HA-trypsin conjugates. Despite varying HAase concentration, incubation time and buffer pH, it was not possible to achieve any further expression of trypsin activity. This may potentially be attributable to a permanent inactivation of the trypsin active site caused by random conjugation to HA. Future work on either dextrin- or HA- trypsin conjugates would ideally aim to utilise a multi-buffer system designed to provide the optimum conditions for both trypsin and amylase or HAase activity.

Finally, the preliminary work utilising a HA-RNase A conjugate (Chapter 6) demonstrated that the conjugate caused 50 % cytoxicity in both the cell lines tested. Testing the cytotoxicity of this conjugate over 72 h may not have been the optimum duration, as this does not necessarily allow enough time for (i) degradation of the conjugate, (ii) RNase A trafficking, (iii) degradation of RNA, and (iv) subsequent apoptosis. Preliminary studies looking at the binding and uptake of fluorescently labelled HA only measured uptake over a 3 h incubation period. Therefore, over 72 h incubation period required for the MTT assay, it is possible that all of the HA-RNase A conjugate was taken up into both cell lines, but may have varied in rate. Further work on this conjugate should examine the uptake and cellular trafficking of fluorescently labelled HA over a 72 h time frame. Similarly, conducting the MTT

assay over 5 days would also be desirable. Furthermore, it would be essential to examine the cellular trafficking and localisation of the HA-RNase A conjugate in order to characterise its mechanism of action. Ideally this would be through the labelling of both the polymer and protein prior to conjugation.

7.4 Potential applications of this concept

This novel concept is very exciting as it could potentially be designed to selectively deliver therapeutic proteins to many different disease states. It is envisaged that polymer-protein conjugates would be administered by IV directly into the systemic circulation. Therefore, there are three potential levels of targeting, which may be summarised as:

(i) Systemic circulation
(ii) Extracellular targeting
(iii) Intracellular targeting

Dextrin would be a suitable candidate for application in a PDEPT-like system. Alternatively, by utilising dextrin of a high degree of succinoylation, it would be possible to formulate a conjugate with CR properties. This would provide optimum delivery of therapeutics, such as asparaginase for the treatment of leukaemia. Current polymer-protein conjugates indicated for the treatment of ALL include PEG-L-asparaginase (Oncaspar®) (Park et al., 1981; reviewed by Graham, 2003).

Delivery of a peptide therapeutic for receptor / ligand interactions would be of benefit in conditions such as Rheumatoid Arthritis (RA), where the soluble TNF receptor p55 and anti-TNF FAB bind to the inflammatory cytokine TNF-α. Both have been conjugated to PEG and are currently in phase II and III of clinical trials as Pegsunercept (PhRMA, 2004) and CDP870 (Chapman et al., 1999) respectively. RA is associated with an over expression of matrix metalloproteinases, located specifically in the joint cavity. This enzyme could be targeted to enable site-specific degradation of the potential polymeric backbones heparan sulfate and chondroitin sulfate (Collins, 1987).

Intracellular targeting *via* receptor-mediated endocytosis of the biodegradable polymer-protein conjugate, could be used to target specific therapeutic enzymes to the lysosomal compartment for enzyme replacement therapy. Alternatively, it could also

be used as a means of selectively delivering a cytotoxic protein such as RNase A (Chapter 6) into the cell.

Bioresponsive polymer-protein conjugates made up of biodegradable polymers have shown the potential to be applied to selective and site-specific delivery. Not only has proof of principle of a masked and reinstated protein activity been demonstrated here, but also in the subsequent work carried out by proceeding researchers (Figure 7.1). Herein lies a great and exciting novel delivery system to pave the way to advancements in the field of polymer-protein conjugates.

Bibliography

A

Abuchowski, A., Davis, F. F. (1979). Preparation and properties of polyethylene glycol-trypsin adducts. *Biochimica et Biophysica Acta*, **578**, 41-46

Abuchowski, A., van Es, T., Palczuk, N. C., Davis, F. F. (1977). Alteration of immunological properties of bovine serum albumin by covalent attachment of polyethylene glycol. *Journal of Biological Chemistry*, **252**, 3578-3581

Aguiar, D. J., Knudson, W., Knudson, C. B. (1999). Internalization of the hyaluronan receptor CD44 by chondrocytes. *Experimental Cell Research*, **252**, 292-302

Aiuti, A., Ficara, F., Cattaneo, F., Bordignon, C., Roncarolo, M. G. (2003). Gene therapy for adenosine deaminase deficiency. *Current Opinion in Allergy and Clinical Immunology*, **3**, 461-466

Alexander, C., Shakesheff, K. M. (2006). Responsive polymers at the biology / materials science interface. *Advanced Materials*, **18**, 3321-3328

Al-Obeidi, F., Hruby, V. J., Yaghoubi, N., Marwan, M. M., Hadley, M. E. (1992). Synthesis and biological activities of fatty acid conjugates of a cyclic lactam alpha-melanotropin. *Journal of Medicinal Chemistry*, **35**, 118-123

Al-Shamkhani, A. (1993). Evaluation of alginates as a soluble drug delivery system for oral and systemic use. PhD thesis; Department of Biological Sciences, University of Keele.

Alsop, M. R. (1994). History, chemical and pharmaceutical development of Icodextrin. *Peritoneal Dialysis International*, **14** (Supplement 2), S5

Andresen, T. L., Jensen, S. S., Jensen, L. T., Kaasgaard, T., Jorgensen, K. (2004). Triggered liposomal drug release in cancer tissue by secretory phospholipase A_2. *Proceedings of the Controlled Release Society. 31st Annual Meeting and Exposition*, **31**

Anika (2004). Orthovisc. High molecular weight hyaluronan. Report; Ortho Biotech, Woburn, 1-8

Arakawa, T., Hung, L., Pan, V., Horan, T. P., Kolvenbach, C. G., Narhi, L.O. (1993). Analysis of the heat induced denaturation of proteins using temperature gradient gel electrophoresis. *Analytical Biochemistry*, **208**, 255-259

Ardelt, B., Ardelt, W., Darzynkiewicz, Z. (2003). Cytotoxic ribonucleases and RNA interference (RNAi). *Cell cycle*, **2**, 22-24

Asteriou, T., Vincent, J-C., Tranchepain, F., Deschrevel, B. (2006). Inhibition of hyaluronan hydrolysis catalysed by hyaluronidase at high substrate concentration and low ionic strength. *Matrix Biology*, **25**, 166-174

B

Balan, S., Choi, J., Godwin, A., Teo, I., Laborde, C. M., Heidelberger, S., Zloh, M., Shaunak, S., Brocchini, S. (2007). Site-specific PEGylation of protein disulfide bonds using a three-carbon bridge. *Bioconjugate Chemistry*, **18**, 61-76

BAXTER (2007). PD (Peritoneal Dialysis) Solutions, BAXTER International Inc. www.baxter.com/products/renal/peritoneal_dialysis/sub/solutions.html (accessed 31/5/2007)

Beecher, J. E., Andrews, A. T., Vulfson, E. N. (1990). Glycosidases in organic solvents. II. Transgalactosylation catalysed by polyethylene glycol-modified beta-galactosidase. *Enzyme Microbial Technology*, **12**, 955-959

Bhardwaj, R., Blanchard, J. (1996). Controlled-release delivery system for the alpha-MSH analog Melanotan-I using poloxamer 407. *Journal of Pharmaceutical Sciences*, **85**, 915-919

Blundell, C. D., Almond, A. (2006). Enzymatic and chemical methods for the generation of pure hyaluronan oligosaccharides with both odd and even numbers of monosaccharide units. *Analytical Biochemistry*, **353**, 236-247

BMA, RPSGB. (2001) 10. Musculoskeletal and joint diseases. In *British National Formulary*, p. 461. Pharmaceutical press and BMJ publishers: London, UK

BMA, RPSGB. (2002). Appendix 7. Borderline substances. In *British National Formulary*, p. 730. Pharmaceutical press and BMJ publishers: London, UK

Bobic, V. (2005). Viscosupplementation for the osteoarthritis of the knee. International Society of Arthroscopy Knee Surgery and Orthopaedic Sports Medicine. www.isakos.com/innovations/bobic2.aspx (accessed 16/3/05)

Boos, J. (2004). The best way to use asparaginase in childhood acute lymphatic leukaemia - still to be defined? *British Journal of Haematology*, **125**, 117-127

Brewerton, L. J., Fung, E., Snyder, F. F. (2003). Polyethylene glycol-conjugated adenosine phosphorylase. Development of alternative enzyme therapy for adenosine deaminase deficiency. *Biochimica et Biophysica Acta,* **1637**, 171-177

Brocchini, S., Duncan, R. (1999). Pendent drugs, release from polymers. In *Encyclopedia of Controlled Drug Delivery*, Mathiowitz, E. (ed) p. 786-816. Wiley: New York, USA.

Brocchini, S., Balan, S., Godwin, A., Choi, J. W., Zloh, M., Shaunak, S. (2006). PEGylation of native disulfide bonds in proteins. *Nature Protocols,* **1** (5), 2241-2252

Bruneel, D., Schacht, E. (1993a). Chemical modification of pullulan. 1. Periodate oxidation. *Polymer,* **34**, 2628-2632

Bruneel, D., Schacht, E. (1993b). Chemical modification of pullulan. 2. Chloroformate activation. *Polymer*, **34**, 2633-2637

Bruneel, D., Schacht, E. (1994). Chemical modification of pullulan. 3. Succinoylation. *Polymer*, **35**, 2656-2658

Bruneel, D., Schacht, E. (1995). Enzymatic degradation of pullulan and pullulan derivatives. *Journal of Bioactive and Compatible Polymers*, **10**, 299-312

Buck, F. F., Vithayathil, A. J., Bier, M., Nord, F. F. (1962). On the mechanism of enzyme action. LXXII. Studies on trypsins from beef, sheep and pig pancreas. *Archives of Biochemistry and Biophysics*, **97**, 417-424

Bulmus, V., Woodward, M., Lin, L., Murthy, N., Stayton, P., Hoffman, A. (2003). A new pH-responsive and glutathione-reactive, endosomal membrane-disruptive polymeric carrier for intracellular delivery of biomolecular drugs. *Journal of Controlled Release*, **93**, 105-120

Bulpitt, P., Aeschlimann, D. (1999). New strategy for chemical modification of hyaluronic acid. Preparation of functionalized derivatives and their use in formation of novel biocompatible hydrogels. *Journal of Biomedical and Materials Research*, **47**, 152-169

C

Caliceti, P., Chinol, M., Roldo, M., Veronese, F. M., Semenzato, A., Salmaso, S., Paganelli, G. (2002). Poly(ethylene glycol)-avidin bioconjugates. Suitable candidates for tumor pretargeting. *Journal of Controlled Release*, **83**, 97-108

Carter, M. C., Meyerhoff, M. E. (1985). Instability of succinyl ester linkages in O2'-monosuccinyl cyclic AMAP-protein conjugates at neutral pH. *Journal of Immunological Methods*, **81**, 245-257

Chaffee, S., Mary, A., Stiehm, R., Girault, D., Fischer, A., Hershfield, M. S. (1992). IgG antibody response to polyethylene glycol-modified adenosine deaminase in

patients with adenosine deaminase deficiency. *Journal of Clinical Investigation*, **89**, 1643-1651

Chang, T. K., Jackson, D.Y., Burnier, J. P., Wells, J. A. (1994). Subtiligase. A tool for semisynthesis of proteins. *Proceedings of the National Academy of Science*, **91**, 12544-12548

Chapman, A. P., Antoniw, P., Spitali, M., West, S., Stephens, S., King, D. J. (1999). Therapeutic antibody fragments with prolonged *in vivo* half-lives. *Nature Biotechnology*, **17**, 780-783

Chaturvedi, D. N., Knittel, J. J., Hruby, V. J., Castrucci, A. M. de L., Hadley, M. E. (1984). Synthesis and biological actions of highly potent and prolonged acting biotin-labelled melanotropins. *Journal of Medicinal Chemistry*, **27**, 1406-1410

Chau, Y., Padera, R. F., Dang, N. M., Langer, R. (2006). Antitumor efficacy of a novel polymer-peptide-drug conjugate in human tumor xenograft models. *International Journal of Cancer*, **118**, 1519-1526

Chen, G., Hoffman, A. S. (1993). Preparation and properties of thermoreversible, phase-separating enzyme-oligo(N-isopropylacrylamide) conjugates. *Bioconjugate Chemistry*, **4**, 509-514

Cheung, R. Y., Ying, Y., Rauth, A. M., Marcon, N., Yu Wu, X. (2005). Biodegradable dextran-based microspheres for delivery of anticancer drug mitomycin C. *Biomaterials*, **26** (26), 5375-5385

Clarke, S., Lock, V., Duddy, J., Sharif, M., Newman, J. H., Kirwan, J. R. (2005). Intra-articular hylan G-F 20 (Synvisc) in the management of patellofemoral osteoarthritis of the knee (POAK). *The Knee*, **12**, 57-62

Collins, P. M. (1987). Carbohydrates. Chapman and Hall Ltd: London, UK

Cornish-Bowden, A. (2004). Fundamentals of enzyme kinetics. Portland press: London, UK

Culty, M., Nguyen, H. A., Underhill, C. B. (1992). The hyaluronan receptor (CD44) participates in the uptake and degradation of hyaluronan. *The Journal of Cell Biology*, **116**, 1055-1062

Cunningham-Rundles, C., Zhuo, Z., Griffith, B., Keenan, J. (1992). Biological activities of polyethylene-glycol immunoglobulin conjugates resistance to enzymatic degradation. *Journal of Immunological Methods*, **152**, 177-190

D

Daly, S. M., Przybycien, T. M., Tilton, R. D. (2005). Adsorption of poly(ethyleneglycol)-modified ribonuclease A to a poly(lactide-co-glycolide) surface. *Biotechnology and Bioengineering*, **90**, 856-868

Danauser-Reidl, S., Hausmann, E., Schick, H., Bender, R., Dietzfelbinger, H., Rastetter, J., Hanauske, A. (1993). Phase-I clinical and pharmacokinetic trial of dextran conjugated doxorubicin (AD-70, DOX-OXD). *Investigational New Drugs*, **11**, 187-195

Davies, D. S. (1994). Kinetics of Icodextrin. *Peritoneal Dialysis International*, **14** (S2), S45-50

Davis, F. F. (2002). The origin of pegnology. *Advanced Drug Delivery Reviews*, **54**, 457-458

Day, A. (2003). Dextrin. In *Handbook of Pharmaceutical Excipients*, Rowe, R.C., Shesky, P.J., Welleb, P.J. (ed) p. 197-199. Pharmaceutical Press and American Pharmaceutical Association: London, UK

DeNardo, G. L., DeNardo, S. J., Peterson, J. J., Miers, L. A., Lam, K. S., Hartmann-Siantar, C., Lamborn, K. R. (2003). Preclinical evaluation of cathepsin-

degradable peptide linkers for radioimmunoconjugates. *Clinical Cancer Research,* **9,** 3865-3872

Ding, Z., Chen, G., Hoffman, A. S. (1998). Unusual properties of thermally sensitive oligomer-enzyme conjugates of poly(N-isopropylacrylamide)-trypsin. *Journal of Biomedical Material Research*, **39**, 498-505

Ding, Z., Long, C. J., Hayashi, Y., Elmus, E. V., Hoffman, A. S., Stayton, P. S. (1999). Temperature control of biotin binding and release with a streptavidin-Poly(N-isopropylacrylamide) site-specific conjugate. *Bioconjugate Chemistry,* **10**, 395-400

Duncan, R. (1986). Lysosomal degradation of polymers used as drug carriers. *CRC Critical Reviews in Biocompatibility*, **2** (2), 127-145

Duncan, R., Gac-Breton, S., Keane, R., Musila, R., Sat, Y. N., Satchi, R., Searle, F. (2001). Polymer-drug conjugates, PDEPT and PELT: basic principles for design and transfer from the laboratory to clinic. *Journal of Controlled Release*, **74**, 135-146

Duncan, R. (2003). The dawning era of polymer therapeutics. *Nature Reviews | Drug Discovery*, **2**, 347-360

Duncan, R. (2005) Targeting and intracellular delivery of drugs. In *Encyclopedia of Molecular Cell Biology and Molecular Medicine,* Meyers, R.A. (ed). Wiley-VHC Verlag: Weinheim, Germany

Duncan, R., Vicent, M. J., Greco, F., Gilbert, H. R. P., Schmaljohann, D. and Ferguson, E. (2006). Novel anticancer polymer conjugates designed to treat hormone-dependant cancers and circumvent resistance. *Proceedings of the Controlled Release Society Meeting in Pamplona.*

Duncan, R. (2007). Designing polymer conjugates as lysosomotropic nanomedicines. *Biochemical Society Transactions,* **35**, 56-60

Duncan, R., Ferguson, E., Gilbert, H., Hardwicke, J., Schmaljohann, D., Moseley, R., Stephens, P., Thomas, D. W. (2007). Polymer therapeutics - Towards new nanomedicines. *Proceedings of the 7th International Symposium on Frontiers in Biomedical Polymers,* **7**, #003

Dust, J. M., Fang, Z. H., Harris, J. M. (1990). Proton NMR characteristics of polyethylene glycol and derivatives. *Macromolecules*, **23**, 3742-3746

E

Eberle, A. N. (1988). *The Melanotropins. Chemistry, Physiology and Mechanisms of Action.* Karger: London, UK.

Eliaz, R. E., Szoka, F. C. (2001). Liposome-encapsulated doxorubicin targeted to CD44. *Cancer Research*, **61**, 2592-2601

Enzon (2004). Enzon Inc clinical trials, Resource informagen, http://informagen.com/Resource_Informagen/Deprecated/2/2602.php (accessed 24/6/2004)

Erickson, H. A., Jund, M. D., Pennell, C. A. (2006). Cytotoxicity of human RNase-based immunotoxins requires cytosolic access and resistance to ribonuclease inhibition. *Protein Engineering, Design and Selection*, **19**, 37-45

ESF (2007). European Science Foundation Forward Look on Nanomedicine. www.esf.org (accessed 07/07)

ETPN (2005). European technology platform on nanomedicine. ftp://ftp.cordis.europa.eu/pub/nanotechnology/docs/nanomedicine_visionpaper.pdf (accessed 07/07)

Eugene Lee, J., Raines, R. T. (2003). Contribution of active-site residues to the function of onconase, a ribonuclease with antitumoral activity. *Biochemistry*, **42**, 11443-11450

Eugene Lee, J., Raines, R. T. (2005). Cytotoxicity of bovine seminal ribonuclease. Monomer versus dimer. *Biochemistry*, **44**, 15760-15767

ExPASy (2004a). Trypsin; porcine pancreas. *ExPASy protein database*, http://Swissmodel.expasy.org/repository/SmS.php?sptr_ac=P00761 (accessed 16/3/04)

ExPASy (2004b). Hyaluronidase; bovine pancreas. *ExPASy protein database*, http://expasy.org/uniprot/Q8SQG8 (accessed 16/3/04)

ExPASy (2007). RNase A; bovine pancreas. *ExPASy protein database*, http://www.expasy.org/uniprot/P61823 (accessed 21/7/07)

F

FDA (2004). Therapeutic biological approvals. U.S. Food and Drug Administration, Department of Health and Human Services. http://www.fda.gov/cder/biologics/biologics_table.htm (accessed 25/6/04)

Feldmann, M. (2001). Pathogenesis of arthritis. Recent research progress. *Nature immunology*, **2**, 771-773

Ferguson, E. L., Schmaljohann, D., Duncan, R. (2006). Polymer-phospholipase conjugates as novel anti-cancer agents: dextrin-phospholipase A_2. *Proceedings of the 33rd Annual Meeting and Exposition of the Controlled Release Society*, **33**, # 660

Ferguson, E. L., Schmaljohann, D., Duncan, R. (2007). Dextrin-phospholipase A_2 conjugates as an enzyme-triggered anti-cancer agent. *Proceedings of the United Kingdom and Ireland Controlled Release Society Annual Symposium*, **13**

Fernandez, M., Fragoso, A., Cao, R., Banos, M., Ansorge-Schumacher, M., Hartmeier, W., Villalonga, R. (2004). Functional properties and application in peptide synthesis of trypsin modified with cyclodextrin-containing dicarboxylic acids. *Journal of Molecular Catalysis B. Enzymatic*, **31**, 47-52

Fernandez, M., Fragoso, A., Cao, R., Banos, M., Villalonga, R. (2002). Chemical conjugation of trypsin with monoamine derivatives of cyclodextrins. Catalytic and stability properties. *Enzyme and Microbial Technology*, **31**, 543-548

Fernandez, M., Fragoso, A., Cao, R., Villalonga, R. (2003). Improved functional properties of trypsin modified by monosubstituted amino-b-cyclodextrins. *Journal of Molecular Catalysis B. Enzymatic*, **21**, 133-141

Fernandez, M., Villalonga, M. L., Fragoso, A., Cao, R., Villalonga, R. (2004). Effect of beta-cyclodextrin-polysucrose polymer on the stability properties of soluble trypsin. *Enzyme and Microbial Technology*, **34**, 78-82

Fernandez-Botran, R., Yan, J., Justus, D. E. (1999). Binding of Interferon gamma by glycosaminoglycans. A strategy for localisation and/or inhibition of its activity. *Cytokine*, **11**, 313-325

Fletcher, S., Stables, A., Turney, J. H. (1998). Icodextrin allergy in a peritoneal dialysis patient. *Nephrology Dialysis Transplantation*, **13**, 2656-2658

Francis, G. E., Fisher, D., Delgado, C., Malik, F., Gardiner, A., Neale, D. (1998). PEGylation of cytokines and other therapeutic proteins and peptides. The importance of biological optimisation of coupling techniques. *International Journal of Hematology*, **68**, 1-18

G

Garman, A. J., Kalindjian, S. B. (1987). The preparation and properties of novel reversible polymer-protein conjugates. *FEBS Letters*, **223**, 361-365

German, L. (2001). Body distribution of dextrin and D-2-S and evaluation of their potential as novel polymeric-drug carriers. PhD thesis: Welsh School of Pharmacy, Cardiff University, UK

Ghanem, G. E., Libert, A., Arnould, R., Vercammen, A., Lejeune, F. (1991). Human melanoma targeting with alpha-MSH-melphalan conjugate. *Melanoma Research*, **1**, 105-114

Ghosh, P., Guidolin, D. (2002). Potential mechanism of action of intra-articular hyaluronan therapy in osteoarthritis. Are the effects molecular weight dependent? *Seminars in Arthritis and Rheumatism*, **32**, 10-37

Gianolio, D. A., Philbrook, M., Avila, L. Z., MacGregor, H., Duan, S. X., Bernasconi, R., Slavsky, M., Dethlefsen, S., Jarrett, P. K., Miller, R. J. (2005). Synthesis and evaluation of hydrolyzable hyaluronan-tethered bupivacaine delivery systems. *Bioconjugate chemistry*, **16**, 1512-1518

Gilbert, H. R. P., Vicent, M. J., Duncan, R. (2004). Design of novel, bioresponsive polymer-protein conjugates. *Journal of Pharmacy and Pharmacology*, **S-17**, # 46

Gilbert, H. R. P., Duncan, R. (2005). Bioresponsive polymer-protein conjugates for site-specific activation. *Proceedings of the 4th Annual meeting of the Cardiff Institute of Tissue Engineering and Repair*, **4**, 3-4

Gilbert, H. R. P., Vicent, M. J., Duncan, R. (2005). Polymer-protein conjugates; optimising design for disease specific targeting. *Proceedings of the 32nd Annual Meeting of the Controlled Release Society*, **32**, # 455

Gilbert, H. R. P., Duncan, R. (2006). Polymer-protein conjugates for triggered activation: hyaluronic acid-trypsin as a model. *Proceedings of the 33rd Annual Meeting of the Controlled Release Society*, **33**, # 601

Glazer, A. N., McKenzie, H. A., Wake, R. G. (1963). The denaturation of proteins. II. Ultraviolet absorption spectra of bovine serum albumin and ovalbumin in urea and in acid solution. *Biochimica et Biophysica Acta*, **69**, 240-248

Glue, P., Fang, J. W., Rouzier-Panis, R., Raffanel, C., Sabo, R., Gupta, S. K., Salfi, M., Jacobs, S. (2000). Pegylated interferon-alpha 2b. Pharmacokinetics, pharmacodynamics, safety, and preliminary efficacy data. Hepatitis C intervention Therapy Group. *Clinical Pharmacology and Therapeutics*, **68**, 556-567

Gokal, R., Mistry, C. D., Peers, E., MIDAS study group. (1994). A United Kingdom multicenter study of Icodextrin in continuous ambulatory peritoneal dialysis. *Peritoneal Dialysis International*, **14** (S2), S22-27

Goldsmith, D., Jayawardene, S., Sabharwal, N., Cooney, K. (2000). Allergic reactions to the polymeric glucose-based peritoneal dialysis fluid icodextrin in patients with renal failure. *The Lancet*, **355**, 897

Gonzalez-Garcia, A., Marchetti, P., Castedo, M., Zamzami, N., Tarazona, R., Martinez-A, C., Kroemer, G. (1996). Polyethylene glycol-modified IL-2 abrogates superantigen-induced anergy without affecting peripheral clonal clonal deletion in vivo. *Clinical Immunology and Immunopathology*, **78**, 215-222

Goorman, S. D., Watanabe, T. K., Miller, E. H., Perry, C. (2000). Functional outcome in knee osteoarthritis after treatment with Hylan G-F 20. A prospective study. *Archives of Physical Medicine and Rehabilitation*, **81**, 479-483

Gopin, A., Rader, C., Shabat, D. (2004). New chemical adaptor unit designed to release a drug from a tumr targeting device by enzymatic triggering. *Bioorganic and Medicinal Chemistry,* **12**, 1853-1858

Graham, M. L. (2003). Pegaspargase. A review of clinical studies. *Advanced Drug Delivery Reviews*, **55**, 1293-1302

Groff, J. L., Cherniak, R., Jones, R. G. (1982). The incorporation of carboxyl groups into dextran and cross-linked agarose by O-succinylation. *Carbohydrate Research*, **101**, 168-173

H

Haag, R., Kratz, F. (2006). Polymer therapeutics: concepts and applications. *Angewandte Chemie,* **45,** 1198-1215

Hamburger, M. I., Lakhanpal, S., Mooar, P. A., Oster, D. (2003). Intra-articular hyaluronans. A review of product-specific safety profiles. *Seminars in Arthritis and Rheumatism,* **32**, 296-309

Hardwicke, J., Moseley, R., Schmaljohann, D., Stephens, P., Duncan, R., Thomas, D. W. (2007). Bioresponsive dextrin-EGF conjugates designed to promote tissue regeneration in impaired human wound healing. *Proceeding of the 7th International Symposium on Polymer Therapeutics,* **7**

Harris, J. M. (1992). 1. Introduction to biotechnical and biomedical applications of poly(ethylene glycol). In *Poly(ethylene glycol) Chemistry, Biotechnical and Biomedical Applications*, p. 1-13. Harris, J. M. (ed). Plenum Publishing Corporation: New York, USA

Harris, J. M., Chess, R. B. (2003). Effect of PEGylation on pharmaceuticals. *Nature Reviews | Drug Discovery,* **2**, 214-221

Harris, J. M., Martin, N. E., Modi, M. (2001). PEGylation. A novel process for modifying pharmacokinetics. *Clinical Pharmacokinetics*, **40**, 539-551

Harzmann, R., Esser, N., Loewe, R., Roberts, J., Leenders, F., Seifert, W., Unger, C., Drevs, J. (2004). Glutaminase (PEG-PGA) increases antitumoral efficacy of cytotoxic agents. *Proceedings of the American Society of Clinical Oncology (ASCO) Annual Meeting*

Hershfield, M. S., Buckley, R. H., Greenberg, M. L., Melton, A. L., Schiff, R., Hatem, C., Kurtzberg, J., Markert, M. L., Kobayashi, R. H., Kobayashi, A. L. (1987). Treatment of adenosine deaminase deficiency with polyethylene glycol-modified adenosine deaminase. *New England Journal of Medicine,* **316**, 589-596

Hershfield, M. S., Chaffee, S., Koro-Johnson, L., Mary, A., Smith, A. A., Short, S. A. (1991). Use of site-directed mutagenesis to enhance the epitope-shielding effect of covalent modification of proteins with polyethylene glycol. *Proceedings of the National Academy of Science*, **88**, 7185-7189

Hinds, K. D., Wan Kim, S. (2002). Effects of PEG conjugation on insulin properties. *Advanced Drug Delivery Reviews*, **54**, 505-530

Hoffman, A. S., Stayton, P. S. (2004). Bioconjugates of smart polymers and proteins. Synthesis and applications. *Macromolecular symposium*, **207**, 139-151

Hooper, N. M. (2002). *Essays in Biochemistry. Proteases in Biology and Medicine.* Portland Press: London, UK

Hosie, K., Gilbert, J. A., Kerr, D., Brown, C. B., Peers, E. M. (2001). Fluid dynamics in man of an intraperitoneal drug delivery solution. 4 % Icodextrin. *Drug Delivery*, **8**, 9-12

Hreczuk-Hirst, D., Chicco, D., German, L., Duncan, R. (2001a). Dextrins as potential carriers for drug targeting. Tailored rates of dextrin degradation by introduction of pendant groups. *International Journal of Pharmaceutics*, **230**, 57-66

Hreczuk-Hirst, D., German, L., Duncan, R. (2001b). Dextrins as carriers for drug targeting. Reproducible succinoylation as a means to introduce pendant groups. *Journal of Bioactive and Compatible Polymers*, **16**, 353-365

Hruby, V. J., Wilkes, B. C., Hadley, M. E., Al-Obeidi, F., Sawyer, T. K. (1987). Melanotropin. The minimal active sequence in the frog skin bioassay. *Journal of Medicinal Chemistry*, **30**, 2126-2130

Huang, Q., Wang, Z., Li, Y., Liu, S., Tang, Y. (1994). Refined 1.8Å resolution crystal structure of the porcine epsilon-trypsin. *Biochimica et Biophysica Acta - Protein Structure and Molecular Enzymology*, **1209**, 77-82

Huber, J. D., Campos, C. R., Egleton, R. D., Witt, K., Guo, L., Roberts, M. J., Bentley, M. D., Davis, T. P. (2003). Conjugation of low molecular weight poly(ethylene glycol) to biphalin enhances antinociceptive profile. *Journal of Pharmaceutical Sciences*, **92**, 1377-1385

Hunt, G., Todd, C., Cresswell, J. E., Thody, A. J. (1994). Alpha-Melanocyte stimulating hormone and its analogue NLe^4DPhe^7 alpha-MSH affect morphology, tyrosinase activity and melanogenesis in cultured human melanocytes. *Journal of Cell Science*, **107**, 205-211

I

Ilinskaya, O. N., Koschinski, A., Mitkevich, V. A., Repp, H., Dreyer, F., Nick Pace, C., Makarov, A. A. (2004). Cytotoxicity of RNases is increased by cationization and counteracted by K_{ca} channels. *Biochemical and Biophysical Research Communications*, **314**, 550-554

Inada, Y., Matsushima, A., Kodera, Y., Nishimura, H. (1990). *Journal of Bioactive and Compatible Polymers*, **5**, 343

Ishii, A., Furukawa, M., Matsushima, A., Kodera, Y., Yamada, A., Kanai, H., Inada, Y. (1995). Alteration of properties of natural pigments by conjugation with fibroin or polyethylene glycol. *Dyes and Pigments*, **27**, 211-217

J

Jackson, C.-J. C., Charlton, J. L., Kuzminski, K. (1987). Synthesis, isolation and characterisation of conjugates of ovalbumin and monomethoxypolyethylene glycol using cyanuric chloride as the coupling agent. *Analytical Biochemistry*, **165**, 114-127

Jain, A., Gupta, Y., Jain, S. K. (2007). Perspectives of biodegradable natural polysaccharides for site-specific drug delivery to the colon. *Journal of Pharmacology and Pharmaceutical Sciences*, **10**, 86-128

John, R. A. (1998). Photometric assays. In *Enzyme Assays. A Practical Approach*, Eisenthal, R., Danson, M.J. (ed) p. 59-92. Oxford University Press: Oxford, UK

Johnson, A., Gautham, N., Pattabhi, V. (1999). Crystal structure at 1.63 Å resolution of the native form of porcine b-trypsin. Revealing an acetate ion binding site and functional water network. *Biochimica et Biophysica Acta*, **1435**, 7-21

Johnson, K. D., Clark, A., Marshall, S. (2002). A functional comparison of ovine and porcine trypsins. *Comparative Biochemistry and Physiology Part B*, **131**, 423-431

Johnston, E., Crawford, J., Blackwell, S., Bjurstrom, T., Lockbaum, P., Roskos, L., Yang, B. B., Gardner, S., Miller-Messana, M. A., Shoemaker, D., Garst, J.,

Schwab, G. (2000). Randomised, dose-escalating study of SD/01 compared with daily filgrastim in patients receiving chemotherapy. *Journal of Clinical Oncology*, **18**, 2522-2528

Juliano, R. (2007). Cellular delivery of therapeutic macromolecules. Challenges to macromolecular drug delivery. *Biochemical Society Transactions*, **35**, 4-6

Jung, S. H., Choi, S. J., Kim, H. J., Moon, T. W. (2006). Molecular characteristics of bovine serum albumin-dextran conjugates. *Bioscience, Biotechnology and Biochemistry*, **70**, 2064-2070

K

Kaufman, P.B., Wu, W., Kim, D., Cseke, L. J. (1995). Electrophoresis, blotting, and hybridization. In *Handbook of Molecular and Cellular Methods in Biology and Medicine*, p. 109-115. CRC Press: London, UK

Kerr, D. J., Young, A. M., Neoptolemos, J. P., Sherman, M., Van-Greene, P., Stanley, A., Ferry, D., Dobbie, J. W., Vincke, B., Gilbert, J., el Eini, D., Dombros, N., Fountzilas, G. (1996). Prolonged intraperitoneal infusion of 5-fluorouracil using a novel carrier solution. *British Journal of Cancer*, **74**, 2032-2035

Kibbe, A. H. (2000). Handbook of Pharmaceutical Excipients. Washington D.C., Pharmaceutical press and American Pharmaceutical Association: London, UK

Kim, Y. H., Park, J H., Lee, M., Kim, Y-H., Park, T. G., Kim, S. W. (2005). Polyethylenimine with acid-labile linkages as a biodegradable gene carrier. *Journal of Controlled Release*, **103**, 209-219

Kinstler, O., Molineux, G., Treuheit, M., Ladd, D., Gegg, C. (2002). Mono-N-terminal poly(ethylene glycol)-protein conjugates. *Advanced Drug Delivery Reviews*, **54**, 477-485

Kohn, D. B., Sadelain, M., Glorioso, J. C. (2003). Occurrence of leukaemia following gene therapy of X-linked SCID. *Nature Reviews / Cancer*, **3**, 477-488

Kolarz, G., Kotz, R., Hochmayer, I. (2003). Long-term benefits and repeated treatment cycles of intra-articular sodium hyaluronate (Hyalgan) in patients with osteoarthritis of the knee. *Seminars in Arthritis and Rheumatism*, **32**, 310-319

Kost, J., Goldbart, R. (1997). Natural and modified polysaccharides. In *Handbook of Biodegradable Polymers*, Domb, J. K. A. J., Wiseman, D. M. (ed). Harwood academic publishers: Singapore

Krown, S. E., Hwu, W. -J., Menell, J. H., Panageas, K. S., Lamb, L. A., Aird, S., Williams, L. J., Chapman, P. B., Livingston, P. O., Wolchok, J. D. (2004). A phase II study of temozolomide (TMZ) and pegylated interferon alpha-2b (PGI) in the treatment of advanced melanoma. *Proceedings of the American Society of Clinical Oncology (ASCO) Annual Meeting*

Kurisawa, M., Chung, J. E., Yang, Y. Y., Gao, S. J., Uyama, H. (2005). Injectable biodegradable hydrogels composed of hyaluronic acid-tyramine conjugates for drug delivery and tissue engineering. *Chemical Communications*, 4312-4314

L

Lackey, C. A., Murthy, N., Press, O. W., Tirrell, D. A., Hoffman, A. S., Stayton, P. S. (1999). Hemolytic activity of pH-responsive polymer-streptavidin bioconjugates. *Bioconjugate Chemistry*, **10**, 401-405

Lee, J. Y., Spicer, A. P. (2000). Hyaluronan. A multifunctional, megaDalton, stealth molecule. *Current Opinion in Cell Biology*, **12**, 581-586

Lee, S. H., Youn, Y. S., Lee, K. C. (2004). Improved hypoglycemic effect and pharmacokinetics of glucagon-like peptide-1 (GLP-1) by PEGylation.

Proceedings of the Controlled Release Society 31st Annual Meeting and Exposition, **31**

Levy, Y., Hershfield, M. S., Fernandez-Mejia, C., Polmar, S. H., Scudiery, D., Berger, M., Sorensen, R. U. (1988). Adenosine deaminase deficiency with late onset of recurrent infections. Response to treatment with polyethylene glycol-modified adenosine deaminase. *The Journal of Paediatrics,* **113**, 312-317

Lewis, R. (2003). Triggered degradation of polymer-protein conjugates. Report: Welsh School of Pharmacy, Cardiff University, UK

M

Maeda, H. (2001). SMANCS and polymer-conjugated macromolecular drugs. Advantages in cancer chemotherapy. *Advanced Drug Delivery Reviews,* **46**, 169-185

Maeda, H., Ueda, M., Morinaga, T., Matsumoto, T. (1985). Conjugation of poly(styrene-co-maleic acid) derivatives to the antitumor protein Neocarzinostatin. Pronounced improvements in pharmacological properties. *Journal of Medicinal Chemistry*, **28**, 455-461

Maeda, H., Matsumura, T. (1989). Tumoritropic and lymphotropic principles of macromolecular drugs. C*ritical Reviews in Therapeutic Drug Carrier Systems*, **6**, 193-210

Maeda, H., Konno, T. (1997). Metamorphosis of Neocarzinostatin to SMANCS. Chemistry, biology, pharmacology, and clinical effect of the first prototype anticancer polymer therapeutic. Neocarzinostain. In *The Past, Present, and Future of an Anticancer Drug*, Maeda, H., Edo, K., Ishida, N. (ed) p. 227-267. Springer-Verlag: Tokyo, Japan

Malik, F., Brew, J., Maidment, S. A., Delgado, C., Francis, G. E. (2000). PEG-modified erythropoietin with improved efficacy. *Experimental Hematology*, **28**, 106

Malik, F., Delgado, C., Knusli, C., Irvine, A. E., Fisher, D., Francis, G. E. (1992). Polyethylene glycol (PEG) modified granulocyte-macrophage colony stimulating factor (GM-CSF) with conserved biological activity. *Experimental Hematology,* **20**, 1028-35

Manjula, B. N., Tsai, A., Upadhya, R., Perumalsamy, K., Smith, P. K., Malavalli, A., Vandegriff, K., Winslow, R. M., Intaglietta, M., Prabhakaran, M., Friedman, J. M., Acharya, A. S. (2003). Site-specific PEGylation of hemoglobin at cys-93(beta). Correlation between the colligative properties of the PEGylated protein and the length of the conjugated PEG chain. *Bioconjugate Chemistry*, **14**, 464-472

Mathews, C. K., van Holde, K. E. (1990). Biochemistry. The Benjamin/Cummings Publishing Company, Redwood city: CA, USA

Matousek, J., Soucek, J., Slavik, T., Tomanek, M., Eugene Lee, J., Raines, R. T. (2003). Comprehensive comparison of the cytotoxic activities of onconase and bovine seminal ribonuclease. *Comparative Biochemistry and Physiology Part C*, **136**, 343-356

Matsuo, I., Fujimoto, H., Isomura, M., Ajisaka, K. (1997). Chemoenzymatic synthesis of GALa1-3GAL, GALa1-3GALb1-4GLCNAC, and their PEG conjugates. *Bio-organic and Medicinal Chemistry Letters*, 7, 255-258

Matsushima, A., Kodera, Y., Hiroto, M., Nishimura, H., Inada, Y. (1996). Bioconjugates of proteins and polyethylene glycol. Potent tools in biotechnological processes. *Journal of Molecular Catalysis B. Enzymatic*, **2**, 1-17

McQuade, P., Miao, Y., Yoo, J., Quinn, T. P., Welch, M. J., Lewis, J. S. (2005). Imaging of melanoma using 64 Cu- and 86 Y- DOTA- ReCCMSH(Arg11), a cyclized peptide analogue of alpha MSH. *Journal of Medicinal Chemistry*, **48**, 2985-2992

Mehvar, R. (2000). Dextrans for targeted and sustained delivery of therapeutic and imaging agents. *Journal of Controlled Release*, **69**, 1-25

Mehvar, R. (2003). Recent trends in the use of polysaccharides for improved delivery of therapeutic agents: pharmacokinetic and pharmacodynamic perspectives. *Current Pharmaceutical Biotechnology*, **4**, 283-302

Meier, K. (2002). Synthesis and biological evaluation of dextrin-protein conjugates. Report: Welsh School of Pharmacy, Cardiff University, UK

Meloan, C. E. (1999). Size exclusion chromatography (gel filtration; gel permeation). In *Chemical Separations. Principles, Techniques, and Experiments*, p. 171-178. John Wiley and Sons: Chichester, UK

Menzel, E. J., Farr, C. (1998). Hyaluronidase and its substrate hyaluronan. Biochemistry, biological activities and therapeutic uses. *Cancer Letters*, **131**, 3-11

Michaelis, M., Cinati, J., Cinati, J., Pouckova, P., Langer, K., Kreuter, J., Matousek, J. (2002). Coupling of the antitumoral enzyme bovine seminal ribonuclease to polyethylene glycol chains increases its systemic efficacy in mice. *Anti-Cancer Drugs*, **13**, 149-154

Mistry, C. D., Gokal, R. (1994). Icodextrin in peritoneal dialysis. Early development and clinical use. *Peritoneal Dialysis International*, **14**, S13-S21

Mok, C. C., Mak, A. (2004). Therapeutic advances in rheumatoid arthritis. APLAR *Journal of Rheumatology*, **7**, 62-70

Monti, D. M., D'Alessio, G. (2004). Cytosolic RNase inhibitor only affects RNases with intrinsic cytotoxicity. *The Journal of Biological Chemistry*, **279**, 39195-39198

Mosmann, T. (1983). Rapid colorimetric assay for cellular growth and survival: application to proliferation and cytotoxicty assays. *Journal of Immunological Methods*, **65**, 55-63

Murakami, Y., Hoshi, R., Hirata, A. (2003). Characterisation of polymer-enzyme complex as a novel biocatalyst for nonaqueous enzymology. *Journal of Molecular Catalysis B. Enzymatic*, **22**, 79-88

Murphy, A., Fagain, C. O. (1996). Stability characteristics of chemically-modified soluble trypsin. *Journal of Biotechnology*, **49**, 163-171

N

Nagle, T., Berg, C., Nassi, R., Pang, K. (2003). The further evolution of biotech. *Nature Reviews | Drug Discovery*, **2**, 75-79

Natarajan, A., Xiong, C., Albrecht, H., DeNardo, G. L., DeNardo, S. J. (2005). Characterization of site-specific ScFv PEGylation for tumor-targeting pharmaceuticals. *Bioconjugate Chemistry*, **16**, 113-121

NIH (1990). Gene transfer therapy for severe combined immunodeficiency disease (SCID) due to adenosine deaminase (ADA) deficiency. *A natural history study, National Library of Medicine.* http://www.clinicaltrials.gov/ct/gui/show/NCT00001255 (accessed 5/8/04)

NIH (1993). PEG-Glucocerebrosidase for the treatment of Gaucher disease. *A natural history study, National Library of Medicine.* www/clinicaltrials.gov/ct/show/NCT00001410?order=1 (accessed 06/07)

NIH (2003a). Bevacizumab and PEG-Interferon alfa-2b in treating patients with metastatic or unresectable carcinoid tumors. *A natural history study, National Library of Medicine.* www.clinicaltrials.gov/ct/show/NCT00055809?order=1 (accessed 06/07)

NIH (2003b). Open label long-term safety study of CDP870 (Certolizumab Pegol) for patients with rheumatoid arthritis. *A natural history study, National Library of Medicine.* www.clinicaltrials.gov/ct/show/NCT00160693?order=4 (accessed 06/07)

NIH (2003c). Ro 50-3821 in treating anaemia in patients receiving antineoplastic therapy for stage IIIB or stage IV non-small cell lung cancer. *A natural history study, National Library of Medicine.* www.clinicaltrials.gov/ct/show/NCT00072059?order=3 (accessed 06/07)

NIH (2003d). ADI-PEG in patients with metastatic melanoma. *A natural history study, National Library of Medicine.* www.clinicaltrials.gov/ct/show/NCT00029900?order=2 (accessed 06/07)

NIH (2003e). Testing of ADI-PEG in hepatocellular carcinoma. *A natural history study, National Library of Medicine.* www.clinicaltrials.gov/ct/show/NCT00056992?order=1 (accessed 06/07)

NIH (2004). PEGylated recombinant mammalian uricase (PEG-Uricase) as treatment for refractory gout. *A natural history study, National Library of Medicine.* www.clinicaltrials.gov/ct/show/NCT00111657?order=1 (accessed 30/07/07)

NIH (2005a). Peginterferon alfa-2a plus ribavirin for chronic hepatitis C / hepatitis B co-infection and chronic hepatitis C. *A natural history study, National Library of Medicine.* www.clinicaltrials.gov/ct/show/NCT00154869?order=21 (accessed 06/07)

NIH (2005b). Efficacy study of CDP870 in subjects with chronic plaque psoriasis who are candidate for systemic therapy and/or phototherapy / photochemotherapy. *A natural history study, National Library of Medicine.* www.clinicaltrials.gov/ct/show/NCT00245765?order=1 (accessed 06/07)

NIH (2005c). Treatment of advanced AIDS patients with dextrin sulfate. *A natural history study, National Library of Medicine.* www.clinicaltrials.gov/ct/show/NCT00004987?order=1 (accessed 06/07)

NIH (2006a). Proteinase 3 PR1 peptide mixed with montanide ISA-51 VG adjuvant and administered with GM-CSF and Peginterferon alfa-2b [PEG-INTRON(R)]. *A natural history study, National Library of Medicine.* www.clinicaltrials.gov/ct/show/NCT00415857?order=1 (accessed 06/07)

NIH (2006b). Clinical study of CDP870/Certolizumab Pegol in patients with active Crohn's disease. *A natural history study, National Library of Medicine.* www.clinicaltrials.gov/ct/show/NCT00291668?order=1 (accessed 06/07)

NIH (2006c). Study of PEG-Intron for Plexiform neurofibromas. *A natural history study, National Library of Medicine.* www.clinicaltrials.gov/ct/show/NCT00396019?order=4 (accessed 30/07/07)

NIH (2007a). PEG-Interferon alfa-2b and Thalidomide in treating patients with recurrent high-grade gliomas. *A natural history study, National Library of Medicine.* www.clinicaltrials.gov/ct/show/NCT00052650?order=1 (accessed 06/07)

NIH (2007b). Gefitinib and PEG-Interferon alfa-2a in treating patients with unresectable or metastatic skin cancer. *A natural history study, National Library of Medicine.* www.clinicaltrials.gov/ct/show/NCT00423397?order=10 (accessed 06/07)

Nucci, M. L., Shorr, R., Abuchowski, A. (1991). The therapeutic value of poly(ethylene glycol)-modified proteins. *Advanced Drug Delivery Reviews,* **6**, 133-151

O

Odaimi, M., El-Jassous, I., Richa, E., Forte, F., Terjanian, T., Vesoniiaraki, M., Lowry, J., Murukutla, S., Dhar, M., Burton, J. (2004). Phase I/II trial of a novel regimen of GM-CSF, IL-2 and pegylated Interferon-alpha2b (PEG-Intron) for stage IV melanoma and renal cell carcinoma (RCC). *Proceedings of the American Society of Clinical Oncology (ASCO) Annual Meeting*

O'Hare, K. B., Duncan, R., Strohalm, J., Ulbrich, K., Kopeckova, P. (1993). Polymeric drug-carriers containing doxorubicin and melanocyte-stimulating hormone. *In vitro* and *in vivo* evaluation against murine melanoma. *Journal of Drug Targeting*, **1**, 217-229

Orlando, J. A. (1962). Acid and alkali denaturation of rhodospirillum haem protein. *Biochimica et Biophysica Acta,* **56**, 252-256

Oupicky, D., Ulbrich, K., Rihova, B. (1999). Conjugates of semitelechelic poly[N-(2-hydroxypropyl)methacrylamide] with enzymes for protein delivery. *Journal of Bioactive and Compatible Polymers*, **14**, 213-231

P

Park, Y. K., Abuchowski, A., Davis, S., Davis, F. (1981). Pharmacology of Escherichia coli-L-asparaginase polyethylene glycol adduct. *Anticancer Research*, **1**, 373-376

Parkinson, C., Scarlett, J. A., Trainer, P. J. (2003). Pegvisomant in the treatment of acromegaly. *Advanced Drug Delivery Reviews*, **55**, 1303-1314

Parveen, S., Sahoo, S. K. (2006). Nanomedicine: clinical applications of polyethylene glycol conjugated proteins and drugs. *Clinical Pharmacokinetics*, **45**, 965-988

Pasut, G., Guiotto, A., Veronese, F. M. (2004). Protein, peptide and non-peptide drug PEGylation for therapeutical application. *Expert Opinion on Therapeutic Patents*, **14**, 859-894

PDB (2007). Ribonuclease A. http://www.rcsb.org/pdb/explore/explore.do?structureId=7RSA (accessed 2/11/07).

PFAM (2004). Trypsin. Wellcome Trust, Sanger Institute. http://www.sanger.ac.uk/cgi-bin/Pfam/getacc?PF00089 (accessed 1/4/04)

PhRMA (2004). New Medicines in Development. Pharmaceutical Research and Manufacturers of America. http://www.phrma.org/newmedicines/newmedsdb/drugs.cfm (accessed 24/6/04)

Phelps, K. (2006). Design of novel biologically active polymers to enhance drug delivery across epithelial barriers. PhD thesis: Welsh School of Pharmacy, Cardiff University, UK

PIERCE (2004). Bicinchoninic acid (BCA) method. Assays: protein. Pierce Chemicals. http://starklab.slu.edu/PhysioLab/bca.pdf. (accessed 18/3/04)

Pouckova, P., Zadinova, M., Hlouskova, D., Strohalm, J., Plocova, D., Spunda, M., Olejar, T., Zitko, M., Matousek, J., Ulbrich, K., Soucek, J. (2004). Polymer-conjugated bovine pancreatic and seminal ribonuclease inhibit growth of human tumors in nude mice. *Journal of Controlled Release*, **95**, 83-92

R

Reddy, K. R., Wright, T. L., Pockros, P. J., Shiffman, M., Everson, G., Reindollar, R., Fried, M. W., Purdum, P. P 3rd., Jensen, D., Smith, C., Lee, W. M., Boyer, T. D., Lin, A., Pedder, S., DePamphilis, J. (2001). Efficacy and safety of pegylated (40-kd) interferon alpha-2a compared with interferon alpha-2a in noncirrhotic patients with chronic hepatitis C. *Hepatology,* **33**, 433-438

Reddy, K. R., Modi, M. W., Pedder, S. (2002). Use of peginterferon alfa-2a (40 kd) (Pegasys®) for the treatment of hepatitis C. *Advanced Drug Delivery Reviews*, **54**, 571-586

Roberts, M. J., Bentley, M. D., Harris, J. M. (2002). Chemistry for peptide and protein PEGylation. *Advanced Drug Delivery Reviews*, **54**, 459-476

Rosenkranz, A. A., Lunin, V. G., Sergienko, O. V., Gilyazova, D. G., Voronina, O. L., Jans, D. E., Kofner, A. A., Shumiantseva, M. A., Mironov, A. F., Sobolev, A. S. (2003). Targeted intracellular site-specific drug delivery. Photosensitizer targeting to melanoma cell nuclei. *Russian Journal of Genetics*, **39**, 198-206

Roy, I., Gupta, M. N. (2003). Smart polymeric materials. Emerging biochemical applications. *Chemistry and Biology*, **10**, 1161-1171

Ruhela, D., Riviere, K., Szoka, F. C. (2006). Efficient synthesis of an aldehyde functionalised hyaluronic acid and its application in the preparation of hyaluronan-lipid conjugates. *Bioconjugate Chemistry,* **17**, 1360-1363

RxMed (2005). Suplasyn. Paladin sodium hyaluronate synovial fluid replacement. RxMed. www.rxmed.com/b.main/b2.pharmaceutical/b2.1.monographs/CPS-%20Monographs/CPS-%20(General%20Monographs-%20S)/SUPLASYN.html (accessed 16/3/05)

S

Sakuragawa, N., Shimizu, K., Kondo, K., Kondo, S., Niwa, M. (1986). Studies on the effect of PEG-modified urokinase on coagulation-fibrinolysis using beagles. *Thrombosis Research*, **41**, 627-635

Samoshina, N. M., Samoshin, V. V. (2005). The Michaelis constants ratio for two substrates with a series of fungal (mould and yeast) beta-galactosidases. *Enzyme and Microbial Technology*, **36**, 239-251

Sato, H. (2002). Enzymatic procedure for site-specific pegylation of proteins. *Advanced Drug Delivery Reviews*, **54**, 487-504

Sato, H., Yamamoto, K., Hayashi, E., Takahara, Y. (2000). Transglutaminase-mediated dual and site-specific incorporation of poly(ethylene glycol) derivatives into a chimeric Interleukin-2. *Bioconjugate Chemistry*, **11**, 502-509

Savoca, K. V., Abuchowski, A., Van Es, T., Davis, F. F., Palczuk, N. C. (1979). Preparation of a non-immunogenic arginase by the covalent attachment of polyethylene glycol. *Biochimica et Biophysica Acta,* **578**, 47-53

Sawyer, T. K., Sanfilippo, P. J., Hruby, V. J., Engel, M. H., Heward, C. B., Burnett, J. B., Hadley, M. E. (1980). 4-Norleucine, 7-D-phenylalanine-alpha-melanocyte-stimulating hormone. A highly potent alpha-melanotropin with ultralong biological activity. *Biochemistry*, **77**, 5754-5758

Schering, C. A., Zhong, B., Woo, J. C. G., Silverman, R. B. (2004). Poly(ethylene glycol)-supported enzyme inactivators. Efficient identification of the site of covalent attachment to alpha-chymotrypsin by PEG-TPCK. *Bioconjugate Chemistry*, **15**, 673-676

Schnaar, R. L., Sparks, T. F., Roseman, S. (1977). Cyanogen bromide activation of polysaccharides. *Analytical Biochemistry*, **79**, 513-525

Seib, F. P. (2005). Endocytosis and trafficking of polymer therapeutics in melanoma cells. PhD thesis: Welsh School of Pharmacy, Cardiff University, UK

Seppala, I., Pelkonen, J., Makela, O. (1985). Isotypes of antibodies induced by plain dextran or a dextran-protein conjugate. *European Journal of Immunology,* **15**, 827-833

Sharma, S. D., Granberry, M. E., Jiang, J., Leong, S. P. L., Hadley, M. E., Hruby, V. J. (1994). Multivalent melanotropic peptide and fluorescent macromolecular conjugates. New reagents for characterization of melanotropin receptors. *Bioconjugate Chemistry*, **5**, 591-601

Sharma, S. D., Jiang, J., Hadley, M. E., Bentley, D. L., Hruby, V. J. (1996). Melanotropic peptide-conjugated beads for microscopic visualization and characterization of melanoma melanotropin receptors. *Biochemistry*, **93**, 13715-13720

Shaunak, A., Thornton, M., John, S., Teo, I., Peers, E., Mason, P., Krausz, T., Davies, D. (1998). Reduction of the viral load of HIV-1 after the intraperitoneal administration of dextrin 2-sulphate in patients with AIDS. *AIDS*, **12**, 399-409

Shimoboji, T., Ding, Z. L., Stayton, P. S., Hoffman, A. S. (2001). Mechanistic investigation of smart polymer-protein conjugates. *Bioconjugate Chemistry,* **12**, 314-319

Shimoboji, T., Ding, Z. L., Stayton, P. S., Hoffman, A. S. (2002). Photoswitching of ligand association with a photoresponsive polymer-protein conjugate. *Bioconjugate Chemistry*, **13**, 915-919

Shimoboji, T., Larenas, E., Fowler, T., Hoffman, A. S., Stayton, P. (2003). Temperature-induced switching of enzyme activity with smart polymer-enzyme conjugates. *Bioconjugate Chemistry*, **14**, 517-525

SIGMA (1995). Trypsin from porcine pancreas. Sigma. www.sigma.co.uk (accessed 1/4/04).

SIGMA (2002). Hyaluronidase from bovine testes. Sigma. www.sigma-aldrich.com (accessed 06/05)

SIGMA (2005). Melanocyte stimulating hormone. Sigma. www.sigmaaldrich.com/catalog/search/ProductDetail/SIGMA/M4135 (accessed 05)

Soucek, J., Pouckova, P., Strohalm, J., Plocova, D., Hlouskova, D., Zadinova, M., Ulbrich, K. (2002). Poly[N-(2-hydroxypropyl)methacrylamide] conjugates of bovine pancreatic ribonuclease (RNase A) inhibit growth of human melanoma in nude mice. *Journal of Drug Targeting*, **10**, 175-183

Stayton, P. S., El-Sayed, M. E. H., Murthy, N., Bulmus, V., Lackey, C., Cheung, C., Hoffman, A. S. (2005). 'Smart' delivery systems for biomolecular therapeutics. *Orthodental and Craniofacial Research,* **8**, 219-225

Stevens, L. (1998). 11. Buffers and the determination of protein concentrations. In *Enzyme Assays. A Practical Approach,* Eisenthal, R., Danson, M.J. (ed) p. 317-335. Oxford University Press: Oxford, UK

Stuart, B. H. (2002). *Polymer Analysis*. John Wiley and Sons: Chichester, UK

Swiss-Prot/TrEMBL (2003). TRYP_PIG (P00761). *ExPASy Protein Database.* http://us.expasy.org/cgi-bin/protparam1?P00761@CHAIN@9@231 (accessed 5/12/03)

T

Takagi, A., Yamashita, N., Yoshioka, T., Sano, K., Yamaguchi, H., Maeda, A., Takakura, Y., Hashida, M. (2007). Enhanced pharmacological activity of

recombinant human interleukin 11 (rhIL11) by chemical modification with polyethylene glycol. *Journal of Controlled Release*, **119**, 271-278

Tawada, A., Masa, T., Oonuki, Y., Watanabe, A., Matsuzaki, Y., Asari, A. (2002). Large-scale preparation, purification, and characterization of hyaluronan oligosaccharides from 4-mers to 52-mers. *Glycobiology*, **12**, 421-426

Thanou, M., Duncan, R. (2003). Polymer-protein and polymer-drug conjugates in cancer therapy. *Current Opinion in Investigational Drugs*, **4**, 701-709

The Royal Society, The Royal Academy of Engineering (2004). Nanoscience and nanotechnologies: opportunities and uncertainties. Report. accessed through www2.cst.gov.uk/cst/business/nanoreview.shtml (accessed 29/07/07)

Thorner, M. O., Strasburger, C. J., Wu, Z., Straume, M., Bidlingmaier, M., Pezzoli, S. S., Zib, K., Scarlett, J. C., Bennett, W. F. (1999). Growth hormone (GH) receptor blockade with a PEG-modified GH (B2036-PEG) lowers serum insulin-like growth factor-1 but does not acutely stimulate serum GH. *Journal of Clinical Endocrinology and Metabolism*, **84**, 2098-2103

Thornton, M., Barkley, L., Mason, J. C., Shaunak, S. (1999). Anti-Kaposi's sarcoma and antiangiogenic activities of sulfated dextrins. *Antimicrobial Agents and Chemotherapy*, **43**, 2528-2533

Tipton, K. F. (1998). 1. Principles of enzyme assay and kinetic studies. In *Enzyme Assays. A Practical Approach,* Eisenthal, R., Danson, M.J. (ed) p. 1-53. Oxford University Press: Oxford, UK

Todorovic, A., Holder, J. R., Bauzo, R. M., Scott, J. W., Kavanagh, R., Abdel-Malek, Z., Haskell-Luevano, C. (2005). N-terminal fatty acylated His-Phe-Arg-Trp-NH2 tetrapeptides. Influence of fatty acid chain length on potency and selectivity at the mouse melanocortin receptors and human melanocytes. *Journal of Medicinal Chemistry*, **48**, 3328-3336

Torchilin, V. P. (2000). Drug Targeting. *European Journal of Pharmaceutical Sciences,* **11**, S81-S91

Torchilin, V. P., Lukyanov, A. N. (2003). Peptide and protein drug delivery to and into tumors. Challenges and solutions. *Drug Discovery Today*, **8**, 259-266

Torchilin, V. P., Voronkov, J. I., Mazoev, A. V. (1982). The use of immobilised streptokinase (Streptodekaza) for the therapy of thromboses. *Therapeutic Archives Russia,* **54**, 21-25

Torsteinsdottir, I., Groth, T., Lindqvist, U. (1999). Production and elimination of hyaluronan in rheumatoid arthritis patients. Estimation with a loading test. *Seminars in Arthritis and Rheumatism*, **28**, 268-279

Tsatmali, M., Ancans, J., Thody, A. J. (2002). Melanocyte function and its control by melanocortin peptides. *The Journal of Histochemistry and Cytochemistry*, **50**, 125-133

Tsutsumi, Y., Onda, M., Nagata, S., Lee, B., Kreitman, R. J., Pastan, I. (2000). Site-specific chemical modification with polyethylene glycol of recombinant immunotoxin anti-Tac(Fv)-PE38(LMB-2) improves antitumor activity and reduces animal toxicity and immunogenicity. *Proceedings of the National Academy of Science*, **97**, 8548-8553

U

Ulbrich, K., Strohalm, J., Plocova, D., Oupicky, D., Subr, V., Soucek, J., Pouckova, P., Matousek, J. (2000). Poly[N-(2-hydroxypropyl)methylacrylamide] conjugates of bovine seminal ribonuclease. Synthesis, physicochemical, and preliminary biological evaluation. *Journal of Bioactive and Compatible Polymers*, **15**, 4-26

V

Varga, J. M., Asato, N., Lande, S., Lerner, A. B. (1977). Melanotropin-daunomycin conjugate shows receptor-mediated cytotoxicity in cultured murine melanoma cells. *Nature*, **267**, 56-58

Varga, J. M., Dipasquale, A., Pawelek, J., McGuire, J. S., Lerner, A. B. (1974). Regulation of melanocyte stimulating hormone action at the receptor level. Discontinuous binding of hormone to synchronised mouse melanoma cells during the cell cycle. *Cell Biology*, **71**, 1590-1593

Varga, J. M., Moellmann, G., Fritsch, P., Godawska, E., Lerner, A. B. (1976). Association of cell surface receptors for melanotropin with the golgi region in mouse melanoma cells. *Cell Biology*, **73**, 559-562

Vercauteren, R., Bruneel, D., Schacht, E., Duncan, R. (1990). Effect of the chemical modification of dextran on the degradation by dextranase. *Journal of Bioactive and Compatible Polymers*, **5**, 4-15

Vercauteren, R., Schacht, E., Duncan, R. (1992). Effect of the chemical modification of dextran on the degradation by rat liver lysosomal enzymes. *Journal of Bioactive and Compatible Polymers*, **7**, 346-357

Veronese, F. M., Morpurgo, M. (1999). Bioconjugation in pharmaceutical chemistry. *Il Farmaco*, **54**, 497-516

Veronese, F. M., Sacca, B., Polverino de Laureto, P., Sergi, M., Caliceti, P., Schiavon, O., Orsolini, P. (2001a). New PEGs for peptide and protein modification, suitable for identification of the PEGylation site. *Bioconjugate Chemistry*, **12**, 62-70

Veronese, F. M. (2001b). Peptide and protein PEGylation. A review of problems and solutions. *Biomaterials*, **22**, 405-417

Veronese, F. M. (2004). New PEGs conjugates for therapeutic and diagnostic application. *Proceedings of the Controlled Release Society 31st Annual Meeting and Exposition*, **31**

Veronese, F. M., Pasut, G. (2005). PEGylation, successful approach to drug delivery. *Drug Discovery Today*, **10**, 1451-1458

Vicent, M. J., Duncan, R. (2006). Polymer conjugates: nanosized medicines for treating cancer. *Trends in Biotechnology*, **24**, 39-47

Villalonga, M. L., Fernandez, M., Fragoso, A., Cao, R., Villalonga, R. (2003). Functional stabilization of trypsin by conjugation with beta-cyclodextrin-modified carboxymethylcellulose. *Preparative Biochemistry and Biotechnology*, **33**, 53-66

Villalonga, R., Villalonga, M. L., Gomez, L. (2000). Preparation and functional poperties of trypsin modified by carboxymethylcellulose. *Journal of Molecular Catalysis B. Enzymatic*, **10**, 483-490

Vold, I. M. N., Christensen, B. E. (2005). Periodate oxidation of chitosans with different chemical compositions. *Carbohydrate Research*, **340**, 679-684

Volpi, N. (2003). Milligram-scale preparation and purification of oligosaccharides of defined length possessing the structure of chondroitin from defructosylated capsular polysaccharide K4. *Glycobiology*, **13**, 635-640

W

Wagner, E. (2007). Programmed drug delivery: nanosystems for tumor targeting. *Expert Opinion on Biological Therapy*, **7**, 587-593

Wang, Y., Youngster, S., Grace, M., Bausch, J., Bordens, R., Wyss, D. F. (2002). Structural and biological characterisation of pegylated recombinant interferon

alpha-2b and its therapeutic implications. *Advanced Drug Delivery Reviews,* **54**, 547-570

White, A. (2002). Polymer-protein conjugates as novel therapeutics. Report: Welsh School of Pharmacy, Cardiff University, UK

Wik (2007). Ribonuclease A. Wikipedia, the free encyclopedia. http://en.wikipedia.org/wiki/Ribonuclease_A (accessed 07/07)

X

Xyloyiannis, M. (2004) Poly(ethylene glycol) (PEG)-poly(ester) dendritic hybrids. Biocompatibility and effect of architecture on cellular pharmacokinetics. PhD thesis: Welsh School of Pharmacy, Cardiff University, UK

Y

Yamaoka, T., Tabata, Y., Ikada, Y. (1994). Distribution and tissue uptake of polyethylene glycol with different molecular weights after intravenous administration to mice. *Journal of Pharmaceutical Sciences*, **83**, 601-606

Youn, Y. S., Na, D. H., Lee, K C. (2007). High-yield production of biologically active mono-PEGylated salmon calcitonin by site-specific PEGylation. *Journal of Controlled Release,* **117**, 371-379

Yu, P., Zheng, C., Chen, J., Zhang, G., Liu, Y., Suo, X., Zhang, G., Su, Z. (2007). Investigation on PEGylation strategy of recombinant human interleukin-1 receptor antagonist. *Bioorganic and Medicinal Chemistry,* **15**, 5396-5405

Yun, Y. H., Goetz, D. J., Yellen, P., Chen, W. (2004). Hyaluronan microspheres for sustained gene delivery and site-specific targeting. *Biomaterials*, **25**, 147-157

Z

Zalipsky, S., Lee, C. (1992). 21. Use of functionalized poly(ethylene glycol)s for modification of polypeptides. In *Poly(ethylene glycol) Chemistry, Biotechnical and Biomedical Applications*, Harris, J. M., Zalipsky, S. (ed) p. 347-370. Plenum: New York, USA

Zaplinsky, S. (1995). Chemistry of polyethylene glycol conjugates with biologically active molecules. *Advanced Drug Delivery Reviews,* **16**, 157-182

Zeuzem, S., Feinman, S. V., Rasenack, J., Heathcote, E. J., Lai, M. Y., Gane, E., O'Grady, J., Reichen, J., Diago, M., Lin, A., Hoffman, J., Brunda, M. J. (2000). Peginterferon alfa-2a in patients with chronic hepatitis C. *New England Journal of Medicine*, **343**, 1666-1672

Zhang, Z., He, Z., He, M. (2001). Stabilization mechanism of MPEG modified trypsin based on thermal inactivation kinetic analysis and molecular modeling computation. *Journal of Molecular Catalysis B. Enzymatic,* **14**, 85-94.

Zhong, Y., Bellamkonda, R. V. (2005). Controlled release of anti-inflammatory agent alpha-MSH from neural implants. *Journal of Controlled Release,* **106**, 309-318

Zhuo, L., Hascall, V. C., Kimata, K. (2004). Inter-alpha-trypsin inhibitor, a covalent protein-glycosaminoglycan-protein complex. *Journal of Biological Chemistry,* **(37)**, 38079-38082

Appendix

PUBLICATIONS

Abstracts

Duncan, R., Ferguson, E., Gilbert, H., Hardwicke, J., Schmaljohann, D., Moseley, R., Stephens, P., Thomas, D.W. (2007). Polymer Therapeutics – Towards New Nanomedicines. *Proceedings of the 7th International Symposium on Frontiers in Biomedical Polymers.* #003

Duncan, R., Vicent, M.J., Greco, F., Gilbert, H.R.P., Schmaljohann, D. and Ferguson, E. (2006). Novel anticancer polymer conjugates designed to treat hormone-dependant cancers and circumvent resistance. *Proceedings of the Controlled Release Society Meeting in Pamplona.*

Gilbert, H.R.P. and Duncan, R. (2006). Polymer-Protein Conjugates for Triggered Activation: Hyaluronic Acid-Trypsin as a Model. *Proceedings of the 33rd Annual Meeting of the Controlled Release Society.* **33,** # 601

Gilbert, H.R.P. and Duncan, R. (2005). Bioresponsive Polymer-Protein Conjugates for site-specific activation. *Proceedings of the 4th Annual Meeting of the Cardiff Institute of Tissue Engineering and Repair.* **4,** 3-4

Gilbert, H.R.P., Vicent, M.J., Duncan, R. (2005). Polymer-protein conjugates; Optimising design for disease specific targeting. *Proceedings of the 32nd Annual Meeting of the Controlled Release Society.* **32,** # 455.

Gilbert, H.R.P., Vicent, M.J., Duncan, R. (2004). Design of novel, bioresponsive polymer-protein conjugates. *Journal of Pharmacy and Pharmacology.* S-17, # 46

Manuscripts in preparation

Gilbert, H.R.P., Vicent, M.J., and Duncan, R. (2007). Novel bioresponsive dextrin-trypsin conjugates; triggered degradation for site specific activity, optimisation of structural and kinetics parameters.
Target: Biomacromolecules.

Gilbert, H.R.P. and Duncan, R. (2007). Bioresponsive Polymer-Protein Conjugates for Triggered Activation; Low Molecular Weight Hyaluronic Acid-Trypsin Conjugates as a Model.
Target: Journal of Controlled Release.

Abstract for poster presentation:
33rd Annual Meeting and Exposition of the Controlled Release Society

Polymer-Protein Conjugates For Triggered Activation: Hyaluronic Acid – Trypsin as a Model

Helena Gilbert and Ruth Duncan.
Centre for Polymer Therapeutics, Welsh School of Pharmacy, Cardiff University,
King Edward VII Avenue, Cardiff, CF10 3XF, UK. GilbertH@cf.ac.uk

ABSTRACT SUMMARY:

Use of polymers to create conjugates that are able to mask protein activity, but then regenerate it slowly (or site-specifically) following triggered polymer degradation offers exciting advantages [1,2]. The aim of this study was to investigate hyaluronic acid (HA)/hyaluronidase (HAase) as a model to fulfil this concept. Hyaluronic acid (~ 135 KDa)-trypsin conjugates were synthesised and their activation by hyaluronidase studied.

Key words: polymer-protein conjugates, hyaluronic acid, bioresponsive polymers

INTRODUCTION:

PEGylation is well recognised as a means of increasing protein circulation half-life, reducing protein antigenicity and increasing protein stability [3]. Despite the success of PEGylation, the lack of biodegradability of PEG restricts the usable molecular weight to below the renal threshold. Additionally, there is also the potential risk of polymer accumulation following chronic administration. Our studies have been investigating several biodegradable polymers (e.g. dextrin [1,2]), to generate improved polymer-protein conjugates. Moreover, judicious choice of the polymer and its mechanism of degradation led us to propose a new concept for triggered activation of polymer-protein conjugates whose activity would be normally masked. Usually researchers try to maximise retained protein activity during PEGylation. In this case conjugation is optimised to create an inactive product that will elicit minimal activity/non-specific toxicity whilst in transit. Following triggered degradation of the bound polymer, the protein activity may be slowly regenerated in the circulation (e.g. dextrin/amylase [1,2]), or localised to a particular target site.

Earlier studies found that the optimum dextrin-trypsin conjugates contained dextrin of Mw ~47,000 g/mol functionalised to ~26 mol % (known to retain biodegradability [4]). Therefore it was considered important to use a relatively low molecular weight HA to create the HA-trypsin conjugates needed for these studies. Methods of acid and HAase degradation were explored as a means to generate this HA intermediate, but acid hydrolysis was preferred.

EXPERIMENTAL METHODS:

Preparation of LMW HA: HA from rooster comb was degraded using HCl (5 M, 12 h) to produce the LMW HA fraction. The products were characterised by FTIR and GPC.

Degradation of LMW HA by HAase: To confirm that LMW HA could be degraded by HAase, polymer was incubated with HAase (50-500 IU/mL) for 2h and degradation was monitored by GPC.

Synthesis and characterisation of HA-trypsin conjugates: The LMW HA was then conjugated to trypsin (1:1 molar ratio), using EDC and S-NHS as coupling agents (Fig. 1).

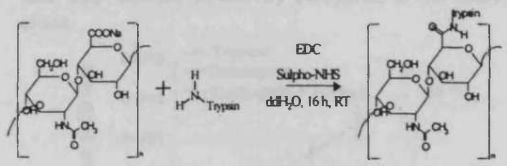

Figure 1. Conjugation of hyaluronic acid to trypsin.

FPLC fractionation was used to purify the conjugate, and the product was further characterised by GPC, SDS-PAGE electrophoresis and a BCA assay to assess total protein content.

Measurement of trypsin activity: Activity of the native and conjugated trypsin was determined using N-benzoyl L-arginine p-nitroanilide (L-BAPNA) as substrate. NAp cleaved from L-BAPNA was measured over 5 min at 400 nm.

Activation of the conjugate by addition of HAase: Activity of the HA-trypsin conjugate in the presence of the polymer degrading enzyme hyaluronidase (HAase; 0.5-25 ui, 37 °C) was measured as above.

RESULTS AND DISCUSSION:

Acid degradation of HA (~900,000 g/mol) was optimised to produce a LMW fraction of ~135,000 g/mol (Fig. 2). The structural integrity of this low molecular weight fraction was confirmed by FTIR.

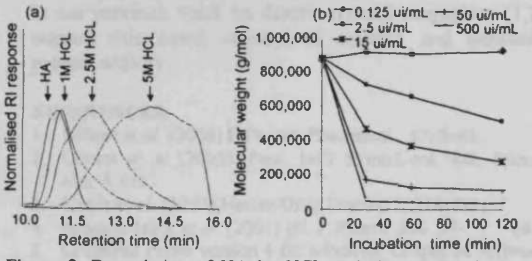

Figure 2. Degradation of HA by HCL and HAase. Panel (a) shows GPC analysis following acid degradation, and panel (b) degradation by HAase at different enzyme concentrations.

The LMW HA remained susceptible to degradation by HAase, an enzyme that cleaves the 1,4 linkage between glucuronic acid and N-acetylglucosamine. HA was rapidly degraded in the first 30 min (Fig 3a). The maximum reduction in polymer molecular weight under these conditions was seen to be to ~12,500 g/mol (Fig 3b).

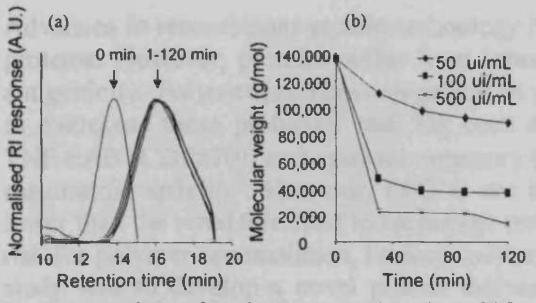

Figure 3. Degradation of HA by HAase. Panel (a) shows GPC analysis of LMW HA incubated with HAase (500 ui/mL), and panel (b) degradation by HAase at different enzyme concentrations.

A library of hyaluronic acid-trypsin conjugates, were synthesised by varying (i) the molar ratio of hyaluronic acid to trypsin and (ii) duration of reaction. Typically, the conjugates produced had a molecular weight (Mw) of ~ 80,000 – 115,000 g/mol and a polydispersity of ~1.4 – 1.7. However, it should be noted that the difference in solution conformation of the polymer standards used and the protein conjugates, provides only an estimate of molecular weight. The total protein content of the conjugates was typically up to 30 % w/w. Characterisation of some conjugates by GPC, SDS-PAGE and FPLC revealed the presence of free trypsin. Consequently, FPLC fractionation to isolate a pure HA-trypsin conjugate (Fig. 4) was conducted.

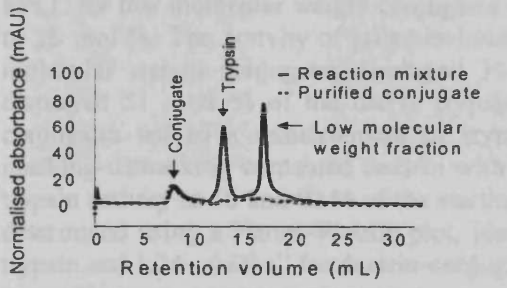

Figure 4. FPLC purification of HA-trypsin conjugates

The trypsin content of this conjugate was 3.7 % w/w and the conjugate molecular weight and polydispersity were ~62,000 g/mol and 1.3 respectively. This isolated conjugate showed negligible free trypsin, and both a reduced hydrodynamic volume and polydispersity compared to unfractionated conjugates.

The activity of polymer-bound trypsin was significantly reduced compared to free trypsin, ($p < 0.05$, One-way ANOVA with Bonferroni's post test [5]).

A reduction in trypsin activity to 6.4 % of trypsin control was measured (Fig. 5).

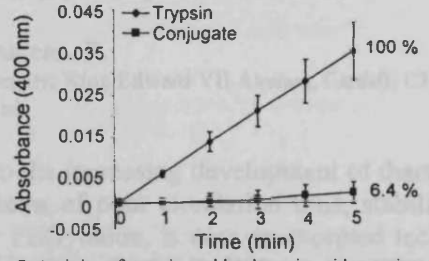

Figure 5. Activity of trypsin and hyaluronic acid-trypsin conjugate against the substrate L-BAPNA. (N=3 ± SD)

After addition of HAase to the HA-trypsin conjugate, there was an immediate increase in trypsin activity (Fig. 6). The conjugate in the presence of HAase, showed ~ a four fold increase in activity compared to the conjugate alone.

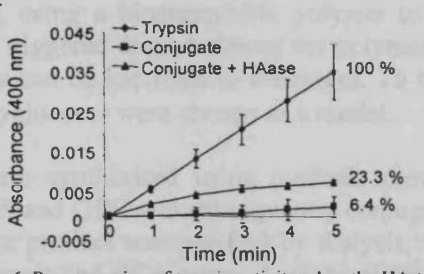

Figure 6. Re-expression of trypsin activity when the HA-trypsin conjugate was incubated with HAase. (N=3 ± SD)

This reinstatement of protein activity supports the previous work on dextrin-trypsin conjugates, where ~ a 1.5 – 2 fold reinstatement of activity was measured.

CONCLUSION:

PH mediated degradation of HA produced a structurally functional LMW HA fraction, retaining enzymatic degradability. Optimisation of the conjugation and purification of LMW HA to trypsin, produced a pure conjugate of low molecular weight and polydispersity. This conjugate expressed a significant masking of conjugated trypsin activity (6.4 %). Additionally, it was also demonstrated that the conjugate activity could be rejuvenated 4 fold over 5 minutes in the presence of the HA degrading enzyme HAase. These results, in addition to our previous work on dextrin-trypsin conjugates (1,2), support this novel concept of masked and reinstated protein activity.

REFERENCES:

1. Gilbert *et al.* (2004) J. Pharm. Pharmacol. **17**, S-46.
2. Gilbert *et al* (2005). Proc. Int'l Symp.Cont. Rel. Bioact. Mat. # 455
3. Harris *et al.* (2003) Nature Drug Discov. **2**, 214-221.
4. Hreczuk-Hirst *et al.* (2001) Int. J. Pharm. **230**, 57- 66.
5. GraphPad Prism version 4 for windows, GraphPad software, San Diego California USA, www.graphpad.com

ACKNOWLEDGEMENTS:
HG would like to thank BBSRC for supporting her PhD studentship.

Abstract for oral presentation:
4th Annual Meeting of the Cardiff Institute of Tissue Engineering and Repair

Bioresponsive polymer-protein conjugates for site-specific activation

Gilbert, H.R.P. and Duncan, R.
Centre for Polymer Therapeutics, Redwood Building, Cardiff University, King Edward VII Avenue, Cardiff, CF10 3XF
GilbertH@cf.ac.uk

Advances in recombinant protein technology have led to the increasing development of therapeutic proteins. However, proteins suffer from inherent problems of poor circulation time, stability and antigenicity. Polymer-protein conjugation, in particular PEGylation, is now an accepted technique to overcome these problems[1] and has been applied to both antibody FAB fragments (PEG-Anti TNF FAB (CDP870)) and cytokine receptors (PEG-sTNF-α-R1 (pegsunercept)) in the treatment of rheumatoid arthritis[2]. However, PEG is not biodegradable and so the molecular weight must be lower than the renal threshold to encourage renal elimination. Chronic administration also remains a risk for polymer accumulation, leading to lysosomal storage diseases. Consequently, the aim of this study was to develop a novel protein delivery system, using a biodegradable polymer to create protein conjugates that are inactivated in transit, but, by triggered degradation of the polymer at the appropriate site of action, unmasking of protein activity can be localised to the target. To test the feasibility of this concept, trypsin and dextrin (α-1,4 polyglucose) were chosen as a model.

Succinoylated dextrin intermediates (9-32 mol %) were synthesised using methods previously described[3,4]. They were characterised by titration, FT-IR and GPC and subsequently conjugated to trypsin using EDC and S-NHS as coupling agents[4]. The product was purified by dialysis, freeze-dried and characterised by GPC, SDS-PAGE electrophoresis and BCA assay. Activity of the native and conjugated trypsin was determined, using the substrate L-BAPNA, prior to, and following incubation with the polymer degrading enzyme α-amylase (16 h at 37 °C).

A library of dextrin-trypsin conjugates were synthesised using dextrins of low (~9 kDa) and high (~51 kDa) molecular weight. The resulting conjugates were typically 14-26 kDa and 49-102 kDa with a trypsin content of 50 to 80 % w/w. Free trypsin was not detected by SDS-PAGE, GPC or FPLC for low molecular weight conjugates and high molecular weight conjugates succinoylated up to 26 mol %. The activity of polymer-bound trypsin was reduced compared to free trypsin. High molecular weight conjugates displayed 34 – 60 % and the lower molecular weight conjugates displayed 51 - 69 % of the native trypsin activity. Addition of amylase to the dextrin-trypsin conjugates led to a reinstatement of trypsin activity. The conjugates that displayed optimum masking-unmasking contained dextrin with a high degree of succinoylation where reinstatment of trypsin activity to 58 and 92 % of the starting level was seen. Michaelis Menten rate constants were determined using a Hanes-Woolfe plot, identifying the turnover rate (Kcat) to be 2.5 – 2.9 s^{-1} for trypsin and 1.24 - 4.09 s^{-1} for dextrin-conjugated trypsin.

Dextrin conjugation to trypsin can be used to mask enzyme activity. This can subsequently be regenerated using amylase-triggered polymer degradation. Use of higher molecular weight dextrin with a high degree of succinoylation was most effective. This concept is now being applied to other polymer-protein combinations, which may have potential to deliver therapeutic proteins site specifically.

1. Harris *et al.* (2003) Nature Drug Discov. **2**, 214-221.
2 Pharmaceutical Research and Manufacturers of America (PhRMA) (2004). New Medicines in Development. http://www.phrma.org/newmedicines/newmedsdb/drugs.cfm
3. Hreczuk-Hirst *et al.* (2001) J. Bioact. Compat. Polymers **16**, 353-365.
4. Gilbert *et al.* (2004) J. Pharm. Pharmacol. **17**, S-46.

HG would like to thank BBSRC for supporting her studentship

Abstract for poster presentation: 32nd Annual Meeting and Exposition of the Controlled Release Society

Polymer-Protein Conjugates : Optimising Design For Triggered Activation

H.R.P. Gilbert, M.J. Vicent, and R. Duncan.
Centre for Polymer Therapeutics, Welsh School of Pharmacy, Cardiff University,
King Edward VII Avenue, Cardiff, CF10 3XF, UK.
GilbertH@cf.ac.uk

SUMMARY:

The aim of this study is to create polymer-protein conjugates where protein activity is masked until triggering of polymer degradation reinstates activity (1). Using dextrin-trypsin conjugates as a model, the effect of i) polymer molecular weight and ii) extent of polymer functionalisation on the reactivation of the conjugate was examined.

Key words: polymer-protein conjugates, dextrin, bioresponsive

INTRODUCTION:

Polymer-protein conjugation, in particular PEGylation, is now an accepted technique to increase protein circulation time, reduce antigenicity and improve the stability of protein therapeutics (2). As PEG is not biodegradable a molecular weight lower than the renal threshold must be used to encourage renal elimination, and even then there is a danger of polymer accumulation following chronic administration, leading to lysosomal storage disease. Consequently the aim of this study was to develop a novel approach for polymer-protein conjugation. A biodegradable polymer is used to create protein conjugates that are inactivated in transit, but, by triggered degradation of the polymer at the appropriate site of action, unmasking of protein activity can be localised to the target (Fig.1).

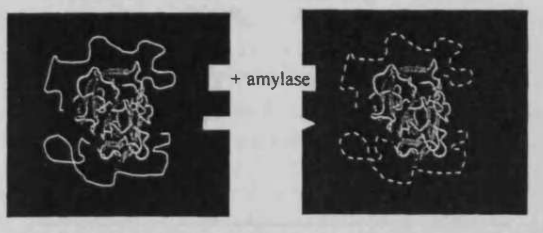

Figure 1. Model showing the dextrin-trypsin conjugate and its activation

To test the feasibility of this concept, trypsin was chosen as a model protein and dextrin selected as the polymer for conjugation. Dextrin, α-1,4 poly(glucose), is routinely administered as the peritoneal dialysis solution (Icodextrin™) (3). Specifically here the aim was to investigate the effect of polymer molecular weight (dextrins of low (≈ 9 kDa) and high (≈ 50 kDa) molecular weight were chosen) and degree of dextrin succinoylation (up to 32 mol %) on the efficiency of protein conjugation and subsequent unmasking of activity.

EXPERIMENTAL METHODS:

Succinoylated dextrin intermediates (9-32 mol %) were synthesised using methods previously described (1,4,5) and characterised by titration, FT-IR and GPC. The intermediates generated were subsequently conjugated to trypsin using EDC and S-NHS as coupling agents (1,5). The product was purified by dialysis, freeze-dried and then characterised by GPC, SDS-PAGE electrophoresis and BCA assay. Activity of the native and conjugated trypsin was determined prior to, and following incubation with the polymer degrading enzyme α-amylase (16 h at 37 °C). The trypsin specific substrate N-benzoyl L-arginine p-nitroanilide (L-BAPNA) was used.

RESULTS AND DISCUSSION:

The characteristics of the conjugates prepared are summarised in Table 1. The trypsin content as determined by BCA assay was 50 to 80 % w/w. There was no clear relationship between degree of polymer functionalisation and trypsin content of the resultant conjugates. GPC characterisation with the aid of polysaccharide standards revealed an apparent Mw of 14-26 kDa (starting from the lower molecular weight polymer) and 49-102 kDa (starting from the higher molecular weight dextrin). The polydispersity ranged from 1.33-1.63. However, it is clear that these are not absolute values due to the difference in solution conformation of polymer standard and protein conjugate. SDS-PAGE analysis showed smearing from the wells to 23 kDa, consistent with the polydispersity of both the succinoylated dextrin (Mw/Mn 1.3-1.5) and conjugates (Mw/Mn 1.3-1.7). Free trypsin was not detected by SDS-PAGE, GPC or FPLC for low molecular weight dextrin conjugates. However, free trypsin was detectable for high molecular weight dextrin conjugates that were extensively succinoylated (26 – 39 mol %).

Table 1 Characteristics of dextrin-trypsin conjugates

Mw Dextrin (g/mol)	Mol % COOH	Trypsin content (% w/w)	Mw (g/mol)	Mw /Mn
9,000	15	72	25,744	1.65
9,000	23	67	14,036	1.47
9,000	32	81	19,784	1.53
51,000	9	51	84,361	1.57
51,000	18	78	101,801	1.63
51,000	26	76	49,774	1.33

The activity of polymer-bound trypsin was reduced compared to free trypsin (Fig 2. and Table 2). For the higher molecular weight dextrin, as the degree of succinoylation of the intermediate increased (9 to 26 mol %), trypsin conjugate activity fell from 63 to 34 % of the starting value. However, when the lower molecular weight dextrin was used, conjugates showed a masking of activity that was unrelated to the extent of modification of the polymer. The remaining activity was in the range 51 - 69 %.

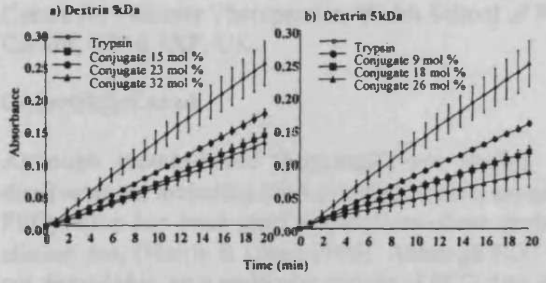

Figure 2 Effect of polymer molecular weight and degree of polymer modification on enzyme activity (n=3 ± SEM).

Addition of amylase to the dextrin-trypsin conjugates led to a reinstatement of trypsin activity (Fig 3a, Table 2). The conjugate that displayed optimum masking-unmasking contained dextrin of molecular weight 51 kDa that had 26 mol % succinoylation. In this case conjugation led to a reduction in trypsin activity to 34 %, and addition of amylase reinstated trypsin activity to 58 % of the starting level. Similarly, the optimum conjugate for the lower molecular weight dextrin was modified to 32 mol % and modulated activity from 51 to 92 %.

Table 2. Enzymatic activity of dextrin-trypsin conjugates, prior to, and following degradation of the polymer.

Dextrin molecular weight (g/mol)	Mol % COOH	Remaining Activity (%)	Amylase activated activity (%)
9,000	15	55	67
9,000	23	69	52
9,000	32	51	92
51,000	9	63	115
51,000	18	46	64
51,000	26	34	58

Analysis of enzyme kinetic was undertaken using a Hanes-Woolfe plot to determine the Michaelis Menten constants for both unmodified trypsin and the dextrin-trypsin conjugates both prior to, and following, amylase degradation of dextrin (Fig 3b). Dextrin-conjugated trypsin had a Kcat of 1.24 - 4.09 s^{-1}. These values are comparable to both the Kcat determined for free trypsin in this study (2.5 – 2.9 s^{-1}), and the published value obtained for porcine trypsin analysed under almost identical conditions using the substrate L-BAPNA (Kcat = 2.89 s^{-1}) (6). There was no obvious relationship between increasing degree of dextrin succinoylation and either the Kcat of the conjugate or the degree of enzyme activity expressed following the degradation of dextrin.

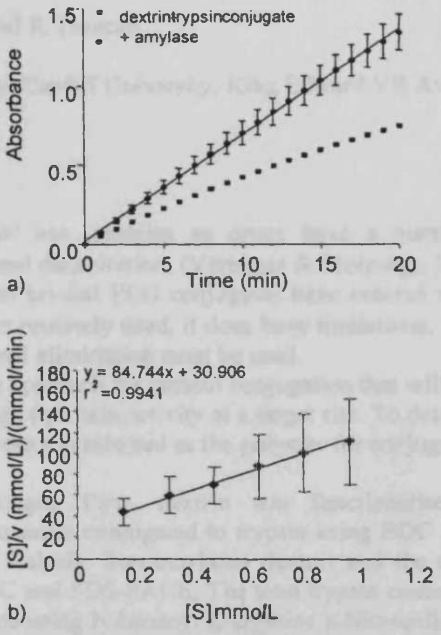

Figure 3a Conjugate activity prior to, and following amylase mediated degradation of the polymer (n=3 ± SEM), 3b) Hanes-Woolfe plot of conjugate activity.

CONCLUSION:

Dextrin conjugation to trypsin can be used to mask enzyme activity. This can subsequently be regenerated using amylase-triggered polymer degradation. Use of higher molecular weight dextrin with a high degree of succinoylation was most effective.

REFERENCES:

1. Gilbert *et al.* (2004) J. Pharm. Pharmacol. **17**, S-46.
2. Harris *et al.* (2003) Nature Drug Discov. **2**, 214-221.
3. Mistry *et al.* (1994) Peritoneal Dialysis Intl **14**, S13-S21.
4. Hreczuk-Hirst *et al.* (2001) Int. J. Pharm. **230**, 57-66.
5. Hreczuk-Hirst *et al.* (2001) J. Bioact. Compat. Polymers **16**, 353-365.
6. Johnson *et al.* (2002) Comp. Biochem. Phys. Part B. **131**, 423-431

Abstract for poster presentation:
British Pharmaceutical Conference, 2004

Design of novel, bioresponsive polymer-protein conjugates

H.R.P. Gilbert, R. Lewis, K. Meier, M.J. Vicent, A. White and R. Duncan.

Centre for Polymer Therapeutics, Welsh School of Pharmacy, Cardiff University, King Edward VII Avenue, Cardiff, CF10 3XF, UK.

GilbertH@cf.ac.uk

Although protein-based therapeutics are finding increased use, proteins as drugs have a number of disadvantages including short circulation time, antigenicity and denaturation, (Veronese & Morpurgo 1999). PEGylation has been used to overcome these problems and several PEG conjugates have entered routine clinical use, (Harris & Chess 2003). Although PEG has been routinely used, it does have limitations, as it is not degradable, so a molecular weight of PEG that allows renal elimination must be used.
The aims of this study are to develop a novel, bioresponsive approach for protein conjugation that will allow complete inactivation of the protein in transit, but unmasking of protein activity at a target site. To determine proof of concept, trypsin was chosen as a model protein and dextrin selected as the polymer for conjugation.

Dextrin-trypsin conjugates were synthesised in two stages. First, dextrin was functionalised, by succinoylation (16-32 mol%). This intermediate was subsequently conjugated to trypsin using EDC and S-NHS as coupling agents. The conjugate was purified by dialysis. Succinoylated dextrin and the trypsin conjugates were characterised by titration, FTIR, GPC, FPLC and SDS-PAGE. The total trypsin content was determined by BCA assay. Free trypsin activity was measured using N-benzoyl L-arginine p-Nitroanilide (L-BAPNA) as a substrate. The activity of the conjugate incubated with α-amylase (16 h at 37 °C) to degrade dextrin was also measured.

Conjugates were synthesised using 16, 24 and 32 mol% modified dextrin. Characterisation of the conjugates by SDS-PAGE revealed smearing from the wells to 23 KDa. This was consistent with the polydispersity of both the succinoylated dextrin (Mw/Mn 1.4-1.7) and conjugates (Mw/Mn 1.4-1.5). No distinct band was observed at 23KDa, indicating minimal free trypsin, undetected by GPC and FPLC. Determination of the trypsin loading by BCA assay (0.07% w/v) enabled calculation of trypsin equivalents for activity studies.

As desired, polymer bound trypsin showed reduced activity compared to free trypsin. The encasement of trypsin by the polymer prevents the masked enzyme from cleaving the substrate. Increasing the degree of modification of the polymer (up to 32 mol%), further masked enzyme activity of the conjugate, decreasing Vmax from 0.028 to 0.014 (50%).
Following degradation of the polymer by amylase, significant trypsin activity was reinstated (unpaired t-test, $p<0.05$). Degradation of conjugates with higher degrees of polymer modification displayed greater activity, implying an increased masking of activity. This increase in activity was significant between 16 and 32 mol% modified polymer conjugates, (Bonferroni, $p<0.05$).

In conclusion, preliminary results are promising and support the concept of masking the activity of the protein payload by increasing the extent of modification of the polymer backbone. Reinstatement of the activity on degradation of the polymer was significant.

Harris, J.M., Chess, R.B. (2003). *Nature Drug Disc*, **2**, 214-221.
Veronese, F.M., Morpurgo, M. (1999). *Il Farm*, **54**, 497-516.

HG is supported by a studentship from BBSRC and MJV is supported by a Marie Curie Fellowship, Contract No. HPMF-CT-2002-01555.